

ON LOAN

RETURN TO:
NUCLEAR ENGINEERING LIBRARY
138 ALBANY STREET
CAMBRIDGE, MASS. 02139

MIT-3903-4

MITNE-132

SOLUTION OF THE
SPACE-DEPENDENT REACTOR KINETICS EQUATIONS
IN THREE DIMENSIONS

by

Donald R. Ferguson, K. F. Hansen

August, 1971

Massachusetts Institute of Technology
Department of Nuclear Engineering
Cambridge, Massachusetts 02139

AEC Research and Development Report

Contract AT (30-1) 3903

U.S. Atomic Energy Commission

MASSACHUSETTS INSTITUTE OF TECHNOLOGY

DEPARTMENT OF NUCLEAR ENGINEERING

Cambridge, Massachusetts 02139

SOLUTION OF THE
SPACE-DEPENDENT REACTOR KINETICS EQUATIONS
IN THREE DIMENSIONS

by

Donald R. Ferguson, K. F. Hansen

August, 1971

ON LOAN

RETURN TO:
NUCLEAR ENGINEERING LIBRARY
138 ALBANY STREET
CAMBRIDGE, MASS. 02139

MIT - 3903 - 4

MITNE - 132

AEC Research and Development Report

Contract AT(30-1) 3903

U. S. Atomic Energy Commission

SOLUTION OF THE
SPACE-DEPENDENT REACTOR KINETICS EQUATIONS
IN THREE DIMENSIONS

by

Donald Ross Ferguson

Submitted to the Department of Nuclear Engineering on August 16, 1971, in partial fulfillment of the requirements for the degree of Doctor of Philosophy.

ABSTRACT

A general class of two-step alternating-direction semi-implicit methods is proposed for the approximate solution of the semi-discrete form of the space-dependent reactor kinetics equations. An exponential transformation of the semi-discrete equations is described which has been found to significantly reduce the truncation error when several alternating-direction semi-implicit methods are applied to the transformed equations. A subset of this class is shown to be a consistent approximation to the differential equations and to be numerically stable. Specific members of this subset are compared in one- and two-dimensional numerical experiments. An "optimum" method, termed the NSADE (Non-Symmetric Alternating-Direction Explicit) method is extended to three-dimensional geometries. Subsequent three-dimensional numerical experiments confirm the truncation error, accuracy, and stability properties of this method.

Thesis Supervisor: Kent F. Hansen
Title: Professor of Nuclear Engineering

TABLE OF CONTENTS

	<u>Page</u>
ABSTRACT	2
LIST OF FIGURES	5
LIST OF TABLES	6
ACKNOWLEDGMENTS	7
BIOGRAPHICAL NOTE	8
Chapter 1. INTRODUCTION	9
1.1 The Space-Dependent Reactor Kinetics Problem	9
1.2 The Space-Dependent Reactor Kinetics Equations	12
1.3 The Spatially Discretized Equations	15
1.4 A Review of Solution Techniques	18
Chapter 2. ALTERNATING-DIRECTION SEMI-IMPLICIT TECHNIQUES	23
2.1 The <u>A</u> Matrix	24
2.2 The Exponential Transformation	26
2.3 A General Two-Step Alternating-Direction Semi-Implicit Method	28
2.4 Properties of the Generalized Method with Transformation	30
2.5 Specific Splittings for Two Dimensions	41
2.6 A Proposed Method for Three Dimensions: NSADE	50
Chapter 3. NUMERICAL RESULTS	51
3.1 One- and Two-Dimensional Studies	51
3.2 Three-Dimensional Studies: Homogeneous Problem	59
3.3 Three-Dimensional Studies: Space-Dependent Problems	64

	<u>Page</u>
Chapter 4. CONCLUSIONS AND RECOMMENDATIONS	78
4.1 Characteristics of the Numerical Results	78
4.2 Applicability of the NSADE Method	81
4.3 Limitations of the NSADE Method	84
4.4 Recommendations for Further Work	85
REFERENCES	86
Appendix A. THE SEMI-DISCRETE FORM OF THE SPACE-DEPENDENT REACTOR KINETICS EQUATIONS	90
Appendix B. THEOREMS	97
Appendix C. TEST PROBLEM DATA	107
Appendix D. THE COMPUTER PROGRAM 3DKIN	116
D.1 Description of the Steady State Section	116
D.2 Description of the Time-Dependent Section	125
D.3 Overlay Structure and Input/Output Devices for 3DKIN	126
D.4 Description of Input for 3DKIN	128
D.5 Input for Sample Problem	140
Appendix E. SOURCE LISTING OF 3DKIN (Only in first six copies)	142

LIST OF FIGURES

<u>No.</u>		<u>Page</u>
3.1	Convergence Rate for Test Case 1	62
3.2	Test Case 1 Results, Centerline Thermal Flux	63
3.3	Test Case 4 Results, Point (1, 5, z)	75
3.4	Test Case 4 Results, Point (1, 21, z)	76
A.1	Coordinate System	91
A.2a	Plane Perpendicular to z-Axis at (l, j, k)	91
A.2b	Plane Perpendicular to y-Axis at (l, j, k)	91
C.1a	x-y Plane for $24 \leq z \leq 136$ cm	109
C.1b	x-y Plane for $0 \leq z \leq 24$, $136 \leq z \leq 160$ cm	109
C.2	x-y Plane for $0 \leq z \leq 120$ cm	111
C.3a	x-y Plane for $30 \leq z \leq 270$ cm	113
C.3b	x-y Plane for $0 \leq z \leq 30$ cm, $270 \leq z \leq 300$ cm	113
D.1	Overlay Structure for 3DKIN	126

LIST OF TABLES

<u>No.</u>		<u>Page</u>
3.1	Group 1 Fluxes at Point (3, 9)	58
3.2	Group 1 Fluxes at Point (12, 3)	58
3.3	Group 4 Fluxes at Point (3, 9)	59
3.4	Group 4 Fluxes at Point (12, 3)	59
3.5	Test Case 1 Results, Group Two Fluxes at Centerpoint	61
3.6	Test Case 2 Results, z-Plane 3	66
3.7	Test Case 2 Results, z-Plane 11	66
3.8	Test Case 2 Results, z-Plane 19	67
3.9	Test Case 3 Results, z-Plane 4, Group 1	70
3.10	Test Case 3 Results, z-Plane 4, Group 4	70
3.11	Test Case 3 Results, z-Plane 12, Group 1	70
3.12	Test Case 3 Results, z-Plane 12, Group 4	71
3.13	Test Case 4 Results, z-Plane 5	73
3.14	Test Case 4 Results, z-Plane 10	74
3.15	Test Case 4 Results, z-Plane 16	74
4.1	Computational Times	81
4.2	Comparison of Computing Speeds	82
D.1	Input/Output Symbolic Devices	128

ACKNOWLEDGMENTS

Several people and organizations are deserving of an expression of appreciation from the author for the assistance and encouragement they rendered during the course of this work. Professor Kent T. Hansen provided valuable guidance and made himself available for discussions whenever requested by the author.

Professor Allan F. Henry and Dr. William H. Reed shared helpful ideas and observations on several occasions. Much of section 2.4 of this thesis is based on work first completed by Dr. Reed and by Dr. Alan L. Wight.

The author's wife, Signe, provided support and never complained about the countless nights spent by the author at the Information Processing Center.

Fellowship support for the author was provided by the U.S. Atomic Energy Commission. The work was performed under USAEC Contract AT(30-1)-3903. All computation was performed on an IBM 360/65 computer at the M. I. T. Information Processing Center.

Finally, Mrs. Mary Bosco displayed a considerable amount of skill in the typing of this thesis.

BIOGRAPHICAL NOTE

Donald Ross Ferguson was born on May 14, 1944, on a farm near Kensington, Kansas. He attended elementary and secondary school in Kensington, Kansas, and was graduated from Kensington Public High School in May, 1962.

He enrolled at Kansas State University in September, 1962. While an undergraduate, he was a member of FarmHouse social fraternity and served as Chairman of the University's Student Senate and as Vice-President of the Student Body. He was elected to Blue Key National Honor Fraternity. In January, 1967, he was graduated Magna Cum Laude with a B.S. degree in Nuclear Engineering.

After spending seven months as a graduate student at Kansas State University, he entered the University of Birmingham, Birmingham, U.K., as a graduate student in the Department of Physics. He was supported by a Fulbright-Hays Scholarship. He received an M.Sc. degree in Reactor Physics and Technology in December, 1968.

In February, 1969, he entered Massachusetts Institute of Technology as a graduate student in the Department of Nuclear Engineering.

Mr. Ferguson is married to the former Signe Louise Burk of Wichita, Kansas.

Chapter 1

INTRODUCTION

1.1 The Space-Dependent Reactor Kinetics Problem

In the past few years, much effort has been devoted to developing methods for solving the time-dependent multigroup neutron diffusion equations in one or more spatial dimensions. This work has been motivated by at least three reasons. First, it is a mathematical certainty that the solution of these equations for any reactor subjected to a perturbation, which is not homogeneous over the entire reactor, will exhibit a spatially nonuniform behavior. Second, and more practically, the present generation of 1000 Mw(e) and larger light water thermal reactors are so large that they behave in a loosely-coupled manner when subjected to localized perturbations. Finally, the inherently more severe safety problems associated with large liquid-metal-cooled fast breeder reactors must be analyzed as exactly as possible. Certainly, methods capable of treating space-time effects should be available for use in this analysis.

The time constants associated with the various phenomena which affect the neutron flux distribution in space span many orders of magnitude. Those associated with the burnout of fissile isotopes, buildup of most fission products, and the production of fissile isotopes from fertile isotopes are on the order of weeks and months. Uneven variations in the xenon concentration in space and time can cause spatial power oscillations, with time constants on the order of several hours.

Sodium voiding, loss of coolant in water-cooled reactors, and rapid control rod motions give rise to flux changes with associated time constants on the order of tens of microseconds to a few seconds.

For the most part, those phenomena which occur on a time scale of hours or longer are adequately treated by quasi-static techniques, where the time dependence is treated by a series of static calculations. Of concern for this thesis are methods for treating the more rapid flux variations, where the transient of interest extends over a few seconds at most. The time derivatives cannot be ignored for these transients. These problems are also of the most concern from the standpoint of accident analysis.

For the purposes of this thesis, it is assumed that the multigroup form of the time-dependent diffusion equation is adequate to describe the spatial and energy distribution of the neutron population in a reactor. This is generally true for assemblies of the size of current power reactors, particularly if more exacting methods have been used to obtain the multigroup constants for the various material compositions in the assembly. A more exact mathematical treatment, such as using the time-dependent transport equation, is usually necessary only for more exotic problems such as weapons calculations.

In addition, only the linear form of the multigroup equation is treated in this thesis. Changes in material properties in time are not coupled to local or assembly-wide flux variations. Perturbations are intended to simulate external factors such as control rod motion. Fortunately, for both the reactor designer and for those concerned with methods development, most feedback mechanisms are relatively

smooth functions of such factors as temperature and pressure. Since the method developed in this thesis treats problems with time-varying coefficients with no difficulty, it is believed that the method should also treat problems with additional variations in coefficients due to nonlinear feedback effects.

As shown later in this thesis, the equations are finite-differenced on a fixed spatial mesh before they are solved. When the fixed mesh has been specified, an error has been incurred in computing the initial spatial flux distribution and largest eigenvalue when these are compared to the solution of the differential form of the equations. This error is due to the finite mesh spacing. It will be carried on into later time-dependent results obtained from the finite-differenced form of the equations. However, discussions of truncation error in the numerical results shown in this thesis do not refer to this error. Of concern here is the error in the approximate solution when compared to the exact solution of the differential-difference system of equations.

The remainder of this chapter presents the form of the space-dependent reactor kinetics equations to be used hereafter. Several methods previously employed to solve these equations are also reviewed. In Chapter 2, a very general solution technique is derived and shown to possess several desirable and mathematically necessary properties. Four specific variants are considered in more detail for comparative numerical testing. Finally, one of these methods is proposed as being most suitable to three spatial dimensions. Chapter 3 begins with the results of the numerical comparisons of the four variants over a range of problems in one and two spatial dimensions.

Numerical results for four problems in three dimensions, obtained with the method proposed in Chapter 2, are presented to conclude the chapter. Chapter 4 summarizes the conclusions which can be reached concerning this method and includes a discussion of its advantages and limitations.

1.2 The Space-Dependent Reactor Kinetics Equations

The diffusion approximation to the reactor kinetics equations may be written as follows:¹

$$\begin{aligned} \frac{1}{v_g} \frac{d\phi_g}{dt}(\vec{r}, t) &= \vec{\nabla} \cdot D_g(\vec{r}, t) \vec{\nabla} \phi_g(\vec{r}, t) + \sum_{g'=1}^G \Sigma_{gg'}(\vec{r}, t) \phi_{g'}(\vec{r}, t) \\ &+ \sum_{i=1}^I f_{gi} C_i(\vec{r}, t) \quad (1 \leq g \leq G) \\ \frac{dC_i}{dt}(\vec{r}, t) &= -\lambda_i C_i(\vec{r}, t) + \sum_{g'=1}^G p_{ig'}(\vec{r}, t) \phi_{g'}(\vec{r}, t) \quad (1 \leq i \leq I), \end{aligned} \tag{1.1}$$

where

g = index number of the energy group

i = index number of the delayed neutron precursor group

ϕ_g = scalar neutron flux in energy group g (neutrons/cm²·sec)

C_i = density of the i^{th} precursor (cm⁻³)

v_g = speed of the neutrons in the g^{th} group (cm/sec)

D_g = diffusion coefficient for neutrons in group g (cm)

$\Sigma_{gg'}$ = intergroup macroscopic transfer cross section from group g' to group g (cm⁻¹), with the following structure:

$$\Sigma_{gg} = \chi_g \nu_g (1-\beta) \Sigma_{fg} - \Sigma_{ag} - \sum_{g' \neq g} \Sigma_{sg'g},$$

χ_g = the fission spectrum yield in group g .

ν_g = average number of neutrons per fission in group g

Σ_{fg} = macroscopic fission cross section in group g

Σ_{ag} = macroscopic absorption cross section in group g

$\Sigma_{sgg'}$ = macroscopic scattering cross section from g' to g

β = total fractional yield of delayed neutrons per fission.

$$\Sigma_{gg'} = \chi_g \nu_g \Sigma_{fg'} (1-\beta) + \Sigma_{sgg'}, \quad g' \neq g.$$

$f_{gi} = \lambda_i \chi_{gi}$ = probability (sec^{-1}) that the i^{th} precursor will yield a neutron in group g , where λ_i is the decay constant and $\vec{\chi}_i$ the energy spectrum of neutrons from the i^{th} precursor

$p_{ig'} = \beta_i \nu_{g'} \Sigma_{fg'}$ = production factor (cm^{-1}) for the i^{th} precursor having fractional yield β_i by fissions in group g' .

Boundary conditions for Eqs. (1.1) will be of the homogeneous Neumann or Dirichlet type. At internal interfaces, continuity of the flux and normal component of the neutron current, $\vec{n} \cdot D \vec{\nabla} \phi$, will be required. An initial flux distribution in energy and space must be specified.

Equations (1.1) may be compacted into the form,¹

$$\frac{d\vec{\theta}}{dt}(\vec{r}, t) = \underline{M}(\vec{r}, t) \vec{\theta}(\vec{r}, t), \quad (1.2)$$

by defining the matrices

$$\vec{\theta}(\vec{r}, t) = \begin{bmatrix} \phi_1(\vec{r}, t) \\ \phi_2(\vec{r}, t) \\ \vdots \\ \phi_G(\vec{r}, t) \\ C_1(\vec{r}, t) \\ \vdots \\ C_I(\vec{r}, t) \end{bmatrix} \quad (1.3a)$$

and

$$\underline{M}(\vec{r}, t) = \begin{bmatrix} v_1(\vec{\nabla} \cdot D_1 \vec{\nabla} + \Sigma_{11}) & v_1 \Sigma_{12} & \cdots & v_1 \Sigma_{1G} & | & v_1^f{}_{11} & \cdots & v_1^f{}_{1I} \\ v_2 \Sigma_{21} & v_2(\vec{\nabla} \cdot D_2 \vec{\nabla} + \Sigma_{22}) & \cdots & v_2 \Sigma_{2G} & | & v_2^f{}_{21} & \cdots & v_2^f{}_{2I} \\ & & \cdot & \cdot & \cdot & & & \\ v_G \Sigma_{G1} & v_G \Sigma_{G2} & \cdots & v_G(\vec{\nabla} \cdot D_G \vec{\nabla} + \Sigma_{GG}) & | & v_G^f{}_{G1} & \cdots & v_G^f{}_{GI} \\ \hline p_{11} & p_{12} & \cdots & p_{1G} & | & -\lambda_1 & & 0 \\ & & \cdot & \cdot & \cdot & 0 & \cdot & \\ p_{I1} & p_{I2} & \cdots & p_{IG} & | & & & -\lambda_I \end{bmatrix} \quad (1.3b)$$

This form of the equations will be used later in discussing various mathematical properties of solution techniques proposed in this thesis.

1.3 The Spatially Discretized Equations

Equations (1.1) are continuous in both spatial and temporal variables. In order to discretize the spatial variables, a three-dimensional spatial mesh is superimposed upon the reactor of interest. Equations (1.1) are then integrated over the volumes associated with each of the mesh points, using the box-integration technique.³ The resulting equations are referred to as the semi-discrete equations.

The semi-discrete forms of the reactor kinetics equations are derived in detail in Appendix A. The resulting equations for the neutron flux at all mesh points for group g , $\vec{\psi}_g$, and the i^{th} precursor concentration at all mesh points, \vec{C}_i , can be written as

$$\frac{d\vec{\psi}_g}{dt} = \underline{D}_g \vec{\psi}_g + \sum_{g'=1}^G \underline{T}_{gg'} \vec{\psi}_{g'} + \sum_{i=1}^I \underline{F}_{gi} \vec{C}_i \quad (1 \leq g \leq G) \quad (1.4)$$

and

$$\frac{d\vec{C}_i}{dt} = -\underline{\Lambda}_i \vec{C}_i + \sum_{g'=1}^G \underline{P}_{ig'} \vec{\psi}_{g'} \quad (1 \leq i \leq I). \quad (1.5)$$

Here, \underline{D}_g is a seven-stripe matrix representing the net neutron leakage across the six sides of the mesh volume. All other square matrices are diagonal. $\underline{T}_{gg'}$ contains terms representing intergroup transfer processes, and \underline{F}_{gi} represents the transfer of delayed neutrons into group g due to decays in precursor group i . $\underline{\Lambda}_i$ contains the precursor decay constants, while $\underline{P}_{ig'}$ represents the production of delayed precursor i due to fissions in group g' .

Equations (1.4) and (1.5) can be combined into the single matrix equation,

$$\frac{d\vec{\psi}}{dt} = \underline{A}\vec{\psi}. \quad (1.6)$$

The matrix \underline{A} is square and of order $N * (G+I)$, where N is the number of spatial mesh points. Here, $\vec{\psi}$ and \underline{A} have been defined as

$$\vec{\psi} = \begin{bmatrix} \vec{\psi}_1 \\ \vec{\psi}_2 \\ \vdots \\ \vec{\psi}_G \\ \vec{c}_1 \\ \vdots \\ \vec{c}_I \end{bmatrix} \quad (1.7)$$

and

$$\underline{A} = \begin{bmatrix} \underline{D}_1 + \underline{T}_{11} & \underline{T}_{12} & \cdots & \underline{T}_{1G} & \underline{F}_{11} & \cdots & \underline{F}_{1I} \\ \underline{T}_{21} & \underline{D}_2 + \underline{T}_{22} & \cdots & \underline{T}_{2G} & \underline{F}_{21} & \cdots & \underline{F}_{2I} \\ & & & \cdots & & & \\ \underline{T}_{G1} & \underline{T}_{G2} & \cdots & \underline{D}_G + \underline{T}_{GG} & \underline{F}_{G1} & \cdots & \underline{F}_{GI} \\ \hline \underline{P}_{11} & \underline{P}_{12} & \cdots & \underline{P}_{1G} & -\underline{\Lambda}_1 & & \\ \underline{P}_{21} & \underline{P}_{22} & \cdots & \underline{P}_{2G} & & \underline{0} & \\ & & & \cdots & & & \\ \underline{P}_{I1} & \underline{P}_{I2} & \cdots & \underline{P}_{IG} & \underline{0} & & -\underline{\Lambda}_I \end{bmatrix}. \quad (1.8)$$

For later reference, several matrices are defined here as follows:

$$\underline{D} = \left[\begin{array}{cccc|c} \underline{D}_1 & \underline{0} & \dots & \underline{0} & \\ \underline{0} & \underline{D}_2 & \dots & \underline{0} & \\ & & \dots & & \underline{0} \\ \underline{0} & \underline{0} & \dots & \underline{D}_G & \\ \hline & & & & -\underline{\Lambda}_1 & \underline{0} \\ & \underline{0} & & & \underline{0} & \dots \\ & & & & & \dots \\ & & & & & -\underline{\Lambda}_I \end{array} \right], \quad (1.9a)$$

$$\underline{U} = \left[\begin{array}{cccc|ccc} \underline{0} & \underline{T}_{12} & \dots & \underline{T}_{1G} & \underline{F}_{11} & \dots & \underline{F}_{1I} \\ \underline{0} & \underline{0} & \dots & \underline{T}_{2G} & \underline{F}_{21} & \dots & \underline{F}_{2I} \\ & & \dots & & & & \\ \underline{0} & \underline{0} & & \underline{0} & \underline{F}_{G1} & \dots & \underline{F}_{GI} \\ \hline & \underline{0} & & & & & \underline{0} \end{array} \right], \quad (1.9b)$$

$$\underline{L} = \left[\begin{array}{cccc|c} \underline{0} & \underline{0} & \dots & \underline{0} & \\ \underline{T}_{21} & \underline{0} & \dots & \underline{0} & \\ & & \dots & & \underline{0} \\ \underline{T}_{G1} & \underline{T}_{G2} & \dots & \underline{0} & \\ \hline \underline{P}_{11} & \underline{P}_{12} & \dots & \underline{P}_{1G} & \\ & & \dots & & \underline{0} \\ \underline{P}_{I1} & \underline{P}_{I2} & \dots & \underline{P}_{IG} & \end{array} \right], \quad (1.9c)$$

and

$$\underline{T} = \underline{A} - (\underline{D} + \underline{L} + \underline{U}). \quad (1.9d)$$

For any period of time, Δt , during which all terms in \underline{A} are constant, Eq. (1.6) has the solution

$$\vec{\psi}(\Delta t) = e^{\underline{A}\Delta t} \vec{\psi}(0). \quad (1.10)$$

All solution techniques for the semi-discrete equations are approximations to Eq. (1.10).

1.4 A Review of Solution Techniques

Calculational methods used for solving the space-dependent kinetics equation can be placed into two broad categories. The first category can be generally classed as modal methods.⁴ More specifically, it can be broken into time synthesis and space-time synthesis, both of which could be termed indirect solution techniques. These methods make some assumption about the shape of the solution over several subregions or the entire reactor. These assumptions are forced into the final solution through a variety of techniques. The second category could be termed direct techniques and consists of methods whereby Eqs. (1.1) are solved directly. Since these equations can be solved analytically only for the most trivial of problems, these direct techniques generally involve finite-differencing them and proceeding to solve some approximation to Eq. (1.6).

All of the indirect methods approach the problem by expanding the solution as a linear combination of some set of functions:

$$\vec{\psi}(\vec{r}, t) = \sum_{k=1}^K \underline{T}_k(\vec{r}, t) \vec{\psi}_k(\vec{r}). \quad (1.11)$$

The time synthesis methods use one or more $\vec{\psi}_k(\vec{r})$, each of which is defined over the entire solution region. The \underline{T}_k then become functions only of time. The $\vec{\psi}_k(\vec{r})$ may consist of eigenmodes of one of several static operators. Among those suggested are the Helmholtz eigenmodes, the ω -modes, and the λ -modes.⁴ None of these have been very successfully applied to any general class of two- or three-dimensional problems.

Alternatively, the $\vec{\psi}_k(\vec{r})$ may be the fundamental modes of a set of operators, each describing the reactor in a different state. Most naturally, these states are chosen to be static states of the reactor at different times during the particular transient of interest.⁵ These states can be computed by standard static methods. However, for three-dimensional problems, even the best methods for computing the $\vec{\psi}_k(\vec{r})$ are very time-consuming. It should be noted that the well-known adiabatic method⁶ and quasi-static method^{7,8} can be considered as variants of time synthesis where only one trial function is used at a time, but new trial functions are used every few time steps.⁴

In space-time synthesis methods, the $\vec{\psi}_k(\vec{r})$ are chosen to represent flux shapes over subregions of the reactor, where the subregion may be a subvolume, plane, or subplane. For example, the so-called single-channel synthesis technique^{9,10,11} divides a three-dimensional reactor into a number of axial zones and uses a set of two-dimensional flux shapes for the $\vec{\psi}_k(\vec{r})$ within each zone. The sets may vary from zone to zone, and are chosen to represent static conditions across planes

perpendicular to the axis in the zones at various times in the transient. Being only two-dimensional, they are relatively easy to compute. Multi-channel synthesis techniques^{12,13} additionally partition the planes perpendicular to the axis into zones and use sets of $\vec{\psi}_k(\vec{r})$ which are allowed to vary independently in these planar zones.

Once the expansion functions have been chosen, equations to be solved for the expansion coefficients are generated using either a variational principle encompassing the multigroup diffusion equations or a weighted residual technique. The great advantage of these methods is that the number of equations to be solved is generally small compared to the number of points at which $\vec{\psi}(\vec{r}, t)$ will be known when the expansion in Eq. (1.11) is carried out, even for three-dimensional calculations. Using a space-time synthesis technique, flux solutions at 10^5 - 10^6 mesh points over the period of interest in a transient can be obtained in reasonable amounts of computer time.

These synthesis techniques are characterized by a lack of definitive error bounds, however. There is little but intuition to indicate when a set of trial functions will give good results for a particular perturbation.

The direct finite difference techniques, in contrast, are characterized by fairly definitive error estimates. Because of this property, they are extremely useful as numerical standards against which the more approximate methods may be compared. As computational capabilities increase, direct methods also become practical for routine production calculations in one and two dimensions. If fine spatial detail is not required, even three-dimensional direct methods become

practical for some types of routine calculations.

In one spatial dimension, the GAKIN¹⁴ and WIGLE¹⁵ methods have been incorporated successfully into codes after which they were named. GAKIN solves Eq. (1.6) by splitting \underline{A} and using the diagonal part of it as an integrating factor to integrate the equation. The behavior of the dependent variables, $\vec{\psi}$, is approximated over each time step so that the integrals can be evaluated.

The WIGLE method approximates the solution to Eq. (1.6) over a series of time steps Δt by

$$\vec{\psi}^{j+1} = \Delta t \underline{\theta} \underline{A} \vec{\psi}^{j+1} + \Delta t (\underline{I} - \underline{\theta}) \underline{A} \vec{\psi}^j, \quad (1.12)$$

where $\underline{\theta}$ is a diagonal matrix of coefficients, θ_{ii} ($0 \leq \theta_{ii} \leq 1$). The θ_{ii} 's are chosen to improve the accuracy of the approximation. Setting $\underline{\theta} = \frac{1}{2} \underline{I}$ would yield the Crank-Nicholson approximation with its favorable $O(\Delta t^3)$ truncation error. Thus, relatively large time steps can be taken, but the inversion of the matrix $(\underline{I} - \Delta t \underline{\theta} \underline{A})$ must be carried out iteratively. This is equivalent to solving a fixed-source subcritical reactor calculation at each time step.

In two dimensions, the WIGLE method has been extended into the code TWIGL.¹⁶ This code is limited to two neutron groups, but the method could treat any number of groups. Practically, a difficulty arises because even two-group, two-dimensional fixed-source calculations must be done by time-consuming iterative techniques. As more groups are added, time requirements increase rapidly for these iterations.

The LUMAC¹⁷ code extends the GAKIN method to two dimensions by approximating the leakage in first one dimension and then the other by a pointwise transverse buckling over two time steps. The matrices to be inverted at each time step are of the same form as in one dimension and are easily inverted.

Finally, the MITKIN^{1,2} method uses a particular alternating-direction, semi-implicit splitting technique referred to as an alternating-direction explicit method.¹⁸ In addition, an exponential transformation is applied to Eq. (1.6), which greatly improves the truncation error. This method is computationally very rapid since all matrices to be inverted are triangular in form. Over a range of problems, it has been shown to be more rapid than the LUMAC algorithm. Increasing the number of mesh points or the number of energy groups results in only a linear increase in computational time. It has also been successfully extended to cylindrical (r-z) and hexagonal geometries.¹⁹

Motivation for extension of one of these or another method to treat a general class of three-dimensional multigroup problems comes primarily from the need for an accurate numerical standard against which the more rapid synthesis techniques can be tested. In three dimensions, the WIGLE method would be straightforward but extremely time-consuming, due to the great increase in time necessary to perform the three-dimensional, fixed-source-like calculations. Because of its demonstrated superiority over the GAKIN method in two dimensions, the alternating-direction semi-implicit method used in MITKIN is the most promising technique for three dimensions. It is the purpose of this thesis to investigate several variations of this method and extend the "optimum" variation to three dimensions.

Chapter 2

ALTERNATING-DIRECTION SEMI-IMPLICIT TECHNIQUES

It is the purpose of this chapter to examine the theoretical foundations of a class of semi-implicit approximations to the solution of Eq. (1.6), given exactly by Eq. (1.10). Thus, approximations to the operator $\exp(\underline{A} \Delta t)$ are examined. Restricting consideration to two-level (first order) approximations of the time derivative, the matrix equivalents of the well-known Padé rational approximations²⁰ are the most straightforward. Equation (1.12), with $\underline{\theta}$ set to $\underline{0}$, \underline{I} , and $\frac{1}{2}\underline{I}$ gives, respectively, the Padé (0, 1), (1, 0), and (1, 1) approximations. However, the (0, 1) approximation suffers from severe stability restrictions,²⁰ while the (1, 0) and (1, 1) approximations require inversion of a matrix containing \underline{A} . This becomes prohibitively time-consuming in problems involving three spatial dimensions and several neutron energy groups.

The class of semi-implicit techniques examined here circumvents this difficulty by "splitting" \underline{A} and inverting only a part of it at a time, a part generally chosen to be easily inverted. The alternating-direction implicit method²¹ and alternating-direction explicit method¹⁸ are members of this class. Treating only a part of \underline{A} implicitly necessarily leads to more severe truncation error difficulties and the requirement of much smaller time steps than for methods which invert \underline{A} in its entirety. Thus, application of several of these methods to the direct solution of Eq. (1.6) has been found to be unsatisfactory.^{1,22,23}

After reviewing properties of the \underline{A} matrix in section 2.1, an exponential transformation to Eq. (1.6) is introduced in section 2.2. This transformation has been found to significantly reduce the truncation error when several of these "splitting" methods are subsequently applied to the transformed equations.^{1,23} Section 2.3 presents a general two-step alternating-direction splitting method for application to the transformed version of Eq. (1.6), and section 2.4 discusses mathematical properties of this method. Four specific splittings of \underline{A} are proposed for further examination in section 2.5. Finally, one of these four is examined in section 2.6 for application to three-dimensional geometries.

2.1 The \underline{A} Matrix

It is instructive to examine the \underline{A} matrix in some detail. The magnitudes of its elements vary over 6 to 8 orders of magnitude. The decay constants λ are on the order of unity, while velocities of order 10^5 to 10^9 multiply absorption and leakage coefficients which may be as large as 10^{-1} . Its eigenvalues likewise span several orders of magnitude, from 10^{-1} sec^{-1} to -10^6 sec^{-1} , giving rise to a property known as "stiffness" to the set of differential equations for reactivities less than prompt critical.¹ Thus, any attempt to represent the derivative in Eq. (1.6) by a finite difference approximation will require that relatively small time steps be taken in order to follow the more rapidly varying components of the solution. At the same time, the interesting part of the transient may span a large number of these time steps.

Additionally, \underline{A} is a real, square irreducible matrix with non-negative off-diagonal elements and negative diagonal elements. In Chapter 8 of Varga,²⁰ this is termed an "essentially positive" matrix. Varga's Theorem 8.1 states that $\exp(\underline{A}t)$ is positive for all $t > 0$. His Theorem 8.2 further states that \underline{A} has a real, simple eigenvalue, ω_0 , which is larger than the real part of any other eigenvalues, ω_1 , and to which corresponds a positive eigenvector, \vec{e}_0 . If any element of \underline{A} increases algebraically, ω_0 increases. Finally, his Theorem 8.3 states that the asymptotic behavior of $\exp(\underline{A}t)$ is given by

$$\|\exp(\underline{A}t)\| \sim K \cdot \exp(\omega_0 t) \quad (2.1)$$

as $t \rightarrow \infty$, where K is some constant, independent of t . This also assumes that \underline{A} is constant. The solution vector $\vec{\psi}(t)$ in Eq. (1.10) will always be non-negative for a non-negative initial condition $\vec{\psi}(0)$. Thus, the desired solution $\vec{\psi}(t)$ is well-behaved and bounded, as physically it must be.

The numerical property of consistency is discussed later in this chapter. The discrete approximation to the $\vec{\nabla} \cdot D\vec{\nabla}$ operator contained in \underline{A} is consistent and accurate to order $(\Delta x)^2$, $(\Delta y)^2$ and $(\Delta z)^2$, the mesh spacings in the three dimensions.²⁵ Stated in another way, if $\vec{\theta}$ is a genuine solution to Eq. (1.2), then

$$\underline{A}\vec{\theta} = \underline{M}\vec{\theta} + O(\Delta x^2) + O(\Delta y^2) + O(\Delta z^2). \quad (2.2)$$

It is also instructive to observe certain properties of \underline{D} as defined in Eq. (1.9a). Use of the box integration technique to discretize the spatial variables assures that $(-\underline{D})$ is symmetric and diagonally dominant with positive diagonal entries and nonpositive off-diagonal entries.

It is also irreducible. A sufficient condition for $(-\underline{D})$ to be irreducibly diagonally dominant is that homogeneous Dirichlet boundary conditions be specified along at least one of the boundaries. If this is the case, then \underline{D} is negative definite.³

2.2 The Exponential Transformation

It is desired to increase the size of the time step size while still controlling truncation error when using alternating-direction splitting methods. A change of variables has been suggested^{1,23} which achieves this end. Let

$$\vec{\psi}(t) = e^{\underline{\Omega}t} \vec{\phi}(t), \quad (2.3)$$

where $\underline{\Omega}$ is a diagonal matrix of free parameters, henceforth referred to as frequencies. Since $\underline{\Omega}$ is diagonal, the exponential is easily computed.

To obtain an equation for $\vec{\phi}$, differentiate Eq. (2.3) to obtain

$$\frac{d\vec{\psi}}{dt} = e^{\underline{\Omega}t} \frac{d\vec{\phi}}{dt} + \underline{\Omega} e^{\underline{\Omega}t} \vec{\phi}. \quad (2.4)$$

Substituting this into Eq. (1.6) yields

$$\frac{d\vec{\phi}}{dt} = e^{-\underline{\Omega}t} (\underline{A} - \underline{\Omega}) e^{\underline{\Omega}t} \vec{\phi}, \quad (2.5)$$

to be solved for $\vec{\phi}$.

This change of variables has been motivated by the idea that since the behavior of $\vec{\psi}$ is basically exponential in nature, the function $\vec{\phi}$ should be relatively slowly-varying, providing that the $\underline{\Omega}$ are properly chosen. Hence, the time derivative in Eq. (2.5) should be approximated by a simple finite difference with less resultant truncation error

than if the same finite difference were used to approximate the time derivative in Eq. (1.6). Equation (2.5) has the same form as does Eq. (1.6), so the same solution techniques are applicable to both.

The choice of $\underline{\Omega}$ is a delicate matter.¹ That such an $\underline{\Omega}$ matrix exists is seen by choosing $\underline{\Omega}$ so that

$$\underline{\Omega} \vec{\psi}(t') = \underline{A} \vec{\psi}(t'). \quad (2.6)$$

Then

$$\left. \frac{d\vec{\phi}}{dt} \right|_{t=t'} = 0, \quad (2.7)$$

so that in some interval about t' , $\vec{\phi}$ should be slowly varying. For many problems, this interval is long compared to the time step sizes necessary to control truncation error when solving the untransformed equation.

Best results are obtained^{1,23} when a new $\underline{\Omega}$ is chosen for each time step, Δt . For the time step from $t=N\Delta t$ to $t=(N+1)\Delta t$, the vector $\vec{\psi}([N+1]\Delta t) = \vec{\psi}^{N+1}$ is not yet known. Using $\vec{\psi}^N$ in Eq. (2.6) to compute $\underline{\Omega}$ for this step has been found to be unstable. Providing $\underline{\Omega}$ does not change very much for $t \leq t' \leq t+\Delta t$, it has been found that the Ω values to be used for the neutron groups at point j for this step may be successfully approximated by

$$\left(\Omega^N \right)_{\text{point } j}^{\text{group } g} = \frac{1}{\Delta t} \ln \frac{\psi_{g,j}^N}{\psi_{g,j}^{N-1}}, \quad 1 \leq g \leq G. \quad (2.8)$$

All of the groups thus use the same frequency at a mesh point. The group \bar{g} to be used in Eq. (2.8) is the thermal group in thermal reactor problems and a representative fast group in fast reactor problems.

The procedure outlined here can equally well be viewed as an extrapolation procedure. Based on past behavior, the desired solution $\vec{\psi}$ is extrapolated from time t to $t+\Delta t$. A relatively small correction factor to this extrapolated behavior is then computed by some finite difference technique. As long as the rate of change of $\vec{\psi}$ is smooth, this extrapolation procedure should work well, thus allowing relatively long time steps to be taken. On the other hand, sudden variations in the rates of change of elements in \underline{A} can cause relatively rapid changes in the behavior of some components of $\vec{\psi}$. When these rapid variations occur, the extrapolation works less well. Smaller time steps must then be taken in order to retain accuracy. This behavior is evidenced in the numerical results shown in Chapter 3.

2.3 A General Two-Step Alternating-Direction Semi-Implicit Method

To apply the general class of alternating-direction splitting methods to Eq. (2.5), the time derivative is replaced by two successive forward differences over a time step, $\Delta t (=2h)$. For notational purposes, let the time step start at $t=0$ so that $\vec{\psi}(0) = \vec{\phi}(0) = \vec{\phi}^0$. For the two halves of the time step, each of duration h , split \underline{A} as follows:

$$\underline{A} = \underline{A}_1 + \underline{A}_2 \tag{2.9a}$$

and

$$\underline{A} = \underline{A}_3 + \underline{A}_4. \tag{2.9b}$$

By evaluating the two exponentials at $t=h$, the midpoint of the step, the difference approximations to Eq. (2.5) become

$$\begin{aligned} \frac{\vec{\phi}(h) - \vec{\phi}(0)}{h} &= e^{-\underline{\Omega}h}(\underline{A}_2 - \alpha \underline{\Omega}) e^{\underline{\Omega}h} \vec{\phi}(h) + e^{-\underline{\Omega}h}(\underline{A}_1 - \gamma \underline{\Omega}) e^{\underline{\Omega}h} \vec{\phi}(0) \\ \frac{\vec{\phi}(2h) - \vec{\phi}(h)}{h} &= e^{-\underline{\Omega}h}(\underline{A}_4 - \alpha \underline{\Omega}) e^{\underline{\Omega}h} \vec{\phi}(2h) + e^{-\underline{\Omega}h}(\underline{A}_3 - \gamma \underline{\Omega}) e^{\underline{\Omega}h} \vec{\phi}(h), \end{aligned} \quad (2.10)$$

where $\alpha + \gamma = 1$.

The unknowns at $t=h$ can be eliminated to yield

$$\begin{aligned} \vec{\phi}(2h) &= e^{-\underline{\Omega}h} [\underline{I} - h(\underline{A}_4 - \alpha \underline{\Omega})]^{-1} [\underline{I} + h(\underline{A}_3 - \gamma \underline{\Omega})] \cdot \\ &\quad \cdot [\underline{I} - h(\underline{A}_2 - \alpha \underline{\Omega})]^{-1} [\underline{I} + h(\underline{A}_1 - \gamma \underline{\Omega})] e^{\underline{\Omega}h} \vec{\phi}(0). \end{aligned}$$

Since $\vec{\psi}(2h) = e^{2h\underline{\Omega}} \vec{\phi}(2h)$, this can be written as

$$\vec{\psi}(2h) = \vec{\psi}^1 = \underline{B}(\underline{\Omega}, h) \vec{\psi}^0, \quad (2.11)$$

where \underline{B} is called the advancement matrix.¹ It is given by

$$\begin{aligned} \underline{B}(\underline{\Omega}, h) &= e^{\underline{\Omega}h} [\underline{I} - h(\underline{A}_4 - \alpha \underline{\Omega})]^{-1} [\underline{I} + h(\underline{A}_3 - \gamma \underline{\Omega})] \cdot \\ &\quad \cdot [\underline{I} - h(\underline{A}_2 - \alpha \underline{\Omega})]^{-1} [\underline{I} + h(\underline{A}_1 - \gamma \underline{\Omega})] e^{\underline{\Omega}h}. \end{aligned} \quad (2.12)$$

Likewise, for any interval Δt ,

$$\vec{\psi}^{N+1} = \underline{B}(\underline{\Omega}, h) \vec{\psi}^N. \quad (2.13)$$

Equations (2.11) and (2.12) represent an arbitrary alternating-direction semi-implicit method. Although it is termed a two-step method because two successive finite differences are taken to advance the solution over time Δt , it is essential to think of the two operators which advance the solution over each half-step h as inseparable from each other. Either used by itself is quite unstable. However, the error modes most strongly excited by one operator are the ones most

strongly damped by the other operator. The solution is thus said to be advanced over one step during time Δt , even though the entire space and energy mesh has been swept twice.

2.4 Properties of the Generalized Method with Transformation

It is imperative to examine the approximation to the solution of Eq. (1.6) given by Eqs. (2.11) and (2.12) with respect to several important numerical properties. This examination has been carried out in a complete and concise fashion in Ref. 1. It is repeated in this thesis for the sake of completeness. The proofs of several theorems and lemmas quoted here are given in Appendix B. The proofs for consistency and stability follow particularly closely those of Ref. 1.

Property 1. Steady State Behavior

For the steady state case where $\underline{A}\vec{\psi}_0 = \vec{0}$,

$$\vec{\psi}(2h) = \underline{B}(\underline{0}, h)\vec{\psi}(0) = \vec{\psi}_0, \quad (2.14)$$

which is the exact solution, independent of h . Thus, operation on a $\vec{\psi}_0$ which represents a just-critical configuration by a $\underline{B}(\underline{0}, h)$ formed from an \underline{A} containing the just-critical parameters will result in no change in $\vec{\psi}_0$.

This can be shown by writing Eq. (2.12) with $\underline{\Omega} = \underline{0}$:

$$\underline{B}(\underline{0}, h) = (\underline{I}-h\underline{A}_4)^{-1}(\underline{I}+h\underline{A}_3)(\underline{I}-h\underline{A}_2)^{-1}(\underline{I}+h\underline{A}_1).$$

Using the splitting relations defined in Eqs. (2.9), this becomes

$$\underline{B}(\underline{0}, h) = (\underline{I}-h\underline{A}_4)^{-1}[\underline{I}-h(\underline{A}_4-\underline{A})](\underline{I}-h\underline{A}_2)^{-1}[\underline{I}-h(\underline{A}_2-\underline{A})].$$

Since $\underline{A}\vec{\psi}_0 = \vec{0}$,

$$\begin{aligned}\underline{B}(\underline{\Omega}, h) \vec{\psi}_0 &= (\underline{I} - h\underline{A}_4)^{-1} [\underline{I} - h(\underline{A}_4 - \underline{A})] (\underline{I} - h\underline{A}_2)^{-1} (\underline{I} - h\underline{A}_2) \vec{\psi}_0 \\ &= (\underline{I} - h\underline{A}_4)^{-1} (\underline{I} - h\underline{A}_4) \vec{\psi}_0 = \vec{\psi}_0.\end{aligned}$$

Property 2. Temporal Truncation Error

This property is concerned with how well the advancement matrix $\underline{B}(\underline{\Omega}, h)$ approximates the exact discrete solution operator $e^{2h\underline{A}}$. For sufficiently small values of h , the difference between the solution computed using $\underline{B}(\underline{\Omega}, h)$ and that computed using $e^{2h\underline{A}}$ over a time step Δt varies approximately as a single power of h . As shown below, for a perfectly symmetric splitting ($\alpha = \gamma = 0.5$, $\underline{A}_1 = \underline{A}_4$, $\underline{A}_2 = \underline{A}_3$), $\underline{B}(\underline{\Omega}, h)$ agrees with the expansion of $e^{2h\underline{A}}$ through terms of order h^2 . For any other splitting, the agreement is through terms of order h .

A Taylor series expansion of the exact operator yields

$$e^{2h\underline{A}} = \underline{I} + 2h\underline{A} + 2h^2 \underline{A}^2 + \dots \quad (2.15)$$

Expanding $\underline{B}(\underline{\Omega}, h)$ likewise gives

$$\begin{aligned}\underline{B}(\underline{\Omega}, h) &= \underline{I} + 2h\underline{A} + h^2 [(\underline{A} - \underline{\Omega})^2 + 2(\underline{\Omega}\underline{A} + \underline{A}\underline{\Omega}) \\ &\quad + (\underline{A}_4 + \underline{A}_2 - 2\alpha\underline{\Omega})(\underline{A} - \underline{\Omega}) - 2\underline{\Omega}^2] + O(h^3).\end{aligned} \quad (2.16)$$

For the symmetric splitting given above,

$$\underline{B}(\underline{\Omega}, h) = \underline{I} + 2h\underline{A} + 2h^2 \underline{A}^2 + O(h^3). \quad (2.17)$$

For any other splitting, terms of order h^2 remain in Eq. (2.16).

For the approximate solution method outlined here to be most useful, the discrete solution $\vec{\psi}^N$ should approach the exact solution $\vec{\theta}(N\Delta t)$ more and more closely as the spatial and temporal meshes are successively decreased in size. Mathematically, this can be stated as requiring

that discrete solutions converge to the solution of the differential equations, Eq. (1.2). A theorem due to Lax²⁶ enables this convergence to be shown. His theorem states that given a properly posed initial-value problem and a consistent finite-difference approximation, stability is the necessary and sufficient condition for convergence.

It has been found most convenient¹ to carry out proofs of consistency and stability in a Hilbert space L_2 . Thus, vector functions $\vec{\theta}(x, y, z, t)$ which are square integrable are to be considered. On this space L_2 , the norm of a linear matrix operator \underline{M} is given by

$$\|\underline{M}\| = \sup_{\vec{\theta}} \frac{\|\underline{M}\vec{\theta}\|}{\|\vec{\theta}\|}.$$

It is assumed that Eq. (1.2) with its associated boundary conditions is a properly-posed initial value problem in the space L_2 . The consistency and stability of the method proposed are proven here; convergence is inferred from these.

Property 3. Consistency¹

The domain of the linear operator \underline{M} in Eq. (1.2) is the set of functions $\vec{\theta}(\vec{r})$ which satisfy the appropriate boundary conditions and for which $\vec{\nabla} \cdot D\vec{\nabla}\vec{\theta}$ exists in L_2 . Any function $\vec{\theta}(\vec{r}, t)$ which is in this domain for all t in the interval $0 \leq t \leq T$ and which satisfies Eq. (1.2) in the sense that

$$\left\| \frac{\vec{\theta}(\vec{r}, t+h) - \vec{\theta}(\vec{r}, t)}{h} - \underline{M}\vec{\theta}(\vec{r}, t) \right\| \rightarrow 0 \text{ as } h \rightarrow 0, \quad 0 \leq t \leq T,$$

is called a genuine solution of the problem.

Informally stated, the consistency condition requires that the temporal finite differencing used to obtain Eq. (2.13) be an approximation to the time derivative of the genuine solution or, equivalently, that

$$\frac{(\underline{\mathbf{B}}(\underline{\Omega}, h) - \underline{\mathbf{I}})}{2h} \vec{\theta}(\vec{r}, t)$$

be an approximation to $\underline{\mathbf{M}} \vec{\theta}(\vec{r}, t)$. How the discrete operator $\underline{\mathbf{B}}$ operates on the continuous function $\vec{\theta}$ must be specified. It is assumed that $\underline{\mathbf{B}}(\underline{\Omega}, h)$ picks out points from $\vec{\theta}$, and an interpolation rule is applied to the result to make it continuous in space. This interpolation need not be specified for the proofs contained in this thesis.

A more formal statement of the consistency condition is that if, for every $\vec{\theta}$ in the class of genuine solutions whose initial elements $\vec{\theta}(\vec{r}, 0)$ are dense in L_2 , the condition²⁶

$$\left\| \left[\frac{\underline{\mathbf{B}}(\underline{\Omega}, h) - \underline{\mathbf{I}}}{2h} - \underline{\mathbf{M}} \right] \vec{\theta}(\vec{r}, t) \right\| \rightarrow 0 \text{ as } h \rightarrow 0, \quad 0 \leq t \leq T,$$

holds, then the operator $\underline{\mathbf{B}}(\underline{\Omega}, h)$ is a consistent approximation to the initial-value problem. With the definition of the derivative,

$$\frac{d\vec{\theta}}{dt} = \lim_{h \rightarrow 0} \frac{\vec{\theta}(t+2h) - \vec{\theta}(t)}{2h},$$

the consistency condition may be modified to be

$$\left\| \frac{\vec{\theta}(t+2h) - \underline{\mathbf{B}}(\underline{\Omega}, h) \vec{\theta}(t)}{h} \right\| \rightarrow 0 \text{ as } h \rightarrow 0, \quad (2.18)$$

the form used in the proof of consistency.

The proof¹ begins by factoring $\underline{B}(\underline{\Omega}, h)$ as follows:

$$\underline{B}(\underline{\Omega}, h) = \underline{C}_1(\underline{\Omega}, h) * \underline{C}_2(\underline{\Omega}, h). \quad (2.19)$$

Here

$$\underline{C}_1(\underline{\Omega}, h) = e^{\underline{\Omega}h} [\underline{I} - h(\underline{A}_4 - \alpha \underline{\Omega})]^{-1} [\underline{I} + h(\underline{A}_3 - \gamma \underline{\Omega})] \quad (2.20a)$$

and

$$\underline{C}_2(\underline{\Omega}, h) = [\underline{I} - h(\underline{A}_2 - \alpha \underline{\Omega})]^{-1} [\underline{I} + h(\underline{A}_1 - \gamma \underline{\Omega})] e^{\underline{\Omega}h}. \quad (2.20b)$$

Lemma 1,¹ stated here and proved in Appendix B, treats the consistency of \underline{C}_1 and \underline{C}_2 .

LEMMA 1. The operators $\underline{C}_1(\underline{\Omega}, h)$ and $\underline{C}_2(\underline{\Omega}, h)$ are consistent.

The only restriction which must be placed on the operator $\underline{B}(\underline{\Omega}, h)$ in order to complete this proof is that as h is decreased, Δx , Δy , and Δz are decreased so that the ratios $h/\Delta x^2$, $h/\Delta y^2$, and $h/\Delta z^2$ are fixed, real constants of any finite size. The need for this restriction is made clear during the discussion concerning the stability of $\underline{B}(\underline{\Omega}, h)$.

Lemma 2,¹ proved in Appendix B, is also necessary for the completion of the consistency proof.

LEMMA 2. If two operators are consistent, then their product is consistent.

With these two lemmas, the consistency proof can be stated in Theorem 1.¹

THEOREM 1. The difference operator $\underline{B}(\underline{\Omega}, h)$ given in Eq. (2.12) is a consistent approximation.

Lemma 1 has shown that $\underline{C}_1(\underline{\Omega}, h)$ and $\underline{C}_2(\underline{\Omega}, h)$ are consistent. Since their product equals $\underline{B}(\underline{\Omega}, h)$, Lemma 2 provides the proof to this theorem.

Property 4. Stability¹

In Eqs. (1.9), the matrix \underline{A} has been split into four parts. Of these four, \underline{D} contains all of the terms which relate to the diffusion of neutrons and, in addition, terms relating to precursor decay. In three-dimensional geometries, the first G submatrices, \underline{D}_g , on the diagonal have seven nonzero stripes containing terms which are inversely proportional to the square of the mesh spacings Δx , Δy , and Δz . \underline{D} is termed the principle part of \underline{A} as it is the part of \underline{A} which determines the property of stability. This arises because of the requirement that the ratios $h/\Delta x^2$, $h/\Delta y^2$, and $h/\Delta z^2$ be fixed, real constants as h goes to zero. Subsequently, terms in the product $h\underline{D}$ do not vanish as h goes to zero.

For convenience, the matrix \underline{E} is defined as

$$\underline{E} = \underline{E}_1 + \underline{E}_2 = \underline{E}_3 + \underline{E}_4 = \underline{A} - \underline{D}. \quad (2.21)$$

The matrices \underline{E}_1 , \underline{E}_2 , \underline{E}_3 , and \underline{E}_4 are those parts of \underline{E} associated with \underline{A}_1 , \underline{A}_2 , \underline{A}_3 , and \underline{A}_4 , respectively. All terms in \underline{E} are independent of the mesh spacings.

Split \underline{D} according to

$$\underline{D} = \underline{D}_1 + \underline{D}_2. \quad (2.22)$$

Let \underline{D}_1 be that part of \underline{D} contained in \underline{A}_1 and \underline{A}_4 and \underline{D}_2 be that part which is contained in \underline{A}_2 and \underline{A}_3 . To complete the proof of stability,

it is necessary to restrict the splitting of \underline{D} such that

$$\underline{D}_1 + \underline{D}_1^T \text{ and } \underline{D}_2 + \underline{D}_2^T \text{ are negative definite.}^1 \quad (2.23)$$

As will be seen later, this is not a serious limitation.

From the proof for consistency, it was required that the ratios $h/\Delta x^2$, $h/\Delta y^2$, and $h/\Delta z^2$ be fixed, real constants. Here, those constants are defined as

$$h/\Delta x^2 = \sigma_1 \quad (2.24a)$$

$$h/\Delta y^2 = \sigma_2 \quad (2.24b)$$

$$h/\Delta z^2 = \sigma_3. \quad (2.24c)$$

The proof for stability examines the case where both the spatial and temporal meshes are taken to zero together. The class of problems where the spatial mesh is fixed and only the temporal mesh is taken to zero is unimportant, because almost any method is stable if h is taken sufficiently small with a given spatial mesh. It is shown that the difference approximation is stable under the conditions of Eqs. (2.24) with σ_1 , σ_2 , and σ_3 arbitrary and thus is unconditionally stable.¹

A third condition imposed upon the proof for stability is that all elements in \underline{A} and $\underline{\Omega}$ be held fixed in time. Thus, stability is shown only for each period of time over which this is true. In the algorithm finally used in numerical calculations in this thesis, $\underline{\Omega}$ is changed with each time step Δt . Additionally, elements of \underline{A} may also vary each step, such as during an insertion of reactivity. The much more difficult question of stability for this nonlinear procedure has not been analytically examined yet. Experimentally, however, stability problems

have not arisen over a series of sample problems in two- and three-dimensional geometries.

With the difference equations written in the form of Eq. (2.13), a sufficient condition for numerical stability²⁶ is that

$$\begin{aligned} \|\underline{B}(\underline{\Omega}, h)^N\| &\leq K, \quad K \text{ some constant,} \\ 0 \leq h &\leq \tau, \quad 0 \leq 2Nh \leq T. \end{aligned} \tag{2.25}$$

This implies that the computed solution will remain bounded as both spatial and temporal meshes are decreased in size so that more and more steps are required to reach a fixed total time T .

The proof of stability proceeds in several steps. A theorem due to Kreiss and Strang²⁶ motivates these steps.

THEOREM 2. If the difference system

$$\vec{U}^{N+1} = \underline{C}(\Delta t) \vec{U}^N$$

is stable, and if $\underline{Q}(\Delta t)$ is a bounded family of operators, then the difference system

$$\vec{U}^{N+1} = [\underline{C}(\Delta t) + \Delta t \underline{Q}(\Delta t)] \vec{U}^N$$

is stable.

It thus must first be shown that the operator $\underline{B}(\underline{\Omega}, h)$ can be written as

$$\underline{B}(\underline{\Omega}, h) = \underline{B}'(h) + h\underline{Q}(\underline{\Omega}, h). \tag{2.26}$$

If $\underline{B}'(h)$ can be shown to be stable and $\underline{Q}(\underline{\Omega}, h)$ bounded, then the stability of $\underline{B}(\underline{\Omega}, h)$ is assured.

With $\underline{C}_1(\underline{\Omega}, h)$ and $\underline{C}_2(\underline{\Omega}, h)$ defined as in Eqs. (2.20), $\underline{B}(\underline{\Omega}, h)$ is again factored as

$$\underline{B}(\underline{\Omega}, h) = \underline{C}_1(\underline{\Omega}, h)\underline{C}_2(\underline{\Omega}, h).$$

The matrix $\underline{C}_1(\underline{\Omega}, h)$ can be factored as

$$\begin{aligned} \underline{C}_1(\underline{\Omega}, h) &= [\underline{I} + h\underline{\Omega} + O(h^2)] [\underline{I} - h(\underline{I} - h\underline{D}_1)]^{-1} (\underline{E}_4 - \alpha \underline{\Omega})^{-1} \cdot \\ &\quad \cdot [\underline{I} - h\underline{D}_1]^{-1} [\underline{I} + h(\underline{D}_2 + \underline{E}_3 - \gamma \underline{\Omega})] \\ &= [\underline{I} + h\underline{\Omega} + O(h^2)] [\underline{I} + h(\underline{I} - h\underline{D}_1)]^{-1} (\underline{E}_4 - \alpha \underline{\Omega}) + O(h^2) \cdot \\ &\quad \cdot [\underline{I} - h\underline{D}_1]^{-1} [\underline{I} + h(\underline{D}_2 + \underline{E}_3 - \gamma \underline{\Omega})]. \end{aligned}$$

Finally,

$$\underline{C}_1(\underline{\Omega}, h) = [\underline{I} - h\underline{D}_1]^{-1} [\underline{I} + h\underline{D}_2] + h\underline{Q}_1(\underline{\Omega}, h). \quad (2.27)$$

Similarly, $\underline{C}_2(\underline{\Omega}, h)$ can be written as

$$\underline{C}_2(\underline{\Omega}, h) = [\underline{I} - h\underline{D}_2]^{-1} [\underline{I} + h\underline{D}_1] + h\underline{Q}_2(\underline{\Omega}, h). \quad (2.28)$$

Combining Eqs. (2.27) and (2.28) gives

$$\underline{B}(\underline{\Omega}, h) = [\underline{I} - h\underline{D}_1]^{-1} [\underline{I} + h\underline{D}_2] [\underline{I} - h\underline{D}_2]^{-1} [\underline{I} + h\underline{D}_1] + h\underline{Q}(\underline{\Omega}, h), \quad (2.29)$$

so that the matrix $\underline{B}'(h)$ in Eq. (2.26) is defined as

$$\underline{B}'(h) = [\underline{I} - h\underline{D}_1]^{-1} [\underline{I} + h\underline{D}_2] [\underline{I} - h\underline{D}_2]^{-1} [\underline{I} + h\underline{D}_1]. \quad (2.30)$$

Proving the boundedness in the various matrices in $\underline{Q}(\underline{\Omega}, h)$ requires careful analysis. This is because the number of mesh points and, hence, the order of these matrices approach infinity as h is taken toward zero. Theorem 3,¹ the proof of which is given in Appendix B, resolves this issue.

THEOREM 3. A family of matrices \underline{M}_n of varying dimension n having at most $\ell < n$ nonzero elements in each row or column, ℓ being

constant for all n , has a uniform L_2 bound if the individual elements of the matrices \underline{M}_n are uniformly bounded for all n .

All elements in \underline{E} and, hence, in \underline{E}_1 , \underline{E}_2 , \underline{E}_3 , and \underline{E}_4 are independent of the mesh spacings. Thus they are uniformly bounded. The number of nonzero elements in each row of \underline{E} is less than or equal to the number of prompt and delayed neutron groups. Thus, \underline{E}_1 , \underline{E}_2 , \underline{E}_3 , and \underline{E}_4 have uniform L_2 bounds.

The matrix $h\underline{D}$ has at most seven nonzero elements in each row (nine for a hexagonal-z mesh configuration). Providing the conditions given in Eqs. (2.24) are obeyed, the magnitudes of its elements are fixed as h tends toward zero. Thus the L_2 norm of $h\underline{D}$ is bounded for all h . This also assures that $(\underline{I}+h\underline{D}_1)$ and $(\underline{I}+h\underline{D}_2)$ are bounded.

The boundedness of $(\underline{I}-h\underline{D}_1)^{-1}$ and $(\underline{I}-h\underline{D}_2)^{-1}$ is given by Theorem 4, which is proved in Appendix B.

THEOREM 4. The matrices $(\underline{I}-h\underline{R})^{-1}$ and $(\underline{I}+h\underline{R})(\underline{I}-h\underline{R})^{-1}$ have L_2 norms of less than unity provided that $(\underline{R}+\underline{R}^T)$ is negative definite.

All matrices which form the matrix $\underline{Q}(\underline{\Omega}, h)$, as given in Eq. (2.29), have been shown to be bounded. Thus $\underline{Q}(\underline{\Omega}, h)$ is bounded as h tends toward zero. It remains only to show that $\underline{B}'(h)$ is stable. This can be done by factoring it in the form:¹

$$\underline{B}'(h) = \underline{R}_1 \underline{R}_2 \underline{R}_3,$$

where

$$\underline{R}_1 = (\underline{I}-h\underline{D}_1)^{-1}$$

$$\underline{R}_2 = (\underline{I}+h\underline{D}_2)(\underline{I}-h\underline{D}_2)^{-1}$$

$$\underline{R}_3 = (\underline{I}+h\underline{D}_1).$$

By Theorem 4, $\|\underline{R}_2\| < 1$ and $\|\underline{R}_3\underline{R}_1\| < 1$. Writing $[\underline{B}'(h)]^N$ in terms of the above factorization,

$$\underline{B}'^N(h) = \underline{R}_1\underline{R}_2\underline{R}_3 \quad \underline{R}_1\underline{R}_2\underline{R}_3 \quad \dots \quad \underline{R}_1\underline{R}_2\underline{R}_3 \quad (\text{N times}).$$

Thus,

$$\begin{aligned} \|\underline{B}'^N(h)\| &\leq \|\underline{R}_1\| \cdot \|\underline{R}_2\| \cdot \|\underline{R}_3\underline{R}_1\| \cdot \|\underline{R}_2\| \cdot \|\underline{R}_3\underline{R}_1\| \cdot \dots \cdot \|\underline{R}_2\| \cdot \|\underline{R}_3\|, \\ \|\underline{B}'^N(h)\| &< \|\underline{R}_1\| \cdot \|\underline{R}_3\|. \end{aligned}$$

Again, \underline{R}_1 has a bounded norm by Theorem 4 and \underline{R}_3 has a bounded norm by Theorem 3, both for $0 < h < \tau$. Thus, $\|\underline{B}'^N(h)\|$ is bounded for $0 < h < \tau$ and $0 < 2Nh < T$ and is stable. Finally, from this fact and Theorem 2, $\underline{B}(\underline{\Omega}, h)$ is seen to be stable. Since no restrictions have been placed on the size of σ_1 , σ_2 , and σ_3 in Eqs. (2.24), except that they be real and finite, this stability is unconditional.

Property 5. Asymptotic Behavior

Because of the form of the exponential transformation, the difference method proposed here can be forced to yield the correct asymptotic behavior. The asymptotic behavior of the exact solution is given by Theorem 5,²⁴ which is proved in Appendix B.

THEOREM 5. As t approaches infinity, the solution vector $\vec{\psi}(t) = e^{(\underline{A}t)}\vec{\psi}_0$ approaches $\alpha e^{\omega_0 t} \vec{e}_0$, where ω_0 is the largest eigenvalue of \underline{A} , \vec{e}_0 the corresponding eigenvector, and $\alpha = (\vec{\psi}_0, \vec{e}_0)$.

Theorem 6² gives the largest eigenvalue and corresponding eigenvector of $\underline{B}(\underline{\Omega}, h)$ under the assumption that $\underline{\Omega} = \omega_0 \underline{I}$. It is also proved in Appendix B.

THEOREM 6. If $\underline{\Omega} = \omega_0 \underline{I}$, the approximate solution operator $\underline{B}(\underline{\Omega}, h)$ has as its largest eigenvalue $e^{2\omega_0 h}$, with corresponding eigenvalue \vec{e}_0 , where $\underline{A} \vec{e}_0 = \omega_0 \vec{e}_0$.

If, at asymptotic times, the matrix $\underline{\Omega}$ were set equal to $\omega_0 \underline{I}$, the action of $\underline{B}(\underline{\Omega}, h)$ on the asymptotic solution would ultimately yield the exact growth of $e^{2h\omega_0}$ over the time step $2h$.

2.5 Specific Splittings for Two Dimensions

Up to this point, the splitting of \underline{A} into \underline{D} and \underline{E} and these into \underline{D}_1 and \underline{D}_2 and \underline{E}_1 , \underline{E}_2 , \underline{E}_3 , and \underline{E}_4 , respectively, has been very general. Specific splittings must be indicated before proceeding to numerical calculations. Any splitting proposed must obey Condition (2.23) in addition to offering relative computational ease.

Four specific splittings are presented for study in this section. Two of these have been extensively tested previous to this work, the Non-Symmetric Alternating-Direction Explicit (hereafter referred to as NSADE) method in Refs. 1 and 2 and the Symmetric Alternating-Direction Implicit (SADI) method in Refs. 23 and 24. This testing was carried out in two spatial dimensions. The NSADE method has been shown to handle a wide variety of test problems successfully, while the SADI method required unreasonably small time steps to treat a difficult asymmetric problem. The four splittings proposed here for further two-dimensional studies are motivated by a desire to understand what has caused the difference in performance of these two methods and to arrive at an "optimum" splitting.

The terminology used above deserves clarification. The "Symmetric" and "Non-Symmetric" have been prefixed to the names originally given to these methods to indicate the placement of the matrices \underline{U} and \underline{L} in the two splittings of \underline{A} . A method is termed symmetric if the matrix \underline{L} is treated implicitly over the first half-step and \underline{U} implicitly over the second half-step. If \underline{L} is treated implicitly over both half-steps, the method is called non-symmetric. If the two-dimensional spatial mesh is swept solving for the new fluxes point by point, the method is termed explicit. It is termed implicit if a whole row or column of points is solved simultaneously for new fluxes.

SADI Method. For this method, let

$$\begin{aligned}\alpha &= \gamma = 0.5 \\ \underline{A}_1 &= \frac{1}{2} \underline{T} + \underline{U} + \underline{D}_1 = \underline{A}_4 \\ \underline{A}_2 &= \frac{1}{2} \underline{T} + \underline{L} + \underline{D}_2 = \underline{A}_3,\end{aligned}\tag{2.31}$$

where \underline{D}_1 is composed of the terms associated with diffusion in one direction and one-half of each term in the submatrices $\underline{\Lambda}_i$. The matrix \underline{D}_2 is composed of the diffusion terms for the other direction and the remaining half of each term in the $\underline{\Lambda}_i$. As discussed under Property 2, this splitting agrees with the Taylor series expansion of the exact solution operator through terms of order h^2 .

NSADI Method. Here let

$$\begin{aligned}
 \alpha &= 1.0, \quad \gamma = 0, \\
 \underline{A}_1 &= \underline{U} + \underline{D}_1 \\
 \underline{A}_2 &= \underline{T} + \underline{L} + \underline{D}_2 \\
 \underline{A}_3 &= \underline{U} + \underline{D}_2 \\
 \underline{A}_4 &= \underline{T} + \underline{L} + \underline{D}_1,
 \end{aligned} \tag{2.32}$$

where \underline{D}_1 and \underline{D}_2 are as defined above. By defining the truncation error over one step as

$$\text{T.E.} = e^{2h\underline{A}} - \underline{B}(\underline{\Omega}, h), \tag{2.33}$$

the NSADI method has a truncation error of

$$\text{T.E.} = h^2(\underline{T} + \underline{L} - \underline{U} - \underline{\Omega})(\underline{A} - \underline{\Omega}) + O(h^3).$$

SADE Method. Let

$$\begin{aligned}
 \alpha &= \gamma = 0.5, \\
 \underline{A}_1 &= \frac{1}{2} \underline{T} + \underline{U} + \underline{D}_1 = \underline{A}_4 \\
 \underline{A}_2 &= \frac{1}{2} \underline{T} + \underline{L} + \underline{D}_2 = \underline{A}_3,
 \end{aligned} \tag{2.34}$$

where \underline{D}_1 contains the two stripes of \underline{D} which lie above the diagonal plus one-half of each term on the diagonal and \underline{D}_2 contains the two stripes below the diagonal plus the remainder of each diagonal term. As with the SADI method, the truncation error for one time step is of order h^3 .

NSADE Method. Let

$$\begin{aligned}
 \alpha &= 1.0, \quad \gamma = 0, \\
 \underline{A}_1 &= \underline{U} + \underline{D}_1 \\
 \underline{A}_2 &= \underline{T} + \underline{L} + \underline{D}_2 \\
 \underline{A}_3 &= \underline{U} + \underline{D}_2 \\
 \underline{A}_4 &= \underline{T} + \underline{L} + \underline{D}_1,
 \end{aligned} \tag{2.35}$$

where \underline{D}_1 and \underline{D}_2 are as defined for the SADE method. Its truncation error is the same as that given for the NSADI method.

It can be seen that all four methods just presented satisfy the conditions for consistency and stability. The box integration technique used to derive the five-point finite difference relations in two dimensions guarantees that the diagonal term in each row of \underline{D} is just the negative of the sum of the other terms in that row. Both implicit and explicit splittings make the diagonal term in each row in both \underline{D}_1 and \underline{D}_2 the negative sum of the other two terms in that row. Thus, both \underline{D}_1 and \underline{D}_2 are diagonally dominant. Since

$$\underline{D}_1 + \underline{D}_1^T = \underline{D}_2 + \underline{D}_2^T = \underline{D}$$

for both splittings and \underline{D} is negative definite, the condition (2.23) is satisfied.

All four methods offer relative computational ease. The matrices to be inverted in the SADE and NSADE methods are always upper or lower triangular or can be made so by rearranging the order of the unknowns. The first half-step is carried out by forward substitution,

sweeping from one corner of the mesh to the diagonally-opposite corner and from the highest energy group to the lowest. The second half-step reverses the direction of the spatial sweep and also from the lowest energy group to the highest in the case of the SADE method.

For the SADI and NSADI methods, the matrices to be inverted are block lower or upper triangular, but the diagonal submatrices are tri-diagonal. In sweeping from one corner of the mesh to the diagonally opposite corner, entire lines of fluxes in one of the two directions must be solved simultaneously by the rapid forward elimination, backward substitution process. In working back across the mesh during the second half-step, lines of fluxes in the second direction are solved simultaneously. For the NSADI method, the groups are solved from the highest to the lowest energy over both half-steps, while the order is reversed for the second half-step of the SADI method.

This section is concluded with a discussion of the factors which could cause these four methods to perform differently on actual numerical experiments. The first difference apparent is the implicit versus explicit spatial treatment. From experience gained in static calculations, it is tempting to state that solving for an entire line of fluxes simultaneously should result in less total error than solving for the fluxes one by one. The analogy is not entirely appropriate, however, since the kinetics problem is an initial-value problem and not a boundary-value problem. Considering the two sweeps of the mesh together, new fluxes at each of the five points in two-dimensional problems are given half of the weighting and old fluxes the other half for both types of methods.

There does appear to be a difference in the spatial distribution of the errors for the two spatial treatments. No analytical examination of error distribution and propagation has yet been completed. Qualitatively, however, experience seems to indicate that the implicit treatment is somewhat more stable with respect to propagation of errors.

For illustrative purposes, consider the first time step, Δt , in a two group homogeneous problem, where the initial condition $\vec{\psi}_0$ is taken to be exact. Let the perturbation be due to uniform step decreases in the absorption cross sections of both groups over the entire system.

Both the implicit and explicit methods are inexact so that some error is introduced into the new group one flux as it is calculated at each mesh point over the first half-step. This error is distributed differently for the two methods, however. In the implicit treatment, each line of fluxes is computed simultaneously, using the old fluxes on each side of it to compute the leakage in the direction perpendicular to that line. Thus, the error in the growth is distributed along the entire line. The new fluxes in other lines see none of the error introduced in that line. At the end of the mesh sweep for group one, it is easily shown that the error at each mesh point is proportional to the initial flux value at that point for this model problem.

The group two fluxes at the end of the first half-step likewise contain an error component which has the same spatial distribution as the initial fundamental mode solution. Part of the error at each point is due to error in the group one flux previously computed, and part is

due to inexact treatment of the growth of group two given the group one flux.

At the end of the second half-step, additional errors have been introduced into both group fluxes at each mesh point. However, the errors still have a fundamental mode distribution for both groups. No spatial flux tiltings have been introduced by the implicit spatial treatment.

This is not the case with the explicit spatial treatment. As group one fluxes are computed one by one over the first mesh sweep, the error introduced at a point due to the inexact operator is carried on across to the computation of all subsequent mesh points. At the end of the first sweep for group one, the spatial distribution is tilted so that the last point calculated has grown proportionately more than any point previously computed.

If this were a one group problem, the tilting would be erased as the sweep is reversed over the second half-step. In the two group problem, however, the second group must first be calculated. The second group now sees a tilted source and is tilted proportionately worse at the end of the first mesh sweep.

This tilted second group is used in computing the source for the reverse mesh sweep for group one. It is difficult to predict exactly how the group one flux will be distributed at the end of the reverse sweep since that depends on the reactor size and composition and the magnitude of the initial perturbation. However, it would be strictly fortuitous if the errors in the group one flux have a fundamental mode distribution. The first mesh sweeps for the two groups have introduced

higher error modes which tend to persist in the solution, although the stability proof in section 2.4 gives assurance that they will not grow without bound for the case of constant $\underline{\Omega}$ and reactor properties.

The really important question is to what degree does the introduction of these higher error modes affect the solution of real problems. In actual practice, it has been found that for realistic perturbations and time step sizes, these higher modes do not severely affect the solution. In addition, the exponential transformation tends to damp out these higher modes, as is shown in the numerical results given in Chapter 3.

There is one situation, however, in which this accumulation of errors can severely hamper the explicit methods. If the initial condition $\vec{\psi}_0$ used to start the transient differs sufficiently from the true fundamental mode initial condition, the presence of these additional errors can affect a sufficient accumulation of error to swamp the true solution.

It should be noted that a fully explicit method cannot properly treat the fluxes at an outer boundary where a zero current normal to that boundary has been specified. This problem was noted in the initial work done in extending the NSADE method to r-z geometry,¹⁹ where the z-axis is always a so-called symmetry boundary. It is easily solved, however, by solving for new fluxes at each point on such a boundary and the interior point closest to it simultaneously for whichever of the two half-steps originates from that boundary.

A second difference to be noted in the methods is the symmetric versus non-symmetric sweeping of the energy groups. Favoring the

symmetric methods is the fact that terms of order h^2 in the truncation error expression vanish for these splittings. On the other hand, most thermal reactor models have group structures which are closely coupled by down-scattering from each group to the next lowest, but are only loosely coupled by the upward flow of neutrons. This is because the higher energy groups have relatively small fission cross sections, while the fission spectrum is nonzero only in the highest groups. During a sweep of the energy mesh from the lowest energy group to the highest group, a perturbation in the thermal group can cause a change only in the high energy groups with nonzero fission fractions during the remainder of that sweep. In a two group thermal reactor problem, this effect should be minimal. With four or more groups, this effect could become important. This effect should also be minimized in a fast reactor problem, where the fission cross section is fairly constant over most of the groups, and the fission spectrum is nonzero over most of the groups.

The concept of truncation error accumulation is complicated by the presence of the exponential transformation. It is generally stated that the total error at time $T=2Nh$ varies as a function of one order less of h than does the local truncation error. The correct asymptotic behavior resulting from the exponential transformation should tend to lessen the severity of error accumulation, however.

2.6 A Proposed Method for Three Dimensions: NSADE

It is the stated purpose of this thesis to develop an alternating-direction semi-implicit method for solving the space-dependent kinetics equations in three-dimensional geometries. The method so proposed is the NSADE (Non-Symmetric Alternating-Direction Explicit) method as outlined in section 2.5. The splitting of the \underline{A} matrix for three dimensions is identical to that presented in Eq. (2.35) for two dimensions. However, \underline{D}_1 now has three nonzero stripes above the diagonal and \underline{D}_2 has three nonzero stripes below it. Because the \underline{L} matrix is treated implicitly over both half-steps, the groups are always to be solved from the highest energy group to the lowest. The spatial sweep starts in one corner of the three-dimensional mesh and works toward the diagonally-opposite corner during the first half-step. It is then exactly reversed for the second half-step.

This particular method has been chosen for three reasons. Based on a number of test problems in one and two dimensions, it is shown in Chapter 3 that the non-symmetric splittings perform far more satisfactorily in thermal reactor problems. Secondly, the NSADI and NSADE methods are shown to perform practically identically over a range of problems. Finally, in addition to being computationally slightly faster, the NSADE method is directly applicable to three-dimensional geometries as a two-step method. Only two dimensions could be treated implicitly if an implicit method as outlined in section 2.5 were to be applied to three-dimensional geometries as a two-step method.

Chapter 3

NUMERICAL RESULTS

Four different members of a general class of alternating-direction semi-implicit methods for solution of the semi-discrete reactor kinetics equations have been proposed in section 2.5 for further study in one- and two-dimensional geometries. The results of several numerical experiments, where these methods have been used to solve reactor problems, are presented and compared in section 3.1 of this chapter. In section 3.2, the behavior of the NSADE method when solving a three-dimensional model problem is compared to the exact solution of this problem. Finally, section 3.3 presents the results of a number of true space-dependent, three-dimensional numerical experiments with the NSADE method.

3.1 One- and Two-Dimensional Studies

Two of the four specific methods that are presented in section 2.5 have been extensively tested previous to this thesis. The NSADE method has been shown to perform satisfactorily over a range of problems in x-y, r-z, and hexagonal geometries.^{1,19} In contrast, the SADI method has been shown to perform poorly in a space-dependent, four group thermal reactor problem.²³ The numerical experiments presented in this section have been performed in an effort to explain the difference in behavior of these two methods.

Four different test cases are examined in this section. They have been chosen in an attempt to compare the methods over a wide range of problem types. The first three cases are in one-dimensional slab geometry, while the fourth is the two-dimensional rectangular multi-region thermal reactor which the SADI method had difficulty in treating.

In order to solve the one-dimensional problems, the computational subroutines of an existing one-dimensional code, GAKIN,¹⁴ were replaced with a single subroutine which, depending on several input parameters, treated problems with one of the four methods. Since one-dimensional problems have diffusion on one direction only, the diffusion terms in that direction were halved, with one-half of each term in the matrix \underline{D} being treated as diffusion in one dimension and the other half as diffusion in a second dimension. For the two-dimensional case, subroutines were added to the code MITKIN¹ so that it had multi-method capabilities.

Both because it is the primary purpose of this thesis to deal with multi-dimensional geometries and because the one-dimensional problems treated for this thesis are relatively simplistic, the three one-dimensional problems are discussed here in a qualitative fashion only. The numerical results are not presented in either tabular or graphical form.

The first one-dimensional problem was a homogeneous thermal slab reactor with four neutron groups and one precursor group. The critical configuration was perturbed by a fifty-cent step insertion of reactivity caused by uniformly decreasing the thermal group capture cross section. Twenty-one mesh points were used to represent the

146-cm slab. Because of the homogeneous composition, the initial flux distribution in each group was cosinusoidal in shape. The exact solution to the time-dependent problem was obtained using an eigenvector expansion technique² and was available for comparison.

Using a time step, Δt , of .0005 sec, both the SADI and SADE methods underestimated the solution throughout the transient. At 1.0 seconds into the transient, both solutions were about 15 % too low. With $\Delta t = .00025$ sec, both methods gave considerably better results, but were still about 1% low at 1.0 sec. Only when Δt was reduced to .0001 sec did the SADI method give the correct result ($< .1\%$ error) throughout the transient. The SADE method was not used at this small time step since it was expected that it would again behave similarly to the SADI method.

In contrast, both the NSADE and NSADI methods gave good results ($< .1\%$ error) for time steps as large as $\Delta t = .001$ sec out to about 0.2 sec into the transient. At around 0.2 sec, however, both methods were overcome by stability problems for time steps of .001 and .0005 sec. The instabilities seemed to result from the feedback of accumulated errors through the frequencies. These instabilities first appeared as a small ripple-like component superimposed on the true solution, but soon grew to the point that negative fluxes resulted.

The characteristic which separated the four methods into two distinct classes is the property which has been termed symmetry. The symmetric methods behaved in one fashion, while the non-symmetric methods behaved in another and different fashion.

These results shed light on several of the conjectures made in section 2.5 about these methods. The group structure for this four group problem was loosely-coupled by the upward flow of neutrons, thus causing the symmetric methods to underpredict the growth of the fluxes at time steps reasonable for this problem. This tendency to underpredict can also be explained from an analytic point of view. In the limit of large h , the advancement matrix goes to the identity matrix for the symmetric methods. For any finite time step, the symmetric methods underpredict the growth over each time step. The feedback effect introduced by the method used to compute the frequencies may offset this to some extent, but the numerical experiment cited here indicates that it does not offset it completely. Once a sufficiently small time step is used, however, these methods converge rapidly to the correct solution.

The non-symmetric methods, even though they have a local truncation error of only order h^2 , followed the solution closely for much large time steps. Physically, this smaller error at each step was the result of sweeping down through the groups at both half steps, taking advantage of the tightly-coupled downward flow of neutrons. The instabilities observed prove that these methods can also become unstable due to the feedback effect of the frequencies. Fortunately, these instabilities have never been noted in problems in two or three dimensions or in one-dimensional problems with a large number of mesh points.

The second one-dimensional problem was a homogenized slab unit cell, 10 cm in width, from a fast gas-cooled reactor with ten neutron

groups and four precursor groups. The initial flux distribution was flat for all groups. The critical configuration was perturbed by a step reduction in the capture cross sections in all groups.

Only the two implicit methods could be used to treat this problem because the explicit options were not programmed to handle homogeneous Neumann boundary conditions. The SADI method followed the transient accurately for as long as the solution was carried out, although relatively small time steps had to be taken. Physically, this problem was better suited to the symmetric techniques because the fission cross section was fairly constant over most of the groups, and the fission spectrum was nonzero over most of the groups. Thus, even though there was no upscattering in this problem, a perturbation could propagate in an upward sweep of the groups as well as in a downward sweep.

The NSADI method followed the early part of the transient as well as did the SADI method, using the same time step sizes. However, at about .0005 seconds into the transient, instabilities again appeared and soon swamped the true solution. A close examination reveals one reason why these non-symmetric methods should be more susceptible to these feedback-induced instabilities. Unlike the symmetric methods, the non-symmetric methods have advancement matrices which do not reduce to the identity matrix in the limit of large time steps. Depending on the problem and the flux vector at a particular time, they can underestimate or overestimate the flux at the end of the next time step. Add to this the feedback effect of the method used to compute the frequencies, and it becomes possible for these oscillations to grow

large. Again it is stressed that these instabilities have been observed only in one-dimensional problems with a relatively small number of spatial mesh points.

The last one-dimensional problem used to compare these four methods was a 240-cm, three-region thermal slab reactor with two neutron groups and six precursor groups. An inner zone, 160 cm thick, of relatively low enrichment, was surrounded on either side with a 40-cm-thick slab of higher enrichment. Ninety-seven equally-spaced mesh points were used. The critical configuration was perturbed by linearly decreasing the thermal capture cross section by 1% over 1.0 second in one of the two outer slabs.

The composition of this test problem was similar to a graphite slab reactor, so that a relatively large time step, Δt , of .0025 second was used. Both the NSADI and NSADE methods followed the transient out to 1.0 second with little error and with no sign of any instabilities. As in the first test case, the SADI and SADE methods initially underestimated the growth in the solution. However, they both improved considerably by the end of the transient.

For two-group problems such as this, the two groups are tightly coupled by both the upward and downward flow of neutrons. This apparently minimized the difference in performance between the symmetric and non-symmetric methods for this problem. Again, the method used to sweep the spatial mesh made little difference in the results.

The final numerical experiment discussed in this section is a highly-asymmetric, two-dimensional problem with four neutron groups

and one delayed precursor group. This problem has been discussed in two previous works,^{1,23} but it is included here because it again demonstrates the validity of the arguments presented in section 2.5.

The geometry for this problem was identical to that of any plane perpendicular to the z-axis taken between z mesh planes 8 and 17 of Configuration 3, found in Appendix C. The material constants for the four materials were also identical to those shown in Configuration 3, except that the critical value of ν for all groups was 1.450679 for the two-dimensional problem. The critical configuration was perturbed by linearly decreasing the group four capture cross section in material 4 by 0.003 cm^{-1} over 0.2 second. From that time, all material properties were held fixed.

Tables 3.1, 3.2, 3.3, and 3.4 list the group one and group four fluxes at two points in the reactor for various times in the transient. The results for the SADI method have been taken from Ref. 24, while the NSADE results represent improved results (more accurate initial flux distribution) of those quoted in Ref. 1.

The NSADE and NSADI methods gave practically identical results for the results shown, with $\Delta t = .001$ sec. Results using the NSADE method and time steps of .0005 sec and .002 sec gave similar results to those listed here, so it is assumed that the results for the two non-symmetric methods represent converged solutions. In contrast, the SADI method gave inconsistent results for time steps as small as .00025 sec and was still nearly 6% in error at 0.3 sec into the transient with a $\Delta t = .000125$ sec.

This problem represented a severe test of these methods because of the large changes in the spatial shape and energy spectrum induced by the perturbation. The results shown here again confirm that the method used to sweep the spatial mesh makes little difference in the final result. For thermal reactors, the critical factor is that the groups be swept from high energy to low energy over both half steps. The non-symmetric methods are thus preferred for any scheme which is to have general applicability.

Table 3.1. Group 1 Fluxes at Point (3, 9)

Time (sec)	$\Delta t =$	NSADE	NSADI	SADI		
		.001	.001	.000125	.0005	.001
.0		.4463	.4463	.4463	.4463	.4463
.05		.4561	.4559	.4525	.4463	.4463
.10		.4670	.4669	.4781	.4464	.4463
.15		.4796	.4795	.4985	—	.4463
.20		.4943	.4944	.5064	.4624	.4463
.30		.4945	.4946	.5194	.4624	.4465

Table 3.2. Group 1 Fluxes at Point (12, 3)

Time (sec)	$\Delta t =$	NSADE	NSADI	SADI		
		.001	.001	.000125	.0005	.001
.0		.1341	.1341	.1341	.1341	.1341
.05		.1383	.1383	.1375	.1346	.1342
.10		.1431	.1430	.1473	.1371	.1346
.15		.1485	.1485	.1554	—	.1359
.20		.1549	.1549	.1604	.1413	.1382
.30		.1549	.1550	.1640	.1489	.1438

Table 3.3. Group 4 Fluxes at Point (3, 9)

Time (sec)	$\Delta t =$	NSADE	NSADI	SADI		
		.001	.001	.000125	.0005	.001
.0		.0359	.0359	.0359	.0359	.0359
.05		.0367	.0367	.0364	.0359	.0359
.10		.0376	.0376	.0385	.0360	.0359
.15		.0386	.0386	.0401	—	.0359
.20		.0398	.0398	.0408	.0361	.0359
.30		.0398	.0398	.0418	.0373	.0360

Table 3.4. Group 4 Fluxes at Point (12, 3)

Time (sec)	$\Delta t =$	NSADE	NSADI	SADI		
		.001	.001	.000125	.0005	.001
.0		.9684	.9684	.9684	.9684	.9684
.05		1.0532	1.0528	1.0474	1.0255	1.0223
.10		1.1513	1.1510	1.1855	1.1006	1.0873
.15		1.2669	1.2668	1.3278	—	1.1614
.20		1.4051	1.4051	1.4565	1.2914	1.2498
.30		1.4060	1.4064	1.4920	1.3498	1.2889

3.2 Three-Dimensional Studies: Homogeneous Problem

As stated in section 2.6, the NSADE method has been chosen as the method to be extended to treat three-dimensional geometries. Four numerical experiments have been designed to test this method. The geometries and compositions for these experiments are presented in Appendix C. The results from the first of these, the only homogeneous problem, are presented in this section. All of the numerical results from three-dimensional experiments have been obtained from

a computer code called 3DKIN, which is discussed in Appendices D and E.

Again, it must be stressed that the truncation error discussed in this chapter is the difference between the particular solution under consideration and the exact solution of the semi-discrete equations. In the case of the homogeneous problem, the exact solution can be generated using an eigenvector expansion technique.² The exact solutions cannot be obtained for the other three-dimensional problems. Thus it is assumed that if two successive solutions are generated, one using a time step half of the size of that used to generate the other, and are in good agreement, then the solution generated with the smaller time step represents a "converged" solution.

TEST CASE 1

Geometry and Composition: Configuration 1

Perturbation: Step change, $\Delta\Sigma_a(\text{group 2}) = -.369 \times 10^{-4}$

This case is a bare, homogeneous cube, 200 cm on a side, with two neutron groups and one precursor group. Ten mesh intervals were used in each direction, and the boundary conditions were homogeneous Dirichlet on all six sides. The perturbation consisted of a uniform step decrease in the thermal group absorption cross section and had a reactivity worth of about 50 cents. Since the geometry is symmetric about the mid-plane in the x-direction, only the right half of the reactor was actually used in the 3DKIN computer runs. It was determined that the half-core and full-core results compared through six significant figures for two different time step sizes.

The results of 3DKIN runs using four different time step sizes at various times in the transient are shown in Table 3.5. The values presented are the thermal group fluxes at the center point of the reactor.

Table 3.5. Test Case 1 Results, Group Two Fluxes at Centerpoint

Time (sec)	$\Delta t =$	3DKIN				EXACT
		.01	.005	.002	.001	
.0		.816	.816	.816	.816	.816
.05		.920	1.043	1.116	1.124	1.127
.10		1.151	1.361	1.403	1.406	1.407
.15		1.454	1.651	1.660	1.660	1.660
.20		1.782	1.904	1.892	1.890	1.890
.30		2.388	2.328	2.294	2.289	2.288
.40		2.840	2.671	2.628	2.622	2.620

Table 3.5 demonstrates the rapid convergence of the NSADE method with the exponential transformation. With a time step of .002 sec, the solution was only .3% in error at .4 second, during which time the thermal flux had more than tripled. That this convergence is approximately of order h^2 is displayed in Fig. 3.1, where the percentage truncation error is plotted as a function of h at 0.4 second into the transient.

The results that are tabulated in Table 3.5 are presented in graphical form in Fig. 3.2 to illustrate an interesting characteristic of this exponentially-transformed method. The semi-discrete equations are a coupled set of first-order differential equations. As such, any change in $\vec{\psi}$ at time t depends only on the values of $\vec{\psi}$ and \underline{A} at that time

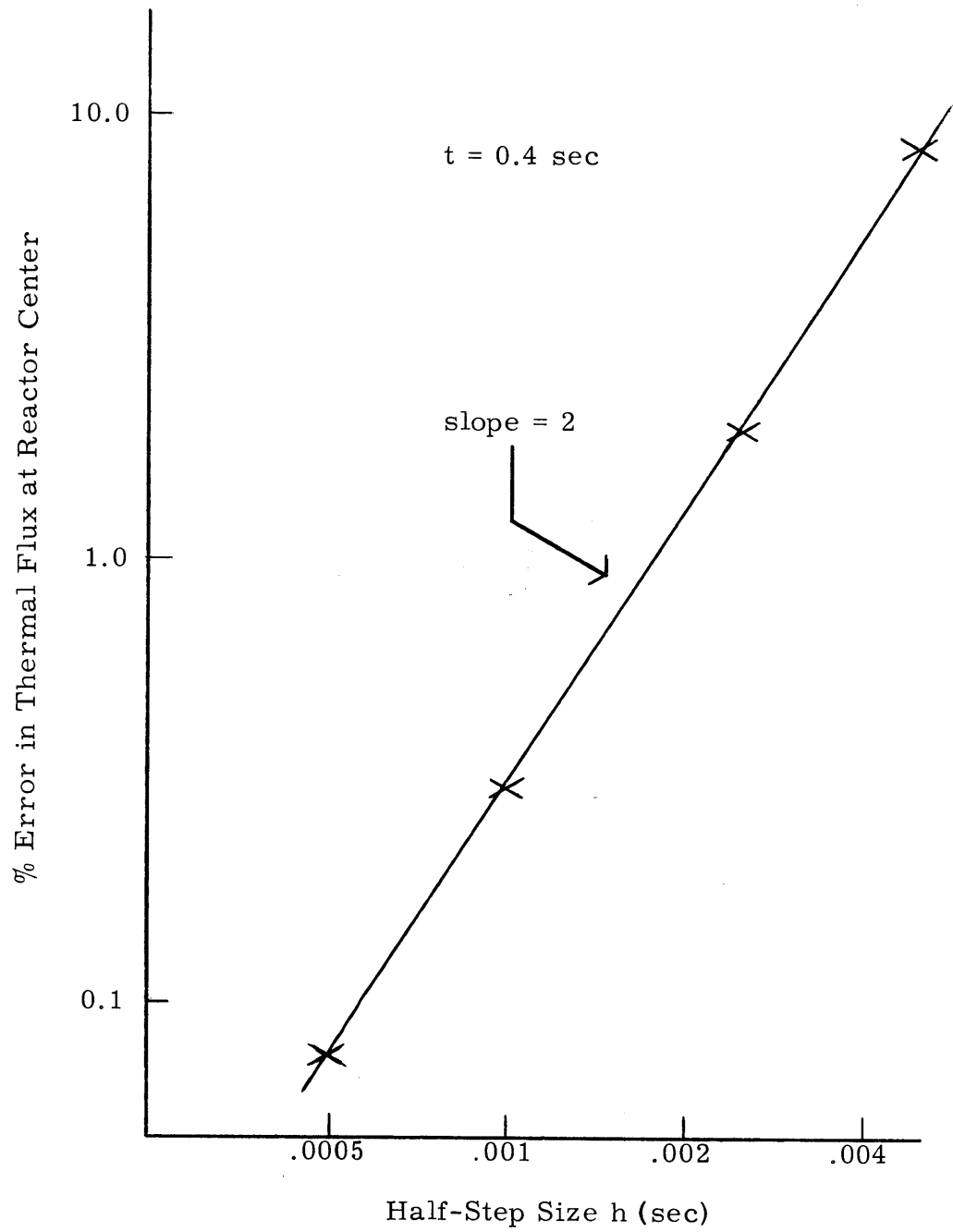


Fig. 3.1. Convergence Rate for Test Case 1

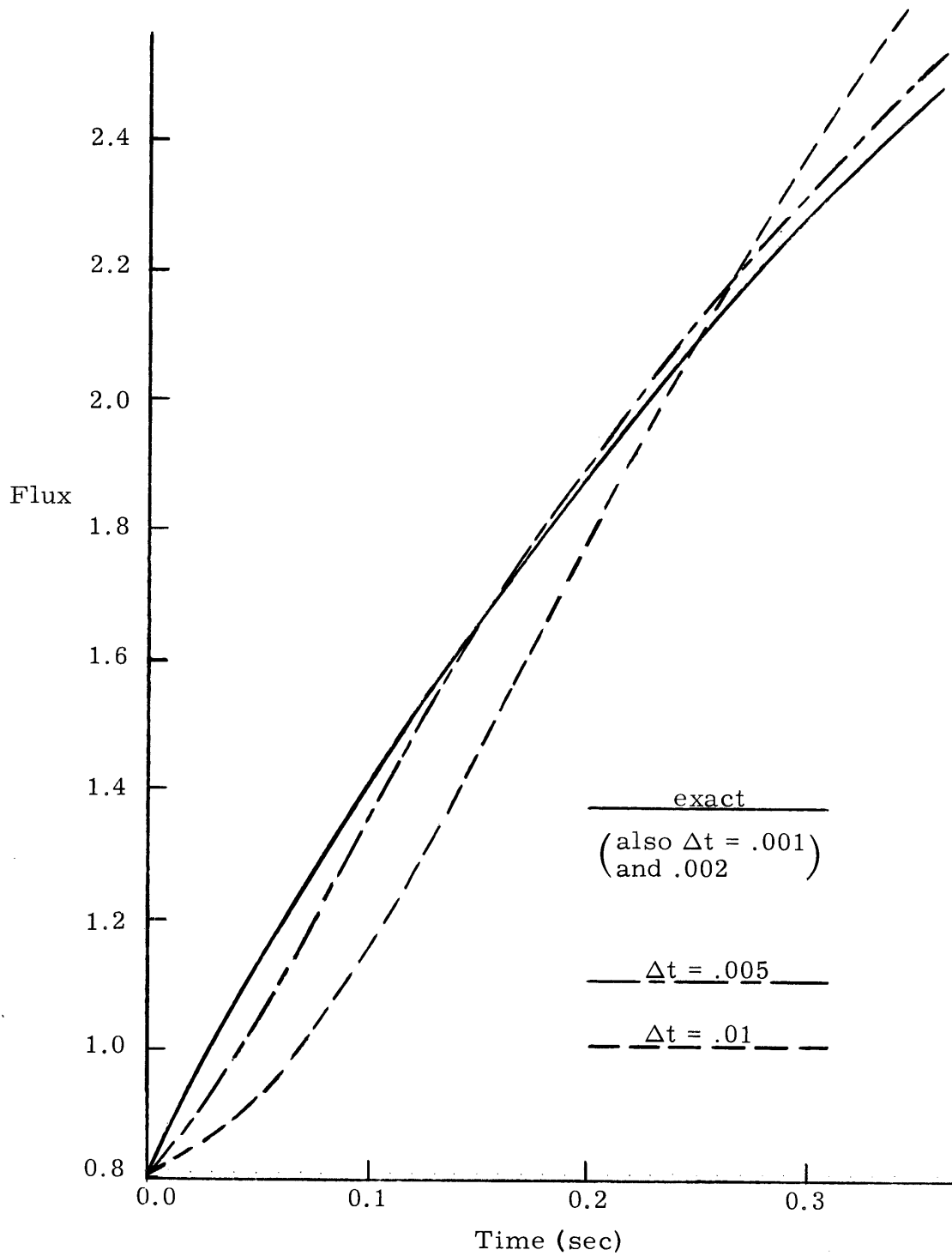


Fig. 3.2. Test Case 1 Results, Centerline Thermal Flux

and not on the past history of the system. By adding the exponential transformation and computing $\underline{\Omega}$ to be used at t_N based on the change in the solution between t_{N-1} and t_N , the behavior of the solution at t_N has been coupled to its rate of change. The system now behaves in the fashion of a second order system in that it builds up "inertia" during a transient. Figure 3.2 clearly displays the damped sinusoidal oscillations superimposed on the true solution which are characteristic of such a system. The amplitude of the "overshoot" is clearly a function of h and decreases as order h^2 .

When material properties are constant or changing in a smooth fashion, this "inertia" enables the time step to be increased without affecting the accuracy seriously. However, when properties or their rates of change are abruptly changed, such as at the end of a ramp insertion of reactivity, time step sizes must be decreased in order to overcome the "inertia."

3.3 Three-Dimensional Studies: Space-Dependent Problems

The three test cases presented in this section are all spatially-dependent problems. Test Cases 2 and 3 are three-dimensional versions of problems already used to test some or all of the methods discussed in section 2.5. Test Case 4 is a new problem, designed with the idea of simulating the withdrawal of a cluster of control rods from two adjacent subassemblies in a medium-sized pressurized-water power reactor. Taken together, these problems provide a stern test of the general applicability of the NSADE method.

TEST CASE 2

Geometry and Composition: Configuration 2

Perturbation: Ramp change, $\Delta\Sigma_a$ (material 1, group 2) = $-.0045(t/0.2)$
for $0 \leq t \leq 0.2$ sec

$\Delta\Sigma_a$ (material 1, group 2) = $-.0045$
for $t > 0.2$ sec

The original two-dimensional version of this problem has been used to test several two-dimensional solution methods.^{1, 23, 17, 15} The original plane was 160 cm square, with a central blanket area surrounded by a highly-enriched seed area. It was in turn surrounded by another blanket region. In three dimensions, this configuration was made 112 cm thick in the z-direction, and a blanket of 24 cm thickness added to the top and bottom. Thus, the overall reactor is cubical, 160 cm on a side. It has two neutron groups and one delayed precursor group.

The four regions containing material 1, each $32 \times 32 \times 124$ cm in size, which were perturbed are located symmetrically with respect to the central x-plane. Only the right half of the cube was considered, with a homogeneous Neumann boundary condition imposed at the exposed mid-plane to preserve symmetry. With 8.0-cm mesh spacings in each direction, a total of 4841 mesh points were needed to represent the half-reactor. The initial flux distribution and eigenvalue were computed with the steady state option of 3DKIN.

Test Case 2 was carried out to 0.3 second into the transient for time step sizes of .001 sec and .002 sec. The results of the 3DKIN runs

for these two time step sizes are presented in Tables 3.6, 3.7, and 3.8. The values tabulated are the thermal flux values. The z-planes 3 and 19 are 8 cm below and above the core, respectively, while z-plane 11 is the central z-plane. Point (6, 6, z) is on the central z-axis of one of the perturbed regions. Values at points (6, 16, z) are not shown in these tables. However, they agreed with corresponding values at points (6, 6, z) to better than 0.05% for every z value, thus preserving symmetry.

Table 3.6. Test Case 2 Results, z-Plane 3

Time (sec)	$\Delta t =$	Point (1, 11, 3)		Point (6, 6, 3)	
		.002	.001	.002	.001
.0		.347	.347	.245	.245
.05		.392	.398	.280	.284
.10		.484	.483	.350	.349
.15		.610	.619	.446	.454
.20		.853	.867	.633	.643
.25		1.094	.994	.811	.737
.30		.998	.991	.740	.735

Table 3.7 Test Case 2 Results, z-Plane 11

Time (sec)	$\Delta t =$	Point (1, 11, 11)		Point (6, 6, 11)	
		.002	.001	.002	.001
.0		1.279	1.279	.422	.422
.05		1.442	1.467	.487	.496
.10		1.784	1.780	.617	.616
.15		2.248	2.284	.796	.809
.20		3.149	3.197	1.144	1.162
.25		4.035	3.666	1.465	1.330
.30		3.679	3.655	1.334	1.326

Table 3.8. Test Case 2 Results, z-Plane 19

Time (sec)	$\Delta t =$	Point(1,11,19)		Point(6,6,19)	
		.002	.001	.002	.001
.0		.347	.347	.245	.245
.05		.388	.395	.278	.283
.10		.480	.479	.348	.348
.15		.605	.615	.444	.452
.20		.847	.860	.630	.640
.25		1.086	.987	.808	.734
.30		.991	.984	.737	.732

The results at a Δt of .001 indicate that the thermal flux grew by factors of 2.86 and 3.16 at the reactor center and in the center of the perturbed regions, respectively. The group one fluxes grew by practically equal amounts. Thus, spatial and energy spectral changes were minimal, as would be expected for this symmetric problem.

From Tables 3.6 and 3.8, it is seen that differences of up to 1% exist in the results at planes 3 and 19, when they should be equal. After these runs were made, an error was discovered in 3DKIN which caused several coefficients for points on z-plane 18 to be incorrectly computed. This was the cause of the slight retardation in growth in z-plane 19 flux values. With the error corrected, a later run was carried out to .10 sec and gave results symmetric to 4 significant figures in the z-direction. The runs shown here were not repeated because of the cost of the 2-1/2 hours of computer time required to do so.

At $\Delta t = .002$ sec, the solution considerably overshoot the true solution during time $0.2 \leq t \leq 0.3$ sec. To overcome this damped oscillatory behavior when the run with $\Delta t = .001$ sec was made, the time step was decreased to .0005 sec for .01 sec just as the ramp was cut off. This was largely successful as the solution then overshoot by only a very small amount. Closer examination of the solution at several times in the range $0.2 \leq t \leq 0.3$ revealed that the peak of the overshoot occurred at .25 sec and that the solution was growing smoothly and asymptotically by $t = 0.3$ sec. It is believed that the solution shown here for $\Delta t = .001$ sec has converged to less than 1% error at all times except perhaps at the peak of the overshoot. A run made out to .10 sec with $\Delta t = .0005$ sec supported this statement for that part of the transient.

TEST CASE 3

Geometry and Composition: Configuration 3

Perturbation: Ramp change, $\Delta \Sigma_a$ (material 4, group 4) = $-.0035(t/0.2)$

for $0 \leq t \leq 0.2$ sec

$\Delta \Sigma_a$ (material 4, group 4) = $-.0035$

for $t \geq 0.2$ sec

As mentioned in section 3.1, this problem, with four neutron groups and one precursor group, is a three-dimensional version of a problem used to compare several methods in two dimensions. Specifically, the original 160 cm \times 80 cm plane was made 120 cm thick in the z-direction. However, the bottom 56 cm of the region with material 4

was changed to material 3 (which was identical to material 4 before the perturbation). Thus, only the top 64 cm was perturbed for this transient.

This problem is asymmetric in all three dimensions so that the full reactor with homogeneous Dirichlet boundary conditions had to be considered. With 8.0-cm mesh spacings, a total of 3696 mesh points were used.

Material 1 is a highly enriched material so that group one fluxes were initially more than five times higher than group four fluxes in it. On the other hand, materials 3 and 4 are strong moderators so that the group four flux peaked in them. Given these spectral variations in the initial condition, which was computed with 3DKIN, and the asymmetric perturbation, it was expected that large spatial and energy spectrum changes would result.

The results of runs made on 3DKIN out to 0.3 second with time step sizes of .002 and .001 sec are shown in Tables 3.9 through 3.12. Point (3, 9, z) is near the center of the highly-enriched core, while point (12, 3, z) is in the center of the perturbed region for $z > 56$ cm. z-plane 4 is the mid-plane of the unperturbed lower portion, while z-plane 12 is near the center of the upper 64 cm region.

As expected, this transient resulted in rather severe spectral changes. At point (3, 9, 4), the group one and group four fluxes grew by only 6%. Meanwhile, the group one and group four fluxes at point (12, 3, 12) grew by 11% and 45%, respectively. The solution overshoot slightly at the end of the ramp for $\Delta t = .002$ sec, but practically all traces of overshoot were wiped out during the run with $\Delta t = .001$ sec.

Table 3.9. Test Case 3 Results, z-Plane 4, Group 1

Time (sec)	$\Delta t =$	Point (3, 9, 4)		Point (12, 3, 4)	
		.002	.001	.002	.001
.0		1.402	1.402	.384	.384
.05		1.416	1.419	.389	.390
.10		1.439	1.438	.396	.396
.15		1.457	1.459	.402	.403
.20		1.487	1.484	.411	.410
.25		1.487	1.484	.411	.411
.30		1.484	1.486	.410	.410

Table 3.10. Test Case 3 Results, z-Plane 4, Group 4

Time (sec)	$\Delta t =$	Point (3, 9, 4)		Point (12, 3, 4)	
		.002	.001	.002	.001
.0		.112	.112	2.742	2.742
.05		.114	.114	2.775	2.781
.10		.115	.115	2.825	2.824
.15		.117	.117	2.867	2.872
.20		.119	.119	2.931	2.928
.25		.119	.119	2.935	2.930
.30		.119	.119	2.928	2.934

Table 3.11. Test Case 3 Results, z-Plane 12, Group 1

Time (sec)	$\Delta t =$	Point (3, 9, 12)		Point (12, 3, 12)	
		.002	.001	.002	.001
.0		1.772	1.772	.486	.486
.05		1.791	1.795	.496	.497
.10		1.821	1.820	.510	.509
.15		1.845	1.848	.522	.523
.20		1.883	1.881	.539	.538
.25		1.885	1.881	.539	.538
.30		1.881	1.883	.538	.539

Table 3.12. Test Case 3 Results, z-Plane 12, Group 4

Time (sec)	$\Delta t =$	Point (3, 9, 12)		Point (12, 3, 12)	
		.002	.001	.002	.001
.0		.142	.142	3.467	3.467
.05		.144	.144	3.755	3.764
.10		.146	.146	4.114	4.112
.15		.148	.148	4.510	4.521
.20		.151	.151	5.010	5.008
.25		.151	.151	5.026	5.012
.30		.151	.151	5.012	5.019

The results at the two time step sizes are in good agreement and are thought to represent a good approximation to the exact solution.

TEST CASE 4

Geometry and Compositions: Configuration 4

Perturbation: Ramp changes, $\Delta\Sigma_a$ (material 5, group 2) = $-.004 (t/.08)$

for $0 \leq t \leq 0.08$ sec

$\Delta\Sigma_a$ (material 5, group 2) = $-.004$

for $t \geq 0.08$ sec

$\Delta\Sigma_a$ (material 6, group 2) = 0

for $0 \leq t \leq 0.08$ sec

$\Delta\Sigma_a$ (material 6, group 2) = $-.004 \left(\frac{t-.08}{.08} \right)$

for $0.08 \leq t \leq 0.16$ sec

$\Delta\Sigma_a$ (material 6, group 2) = $-.004$

for $t > 0.16$ sec

(continued)

$$\Delta\Sigma_a(\text{material 7, group 2}) = 0$$

$$\text{for } 0 \leq t \leq 0.16 \text{ sec}$$

$$\Delta\Sigma_a(\text{material 7, group 2}) = -.004 \left(\frac{t-.16}{.08} \right)$$

$$\text{for } 0.16 \leq t \leq 0.24 \text{ sec}$$

$$\Delta\Sigma_a(\text{material 7, group 2}) = -.004$$

$$\text{for } t \geq 0.24 \text{ sec}$$

This problem represents an attempt to simulate the withdrawal of control rods from two adjacent subassemblies in a medium-sized pressurized-water power reactor with two neutron groups and one precursor group. The central core zone consists of 16 square subassemblies, each 30 cm on a side, containing 2.8% enriched U^{235} . Four subassemblies of the same size, but containing 3.3% enriched U^{235} , are located along each side of the inner zone. The four 30-cm-square corners plus a 20-cm-thick band around the entire reactor consist of a water and steel reflector. The active core height is 240 cm, with a reflector of 30-cm thickness located above and below it.

The two subassemblies which were perturbed were adjacent to each other with the x mid-plane passing between them. Thus, only the right half of the reactor was considered for the computer calculations. A spatial mesh with $13 \times 25 \times 20$ mesh points was used. A homogeneous Neumann boundary condition was imposed on the exposed mid-plane of the reactor.

The rod withdrawal was simulated by linearly decreasing the thermal absorption cross section over three successive time zones of 0.08 sec length. During the first zone, only the bottom third of the

subassembly was perturbed. The middle and upper thirds followed successively in the next two zones. With the full perturbation inserted, the reactor had about fifty cents of excess reactivity.

The thermal group fluxes at three heights in the core, both in the center of the perturbed subassembly and in the center of the subassembly located symmetrically across the y mid-plane from it, are tabulated in Tables 3.13 through 3.15. Runs were made on 3DKIN with time steps of .002 and .001 sec. The results for $\Delta t = .001$ sec are also plotted on Figs. 3.3 and 3.4.

Table 3.13. Test Case 4 Results, z-Plane 5

Time (sec)	$\Delta t =$	Point (1, 5, 5)		Point (1, 21, 5)	
		.002	.001	.002	.001
.0		.291	.291	.291	.291
.04		.296	.299	.364	.369
.08		.313	.313	.492	.493
.12		.330	.337	.556	.567
.16		.376	.381	.684	.694
.20		.439	.415	.803	.768
.24		.439	.442	.819	.828
.28		.466	.456	.879	.857
.32		.463	.457	.870	.859
.35		.453	.458	.850	.861

Table 3.14. Test Case 4 Results, z-plane 10

Time (sec)	$\Delta t =$	Point (1, 5, 10)		Point (1, 21, 10)	
		.002	.001	.002	.001
.0		.547	.547	.547	.547
.04		.552	.559	.570	.577
.08		.581	.579	.625	.624
.12		.615	.625	.821	.838
.16		.696	.706	1.212	1.236
.20		.816	.773	1.473	1.401
.24		.824	.828	1.544	1.557
.28		.874	.855	1.660	1.616
.32		.868	.857	1.642	1.619
.35		.850	.859	1.604	1.623

Table 3.15. Test Case 4 Results, z-Plane 16

Time (sec)	$\Delta t =$	Point (1, 5, 16)		Point (1, 21, 16)	
		.002	.001	.002	.001
.0		.291	.291	.291	.291
.04		.292	.297	.294	.298
.08		.306	.305	.309	.308
.12		.324	.328	.345	.349
.16		.365	.369	.416	.422
.20		.431	.407	.606	.581
.24		.438	.441	.806	.820
.28		.466	.456	.877	.858
.32		.462	.457	.868	.858
.35		.453	.458	.851	.860

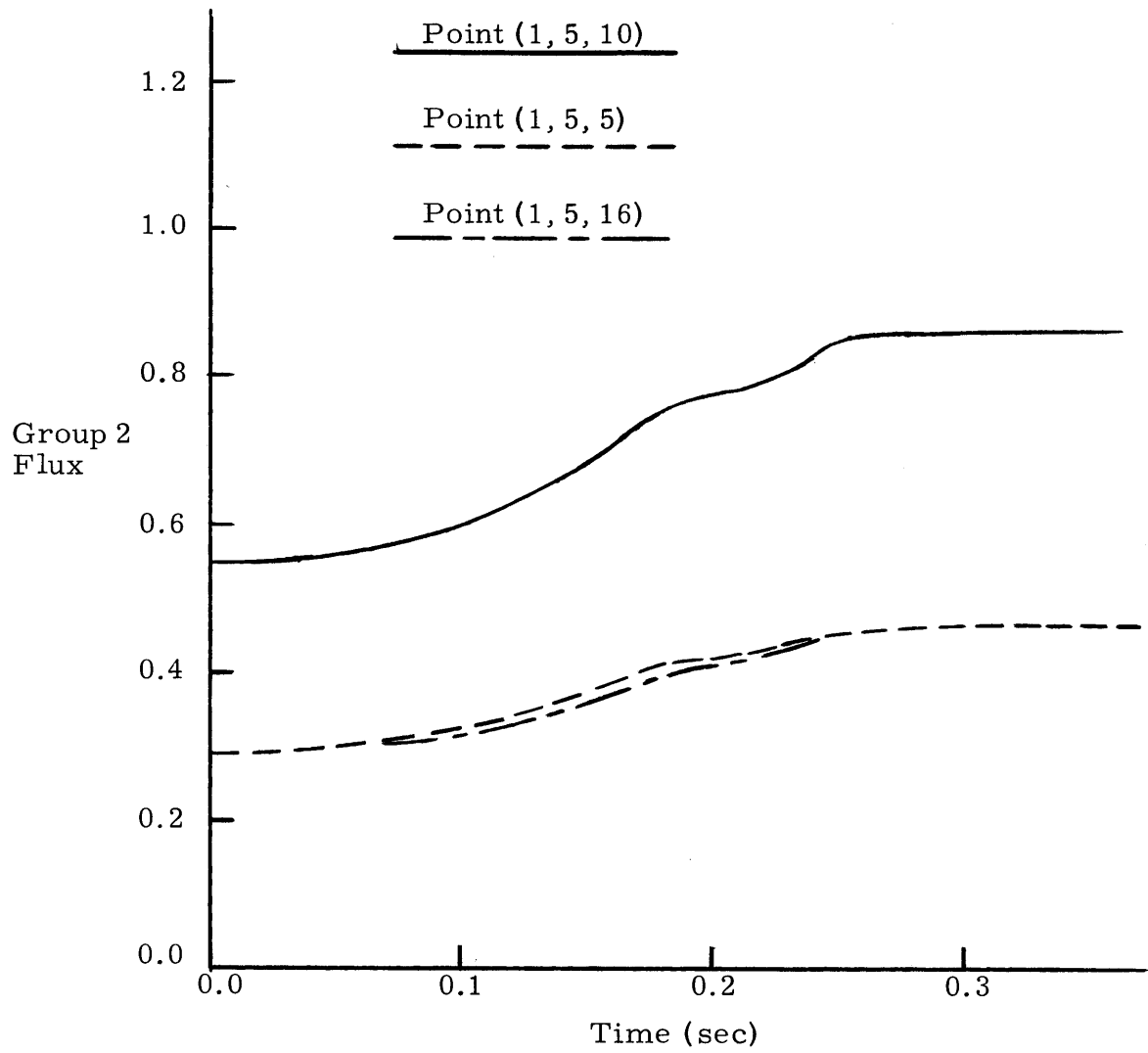


Fig. 3.3. Test Case 4 Results, Point (1, 5, z)

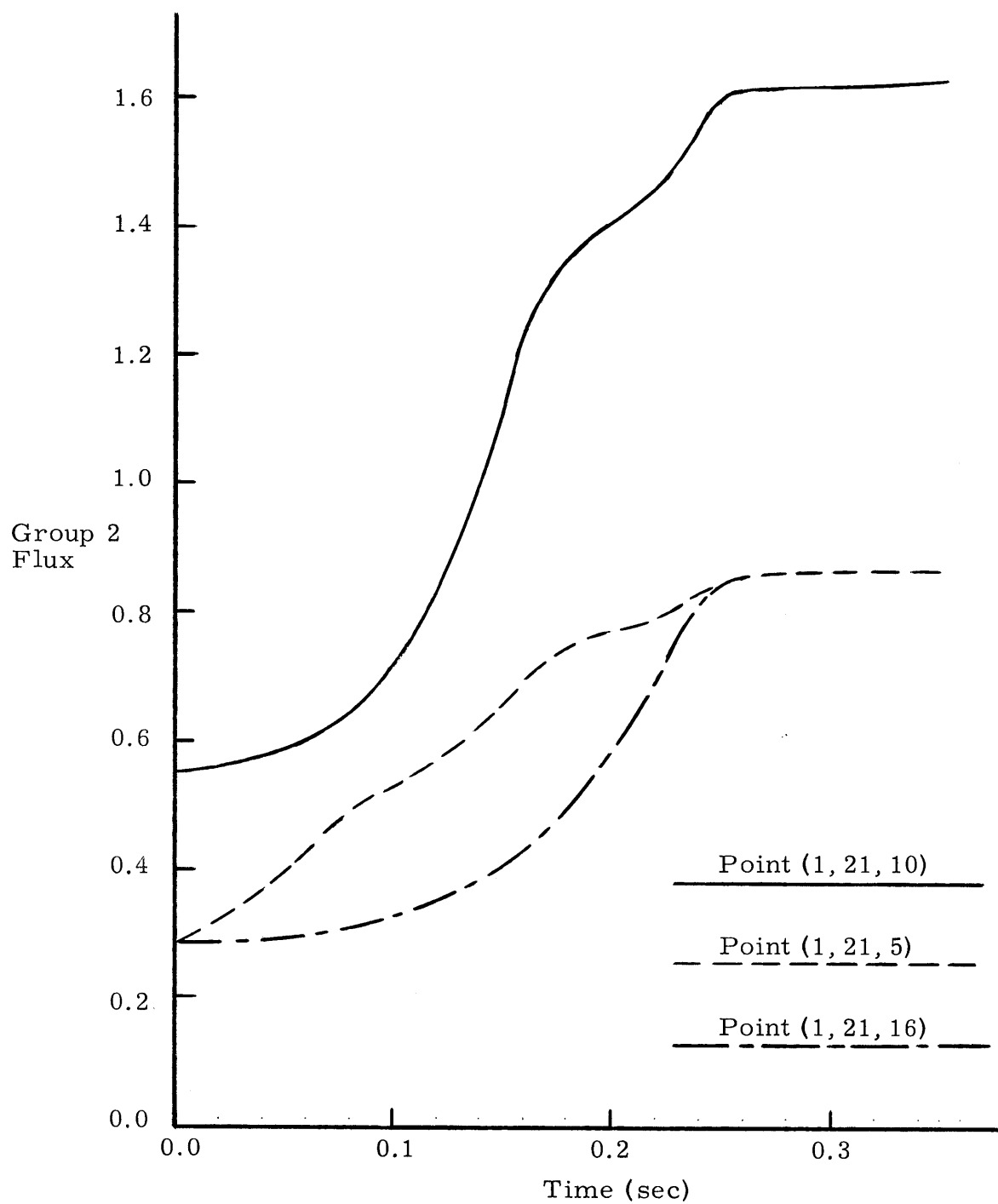


Fig. 3.4. Test Case 4 Results, Point (1, 21, z)

As expected, this perturbation caused severe flux tilting in the reactor. The flux at point (1, 21, 10) grew by a factor of 2.97 during .35 sec, while the flux at point (1, 5, 10) grew by only a factor of 1.57. Likewise, the flux in the upper portion of the core lagged that in the lower third considerably early in the transient, but caught up nicely within .10 sec after the perturbation had become symmetric in the z-direction.

As in earlier cases, the solution at $\Delta t = .002$ behaved in a damped oscillatory fashion at the end of the ramp, due to the frequency calculation. Again, these oscillations disappeared when Δt was halved to .001 sec and halved again for .02 sec just after the end of the ramp. Based on the smoothness of the solution with $\Delta t = .001$ sec and the relatively good agreement of the two solutions except at the end of the ramp, it is again believed that the solution obtained with $\Delta t = .001$ sec is a good approximation to the exact solution.

Chapter 4

CONCLUSIONS AND RECOMMENDATIONS

To be a truly useful numerical technique, a proposed method must treat difficult, practical problems successfully with reasonable computational costs, as well as possess desirable analytical properties. It has been concluded in section 2.4 that the NSADE method satisfies certain analytical criteria necessary for success. This chapter summarizes the practical experience gained from the several numerical experiments presented in Chapter 3.

4.1 Characteristics of the Numerical Results

Several important characteristics are easily observed in the numerical experiments. The property of truncation error behavior for the NSADE method has been shown to be approximately of order h^2 , as predicted by the theoretical analysis, for the one problem where it could be accurately measured.

Closely related to truncation error is accuracy. Over several test cases, the NSADE method has been seen to give acceptably accurate solutions at reasonable time step sizes. It is unfortunate that solutions with even smaller Δt 's are not available for Test Cases 2, 3, and 4 to further verify the accuracy of the solutions shown. Given the relatively slow computer available for numerical experiments for this thesis, this was just too costly.

It is granted that the time steps required by the NSADE method are probably an order of magnitude smaller than those which would be required for similar accuracy by a direct solution technique where the A matrix is not split before inversion. However, it is difficult to imagine any such method, which would necessarily require an iterative technique to carry out the inversion process, requiring less than an order of magnitude more computational effort per time step.

The time step size used by the NSADE method is limited by two factors. These generally come into play during different parts of a transient. During that part of the transient where reactivity is being inserted, usually by an externally-controlled factor such as control rod motion, the time steps are initially limited by the rate of reactivity insertion. This is necessary so that truncation error is controlled while the frequencies used in the exponential transformation are "seeking" the rates of flux change in the various regions of the reactor. Once this has happened, the time steps can be gradually increased in size with little effect on accuracy, so long as the rate of reactivity change remains fairly constant.

During any part of the transient when the rate of reactivity change is suddenly altered, the time steps must be decreased in size. This is necessary if accuracy is to be retained while the frequencies again "seek" the new rates of flux change. This must be done to control the damped oscillations that arise if a time step too large is used through this part of the transient.

A rule of thumb which was first offered for the NSADE method in two dimensions¹ and which has been found to hold approximately for

three dimensions relates the truncation error to the rate of solution change over one time step. A 1% change in the solution over each time step generally produces about 1% error in about 100 steps. For a given problem, this implies that about 100 steps are required to predict a doubling in the flux to 1% accuracy.

The numerical stability of the NSADE method has never been found to be a limiting factor in two- and three-dimensional calculations. The oscillations which plague the solution during periods of abrupt change in the rate of reactivity change affect the accuracy of the solution temporarily. They quickly damp out, however, so that the solution returns to the correct rate of change. This correct asymptotic behavior is a result of the exponential transformation. The time step sizes to be used for a particular problem are thus primarily limited by the accuracy desired in the solution.

One great advantage of the NSADE method is its computational ease. All matrix inversions required by it are simple back-substitutions. Because of this, computational times per time step for a range of problems vary approximately linearly with the number of mesh points and neutron groups. It has thus been found possible¹ to derive an expression of the form

$$\text{Time/Step} = \alpha N(G + \beta I),$$

which relates the time necessary to advance the solution over one time step, Δt , to the number of unknowns in the problem. Here, N is the number of mesh points in the problem, and G and I are the number of neutron and precursor groups, respectively.

Listed in Table 4.1 below are running times per step required by 3DKIN for four different problems. The computer used for these runs was an IBM 360/65 running under OS/360-MVT. All unknowns were stored in fast memory.

Table 4.1. Computational Times

Mesh Points	Groups	Precursors	Seconds/Step
1331	2	1	3.09
3696	4	1	16.0
4851	2	1	13.3
6500	2	1	18.3

Since only problems with one precursor are available, a value of $\beta = 0.3$ will be used as determined in previous two-dimensional work. From Table 4.1, two values of α are obtained:

$$\alpha = 1.2 \times 10^{-3} \quad \text{for } G = 2$$

$$\alpha = 1.0 \times 10^{-3} \quad \text{for } G = 4.$$

As G increases, the work per group decreases in 3DKIN since only one frequency is computed for all neutron groups at each mesh point.

4.2 Applicability of the NSADE Method

The numerical experiments presented in Chapter 3 offer strong evidence that the NSADE method is capable of treating a general class of transients in three spatial dimensions with reasonable time step sizes. These include difficult sub-prompt critical transients which

result in significant spatial flux tilting and energy spectrum changes.

It is obvious that it would not be feasible to solve problems of a really practical size with the computer which was used for the numerical experiments for this thesis. Table 4.2 compares the floating-point add time (for 64-bit words) of the IBM 360/65 to those of several of the fastest computer systems currently in use or being installed. An extrapolation from the relation developed in the last section for the IBM 360/65 should be approximately correct if it is based on the information in the table.

Table 4.2. Comparison of Computing Speeds

Computer Model	Floating Point Add Time (microseconds)
IBM 360/65	1.8
CDC 6600	0.4
IBM 370/195	0.11
CDC 7600	0.1
CDC STAR	0.02

It seems reasonable to expect that increases in computing speeds over the IBM 360/65 by factors of at least 16, 18, and 50, respectively, can be expected from the last three machines listed in Table 4.2. These last three machines can be obtained with 5×10^5 words or more of either fast core storage or slower extended core storage which, through clever programming, slows down computing speed only slightly. Thus, a program like 3DKIN could treat a problem with three neutron groups, one

precursor group, and 5×10^4 or more spatial mesh points with all unknowns stored in fast or extended core storage, provided an excessive amount of geometrical detail were not specified for the problem.

Consider, then, the time which would be required on a machine which is 20 times faster than the IBM 360/65. Table 4.2 gives assurance that such machines are being built. A reasonable estimate for a problem with three neutron groups, one precursor group, and 5×10^4 mesh points on this machine would be

$$\begin{aligned} \text{time/step} &= (1.1 \times 10^{-3})(.05)(5 \times 10^4)(3+.3) \text{ sec} \\ &= 9.1 \text{ sec.} \end{aligned}$$

Two hours of computing time would traverse about 800 time steps, enough to describe many interesting transients.

One goal set for the direct solution technique developed in this thesis has been that it provide benchmark solutions for difficult, practical problems. Solutions from the more rapid but more approximate synthesis techniques can then be compared against these. At the same time, the cost of obtaining these benchmark solutions must not be unduly great. The NSADE method appears to satisfy both of these criteria.

More importantly, the NSADE method is a practical method for the routine solution of several classes of problems, given that a very fast computer is available. One such class includes survey calculations where fine spatial detail is not required. Since more effort is required to prepare a problem for solution by a space-time synthesis

method than for solution by the NSADE method, the synthesis methods lose much of their speed advantage when a number of different problems are to be run during a survey.

Space-time synthesis methods also have difficulty in treating problems where severe spatial flux tiltings and energy spectrum changes result. Selection of trial functions for such problems requires much insight and intuition. In contrast, the NSADE method requires only an initial flux distribution to start such a problem. Little insight is required as to how the solution will behave during the transient.

4.3 Limitations of the NSADE Method

The NSADE method is a more costly method than are space-time synthesis methods for a number of problems of interest to reactor designers. Once a reactor design has been finalized, there are a number of operating transients which need to be analyzed with fine spatial detail. Here, space-time synthesis methods are capable of providing sufficiently accurate solutions at a significantly lower cost.

Another factor may limit the effectiveness of the NSADE method on some current computing systems. Because this method tends to accumulate errors during the first few steps of a transient, a very accurate initial flux distribution and eigenvalue estimate must be used to start the calculations. All initial conditions used in this thesis were accurate to better than one part in 10^7 in the flux distribution and one part in 10^8 in the eigenvalue. Not only is it costly to obtain such an accurate initial condition, but it also is necessary to be able to carry 10 or more significant digits in all calculations. It would be difficult

to utilize this method on any computing system which did not have floating-point capabilities which carry at least 10 significant decimal digits.

4.4 Recommendations for Further Work

The NSADE method can be easily extended to r - θ - z cylindrical geometry and to hexagonal- z geometry. Such extension would greatly increase the utility of the method in treating problems associated with several types of reactors.

It has been mentioned that it is possible to increase the time step size during certain parts of a transient, while it is necessary to decrease it during other parts if accuracy is to remain fairly constant throughout the transient. Algorithms which would automate this time step size variation should be investigated. It is probable that the rate of change of the frequencies, $\underline{\Omega}$, would provide an indication of when the time step size should be changed.

A final recommendation concerns the selection of the frequencies. There may well be algorithms which would select frequencies which would allow even larger time steps to be taken. This area of investigation deserves a great deal of attention.

REFERENCES

1. William H. Reed and K. F. Hansen, "Alternating Direction Methods for Reactor Kinetics Equations," Nucl. Sci. Eng. 41, 431 (1970).
2. William H. Reed, "Finite Difference Techniques for the Solution of the Reactor Kinetics Equations," Sc.D. Thesis, Department of Nuclear Engineering, Massachusetts Institute of Technology, MIT-NE-100 (May, 1969).
3. Richard S. Varga, Matrix Iterative Analysis, Chap. 6, Prentice-Hall, Englewood Cliffs, N. J. (1962).
4. A. F. Henry, "Space-Time Reactor Kinetics," 22.243 Course Notes, Massachusetts Institute of Technology (1969), unpublished.
5. S. Kaplan, O. J. Marlowe, and J. Bewick, "Application of Synthesis Techniques to Problems Involving Time Dependence," Nucl. Sci. Eng. 18, 163 (1964).
6. A. F. Henry, "The Application of Reactor Kinetics to the Analysis of Experiments," Nucl. Sci. Eng. 3, 52 (1958).
7. K. Ott, "Quasistatic Treatment of Spatial Phenomena in Reactor Dynamics," Nucl. Sci. Eng. 26, 563 (1966).
8. D. A. Meneley, K. Ott, and E. S. Wiener, "Space-Time Kinetics, the QX1 Code," ANL-7310, Argonne National Laboratory (1967).
9. J. B. Yasinsky and S. Kaplan, "Synthesis of Three-Dimensional Flux Shapes Using Discontinuous Sets of Trial Functions," Nucl. Sci. Eng. 28, 426 (1967).
10. J. B. Yasinsky, "Combined Space-Time Synthesis with Axially Discontinuous Trial Functions," WAPD-TM-736, Bettis Atomic Power Laboratory (1967).
11. J. B. Yasinsky, "The Solution of the Space-Time Neutron Group Diffusion Equations by a Time-Discontinuous Synthesis Method," Nucl. Sci. Eng. 29, 381 (1967).
12. E. L. Wachspress and M. Becker, "Variational Multichannel Synthesis with Discontinuous Trial Functions," KAPL-3095, Knolls Atomic Power Laboratory (1965).

13. W. M. Stacey, Jr., "A Variational Multichannel Space-Time Synthesis Method for Nonseparable Reactor Transients," Nucl. Sci. Eng. 34, 45 (1968).
14. K. F. Hansen and S. R. Johnson, "GAKIN, A Program for the Solution of the One-Dimensional, Multigroup, Space-Time Dependent Diffusion Equations," GA-7543, General Atomic (1967).
15. W. R. Cadwell, A. F. Henry, and A. J. Vigilotti, "WIGLE - A Program for the Solution of the Two-Group, Space-Time Diffusion Equations in Slab Geometry," WAPD-TM-416, Bettis Atomic Power Laboratory (1964).
16. J. B. Yasinsky, M. Natelson, and L. A. Hageman, "TWIGL - A Program to Solve the Two-Dimensional, Two-Group, Space-Time Neutron Diffusion Equations with Temperature Feedback," WAPD-TM-743, Bettis Atomic Power Laboratory (1968).
17. W. T. McCormick, Jr., "Numerical Solution of the Two-Dimensional Multigroup Kinetics Equations," Ph. D. Thesis, Department of Nuclear Engineering, Massachusetts Institute of Technology, MIT-NE-99 (May, 1969).
18. B. K. Larkin, "Some Stable Explicit Difference Approximations to the Diffusion Equation," Math. Comp. 18, 196 (1964).
19. S. J. Kast, "Solution of the Reactor Kinetics Equations in Two Dimensions by Finite Difference Methods," S. M. Thesis, Department of Nuclear Engineering, Massachusetts Institute of Technology (August, 1970).
20. Richard S. Varga, op. cit., Chap. 8.
21. D. W. Peaceman and H. H. Rachford, Jr., "The Numerical Solution of Parabolic and Elliptic Differential Equations," J. Soc. Ind. Appl. Math. 3, 28 (1955).
22. L. A. Hageman and J. B. Yasinsky, "Comparison of Alternating-Direction Time-Differencing Methods with Other Implicit Methods for the Solution of the Neutron Group-Diffusion Equations," Nucl. Sci. Eng. 38, 8 (1969).
23. A. L. Wight, K. F. Hansen, and D. R. Ferguson, "Application of Alternating-Direction Implicit Methods to the Space-Dependent Kinetics Equations," Nucl. Sci. Eng. 44, 239 (1971).
24. A. L. Wight, "The Application of Alternating-Direction Implicit Methods to the Space-Dependent Kinetics Equations," Ph. D. Thesis, Department of Nuclear Engineering, Massachusetts Institute of Technology (August, 1969).

25. Eugene L. Wachspress, Iterative Solution of Elliptic Systems, Chap. 3, Prentice-Hall, Englewood Cliffs, N. J. (1966).
26. Robert D. Richtmeyer and K. W. Morton, Difference Methods for Initial-Value Problems, Chap. 3, John Wiley and Sons, New York (1967).
27. L. A. Hageman, "Numerical Methods and Techniques Used in the Two-Dimensional Neutron-Diffusion Program PDQ-5," WAPD-TM-364, Bettis Atomic Power Laboratory (1963).

APPENDICES

Appendix A
THE SEMI-DISCRETE FORM OF THE
SPACE-DEPENDENT REACTOR KINETICS EQUATIONS

The differential form of the space-dependent reactor kinetics equations has been given in Eqs. (1.1). These equations are repeated here for the sake of clarity.

$$\begin{aligned} \frac{1}{v_g} \frac{d\phi_g(\vec{r}, t)}{dt} = & \vec{\nabla} \cdot D_g(\vec{r}, t) \vec{\nabla} \phi_g(\vec{r}, t) + \sum_{g'=1}^G \Sigma_{gg'}(\vec{r}, t) \phi_{g'}(\vec{r}, t) \\ & + \sum_{i=1}^I f_{gi} C_i(\vec{r}, t) \quad (1 \leq g \leq G) \end{aligned} \tag{1.1}$$

$$\frac{dC_i(\vec{r}, t)}{dt} = -\lambda_i C_i(\vec{r}, t) + \sum_{g'=1}^G p_{ig'}(\vec{r}, t) \phi_{g'}(\vec{r}, t)$$

All of the symbols used here have been defined in section 1.2.

The discretization is carried out here in rectangular Cartesian coordinates. The region of interest is a rectangular parallelepiped. The origin of coordinates is placed in the lower front left corner of the parallelepiped, as shown in Fig. A.1.

The three-dimensional mesh is created by passing a series of planes, each of which is perpendicular to one of the three axes, entirely through the parallelepiped. The points of intersection of these planes, which lie within or on the boundaries of the parallelepiped, form the mesh. It is assumed that six of the planes are

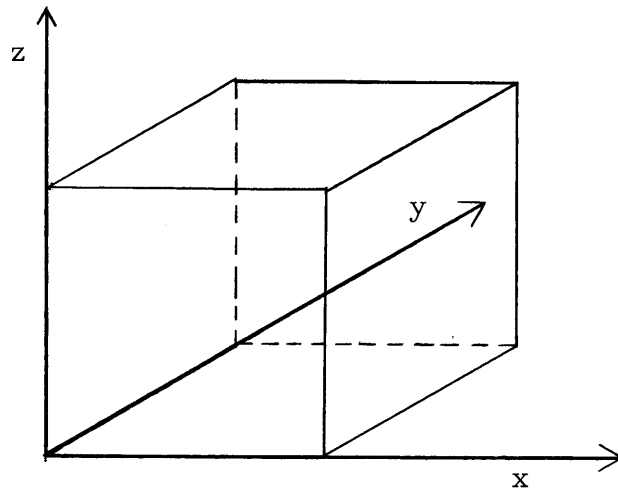


Fig. A.1. Coordinate System

coincident with the six faces so that planes of mesh points lie on the six faces. If a total of L , J , and K planes are passed perpendicular to the x -, y -, and z -axis, respectively, there are a total of $L \times J \times K$ points in the mesh within or on the boundaries of the parallelepiped.

Figures A.2a and A.2b depict, respectively, planes perpendicular to the z -axis and y -axis which pass through mesh point (l, j, k) .

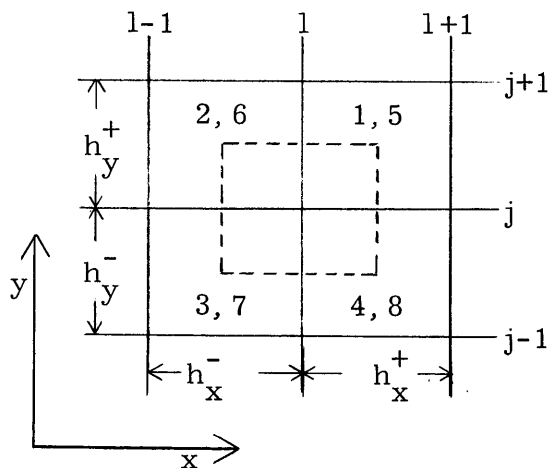


Fig. A.2a. Plane Perpendicular to z -Axis at (l, j, k)

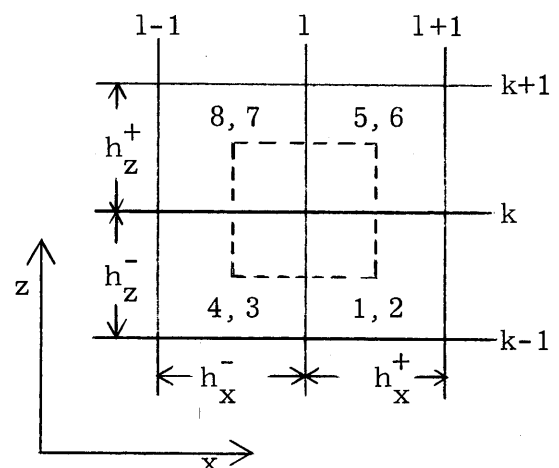


Fig. A.2b. Plane Perpendicular to y -Axis at (l, j, k)

The broken lines lie exactly halfway between the solid mesh lines. The eight octants which touch on point $(1, j, k)$ are numbered as shown above. Octants 1, 2, 3, and 4 lie below the z -plane passing through point $(1, j, k)$, while octants 5, 6, 7, and 8 lie above it.

The discrete equations for point (i, j, k) are obtained by integrating Eqs.(1.1) over the volume contained within $x_1 - h_x^-/2 \leq x \leq x_1 + h_x^+/2$, $y_j - h_y^-/2 \leq y \leq y_j + h_y^+/2$, and $z_k - h_z^-/2 \leq z \leq z_k + h_z^+/2$. It is assumed that the material within each octant is homogeneous. In the derivation that follows, superscripts on material constants denote the octants in which the materials lie.

$$\begin{aligned} & \frac{1}{v_g} \frac{d}{dt} \int_{z_k - h_z^-/2}^{z_k + h_z^+/2} dz \int_{y_j - h_y^-/2}^{y_j + h_y^+/2} dy \int_{x_1 - h_x^-/2}^{x_1 + h_x^+/2} dx \phi_g(x, y, z, t) = \\ & \int_{z_k - h_z^-/2}^{z_k + h_z^+/2} dz \int_{y_j - h_y^-/2}^{y_j + h_y^+/2} dy \int_{x_1 - h_x^-/2}^{x_1 + h_x^+/2} dx \times \\ & \left\{ \bar{\nabla} \cdot D_g(x, y, z, t) \bar{\nabla} \phi_g(x, y, z, t) + \sum_{g'=1}^G \Sigma_{gg'}(x, y, z, t) \phi_{g'}(x, y, z, t) + \right. \\ & \left. \sum_{i=1}^I f_{gi} C_i(x, y, z, t) \right\}, \quad (1 \leq g \leq G). \end{aligned} \quad (A.1)$$

With the following definitions,

$$\phi_{g,1,j,k} = \frac{1}{V_{1,j,k}} \int \int \int \phi_g(x, y, z) dx dy dz \quad (A.2a)$$

$$C_{i,1,j,k} = \frac{1}{V_{1,j,k}} \int \int \int C_i(x, y, z) dx dy dz \quad (A.2b)$$

$$V_{1,j,k} = \frac{1}{8} (h_x^+ + h_x^-) (h_y^+ + h_y^-) (h_z^+ + h_z^-) \quad (\text{A.2c})$$

and

$$\begin{aligned} \Sigma_{gg',1,j,k} = \frac{1}{8} \left[h_x^+ h_y^+ h_z^- \Sigma_{gg'}^1 + h_x^- h_y^+ h_z^- \Sigma_{gg'}^2 + h_x^- h_y^- h_z^- \Sigma_{gg'}^3 + h_x^+ h_y^- h_z^- \Sigma_{gg'}^4 + \right. \\ \left. h_x^+ h_y^+ h_z^+ \Sigma_{gg'}^5 + h_x^- h_y^+ h_z^+ \Sigma_{gg'}^6 + h_x^- h_y^- h_z^+ \Sigma_{gg'}^7 + h_x^+ h_y^- h_z^+ \Sigma_{gg'}^8 \right], \end{aligned} \quad (\text{A.2d})$$

where the integrals are taken over the limits shown in Eq. (A.1), Eq. (A.1) becomes

$$\begin{aligned} \frac{V_{1,j,k}}{v_g} \frac{d\phi_{g,1,j,k}}{dt} = \sum_{m=1}^6 \left\{ \int d\vec{s}_m \cdot D_g(x,y,z) \vec{\nabla} \phi_g(x,y,z) \right\} + \\ \sum_{g'=1}^G \Sigma_{gg',1,j,k} \phi_{g',1,j,k} + \\ V_{1,j,k} \sum_{i=1}^I f_{gi} C_{i,1,j,k}. \end{aligned} \quad (\text{A.3})$$

In Eq. (A.3), the volume integral for the diffusion terms has been changed to a surface integral, using Gauss' theorem. The summation over m indicates that the integral has been broken into integrals over the six faces of the volume. For illustrative purposes, consider the face which is perpendicular to the x -axis at $x=x_1+h_x^+/2$. The surface integral for this face is given by

$$\int_{z-h_z^-/2}^{z+h_z^+/2} dz \int_{y-h_y^-/2}^{y+h_y^+/2} dy \left\{ D_g(x,y,z) \vec{\nabla} \phi_g(x,y,z) \cdot \vec{n}_x \right\} \Big|_{x=x_1+h_x^+/2},$$

where \vec{n}_x is a unit vector in the positive x -direction.

In order to carry out this integration, the current normal to the face is approximated by a simple finite difference:

$$\vec{\nabla} \phi_g(x, y, z) \cdot \vec{n}_x \doteq \frac{\phi_{g, l+1, j, k} - \phi_{g, l, j, k}}{h_x^+}. \quad (\text{A.4})$$

With this approximation, the surface integral representing leakage across the face at $x=x_1+h_x^+/2$ becomes

$$\begin{aligned} & \int_{z-h_z^-/2}^{z+h_z^+/2} dz \int_{y-h_y^-/2}^{y+h_y^+/2} dy \left\{ D_g(x, y, z) \vec{\nabla} \phi_g(x, y, z) \cdot \vec{n}_x \right\} \Big|_{x=x_1+h_x^+/2} \doteq \\ & \left(\frac{\phi_{g, l+1, j, k} - \phi_{g, l, j, k}}{h_x^+} \right) \cdot \left(\frac{D_g^1 h_y^+ h_z^-}{4} + \frac{D_g^5 h_y^+ h_z^+}{4} + \frac{D_g^8 h_y^- h_z^+}{4} + \frac{D_g^4 h_y^- h_z^-}{4} \right) \\ & = R_{g, l+\frac{1}{2}, j, k} (\phi_{g, l+1, j, k} - \phi_{g, l, j, k}), \end{aligned} \quad (\text{A.5})$$

where $R_{g, l+\frac{1}{2}, j, k}$ has been defined as

$$R_{g, l+\frac{1}{2}, j, k} = \frac{1}{4h_x^+} \left(D_g^1 h_y^+ h_z^- + D_g^5 h_y^+ h_z^+ + D_g^8 h_y^- h_z^+ + D_g^4 h_y^- h_z^- \right). \quad (\text{A.6a})$$

By defining five more leakage coefficients as

$$R_{g, l-\frac{1}{2}, j, k} = \frac{1}{4h_x^-} \left(D_g^2 h_y^+ h_z^- + D_g^6 h_y^+ h_z^+ + D_g^7 h_y^- h_z^+ + D_g^3 h_y^- h_z^- \right), \quad (\text{A.6b})$$

$$R_{g, l, j+\frac{1}{2}, k} = \frac{1}{4h_y^+} \left(D_g^1 h_x^+ h_z^- + D_g^5 h_x^+ h_z^+ + D_g^6 h_x^- h_z^+ + D_g^2 h_x^- h_z^- \right), \quad (\text{A.6c})$$

$$R_{g, l, j-\frac{1}{2}, k} = \frac{1}{4h_y^-} \left(D_g^4 h_x^+ h_z^- + D_g^8 h_x^+ h_z^+ + D_g^7 h_x^- h_z^+ + D_g^3 h_x^- h_z^- \right), \quad (\text{A.6d})$$

$$R_{g, l, j, k+\frac{1}{2}} = \frac{1}{4h_z^+} \left(D_g^8 h_x^+ h_y^- + D_g^7 h_x^- h_y^- + D_g^6 h_x^- h_y^+ + D_g^5 h_x^+ h_y^+ \right), \quad (\text{A.6e})$$

$$R_{g, l, j, k-\frac{1}{2}} = \frac{1}{4h_z^-} \left(D_g^4 h_x^+ h_y^- + D_g^3 h_x^- h_y^- + D_g^2 h_x^- h_y^+ + D_g^1 h_x^+ h_y^+ \right), \quad (\text{A.6f})$$

Eq. (A.3) can be written in its final form as

$$\begin{aligned} \frac{d\phi_{g,1,j,k}}{dt} = v_g \left\{ \frac{1}{V_{1,j,k}} \left[R_{g,1+\frac{1}{2},j,k}(\phi_{g,1+1,j,k} - \phi_{g,1,j,k}) + \right. \right. \\ R_{g,1-\frac{1}{2},j,k}(\phi_{g,1-1,j,k} - \phi_{g,1,j,k}) + R_{g,1,j+\frac{1}{2},k}(\phi_{g,1,j+1,k} - \\ \phi_{g,1,j,k}) + R_{g,1,j-\frac{1}{2},k}(\phi_{g,1,j-1,k} - \phi_{g,1,j,k}) + \\ R_{g,1,j,k+\frac{1}{2}}(\phi_{g,1,j,k+1} - \phi_{g,1,j,k}) + R_{g,1,j,k-\frac{1}{2}}(\phi_{g,1,j,k-1} - \\ \left. \left. \phi_{g,1,j,k}) + \sum_{g'=1}^G \Sigma_{gg',1,j,k} \phi_{g',1,j,k} \right] + \right. \\ \left. \sum_{i=1}^I f_{gi} C_{i,1,j,k} \right\}, \quad (1 \leq g \leq G). \end{aligned} \quad (A.7)$$

Furthermore, by defining the (LJK) \times (LJK) square matrices

$$\underline{T}_{gg'} = \text{diag}\{v_g \Sigma_{gg',1,j,k} / V_{1,j,k}\}, \quad (A.8a)$$

$$\underline{F}_{gi} = \text{diag}\{v_g f_{gi}\}, \quad (A.8b)$$

and \underline{D}_g such that

$$\begin{aligned} \underline{D}_g \vec{\psi}_g = v_g \text{col} \left\{ \frac{1}{V_{1,j,k}} \left[R_{g,1+\frac{1}{2},j,k}(\phi_{g,1+1,j,k} - \phi_{g,1,j,k}) + \right. \right. \\ R_{g,1-\frac{1}{2},j,k}(\phi_{g,1-1,j,k} - \phi_{g,1,j,k}) + R_{g,1,j+\frac{1}{2},k}(\phi_{g,1,j+1,k} - \\ \phi_{g,1,j,k}) + R_{g,1,j-\frac{1}{2},k}(\phi_{g,1,j-1,k} - \phi_{g,1,j,k}) + \\ R_{g,1,j,k+\frac{1}{2}}(\phi_{g,1,j,k+1} - \phi_{g,1,j,k}) + \\ \left. \left. R_{g,1,j,k-\frac{1}{2}}(\phi_{g,1,j,k-1} - \phi_{g,1,j,k}) \right] \right\}, \end{aligned} \quad (A.8c)$$

the equations for all mesh points can be combined into the single

matrix equation

$$\frac{d\vec{\psi}_g}{dt} = \underline{D}_g \vec{\psi}_g + \sum_{g'=1}^G \underline{T}_{gg'} \vec{\psi}_{g'} + \sum_{i=1}^I \underline{F}_{gi} \vec{C}_i, \quad (1 \leq g \leq G). \quad (1.4)$$

Here, the vectors $\vec{\psi}_g$ and \vec{C}_i are formed by ordering the group g fluxes and delayed precursor group i concentrations, respectively, in a consistent manner.

The discrete equation for the i^{th} delayed precursor concentration at point (l, j, k) is derived in an analogous fashion. It is given by

$$\frac{dC_{i,1,j,k}}{dt} = -\lambda_i C_{i,1,j,k} + \frac{1}{V_{1,j,k}} \sum_{g'=1}^G P_{ig',1,j,k} \phi_{g',1,j,k}, \quad (1 \leq i \leq I), \quad (A.9)$$

where

$$P_{ig',1,j,k} = \frac{\beta_i}{8} \left[h_{x,y,z}^+ h_{x,y,z}^+ h_{x,y,z}^- \nu_{g',\Sigma_{fg'}}^1 + h_{x,y,z}^- h_{x,y,z}^+ h_{x,y,z}^- \nu_{g',\Sigma_{fg'}}^2 + h_{x,y,z}^- h_{x,y,z}^- h_{x,y,z}^- \nu_{g',\Sigma_{fg'}}^3 + \right. \\ \left. h_{x,y,z}^+ h_{x,y,z}^- h_{x,y,z}^- \nu_{g',\Sigma_{fg'}}^4 + h_{x,y,z}^+ h_{x,y,z}^+ h_{x,y,z}^+ \nu_{g',\Sigma_{fg'}}^5 + h_{x,y,z}^- h_{x,y,z}^+ h_{x,y,z}^+ \nu_{g',\Sigma_{fg'}}^6 + \right. \\ \left. h_{x,y,z}^- h_{x,y,z}^- h_{x,y,z}^+ \nu_{g',\Sigma_{fg'}}^7 + h_{x,y,z}^+ h_{x,y,z}^- h_{x,y,z}^+ \nu_{g',\Sigma_{fg'}}^8 \right]. \quad (A.10)$$

By defining the (LJK) by (LJK) matrices

$$\underline{\Lambda}_i = \lambda_i \underline{I} \quad (A.11a)$$

and

$$\underline{P}_{ig'} = \text{diag} \{ P_{ig',1,j,k} / V_{1,j,k} \}, \quad (A.11b)$$

Eq. (A.9) for all mesh points can be written in matrix form as

$$\frac{d\vec{C}_i}{dt} = -\underline{\Lambda}_i \vec{C}_i + \sum_{g'=1}^G \underline{P}_{ig'} \vec{\psi}_{g'}. \quad (1.5)$$

Appendix B

THEOREMS

Several theorems and lemmas were offered without proof in Chapter 2. They are restated and proved here.

LEMMA 1.¹ The operators $\underline{C}_1(\underline{\Omega}, h)$ and $\underline{C}_2(\underline{\Omega}, h)$ are consistent.

Proof. The consistency condition requires that

$$\left\| \frac{\vec{\theta}(t+h) - \underline{C}_1(\underline{\Omega}, h)\vec{\theta}(t)}{h} \right\| \rightarrow 0 \text{ as } h \rightarrow 0. \quad (\text{B.1})$$

An identical condition must hold for $\underline{C}_2(\underline{\Omega}, h)$. Only $\underline{C}_1(\underline{\Omega}, h)$ will be treated here. The proof for $\underline{C}_2(\underline{\Omega}, h)$ is identical.

The numerator in Eq. (B.1) can be written in the form

$$\begin{aligned} \vec{\theta}(t+h) - \underline{C}_1\vec{\theta}(t) &= e^{\underline{\Omega}h} [\underline{I} - h(\underline{D}_1 + \underline{E}_4 - \alpha\underline{\Omega})]^{-1} \\ &\quad \times \{ [\underline{I} - h(\underline{D}_1 + \underline{E}_4 - \alpha\underline{\Omega})] e^{-\underline{\Omega}h} \vec{\theta}(t+h) \\ &\quad - [\underline{I} + h(\underline{D}_2 + \underline{E}_3 - \gamma\underline{\Omega})] \} \vec{\theta}(t). \end{aligned}$$

Expanding $e^{\underline{\Omega}h}$ and $\vec{\theta}(t+h)$ in a Taylor's series gives

$$\begin{aligned} \vec{\theta}(t+h) - \underline{C}_1\vec{\theta}(t) &= e^{\underline{\Omega}h} [\underline{I} - h(\underline{D}_1 + \underline{E}_4 - \alpha\underline{\Omega})]^{-1} \\ &\quad \times \left\{ h \frac{d\vec{\theta}(t)}{dt} - h\underline{A}\vec{\theta}(t) + O(h^2) \right\}. \end{aligned}$$

It has been stated in section 2.1 that

$$\underline{M}\vec{\theta}(t) = \underline{A}\vec{\theta}(t) + O(\Delta x^2) + O(\Delta y^2) + O(\Delta z^2).$$

Therefore,

$$\begin{aligned} \left\| \frac{\vec{\theta}(t+h) - \underline{C}_1 \vec{\theta}(t)}{h} \right\| &= \left\| e^{\underline{\Omega}h} [\underline{I} - h(\underline{D}_1 + \underline{E}_4 - \alpha \underline{\Omega})]^{-1} \right\| \\ &\quad \times \{O(h) + O(\Delta x^2) + O(\Delta y^2) + O(\Delta z^2)\}, \\ & \\ \left\| \frac{\vec{\theta}(t+h) - \underline{C}_1 \vec{\theta}(t)}{h} \right\| &\leq \left\| e^{\underline{\Omega}h} [\underline{I} - h(\underline{D}_1 + \underline{E}_4 - \alpha \underline{\Omega})]^{-1} \right\| \\ &\quad \times \|O(h) + O(\Delta x^2) + O(\Delta y^2) + O(\Delta z^2)\|. \end{aligned} \tag{B.2}$$

Theorem 3, proved later in this Appendix gives assurance that $\|e^{\underline{\Omega}h} [\underline{I} - h(\underline{D}_1 + \underline{E}_4 - \alpha \underline{\Omega})]^{-1}\|$ is bounded for the L_2 norm provided the ratios $h/\Delta x^2$, $h/\Delta y^2$, and $h/\Delta z^2$ are fixed, real constants of any finite size. Calling this bound K allows Eq. (B.2) to be written as

$$\left\| \frac{\vec{\theta}(t+h) - \underline{C}_1(\underline{\Omega}, h) \vec{\theta}(t)}{h} \right\| \leq K \|O(h)\|$$

for the L_2 norm. Thus, $\underline{C}_1(\underline{\Omega}, h)$ satisfies the consistency condition.

LEMMA 2.¹ If two operators are consistent, then their product is consistent.

Proof. Let \underline{C}_1 and \underline{C}_2 be two consistent operators, i.e.,

$$\left\| \frac{\vec{\theta}(t+h) - \underline{C}_2 \vec{\theta}(t)}{h} \right\| \rightarrow 0 \text{ as } h \rightarrow 0$$

$$\left\| \frac{\vec{\theta}(t+2h) - \underline{C}_1 \vec{\theta}(t+h)}{h} \right\| \rightarrow 0 \text{ as } h \rightarrow 0.$$

Since \underline{C}_1 is consistent, it has a bounded norm so that

$$\| \underline{C}_1 \| \left\| \frac{\vec{\theta}(t+h) - \underline{C}_2 \vec{\theta}(t)}{h} \right\| \rightarrow 0 \text{ as } h \rightarrow 0.$$

The definition of a norm provides that $\| \underline{C} \vec{x} \| \leq \| \underline{C} \| \| \vec{x} \|$. Therefore,

$$\| \underline{C}_1 \vec{\theta}(t+h) - \underline{C}_1 \underline{C}_2 \vec{\theta}(t) \| \rightarrow 0 \text{ as } h \rightarrow 0.$$

Using the triangle inequality, $\| \vec{x} + \vec{y} \| \leq \| \vec{x} \| + \| \vec{y} \|$, this becomes

$$\left\| \frac{\vec{\theta}(t+2h) - \underline{C}_1 \vec{\theta}(t+h)}{h} + \frac{\underline{C}_1 \vec{\theta}(t+h) - \underline{C}_1 \underline{C}_2 \vec{\theta}(t)}{h} \right\| \rightarrow 0 \text{ as } h \rightarrow 0$$

or

$$\left\| \frac{\vec{\theta}(t+2h) - \underline{C}_1 \underline{C}_2 \vec{\theta}(t)}{h} \right\| \rightarrow 0 \text{ as } h \rightarrow 0, \quad (\text{B.3})$$

which is the consistency requirement for the product.

THEOREM 3.¹ A family of matrices \underline{M}_n of varying dimension n having at most $\ell < n$ nonzero elements in each row or column, ℓ being constant for all n , has a uniform L_2 bound if the individual elements of the matrices \underline{M}_n are uniformly bounded for all n .

Proof. Let $c > 0$ be a bound on the absolute value of the individual elements, $m_{j,k}^n$, of the matrices \underline{M}_n . Then

$$\max_k \sum_{j=1}^n |m_{j,k}^n| \leq c\ell$$

$$\max_j \sum_{k=1}^n |m_{j,k}^n| \leq c\ell$$

for all n . However, by definition,

$$\|\underline{M}_n\|_2^2 = \sup_{\|\vec{x}\|_2=1} \sum_{j=1}^n \left| \sum_{k=1}^n m_{j,k}^n x_k \right|^2.$$

The Cauchy-Schwarz inequality gives

$$\begin{aligned} \|\underline{M}_n\|_2^2 &\leq \sup_{\|\vec{x}\|_2=1} \sum_{j=1}^n \left\{ \left[\sum_{k=1}^n |m_{j,k}^n| \right] \left[\sum_{k=1}^n |m_{j,k}^n x_k^2| \right] \right\} \\ &\leq \sup_{\|\vec{x}\|_2=1} \sum_{j=1}^n \left\{ c\ell \sum_{k=1}^n |m_{j,k}^n x_k^2| \right\} \\ &\leq \sup_{\|\vec{x}\|_2=1} c\ell \sum_{k=1}^n \left\{ |x_k|^2 \sum_{j=1}^n |m_{j,k}^n| \right\} \\ &\leq (c\ell)^2 \sup_{\|\vec{x}\|_2=1} \sum_{k=1}^n |x_k|^2, \end{aligned}$$

$$\|\underline{M}_n\|_2^2 \leq (c\ell)^2,$$

or

$$\|\underline{M}_n\| \leq c\ell, \tag{B.4}$$

and the theorem is proved.

THEOREM 4.¹ The matrices $(\underline{I} - h\underline{R})^{-1}$ and $(\underline{I} + h\underline{R})(\underline{I} - h\underline{R})^{-1}$ have L_2 norms of less than unity provided that $(\underline{R} + \underline{R}^T)$ is negative definite.

Proof. By definition,

$$\|(\underline{I} - h\underline{R})^{-1}\|_2^2 = \max_{\vec{v}} \frac{\vec{v}^T (\underline{I} - h\underline{R}^T)^{-1} (\underline{I} - h\underline{R})^{-1} \vec{v}}{\vec{v}^T \vec{v}}.$$

Let $\vec{u} = (\underline{\mathbf{I}} - h\underline{\mathbf{R}})^{-1}\vec{v}$. Then

$$\begin{aligned} \left\| (\underline{\mathbf{I}} - h\underline{\mathbf{R}})^{-1} \right\|_2^2 &= \max_{\vec{u}} \frac{\vec{u}^T \vec{u}}{\vec{u}^T (\underline{\mathbf{I}} - h\underline{\mathbf{R}}^T) (\underline{\mathbf{I}} - h\underline{\mathbf{R}}) \vec{u}} \\ &= \max_{\vec{u}} \frac{\vec{u}^T \vec{u}}{\vec{u}^T [\underline{\mathbf{I}} - h(\underline{\mathbf{R}}^T + \underline{\mathbf{R}}) + h^2 \underline{\mathbf{R}}^T \underline{\mathbf{R}}] \vec{u}}. \end{aligned} \quad (\text{B.5})$$

If $(\underline{\mathbf{R}}^T + \underline{\mathbf{R}})$ is negative definite, the denominator of Eq. (B.5) is positive and larger than the numerator. Therefore,

$$\left\| (\underline{\mathbf{I}} - h\underline{\mathbf{R}})^{-1} \right\|_2 < 1.$$

Likewise, for the product $(\underline{\mathbf{I}} + h\underline{\mathbf{R}})(\underline{\mathbf{I}} - h\underline{\mathbf{R}})^{-1}$, the L_2 norm is defined as

$$\left\| (\underline{\mathbf{I}} + h\underline{\mathbf{R}})(\underline{\mathbf{I}} - h\underline{\mathbf{R}})^{-1} \right\|_2^2 = \max_{\vec{v}} \frac{\vec{v}^T (\underline{\mathbf{I}} - h\underline{\mathbf{R}}^T)^{-1} (\underline{\mathbf{I}} + h\underline{\mathbf{R}}^T) (\underline{\mathbf{I}} + h\underline{\mathbf{R}}) (\underline{\mathbf{I}} - h\underline{\mathbf{R}})^{-1} \vec{v}}{\vec{v}^T \vec{v}}$$

With \vec{u} defined as before, this becomes

$$\begin{aligned} \left\| (\underline{\mathbf{I}} + h\underline{\mathbf{R}})(\underline{\mathbf{I}} - h\underline{\mathbf{R}})^{-1} \right\|_2^2 &= \max_{\vec{u}} \frac{\vec{u}^T (\underline{\mathbf{I}} + h\underline{\mathbf{R}}^T) (\underline{\mathbf{I}} + h\underline{\mathbf{R}}) \vec{u}}{\vec{u}^T (\underline{\mathbf{I}} - h\underline{\mathbf{R}}^T) (\underline{\mathbf{I}} - h\underline{\mathbf{R}}) \vec{u}} \\ &= \max_{\vec{u}} \frac{\vec{u}^T [\underline{\mathbf{I}} + h(\underline{\mathbf{R}}^T + \underline{\mathbf{R}}) + h^2 \underline{\mathbf{R}}^T \underline{\mathbf{R}}] \vec{u}}{\vec{u}^T [\underline{\mathbf{I}} - h(\underline{\mathbf{R}}^T + \underline{\mathbf{R}}) + h^2 \underline{\mathbf{R}}^T \underline{\mathbf{R}}] \vec{u}}. \end{aligned} \quad (\text{B.6})$$

Again, if $(\underline{\mathbf{R}}^T + \underline{\mathbf{R}})$ is negative definite, the denominator of Eq. (B.6) is larger than the numerator so that

$$\left\| (\underline{\mathbf{I}} + h\underline{\mathbf{R}})(\underline{\mathbf{I}} - h\underline{\mathbf{R}})^{-1} \right\|_2 < 1.$$

THEOREM 5.²⁴ As t approaches infinity, the solution vector $\vec{\psi}(t) = e^{\underline{A}t} \vec{\psi}_0$ approaches $\alpha e^{\omega_0 t} \vec{e}_0$, where ω_0 is the largest eigenvalue of \underline{A} , \vec{e}_0 the corresponding eigenvector, and $\alpha = (\vec{\psi}_0, \vec{e}_0)$.

Proof. Write $\vec{\psi}_0$ as a linear combination of \vec{e}_0 and \vec{v} , where $(\vec{v}, \vec{e}_0) = 0$, that is, $\vec{\psi}_0 = \alpha \vec{e}_0 + \beta \vec{v}$. Now,

$$\alpha (\vec{e}_0, \vec{e}_0) + \beta (\vec{e}_0, \vec{v}) = (\vec{e}_0, \vec{\psi}_0)$$

or

$$\alpha = (\vec{e}_0, \vec{\psi}_0),$$

if (\vec{e}_0, \vec{e}_0) is normalized to unity.

Write $\vec{\psi}(t)$ as

$$\begin{aligned} \vec{\psi}(t) &= e^{\underline{A}t} (\alpha \vec{e}_0 + \beta \vec{v}) \\ &= \alpha e^{\omega_0 t} \vec{e}_0 + \beta e^{\underline{A}t} \vec{v} \\ &= \alpha e^{\omega_0 t} \left[\vec{e}_0 + (\beta/\alpha) e^{\underline{B}t} \vec{v} \right], \end{aligned} \tag{B.7}$$

where

$$\underline{B} = \underline{A} - \omega_0 \underline{I}.$$

Note that the largest eigenvalue of \underline{B} is 0, and all the others are given by $\lambda_i = \omega_i - \omega_0$ and have real parts less than zero.

Now, put \underline{B} in Jordan form:

$$\underline{J} = \underline{S}^{-1} \underline{B} \underline{S} = \begin{bmatrix} \underline{J}_1 & & & & \\ & \underline{J}_2 & & & \\ & & \underline{J}_3 & & \\ & & & \ddots & \\ & & & & \ddots \end{bmatrix}, \tag{B.8}$$

where each of the blocks on the diagonal is of the form

$$\underline{J}_i = \begin{bmatrix} \lambda_i & 1 & & 0 \\ & \lambda_i & 1 & \\ & & \lambda_i & 1 \\ 0 & & & \ddots \end{bmatrix}. \quad (\text{B.9})$$

\underline{J}_i is a p_i by p_i matrix, p_i being less than or equal to the multiplicity of the i^{th} eigenvalue, and the λ_i 's are arranged in order of non-increasing real part. \underline{J}_1 is a 1×1 matrix since the largest eigenvalue of \underline{B} is simple.

Now

$$\begin{aligned} e^{\underline{B}t} \vec{v} &= e^{\underline{S}^{-1} \underline{J} \underline{S} t} \vec{v} \\ &= (\underline{I} + \underline{S}^{-1} (\underline{J}t) \underline{S} + (1/2!) \underline{S}^{-1} (\underline{J}t)^2 \underline{S} + \dots) \vec{v} \\ &= \underline{S}^{-1} e^{\underline{J}t} \underline{S} \vec{v} = \underline{S}^{-1} e^{\underline{J}t} \underline{a}, \end{aligned} \quad (\text{B.10})$$

where $\vec{a} = \underline{S} \vec{v}$. But

$$e^{\underline{J}t} = \begin{bmatrix} 1 & & & 0 \\ & e^{\underline{J}_2 t} & & \\ & & e^{\underline{J}_3 t} & \\ \underline{0} & & & \ddots \end{bmatrix}. \quad (\text{B.11})$$

Since \underline{A} and \underline{B} share the same eigenvectors, \vec{e}_0 is the eigenvector of \underline{B} corresponding to eigenvalue 0, and the transformation \underline{S} also puts \underline{A} into Jordan form. That is,

$$\underline{J}' \underline{S} = \underline{S} \underline{A}, \quad \underline{S}^{-1} \underline{J}' \underline{S} \vec{e}_0 = \underline{A} \vec{e}_0 = \omega_0 \vec{e}_0, \quad \underline{J}' \underline{S} \vec{e}_0 = \omega_0 \underline{S} \vec{e}_0,$$

where

$$\underline{J}' = \begin{bmatrix} \omega_0 & & 0 \\ & \underline{J}'_2 & \\ 0 & & \underline{J}'_3 \\ & & \cdot \\ & & \cdot \\ & & \cdot \end{bmatrix}. \quad (\text{B.12})$$

Thus

$$\underline{S} \underline{e}_0 = \begin{bmatrix} 1 \\ 0 \\ 0 \\ \cdot \\ \cdot \\ \cdot \end{bmatrix} \quad \text{and} \quad \underline{S} = \begin{bmatrix} \underline{e}_0^T \\ \cdot \\ \cdot \\ \cdot \\ \dots \end{bmatrix},$$

so that

$$\underline{S} \underline{v} = \begin{bmatrix} \underline{e}_0^T \underline{v} \\ \cdot \\ \cdot \\ \cdot \\ \cdot \\ \cdot \end{bmatrix} = \begin{bmatrix} 0 \\ \cdot \\ \cdot \\ \cdot \\ \cdot \\ \cdot \end{bmatrix}.$$

The first element of $\underline{S} \underline{v}$ is zero since \underline{e}_0 is orthogonal to \underline{v} .

Now

$$\begin{aligned}
 e^{\underline{J}t} \underline{S} \vec{v} &= \begin{bmatrix} 1 & & & & \\ & e^{\underline{J}_2 t} & & & \\ & & e^{\underline{J}_3 t} & & \\ & & & \ddots & \\ \underline{0} & & & & \ddots \end{bmatrix} \begin{bmatrix} 0 \\ \vec{a}_2 \\ \vec{a}_3 \\ \vdots \\ \vdots \end{bmatrix} \\
 &= \begin{bmatrix} 0 \\ e^{\underline{J}_2 t} \vec{a}_2 \\ e^{\underline{J}_3 t} \vec{a}_3 \\ \vdots \\ \vdots \end{bmatrix}. \tag{B.13}
 \end{aligned}$$

Hence, $\|\underline{S}^{-1} e^{\underline{J}t} \underline{S} \vec{v}\| \leq \|\underline{S}^{-1}\| \sum_{i=2}^n \|e^{\underline{J}_i t}\| \cdot \|\vec{a}_i\|$, which approaches

$$\|\underline{S}^{-1}\| \sum_{i=2}^n \|\vec{a}_i\| \frac{t^{p_i-1}}{(p_i-1)!} e^{t \cdot \text{Re}(\lambda_i)}$$

as t approaches infinity, using Lemma 8.1 from Ref. 20. Since $\text{Re}(\lambda_i)$ is less than zero, all $i > 1$, this norm goes to zero for large t . Hence, $\|(\beta/\alpha) e^{\underline{B}t} \vec{v}\|$ approaches zero as t approaches infinity, and the vector $\vec{e}_0 + (\beta/\alpha) e^{\underline{B}t} \vec{v}$ approaches \vec{e}_0 , completing the proof.

THEOREM 6.² If $\underline{\Omega} = \omega_0 I$, the approximate solution operator $\underline{B}(\underline{\Omega}, h)$ has as its largest eigenvalue $e^{2\omega_0 h}$ with corresponding eigenvalue \vec{e}_0 , where $\underline{A} \vec{e}_0 = \omega_0 \vec{e}_0$.

Proof. Letting $\underline{\Omega} = \omega_o \underline{I}$,

$$\begin{aligned} \underline{B}(\omega_o \underline{I}, h) \vec{e}_o &= e^{\omega_o h} [\underline{I} - h(\underline{A}_4 - \alpha \omega_o \underline{I})]^{-1} [\underline{I} + h(\underline{A}_3 - \alpha \omega_o \underline{I})] \\ &\quad \times [\underline{I} - h(\underline{A}_2 - \alpha \omega_o \underline{I})]^{-1} [\underline{I} + h(\underline{A}_1 - \gamma \omega_o \underline{I})] e^{\omega_o h} \vec{e}_o . \end{aligned}$$

But

$$[\underline{I} + h(\underline{A}_3 - \gamma \omega_o \underline{I})] \vec{e}_o = [\underline{I} - h(\underline{A}_4 - \alpha \omega_o \underline{I})] \vec{e}_o$$

and

$$[\underline{I} + h(\underline{A}_1 - \gamma \omega_o \underline{I})] \vec{e}_o = [\underline{I} - h(\underline{A}_2 - \alpha \omega_o \underline{I})] \vec{e}_o .$$

Therefore,

$$\begin{aligned} \underline{B}(\omega_o \underline{I}, h) \vec{e}_o &= e^{\omega_o h} [\underline{I} - h(\underline{A}_4 - \alpha \omega_o \underline{I})]^{-1} [\underline{I} + h(\underline{A}_3 - \gamma \omega_o \underline{I})] \\ &\quad \times [\underline{I} - h(\underline{A}_2 - \alpha \omega_o \underline{I})]^{-1} [\underline{I} - h(\underline{A}_2 - \alpha \omega_o \underline{I})] e^{\omega_o h} \vec{e}_o \\ &= e^{\omega_o h} [\underline{I} - h(\underline{A}_4 - \alpha \omega_o \underline{I})]^{-1} [\underline{I} - h(\underline{A}_4 - \alpha \omega_o \underline{I})] e^{\omega_o h} \vec{e}_o \end{aligned}$$

or

$$\underline{B}(\omega_o \underline{I}, h) \vec{e}_o = e^{2\omega_o h} \vec{e}_o . \tag{B.14}$$

Appendix C
TEST PROBLEM DATA

The reactor parameters for the four configurations used in Chapter 3 for three-dimensional experiments are presented in this appendix. The symbols used in this appendix are defined as follows:

Δx = mesh spacing (cm) in x-direction

Δy = mesh spacing (cm) in y-direction

Δz = mesh spacing (cm) in z-direction

λ_i = decay constant (sec^{-1}) of i^{th} precursor

β_i = delay fraction of i^{th} precursor

χ_{gi} = fraction of decays of i^{th} precursor which yield neutrons in group g

v_g = velocity of g^{th} neutron group (cm/sec)

χ_g = prompt fission spectrum component for group g

Σ_{tr} = macroscopic transport cross section (cm^{-1})

$D = 1/(3\Sigma_{\text{tr}})$ = diffusion coefficient (cm)

Σ_a = macroscopic absorption cross section (cm^{-1})

Σ_f = macroscopic fission cross section (cm^{-1})

ν = average number of neutrons per fission

$\Sigma_{J \rightarrow J+1}$ = macroscopic scattering cross section from group J to group $J+1$ (cm^{-1}).

Unless otherwise noted, all boundary conditions are homogeneous Dirichlet.

Configuration 1

Number of neutron groups = 2

Number of precursor groups = 1

Geometry: Homogeneous cube, 200 cm on a side

$$\Delta x = \Delta y = \Delta z = 20 \text{ cm}$$

Precursor Constants:

$$\lambda_i = .08, \quad \beta_i = .0064, \quad \chi_{11} = 1.0, \quad \chi_{21} = 0.0$$

Material Properties:

	<u>Group 1</u>	<u>Group 2</u>
ν	3.0×10^7	2.2×10^5
χ	1.0	0.0
Σ_{tr}	.2468	.3084
Σ_a	.001382	.0054869
ν	2.41	2.41
Σ_f	.000242	.00408
$\Sigma_{J \rightarrow J+1}$.0023	0.0

Initial Conditions:

Spatial shape: cosine

Critical k_{eff} : .895285417

Configuration 2

Number of neutron groups = 2

Number of precursor groups = 1

Geometry:

$$\Delta x = \Delta y = \Delta z = 8.0 \text{ cm}$$

$$\text{height} = 160 \text{ cm (z-direction)}$$

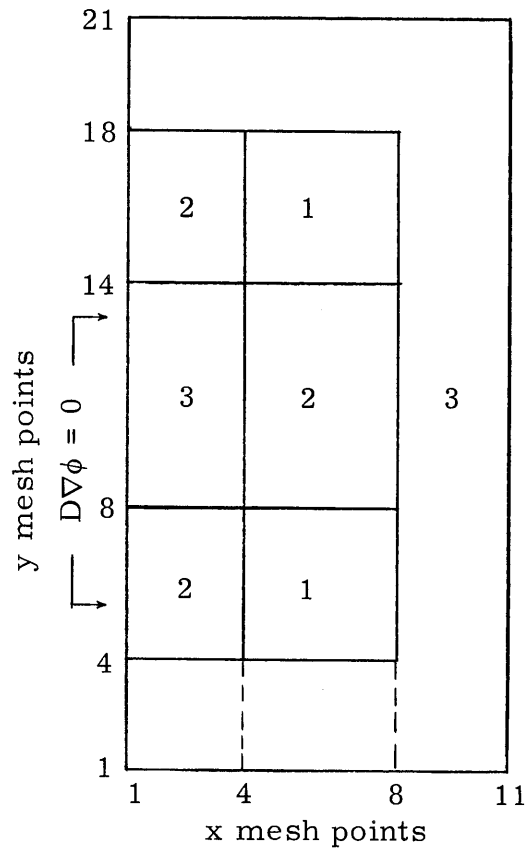


Fig. C.1a. x-y Plane for
 $24 \leq z \leq 136 \text{ cm}$

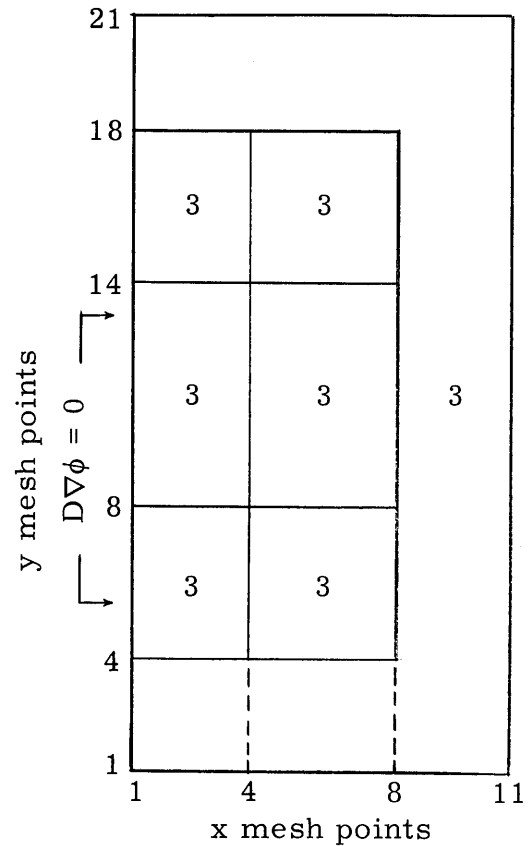


Fig. C.1b. x-y Plane for
 $0 \leq z \leq 24, 136 \leq z \leq 160 \text{ cm}$

The numbers in the various regions indicate the material number in that region. Only the right half of this reactor is shown since the left half is symmetrical to it.

Precursor Constants:

$$\lambda_1 = .08, \quad \beta_1 = .0075, \quad \chi_{11} = 1.0, \quad \chi_{21} = 0.0$$

	<u>Group 1</u>	<u>Group 2</u>
ν	1.0×10^7	2.0×10^5
χ	1.0	0.0

Material Properties:

	<u>Material 1</u>	
	<u>Group 1</u>	<u>Group 2</u>
Σ_{tr}	.238095	.833333
Σ_a	.01	.15
ν	2.40	2.40
Σ_f	.0035	.10
$\Sigma_{J \rightarrow J+1}$.01	0.0

Material 2
(Same as Material 1)

	<u>Material 3</u>	
	<u>Group 1</u>	<u>Group 2</u>
Σ_{tr}	.25461	.666667
Σ_a	.008	.05
ν	2.40	2.40
Σ_f	.0015	.03
$\Sigma_{J \rightarrow J+1}$.01	0.0

Initial Condition:

$$\text{Critical } k_{eff}: 1.06432742$$

Configuration 3

Number of neutron groups = 4

Number of precursor groups = 1

Geometry:

$$\Delta x = \Delta y = \Delta z = 8.0 \text{ cm}$$

height = 120 cm (z-direction)

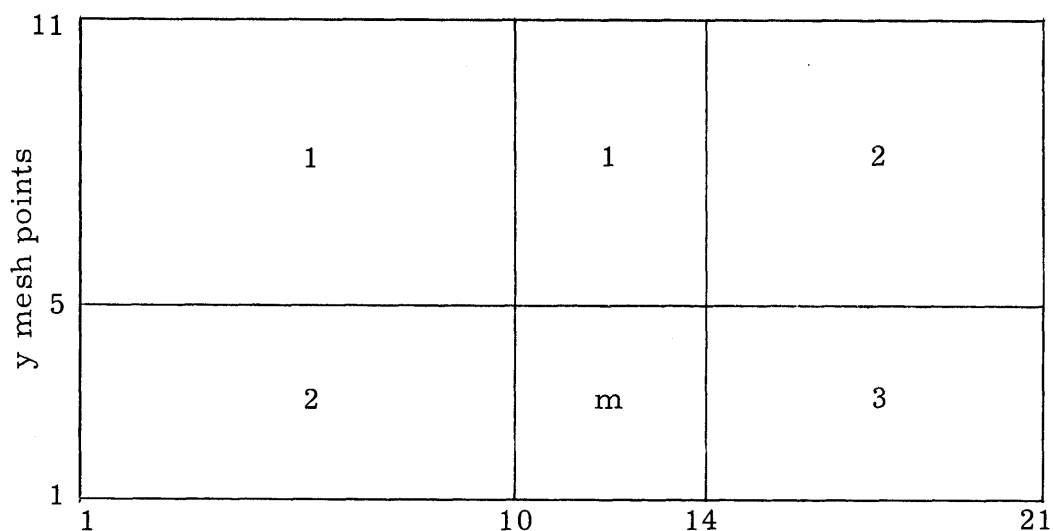


Fig. C.2. x-y Plane for $0 \leq z \leq 120 \text{ cm}$

$$m = 3 \quad \text{for} \quad 0 \leq z \leq 56 \text{ cm}$$

$$m = 4 \quad \text{for} \quad 56 \leq z \leq 120 \text{ cm}$$

Precursor Constants:

$$\lambda_1 = .08, \quad \beta_1 = .0064, \quad \chi_{11} = 0.0, \quad \chi_{21} = 1.0, \quad \chi_{31} = 0.0,$$

$$\chi_{41} = 0.0$$

	<u>Group 1</u>	<u>Group 2</u>	<u>Group 3</u>	<u>Group 4</u>
ν	1.0×10^9	1.0×10^8	5.0×10^6	2.0×10^5
χ	0.755	0.245	0.0	0.0

Material Properties:

	<u>Material 1</u>			
	<u>Group 1</u>	<u>Group 2</u>	<u>Group 3</u>	<u>Group 4</u>
Σ_{tr}	.120	.310	.520	2.050
Σ_a	.00266	.00297	.0359	.655
ν	1.60	1.60	1.60	1.60
Σ_f	.00136	.00197	.0262	.540
$\Sigma_{J \rightarrow J+1}$.0586	.0828	.0850	0.0

	<u>Material 2</u>			
	<u>Group 1</u>	<u>Group 2</u>	<u>Group 3</u>	<u>Group 4</u>
Σ_{tr}	.100	.240	.400	1.600
Σ_a	.00135	.00140	.0176	.332
ν	1.60	1.60	1.60	1.60
Σ_f	.0007	.0009	.0131	.274
$\Sigma_{J \rightarrow J+1}$.0586	.0828	.0850	0.0

	<u>Material 3</u>			
	<u>Group 1</u>	<u>Group 2</u>	<u>Group 3</u>	<u>Group 4</u>
Σ_{tr}	.080	.160	.310	1.270
Σ_a	.00077	.00072	.00051	.012
ν	0.0	0.0	0.0	0.0
Σ_f	0.0	0.0	0.0	0.0
$\Sigma_{J \rightarrow J+1}$.0570	.0822	.0847	0.0

Material 4

(Same as Material 3)

Initial Condition:

Critical k_{eff} : 1.06601870

Configuration 4

Number of neutron groups = 2

Number of precursor groups = 1

Geometry:

Height = 300 cm (z-direction)

$\Delta x = 10.0$ cm, $0 \leq x \leq 20$ cm, $50 \leq x \leq 170$ cm, $200 \leq x \leq 220$ cm

$\Delta x = 7.5$ cm, $20 \leq x \leq 50$ cm, $170 \leq x \leq 200$ cm

$\Delta y = 7.5$ cm, $0 \leq y \leq 30$ cm

$\Delta y = 10.0$ cm, $30 \leq y \leq 110$ cm

$\Delta z = 15.0$ cm, $0 \leq z \leq 30$ cm, $270 \leq z \leq 300$ cm

$\Delta z = 16.0$ cm, $30 \leq z \leq 270$ cm

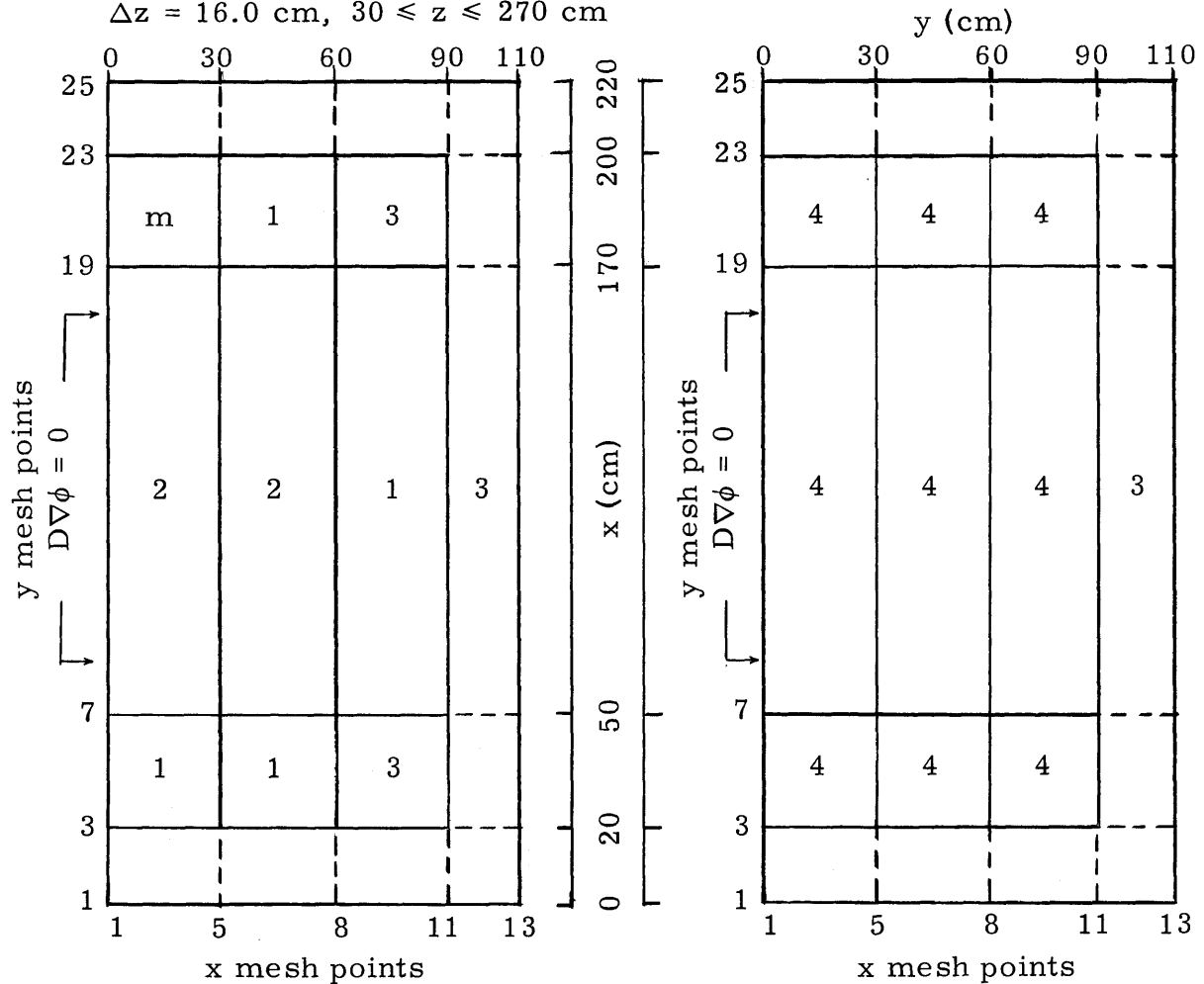


Fig. C.3a. x-y Plane for
 $30 \leq z \leq 270$ cm

Fig. C.3b. x-y Plane for
 $0 \leq z \leq 30$ cm, $270 \leq z \leq 300$ cm

5, for $30 \leq z \leq 110$ cm
 $m = 6$, for $110 \leq z \leq 190$ cm
 7, for $190 \leq z \leq 270$ cm

Precursor Constants:

$$\lambda_1 = .08, \quad \beta_1 = .0064, \quad \chi_{11} = 1.0, \quad \chi_{21} = 0.0$$

	<u>Group 1</u>	<u>Group 2</u>
ν	1.0×10^8	4.4×10^5
χ	1.0	0.0

Material Properties:

Material 1

	<u>Group 1</u>	<u>Group 2</u>
Σ_{tr}	.2246	.8375
Σ_a	.009434	.07345
ν	2.571	2.441
Σ_f	.002437	.05112
$\Sigma_{J \rightarrow J+1}$.01872	0.0

Material 2

	<u>Group 1</u>	<u>Group 2</u>
Σ_{tr}	.2264	.8445
Σ_a	.009223	.06737
ν	2.584	2.442
Σ_f	.002236	.04557
$\Sigma_{J \rightarrow J+1}$.01893	0.0

Material 3

	<u>Group 1</u>	<u>Group 2</u>
Σ_{tr}	.1971	.8685
Σ_a	.0001984	.007207
ν	0.0	0.0
Σ_f	0.0	0.0
$\Sigma_{J \rightarrow J+1}$.03010	0.0

Material 4

	<u>Group 1</u>	<u>Group 2</u>
Σ_{tr}	.1487	.5490
Σ_a	.0003288	.004677
ν	0.0	0.0
Σ_f	0.0	0.0
$\Sigma_{J \rightarrow J+1}$.01798	0.0

Material 5

(Same as Material 1)

Material 6

(Same as Material 1)

Material 7

(Same as Material 1)

Initial Condition:

Critical k_{eff} : 1.28041608

Appendix D

THE COMPUTER PROGRAM 3DKIN

The computer program used to conduct the three-dimensional numerical experiments for this thesis has been named 3DKIN. It is written entirely in Fortran IV for IBM System 360 computers. It can be easily converted to run on any computer with a Fortran IV compiler, however.

The program 3DKIN is described in the several sections of this appendix. It is intended that the description given here be adequate for this appendix to serve as a user's manual for the code. A more detailed description would be necessary for anyone wishing to make modifications to the code, however.

Section D.1 discusses the methods used to obtain an initial steady state solution for a problem. Section D.2 then describes the organization of that part of the code used in a subsequent time-dependent calculation. The overlay structure used to reduce core storage requirements and the input/output devices necessary to run 3DKIN are presented in section D.3. A detailed description of the input information for 3DKIN follows in section D.4. Section D.5 lists the card images of the input data for 3DKIN for a sample problem.

D.1 Description of the Steady State Section

Several comments of a general nature concerning 3DKIN should be made before proceeding to the algorithms used to obtain the initial critical flux distribution and k_{eff} . The first concerns the overall

organization of the code. It has been written in a modular fashion, where each subroutine or set of subroutines performs one task or several closely-related tasks. This facilitates the division of the code into segments for subsequent use of the overlay feature of OS/360. It also allows additional code options such as new geometries to be added to the code without severely altering existing subroutines.

The second comment concerns the use of directly-addressable core storage for the storage of program variables. The variable dimensioning feature of Fortran IV is used throughout the code. In the MAIN routine, a vector named A is placed in the labeled common area ARAY and given a length which corresponds to the total core area which the user desires to allot to program variable storage. Based on input parameters which describe the size of the problem to be considered, a subroutine called MEMORY computes a series of pointer variables. Each pointer variable indicates a location in A where the first member of a program array will be located. The remaining members of that array are then stored in successive locations in A.

The obvious advantage of this technique is that each program array is dimensioned to exactly the size necessary for each particular problem. Core storage is thus used very efficiently. In addition, the total amount of core storage allotted to program variable storage can be changed merely by recompiling the short MAIN routine after changing two statements.

For both the steady state and time-dependent parts of the code, the total core storage necessary to store program variables for each problem is computed. If this amount exceeds the amount allocated to

the vector A in MAIN, another attempt is automatically made to allot storage for program variables. This time, however, the flux and fission source vectors are stored on input/output devices for the steady state section, as are the fluxes and precursor concentrations for the time-dependent section. This greatly reduces the amount of core storage required and allows very large problems to be run.

The remainder of this section describes the program flow in the steady state section. The program entry point is in the MAIN routine. The MAIN routine zeroes out the entire A array and reads in the title card and second card for a particular problem. The second card contains the parameters which completely define the amount of storage required for that problem. Subroutine MEMORY is called to allocate storage for program variables and to determine whether or not input/output devices are required to store several large arrays. If these input/output devices are required, MAIN opens the datasets on these devices. Program control is then passed to subroutine CALLER, which calls the subroutines which control the various first overlay level segments.

Subroutine INPUT is called first to read in the remaining input data for the problem. Subroutine IOEDIT prints out an edited version of the problem description. The flux vector needed to start the iterative solution process is read in either from cards or from a dataset on an input/output device or is generated as a cosine in each dimension. Subroutine FLUXIN performs whichever of these options is requested.

The iterative solution process is controlled by subroutine SSTATE. To detail the form of this iterative process, several equations need to

be restated. The time-dependent equation for the group g flux at all points has been given in Eq. (1.4) as

$$\frac{d\vec{\psi}_g}{dt} = \underline{D}_g \vec{\psi}_g + \sum_{g'=1}^G \underline{T}_{gg'} \vec{\psi}_{g'} + \sum_{i=1}^I \underline{F}_{gi} \vec{C}_i. \quad (1.4)$$

To obtain the initial condition, the time derivative is set to zero.

Further, given the definitions of χ_g and χ_{gi} in section 1.2, a weighted prompt fission spectrum, χ'_g , can be defined as

$$\chi'_g = (1-\beta) \chi_g + \sum_{i=1}^I \beta_i \chi_{gi}. \quad (D.1)$$

If χ'_g replaces χ_g in Eq. (1.4), the precursor concentration term in it can also be ignored for the steady state calculation.

Several additional matrices need to be defined. Let

$$\underline{T}_{gg'} = \underline{v}_g \underline{V}^{-1} (\chi'_g \underline{F}_{g'} + \underline{R}_{gg'}), \quad g' \neq g \quad (D.2a)$$

$$\underline{T}_{gg} = \underline{v}_g \underline{V}^{-1} (\chi'_g \underline{F}_g - \underline{\Sigma}_g) \quad (D.2b)$$

$$\underline{D}_g = \underline{v}_g \underline{V}^{-1} \underline{D}'_g. \quad (D.2c)$$

Here, $\underline{v}_g = v_g \underline{I}$ and \underline{V} is the diagonal matrix of volumes associated with each mesh point. $\underline{F}_{g'}$ is a diagonal matrix containing the $v_{g'} \Sigma_{fg'}$ term for each mesh volume. The matrix $\underline{R}_{gg'}$ is also diagonal and describes the scattering from group g' to g in each mesh volume.

Finally, $\underline{\Sigma}_g$ contains the absorption and out-scattering terms for group g at each mesh volume.

The form of Eq. (1.4) to be solved for the initial condition becomes

$$\underline{v}_g \underline{V}^{-1} (\underline{D}'_g - \underline{\Sigma}_g) \underline{\psi}_g + \underline{v}_g \underline{V}^{-1} \left(\sum_{g' \neq g}^G \underline{R}_{gg'} \underline{\psi}_{g'} + \frac{\chi'_g}{k_{\text{eff}}} \sum_{g'=1}^G \underline{F}_{g'} \underline{\psi}_{g'} \right) = \underline{0},$$

(1 ≤ g ≤ G). (D.3)

In 3DKIN, only downscattering is allowed so that $\underline{R}_{gg'} = \underline{0}$ for $g' > g$.

Equation (D.3) can be reduced to

$$(-\underline{D}'_g + \underline{\Sigma}_g) \underline{\psi}_g = \sum_{g'=1}^{g-1} \underline{R}_{gg'} \underline{\psi}_{g'} + \frac{\chi'_g}{k_{\text{eff}}} \sum_{g'=1}^G \underline{F}_{g'} \underline{\psi}_{g'}.$$

(D.4)

In 3DKIN, Eq. (D.4) is solved by a two-level iterative process.

This is the standard inner iteration-outer iteration method.²⁷ Let the

inner iteration index be m and the outer iteration index be ℓ . The

inner iterations involve solving the equation

$$(-\underline{D}'_g + \underline{\Sigma}_g) \underline{\psi}_g^{\ell+1} = \sum_{g'=1}^{g-1} \underline{R}_{gg'} \underline{\psi}_{g'}^{\ell+1} + \frac{\chi'_g}{\sigma^\ell} \underline{S}^\ell$$

(D.5)

for each group, starting with $g=1$. Here, \underline{S}^ℓ , the fission source vector, and σ^ℓ have been obtained from

$$\sigma^\ell = \frac{\left\| \sum_{g=1}^G \underline{F}_g \underline{\psi}_g^\ell \right\|_1}{\left\| \sum_{g=1}^G \underline{F}_g \underline{\psi}_g^{\ell-1} \right\|_1},$$

(D.6)

$$\underline{S}^\ell = \frac{\mu}{\sigma^\ell} \sum_{g=1}^G \underline{F}_g \underline{\psi}_g^\ell + \frac{(1-\mu)}{\sigma^\ell} \sum_{g=1}^G \underline{F}_g \underline{\psi}_g^\ell.$$

(D.7)

Here, μ is an input fission source overrelaxation parameter bounded

by $1 \leq \mu \leq 2$. The outer iteration consists of the computation of σ^ℓ and an \vec{S}^ℓ , used to start a new set of inner iterations.

The inner iterations in 3DKIN are carried out by a one-line successive overrelaxation method. Lines of fluxes in the x-direction are overrelaxed successively across each z-plane of mesh points, starting with the bottom z-plane. An optimum overrelaxation parameter is computed for each group, using a method prescribed in Ref. 27. The iterative process continues on a particular group until convergence is obtained for that group, where convergence is defined as

$$\max_{l,j,k} \left| \frac{\phi_{g,l,j,k}^m - \phi_{g,l,j,k}^{m-1}}{\phi_{g,l,j,k}^m} \right| \leq \epsilon_2. \quad (\text{D.8})$$

The parameter ϵ is input by the user, as is a parameter m_{\max} . If the condition (D.8) is not satisfied for $m \leq m_{\max}$, the iterative process is stopped for that group automatically for that outer iteration.

As can be seen from Eq. (D.6), the L_1 norm is used as an indication of the total solution change during an outer iteration. In an attempt to speed convergence of the outer iterations, the fission source vector, \vec{S}^ℓ , is overrelaxed in a rather crude fashion. The entire iterative process is completed after the ℓ^{th} outer iteration if condition (D.8) has been satisfied for all groups during that outer iteration and if

$$|1.0 - \sigma^\ell| \leq \epsilon_1. \quad (\text{D.9})$$

At this point, k_{eff} is computed from

$$k_{\text{eff}} = \prod_{n=1}^{\ell} \sigma^n. \quad (\text{D.10})$$

Before starting the iterative process just described, subroutine SSTATE calls subroutine SETUP1 to compute the necessary coefficients. SETUP1 uses subroutine COEF1 to do this.

SSTATE also calls subroutine ORPEST to compute the groupwise optimum overrelaxation parameters. SSTATE computes the fission and scattering source for each group during an outer iteration. Subroutine INNER0 or INNER1 is called to carry out the actual inner iterations for the groups. INNER0 is used if all program variables are stored in core, while INNER1 is used if the flux and fission source vectors are stored on input/output devices. SSTATE completes the outer iteration by computing a new estimate of σ and overrelaxing the fission source vector. It also tests for convergence of the outer iterations. Subroutine SSTOUT prints out a one-line summary of each outer iteration and saves the converged fluxes if requested.

Two additional features of the steady state section of 3DKIN are worthy of note, although they are invisible to the user of 3DKIN. The first is an additional technique used to accelerate convergence of the inner iterations. Before the inner iterations are started for group g during outer iteration $\ell + 1$, the quantities

$$\alpha_1 = \left\| \sum_{g'=1}^{g-1} \underline{R}_{gg'} \vec{\psi}_{g'}^{\ell+1} + \frac{\chi'_g}{\sigma^\ell} \vec{S}^\ell \right\|_1$$

and

$$\alpha_2 = \left\| (-\underline{D}'_g + \underline{\Sigma}_g) \vec{\psi}_g^\ell \right\|_1$$

are computed. The vector $\vec{\psi}_g^\ell$ is multiplied by the ratio (α_1/α_2) , and

the result is used as an initial guess for the inner iterations for group g . This has the effect of scaling the initial guess so that the neutron balance is satisfied in an integral sense when the inner iterations are started. This so-called group rebalancing is carried out by subroutines GRBAL0 and GRBAL1, which are called by INNER0 and INNER1, respectively.

The second feature is the manner in which the coefficients for Eqs. (D.4) are stored in 3DKIN for the x-y-z geometry option. The manner in which planes are passed through the parallelepiped of interest to create the three-dimensional fine mesh has been presented in Appendix A. The only restriction placed on these planes at that time was that every boundary of a homogeneous material region must lie on a fine-mesh plane.

In 3DKIN, an additional restriction is introduced. Each of the fine-mesh planes which has a homogeneous material region boundary coincident on any part of it becomes a coarse-mesh plane. Between two successive coarse-mesh planes in a particular direction, all fine-mesh planes parallel to these coarse-mesh planes must be equidistant.

The reactor of interest is thus divided into a three-dimensional array of rectangular parallelepipeds by the coarse-mesh planes. These rectangular parallelepipeds are hereafter referred to as material regions. Within a given material region, only one material is present. Additionally, fine-mesh spacings are constant across that material region for each of the three directions.

Each material region has a total of 26 faces, edges, and corners associated with it. Thus, regardless of how many fine-mesh points lie

within or on its boundaries, only 27 sets of coefficients need to be computed and stored. The extra set is for all of the fine-mesh points which lie within the boundaries of the material region.

Because of the manner in which faces, edges, and corners are shared by more than one material region, however, an average of only 8 sets need to be associated with each material region. This assumes that the right, upper, and back outer boundaries of the parallelepiped as shown in Fig. A.1 have homogeneous Dirichlet boundary conditions.

In 3DKIN, a so-called problem region number is assigned to each set of coefficients. A three-dimensional array, called a problem region map, is created, with one entry per fine-mesh point. In this problem region map, all fine-mesh points which have the same set of coefficients are assigned the same unique problem region number. Coefficients are computed and stored by problem region number, and the problem region map is used to obtain the proper set of coefficients to be used at a particular fine-mesh point.

The advantages of this method are two-fold. No coefficients ever have to be recomputed during the entire steady state calculation, and each fine-mesh point has a set of coefficients correct for it. At the same time, the amount of storage necessary to contain the coefficients is reduced drastically over that required if a set of coefficients were computed and stored for each fine-mesh point.

D.2 Description of Time-Dependent Section

The program flow for the time-dependent section of 3DKIN is much less complicated than that for the steady state section. This is primarily due to the simplicity of the NSADE algorithm. When the initial condition has been computed, SSTATE returns program control to CALLER. CALLER calls subroutine FLUXTR, which writes the converged fluxes out on an input/output device. CALLER then calls subroutine TIMDEP, which controls the remainder of the time-dependent section.

Subroutine TIMDEP first redefines several coefficients in each problem region. It then calls subroutine DELAYS, which reads the fluxes back in from the input/output device and computes the corresponding pointwise initial precursor concentrations. After zeroing out the frequency array and dividing the various $\nu\Sigma_f$ values by the critical value of k_{eff} , the main time-dependent loop in TIMDEP is entered.

Within this main loop, time is divided into a series of time zones. Within each time zone, a number of materials are allowed to have properties which undergo a step change at the beginning of the time zone and/or a ramp change throughout the time zone. Subroutine TIMINP reads in the data describing each of these time zones.

Within each time zone, subroutine CHANGE is called whenever necessary to recompute coefficients which vary with time. The coefficients are recomputed consistent with the problem region concept. Coefficients are recomputed only for those problem regions which have time-varying properties.

For the case where all problem variables are stored in core, the initial $e^{\Omega h}$ transformation and forward sweep of the spatial mesh for all groups is performed in subroutine STEPA0 for each time step. Subroutine STEPB0 performs the reverse sweep and the second $e^{\Omega h}$ transformation for each time step. Subroutine FREQ0 computes the frequencies for the next time step according to Eq. (2.8). For the case where the fluxes and precursor concentrations are stored on input/output devices, subroutines STEPA1, STEPB1, and FREQ1 perform the same functions as their similarly-named counterparts.

At regular intervals, the fluxes at a number of specified test points are printed out. At the end of each time zone, the entire flux and precursor vector can be printed out if requested. These printouts are obtained from the subroutine TIMEOUT.

D.3 Overlay Structure and Input/Output Devices for 3DKIN

Two levels of overlay are used in 3DKIN. There are a total of 11 segments. The overlay structure is shown in Fig. D.1.

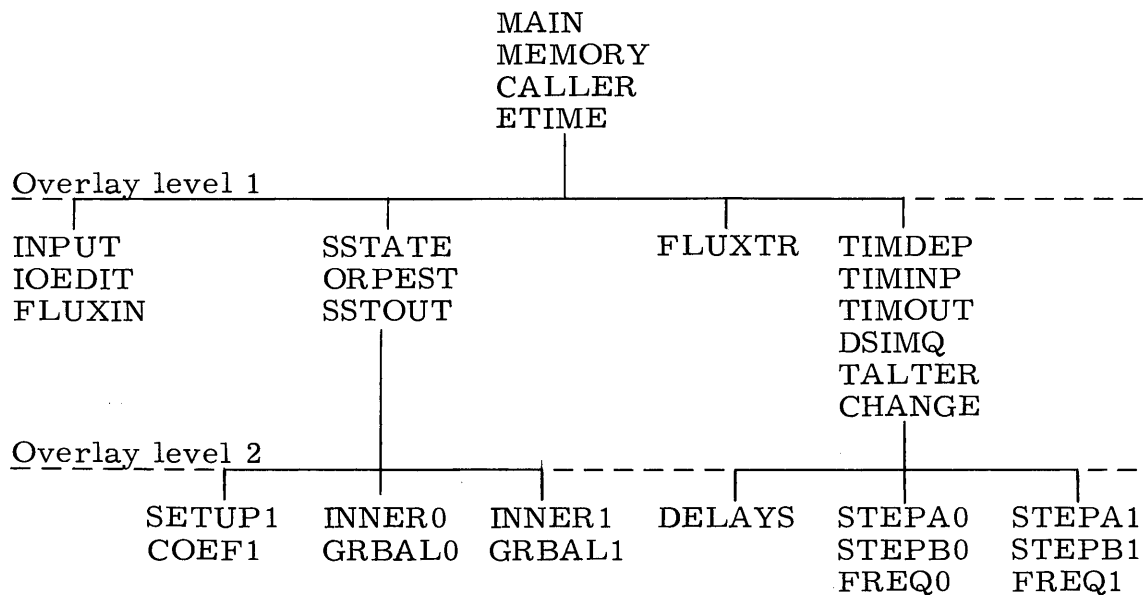


Fig. D.1. Overlay Structure for 3DKIN

Card input to 3DKIN is read in on symbolic device 5, while output to the printer is on device 6. If the option where the fluxes are punched onto cards is requested, the card punch is specified as device 7.

Up to seven sequential datasets on different symbolic devices may be required by 3DKIN. These datasets may each be placed on a separate magnetic tape drive, or they may be placed on one or more disk drives. The disk drives are preferable because their use generally results in faster execution times.

If the option is requested where steady state fluxes are to be stored on an input/output device between runs, this dataset is placed on symbolic device 8. Additionally, symbolic devices 11 and 12 are required for every run in which a time-dependent calculation is to be made. These datasets are used for scratch purposes only.

If the problem is large enough to require that several program vectors be stored on input/output devices, symbolic devices 11 and 12 are required during the steady state calculation as well. The fluxes for each group are spooled back and forth from one to the other during the inner iterations for that group.

In addition, four more symbolic devices are required for scratch purposes for these large problems. During the steady state calculation, old and new fission source vectors alternate on devices 1 and 2. During the time-dependent calculation, the flux for the group used in the frequency calculation is saved from one time step to the next, alternately, on these two devices. Devices 3 and 4 alternate in storing the complete flux vector (and precursors as well during the time-dependent calculation) for both sections of the code. All of these seven datasets are

written with unformatted write statements. Table D.1 summarizes the usage of these datasets.

Table D.1. Input/Output Symbolic Devices

Device Number	Logical Record Length		Number of Records		When Used
	Steady State	Time-Dependent	Steady State	Time-Dependent	
1	L * J	L * J	K	K	IOPT = 1
2	L * J	L * J	K	K	IOPT = 1
3	L * J	L * J * (G+I)	K * G	K	IOPT = 1
4	L * J	L * J * (G+I)	K * G	K	IOPT = 1
8	L * J	L * J	K * G	K * G	When fluxes saved
11	L * J	L * J	K	K * G	Always
12	L * J	L * J	K	K * G	Always

The variables L, J, and K are the number of fine-mesh x-planes, y-planes, and z-planes, respectively. In order to minimize execution time, symbolic devices 1, 3, and 11 should be placed on different disk drives from symbolic devices 2, 4, and 12, respectively.

D.4 Description of Input for 3DKIN

The only geometry currently available in 3DKIN is x-y-z rectangular geometry, as shown in Fig. A.1. For both steady state and time-dependent sections, the right, back, and top faces of the rectangular parallelepiped must have homogeneous Dirichlet boundary conditions.

In the steady state section, the left, front, and bottom faces may each have homogeneous Dirichlet or Neumann boundary conditions specified, independent of what condition is specified for the other two faces. In the time-dependent section, however, the bottom face must always have the homogeneous Dirichlet condition. If only one face is to have a homogeneous Neumann condition, it must be the left face. If quarter-core symmetry is desired, both left and front faces are specified to have a homogeneous Neumann boundary condition.

At the time that the input description of a problem is formulated, an estimate of the amount of core required for program variable storage can be made. Equation (D.11) gives the total number of double precision (64-bit) words required on an IBM System 360 computer in the vector A for each problem. The variables in the equation are defined in the input description.

$$\begin{aligned}
 \text{Min. length of A} = & \text{NNG} * [3+(4+\text{NDNSCT})*\text{NMAT}+\text{NDG}] + 2 * \text{NDG} \\
 & + \text{IM} + \text{JM} + \text{KM} + 3 * (\text{IRM}+\text{JRM}+\text{KRM}+1)/2 \\
 & + 8 * \text{IRM} * \text{JRM} * \text{KRM} * [6*\text{NNG}+(\text{NNG}-1) \\
 & * \text{NDNSCT}+1] + (\text{IRM}*\text{JRM}*\text{KRM}+3)/4 \\
 & + (\text{IM}*\text{JM}*\text{KM}+3)/4 + V_{\text{core}} . \qquad \qquad \qquad (\text{D.11})
 \end{aligned}$$

For the steady state section,

$$\begin{aligned}
 V_{\text{core}} = & 3 * \text{IM} + 5 * \text{NNG} + \text{IM} * \text{JM} * \text{KM} + \\
 & (1-\text{IOPT}) * [\text{IM}*\text{JM}*\text{KM}*(\text{NNG}+2)+5] + \\
 & \text{IOPT} * (5*\text{IM}*\text{JM}+5) .
 \end{aligned}$$

For the time-dependent section,

$$V_{\text{core}} = \text{IM} * \text{JM} * \text{KM} + (1 - \text{IOPT}) * [\text{IM} * \text{JM} * \text{KM} * (\text{NNG} + \text{NDG} + 1) + 5] + \text{IOPT} * [\text{IM} * \text{JM} * (3 * \text{NNG} + 3 * \text{NDG} + 2) + 2].$$

Setting IOPT = 0 gives the minimum length of A required if all variables are to be stored in core. Likewise, setting IOPT = 1 gives the core storage requirement for the option where several vectors are stored on input/output devices.

Using the Fortran H compiler with optimization level 2 and the level 18.6 version of OS-MVT for the IBM 360/65, a total of 77,500 bytes are required to store 3DKIN in core, exclusive of the number of bytes allocated to the vector A. In addition, when the code is actually executed, some additional core is needed for input/output device buffers. With 46,000 8-byte words allocated to A and with about 12,000 bytes allocated to buffers, 3DKIN requires 458,000 bytes of core. A load module of this size was necessary to run Test Case 4 in Chapter 3.

What follows is a card-by-card description of the input for 3DKIN.

Card Type 1

FORMAT(20A4)

Columns 1-80: (ITITLE(I), I=1, 20). This is the alphanumeric problem title.

Card Type 2

FORMAT(20I4)

Columns 1-4: NNG. This is the number of prompt neutron groups.

Columns 5-8: NDG. This is the number of precursor groups.

Columns 9-12: NTG. This is the number of the group to be used in the frequency calculation for the time-dependent section.

Columns 13-16: NDNSCT. This is the maximum number of down-scatter groups for any of the neutron groups. No upscattering is allowed in 3DKIN.

Columns 17-20: NMAT. The code expects to read in a total of NMAT macroscopic cross-section sets. These sets are numbered consecutively, from 1 to NMAT.

Columns 21-24, 25-28, 29-32: IM, JM, KM. These variables give, respectively, the number of fine-mesh x-planes, y-planes, and z-planes. The outer boundary planes are included.

Columns 33-36, 37-40, 41-44: IRM, JRM, KRM. These variables indicate the number of coarse-mesh zones in the x-, y-, and z-direction, respectively.

Columns 45-48, 49-52, 53-56: NXTP, NYTP, NZTP. These are the number of x, y, and z points, respectively, that are to be used in printing out fluxes during the time-dependent calculation. Every IPRSTP steps, a total of NXTP*NYTP*NZTP points will have their flux values printed out.

Columns 57-60: NSTEAD. If NSTEAD = 0, only a time-dependent calculation will be performed. The input fluxes will be taken as the initial condition. If NSTEAD = 1, a steady state calculation will first be performed. If the solution converges within NOIT outer iterations, a time-dependent calculation will follow. If NSTEAD = 2, only a steady state calculation will be performed.

Columns 61-64: IFLIN. If IFLIN = 0, the initial flux will be generated by 3DKIN as a cosine in each direction for each group. If IFLIN = 1, the initial fluxes are to be input on cards. If IFLIN = 2, the initial fluxes are to be read in as a sequential dataset from device 8.

Columns 65-68: IFLOUT. This variable applies only to the output of fluxes at the end of a steady state calculation. If IFLOUT = 0, no fluxes will be output. If IFLOUT = 1, the fluxes will be printed out. If IFLOUT = 2, the fluxes will be printed and also punched onto cards in a 5D16.10 format. If IFLOUT = 3, the fluxes will be printed and also written on device 8 as a sequential dataset. If IFLOUT = 4, the fluxes are only written on device 8.

Columns 69-72: IGEOM. This is the geometry indicator. At present, IGEOM = 1 gives x-y-z geometry, the only option available.

Columns 73-76: IETIME. If IETIME > 0, the outer iteration completed after accumulated computing time exceeds IETIME will be the last. The fluxes at that point are output as indicated by IFLOUT, and the program stops. If IETIME = 0, it is ignored.

Card Type 3

FORMAT(E16.10,4X,3E10.4,3I4)

Columns 1-16: EFFK. This is the initial estimate of k_{eff} . If it is not in the range $.1 \leq k_{\text{eff}} \leq 10.0$, it is set to 1.0.

Columns 21-30: ORFP. This is the parameter used to overrelax the fission source vector, as in Eq. (D.7). It should be in the range $1.0 \leq \text{ORFP} \leq 2.0$.

Columns 31-40: EPS1. This is the eigenvalue convergence parameter, ϵ_1 , from Eq. (D.9).

Columns 41-50: EPS2. This is the flux convergence parameter, ϵ_2 , from Eq. (D.8).

Columns 41-44: NOIT. This is the maximum number of outer iterations allowed in the steady state section. If convergence has not been obtained after NOIT outer iterations, the eigenvalue estimate is printed, the fluxes at that time are output as indicated, and the program is stopped. Provided the fluxes have been saved on cards or on device 8, the latest k_{eff} can be input to a new run with these fluxes and the calculation restarted.

Columns 45-48: NIIT. This is the maximum number of inner iterations per group per outer iteration.

Columns 49-52: NPIT. If the flux and fission source vectors are stored on input/output devices (IOPT=1), then the fluxes for a group are recomputed across each plane a total of NPIT times before going to the next plane during the inner iterations.

Card Type 3'

FORMAT(8E10.4)

Use as many cards as are necessary.

Columns 1-10, 11-20, . . . : (OMEG(NG), NG=1, NNG). These are estimates of the overrelaxation parameters for the inner iterations. If any OMEG(NG) is in the range $.95 \leq \text{OMEG(NG)} \leq 1.05$, all of them will be computed by 3DKIN to be the optimum values. Once the optimum values are known, they can be input and the calculation thus avoided.

Card Type 4

FORMAT (I5, 5(I5,E10.4)/5(I5, E10.4))

One set of these cards is needed for each of the three directions.

First set –

Columns 1-5: NLBC. This is the boundary condition at $x=0$.

NLBC = 0 indicates a zero flux (homogeneous Dirichlet) condition, while NLBC = 1 indicates a zero current (homogeneous Neumann) condition.

Columns 6-10, 11-20; 21-25, 26-35; . . . : (IBP(IR),HX(IR),IR=1,IRM).

IBP(IR) is the right x fine-mesh plane number for the IR^{th} x coarse-mesh region. HX(IR) is the total x -width for that region in centimeters. Additional cards may be used for these pairs of boundary planes and widths. If the last card has five pairs on it, a blank card must follow it.

Second set –

Columns 1-5: NFBC. This is the boundary condition at $y=0$. For

the steady state section, it can be either 0 (zero flux) or 1 (zero current). It can be 1 only if NLBC = 1 for the time-dependent section.

Columns 6-10, 11-20; 21-25, 26-35; . . . : (JBP(JR),HY(JR),JR=1,

JRM). These are the pairs of back fine-mesh y -planes and total y -widths for the y coarse-mesh zones.

Third set –

Columns 1-5: NBBC. This is the boundary condition at $z=0$.

Either a 0 or a 1 can be used for a steady state calculation, but only a zero flux boundary condition is allowed here for the time-dependent calculation.

Columns 6-10, 11-20; 21-25, 26-35; . . . : (KBP(KR),HZ(KR),

KR=1,KRM). These are the pairs of upper fine-mesh z -planes and total z -widths for the z coarse-mesh zones.

Card Type 5

FORMAT(20I4)

Use as many cards as necessary.

Columns 1-4, 5-8, ... : (IXTP(I), I=1, NXTP), (IYTP(I), I=1, NYTP), (IZTP(I), I=1, IZTP). These are the points at which fluxes will be printed out every IPRSTP steps during the time-dependent calculation.

Card Type 6

FORMAT(20I4)

One set of cards is required for each coarse-mesh z-region. Use as many cards as necessary for each set, with 20 values on each card.

Columns 1-4, 5-8, ... : ((MMAPIR, JR, KR), IR=1, IRM), JR=1, JRM). These are the material numbers assigned to each material region in the KRth coarse-mesh z-region.

Card Type 7

FORMAT(6E12.6)

Columns 1-12, 13-24, ... : (V(NG), NG=1, NNG). These are the group velocities in cm/sec.

Card Type 8

FORMAT(6E12.6)

Columns 1-12, 13-24, ... : (XI(NG), NG=1, NNG). This is the prompt fission spectrum.

A set of NNG card type 9's and as many card type 10's as are necessary is input as a package for each material NM, $1 \leq NM \leq NMAT$. The sets start with material 1 and proceed consecutively to material NMAT.

Card Type 9

FORMAT(4E12.6)

Columns 1-12: XNU(NM, NG). This is ν for group NG.

Columns 13-24: SIGF(NM,NG). This is Σ_f for group NG in cm^{-1} .

Columns 25-36: SIGR(NM,NG). This is Σ_a for group NG in cm^{-1} .

Columns 37-48: SIGT(NM,NG). This is Σ_{tr} for group NG in cm^{-1} .

In each set, the NNG card type 9's are arranged consecutively from group 1 to group NNG.

Card Type 10 FORMAT(6E12.6)

Columns 1-12, 13-24, . . . : ((SIGS(NM, NG, NDN), NDN=1, NDNSCT), NG=1, NGX). This is $\Sigma_{s_{g'g}}$ for $g' = \text{NG}+1$ to $g' = \text{NG} + \text{NDNSCT}$ for each group $g = \text{NG}$. $\text{NGX} = \text{NNG}-1$, so no values are read in for group NNG.

Card Type 11 FORMAT(6E12.6)

One or more card type 11 is required for each precursor group. Begin on a new card for each precursor group.

Columns 1-12: ALAM(ND). This is the λ for precursor group ND in sec^{-1} .

Columns 13-24: BETA(ND). This is β for each precursor group ND.

Columns 25-36, 37-48, . . . : (XIP(NG, ND), NG=1, NNG). This is χ_{gi} for all groups g , $1 \leq g \leq \text{NNG}$, for precursor group ND.

Card Type 12 FORMAT(5E16.10)

These cards are needed only if $\text{IFLIN} = 1$. There are a total of $\text{NNG} * \text{KM}$ sets of card type 12's required then. Each set begins on a new card and contains the fluxes for one z-plane and one group. The sets are arranged from plane 1 to plane KM for each group, with those for group 1 coming first.

Columns 1-16, 17-32, . . . : ((PSI(NG, I, J, K), I=1, IM), J=1, JM).

These are the fluxes at all points on z-plane KR for group NG.

For a time-dependent calculation, a set of one card type 13, NNG*ISTPCH card type 14's, and NNG*ILINCH card type 15's are needed for each time zone.

Card Type 13

FORMAT (6I5, 3E12.5)

Columns 1-5: LASZON. If >0, this is the time zone number. If LASZON = 0, this is the last time zone for this problem.

Columns 6-10: ISTPCH. If ISTPCH = 0, no step change in any material properties will occur at the beginning of this time zone. If ISTPCH > 0, then a total of ISTPCH materials have one or more properties which undergo step changes at the beginning of this time zone.

Columns 11-15: ILINCH. ILINCH indicates the total number of materials in which one or more properties will vary as a linear function of time over this time zone.

Columns 16-20: IPRSTP. During the time-dependent calculation, the fluxes at NXTP*NYTP*NZTP points are printed out every IPRSTPth step.

Columns 21-25: ICHHT. This variable is not used at present.

Columns 26-30: IFLOUT. If IFLOUT = 0, fluxes at only the test points are printed out at the end of this time zone. If IFLOUT = 1, the entire flux and precursor vector is printed out at the end of this time zone.

Columns 31-42: HMIN. The value of h ($=\Delta t/2$) to be used throughout this time zone is given here in sec.

Columns 43-54: HMAX. This variable is not used at present.

Columns 55-66: TEND. This is the time at the end of this time zone in sec. It should be an integer multiple of Δt .

Card Type 14

FORMAT (I5, 5X, 5E12.5)

For each material which has a property undergoing a step change, the NNG card type 14's are ordered by group, from group 1 to group NNG. There is a total of $NNG * ISTPCH$ card type 14's in a time zone set.

Columns 1-5: MNSCH(I). This is the material number for which this change takes place.

Columns 11-22: DELSFS(MN, NG). This is the step change in $SIGF(MN, NG)$ for this time zone.

Columns 23-34: DELSRS(MN, NG). This is the step change in $SIGR(MN, NG)$ for this time zone.

Columns 35-46: DELSTS(MN, NG). This is the step change in $SIGT(MN, NG)$ for this time zone.

Columns 47-58: DELS1S(MN, NG). This is the step change in $SIGS(MN, NG, 1)$ for this time zone.

Columns 59-70: DELS2S(MN, NG). This is the step change in $SIGS(MN, NG, 2)$ for this time zone. It is necessary only if $NDNSCT \geq 2$.

The MN above corresponds to the value of MNSCH(I) for this card. At the present time, this option is limited to problems having 4 groups or less. Also, the maximum number of materials which can be changed in each time zone is five. However, both of these limitations can be changed by altering several COMMON statements in the code.

Card Type 15

FORMAT (I5, 5X, 5E12.5)

For each material which has a property undergoing a linear variation, the NNG card type 15's are ordered by group, from group 1 to group NNG. There are a total of $NNG * ILINCH$ card type 15's in a time zone set.

Columns 1-5: MNLCH(I). This is the material number for which this change takes place.

Columns 11-22: DELSFL(MN, NG). This is the total amount by which SIGF(MN, NG) is to vary over this time zone.

Columns 23-34: DELSRL(MN, NG). This is the total amount by which SIGR(MN, NG) is to vary over this time zone.

Columns 35-46: DELSTL(MN, NG). This is the total amount by which SIGT(MN, NG) is to vary over this time zone.

Columns 47-58: DELS1L(MN, NG). This is the total amount by which SIGS(MN, NG, 1) is to vary over this time zone.

Columns 59-70: DELS2L(MN, NG). This is the total amount by which SIGS(MN, NG, 2) is to vary over this time zone. It is required only if $NONSC T \geq 2$.

The MN above corresponds to the value of MNLCH(I) for this card. The limitations concerning number of groups and number of materials apply to card type 15 as they do to card type 14.

Card Type 16

FORMAT (I4)

Columns 1-4: If the number 9999 is placed in these 4 columns, this problem is the last problem in this computer run. If any sequence of numbers other than 9999 is placed here, another problem may be

placed immediately after this card. Each problem must have a complete set of input data.

D.5 Input for Sample Problem

On the pages that follow, the data for running a problem on 3DKIN are presented in card image format. This sample problem is actually the data for Test Case 2. For the steady state calculation, the initial flux guess is generated by 3DKIN. A total of 120 outer iterations are allowed. The time-dependent calculation is set to run out to .3 seconds with a Δt of .001 second. This problem requires about two hours of running time on an IBM 360/65.

FIRST THREE LINES NOT 3DKIN INPUT
 RIGHT DIGIT OF EACH NUMBER IS OVER COLUMN

1	10	20	30	40	50	60	70	80										
THESIS CASE 3: 3-D VERSION OF TWIGLE PROBLEM WITH HALF CORE SYMMETRY																		
2	1	2	1	3	11	21	21	3	5	3	3	5	3	1	0	3	1	0
1.0	1.40000 001.00000-091.00000-08 200 10 1																	
1.0	1.0																	
1	42.4000D 01		83.2000D 01		112.4000D 01													
0	42.4000D 01		83.2000D 01		144.8000D 01		183.2000D 01 212.4000D 01											
0	42.4000D 01		181.1200D 02		212.4000D 01													
1	6	9	3	6	11	16	19	3	11	19								
3	3	3	3	3	3	3	3	3	3	3	3	3	3					
3	3	3	2	1	3	3	2	3	2	1	3	3	3					
3	3	3	3	3	3	3	3	3	3	3	3	3	3					
1.000000D 072.000000D 05																		
1.0	0.0																	
2.400000D 003.500000D-031.000000D-022.380952D-01																		
2.400000D 001.000000D-011.500000D-018.333333D-01																		
1.000000D-020.0																		
2.400000D 003.500000D-031.000000D-022.380952D-01																		
2.400000D 001.000000D-011.500000D-018.333333D-01																		
1.000000D-020.0																		
2.400000D 001.500000D-038.000000D-032.564103D-01																		
2.400000D 003.000000D-025.000000D-026.666667D-01																		
1.000000D-020.0																		
8.000000D-027.500000D-031.000000D 000.0																		
1	0	1	10	0	15.000000D-045.000000D-042.000000D-01													
1	0.00000D 00 0.00000D 00 0.00000D 00 0.00000D 00 0.00000D 00																	
1	0.00000D 00-0.00450D 00 0.00000D 00 0.00000D 00 0.00000D 00																	
2	0	0	10	0	02.500000D-042.500000D-042.100000D-01													
0	0	0	10	0	15.000000D-045.000000D-043.000000D-01													
9999																		

Appendix E
SOURCE LISTING OF 3DKIN

***** STATUS OF 3DKIN AS OF JULY 28, 1971 *****

ALL FEATURES OF 3DKIN AS DESCRIBED IN APPENDIX D HAVE BEEN TESTED AND ARE WORKING EXCEPT FOR THE FOLLOWING ITEMS:

1. THERE IS A BUG SOMEWHERE IN THE STEADY STATE SECTION FOR THE OPTION WHERE FLUX AND FISSION SOURCE VECTORS ARE STORED ON INPUT/OUTPUT DEVICES (IOPT=1).
2. THE SUBROUTINES FOR THE TIME-DEPENDENT SECTION WHICH PERFORM THE FORWARD AND BACKWARD SWEEP AND CALCULATE NEW FREQUENCIES WHEN IOPT=1 (STEP1,STEPB1,FREQ1) HAVE NOT BEEN THOROUGHLY TESTED AND ARE NOT INCLUDED IN THIS LISTING.
3. THE QUARTER-CORE SYMMETRY OPTION (NLBC=1,NFBC=1) FOR THE TIME-DEPENDENT SECTION HAS A BUG IN IT.

VARIABLE DIMENSIONING IS USED THROUGHOUT 3DKIN. SPACE FOR ALL ARRAYS IS ALLOCATED IN THE VECTOR A IN LABELLED COMMON ARAY. A NUMBER OF POINTERS ARE COMPUTED IN SUBROUTINE MEMORY WHICH INDICATE THE LOCATIONS IN A WHERE EACH OF THE FIRST ELEMENTS OF THE ARRAYS ARE STORED. THE POINTERS ARE NAMED SO THAT EACH CONSISTS OF THE LETTER L PREFIXED TO THE ARRAY NAME.

```

MAIN PROGRAM FOR 3DKIN .                                0000010
  IMPLICIT REAL*8 (A-H,O-Z)                             0000020
  INTEGER*2 MMAP,NPRMP                                   0000030
  COMMON/INT3/IASIZE,NNG,NDG,NTOG,NMAT,IM,JM,KM,IRM,JRM,KRM,NLBC, 0000040
  1NFBC,NBBC,NDNSCT,NPRG,IOPT,NTG,NXTP,NYTP,NZTP,IXTP(5),IYTP(5), 0000050
  2IZTP(5),NSTEAD,IFLIN,IGEOM,ITITLE(20),NDIT,NIIT,NPIT,IOPSI,IODUMP, 0000060
  3IOFN,IQFO,IOPN,IQPO,ITEMP,ITEMP1,ITEMP2,ITEMP3,ITEMP4,ITEMP5, 0000070
  4NTIT,IETIME,IFLOUT,IMX,JMX,KMX,IOSC1,IOSC2,NGX        0000080
  COMMON/POINT/LV,LXI,LXIM,LXNU,LSIGF,LSIGR,LSIGT,LSIGS,LALAM,LBETA, 0000090
  1LXIP,LX,LV,LZ,LHX,LHY,LHZ,LIBP,LJBP,LKBP,LDD1,LDD2,LDD3,LDD4,LDD5, 0000100
  2LDD6,LDD7,LVD,LMMAP,LNPRMP,LPSI,LP1,LP2,LP3,LFRO,LFN,LFN,LSRC 0000110
  3,LWA,LGA,LSOLN,LOMEG,LXFISS,LXINSC,LXREM,LXLEK,LTOT,LPSO,LW,LPO,LW 0000120

```


41	COMMON/FLOTE/EFFK, JRFP, EPS1, EPS2, TEMP, TEMP1, TEMP2, TEMP3, TEMP4,	0000121
	1TEMP5, TEMPS, XFISST, XFISSO, ALAMN, ALAMO, TIME, FLXCON, BETAT	0000130
	COMMON/ARAY/A(46000)	0000140
	CALL ETIME	0000150
	IASIZE=46000	0000160
99	DO 100 I=1, IASIZE	0000170
	A(I)=0.000	0000180
100	CONTINUE	0000190
	IOPSI=8	0000200
	IODUMP=10	0000210
	IOFN=1	0000220
	IOFO=2	0000230
	IOPN=3	0000240
	IOPD=4	0000250
	IOSC1=11	0000260
	IOSC2=12	0000270
C	READ CARD 1	0000280
	READ(5,1000)(ITITLE(I),I=1,20)	0000290
1000	FORMAT(20A4)	0000300
	WRITE(6,1010)(ITITLE(I),I=1,20)	0000310
1010	FORMAT(1H1,10X,20A4)	0000320
C	READ CARD 2	0000330
	READ(5,1020)NNG,NDG,NTG,NDNSCT,NMAT,IM,JM,KM,IRM,JRM,KRM,NXTP,NYTP	0000340
	1,NZTP,NSTEAD,IFLIN,IFLOUT,IGEOM,IETIME	0000350
1020	FORMAT(20I4)	0000360
	WRITE(5,1030)NNG,NDG,NTG,NDNSCT,NMAT,IM,JM,KM,IRM,JRM,KRM,NXTP,	0000370
	1NYTP,NZTP,NSTEAD,IFLIN,IFLOUT,IGEOM,IETIME	0000380
1030	FORMAT(11X,20I4)	0000390
	NPRG=8*IRM*JRM*KRM	0000400
	NTDG=NNG+NDG	0000410
	IMX=IM-1	0000420
	JMX=JM-1	0000430
	KMX=KM-1	0000440
	NGX=NNG-1	0000450
	TIME=1.0D+10	0000460

IF(IETIME.NE.0)TIME=IETIME	0000470
IMEM=1	0000480
CALL MEMORY(IMEM)	0000490
IF(IMEM.EQ.5) GO TO 999	0000500
IF(IOPT.EQ.0) GO TO 110	0000510
REWIND IOFN	0000520
REWIND IOFD	0000530
REWIND IOPN	0000540
REWIND IOPD	0000550
REWIND IOSC1	0000560
REWIND IOSC2	0000570
110 CALL CALLER	0000580
READ(5,1040) INDIC	0000590
ITEMP4=9999	0000600
1040 FORMAT(I4)	0000610
IF(INDIC.NE.ITEMP4)GO TO 99	0000620
IF(INDIC.EQ.ITEMP4)WRITE(6,1050)	0000630
1050 FORMAT(1H0,10X,'LAST CASE COMPLETED')	0000640
999 STOP	0000650
END	0000660

SUBROUTINE MEMORY(IMEM)	MEM00010
IMPLICIT REAL*8 (A-H,O-Z)	MEM00020
INTEGER*2 MMAP,NPRMP	MEM00030
COMMON/POINT/LV,LXI,LXIM,LXNU,LSIGF,LSIGR,LSIGT,LSIGS,LALAM,LBETA,	MEM00040
1LXIP,LX,LY,LZ,LHX,LHY,LHZ,LIBP,LJBP,LKBP,LDD1,LDD2,LDD3,LDD4,LDD5,	MEM00050
2LDD6,LDD7,LVD,LMMAP,LNPRMP,LPSI,LP1,LP2,LP3,LFRD,LFRN,LFO,LFN,LSRCMEM	MEM00060
3,LWA,LGA,LSOLN,LOMEG,LXFISS,LXINSC,LXREM,LXLEK,LTOT,LPSO,LW,LPO,LWMEM	MEM00070
41	MEM00071
COMMON/INTG/IASIZE,NNG,NDG,NTOG,NMAT,IM,JM,KM,IRM,JRM,KRM,NLBC,	MEM00080
INFBC,NB3C,NDNSCT,NPRG,IOPT,VTG,NXTP,NYTP,NZTP,IXTP(5),IYTP(5),	MEM00090
2IZTP(5),NSTFAD,IFLIN,IGEOM,ITITLE(20),NJIT,NIIT,NPIT,IJPSI,IODUMP,	MEM00100
3IOFN,IJFO,IOPN,IOPD,ITEMP,ITEMP1,ITEMP2,ITEMP3,ITEMP4,ITEMP5,	MEM00110
4NTIT,IETIME,IFLOUT,IMX,JMX,KMX,IOSC1,IOSC2,NGX	MEM00120
COMMON/FLOTE/EFFK,DRFP,EPS1,EPS2,TEMP,TEMP1,TEMP2,TEMP3,TEMP4,	MEM00130
IEMP5,TEMP6,XFISST,XFISSO,ALAMN,ALAMO,TIME,FLXCON,BETAT	MEM00140
GD TD(100,200),IMEM	MEM00150
100 IOPT=0	MEM00160
LV=1	MEM00170
LXI=LV+NNG	MEM00180
LXIM=LXI+NNG	MEM00190
LXNU=LXIM+NNG	MEM00200
LSIGF=LXNU+NMAT*NNG	MEM00210
LSIGR=LSIGF+NMAT*NNG	MEM00220
LSIGT=LSIGR+NMAT*NNG	MEM00230
LSIGS=LSIGT+NMAT*NNG	MEM00240
LALAM=LSIGS+NMAT*NNG*NDNSCT	MEM00250
LBETA=LALAM+NDG	MEM00260
LXIP=LBETA+NDG	MEM00270
LX=LXIP+NNG*NDG	MEM00280
LY=LX+IM	MEM00290
LZ=LY+JM	MEM00300
LHX=LZ+KM	MEM00310
LHY=LHX+IRM	MEM00320
LHZ=LHY+JRM	MEM00330
LIBP=LHZ+KRM	MEM00340
LJBP=LIBP+(IRM+1)/2	MEM00350

```

LKBP=LJBP+(JRM+1)/2
LDD1=LKBP+(KRM+1)/2
LDD2=LDD1+NPRG*NNG
LDD3=LDD2+NPRG*NNG
LDD4=LDD3+NPRG*NNG
LDD5=LDD4+NPRG*NNG
LDD6=LDD5+NPRG*NNG
LDD7=LDD6+NPRG*NNG
LVD=LDD7+NPRG*NGX*NDNSCT
LMMAP=LVD+NPRG
LNPRMP=LMMAP+(IRM*JRM*KRM+3)/4
C  NOW COMPUTE THOSE POINTERS WHICH MAY VARY WITH IOPT
110 LPSI=LNPRMP+(IM*JM*KM+3)/4
    LP1=LPSI+(1-IOPT)*IM*JM*KM*NNG+IOPT
    LP2=LP1+IM*JM*IOPT+(1-IOPT)
    LP3=LP2+IM*JM*IOPT+(1-IOPT)
    LFR0=LP3+IM*JM*IOPT+(1-IOPT)
    LFRN=LFR0+(1-IOPT)*IM*JM*KM+IOPT
    LFO=LFRN+(1-IOPT)*IM*JM*KM+IOPT
    LFN=LFO+IM*JM*IOPT+(1-IOPT)
    LSRC=LFN+IM*JM*IOPT+(1-IOPT)
    LWA=LSRC+IM*JM*KM
    LGA=LWA+IM
    LSOLN=LGA+IM
    LOMEG=LSOLN+IM
    LXFISS=LOMEG+NNG
    LXINSC=LXFISS+NNG
    LXREM=LXINSC+NNG
    LXLEK=LXREM+NNG
    LTOT=LXLEK+NNG
    IF(IASIZE-LTOT)120,140,140
120 IOPT=IOPT+1
    IF(IOPT.GT.1)GO TO 130
    GO TO 110
130 IMEM=5
    WRITE(6,1000)IASIZE,LTOT

```

```

MEM00360
MEM00370
MEM00380
MEM00390
MEM00400
MEM00410
MEM00420
MEM00430
MEM00431
MEM00440
MEM00450
MEM00460
MEM00470
MEM00480
MEM00490
MEM00500
MEM00510
MEM00520
MEM00530
MEM00540
MEM00550
MEM00560
MEM00570
MEM00580
MEM00590
MEM00600
MEM00610
MEM00620
MEM00630
MEM00640
MEM00650
MEM00660
MEM00670
MEM00680
MEM00690
MEM00700

```

1000	FORMAT(1H ,10X,I6,2X,'WORDS ALLOTTED,',2X,I6,2X,'WORDS NEEDED,COREMEM00710	
	1 CAPACITY EXCEEDED')	MEM00720
	GO TO 300	MEM00730
140	WRITE(6,1010)IASIZE,LTOT	MEM00740
1010	FORMAT(1H ,10X,I6,2X,'WORDS ALLOTTED,',2X,I6,2X,'WORDS USED')	MEM00750
	GO TO 300	MEM00760
C	BRANCH TO HERE TO COMPUTE DIMENSION POINTERS THAT CHANGE FOR	MEM00770
C	KINETICS CALCULATION	MEM00780
200	LP1=LPSI+(1-IOPT)*IM*JM*KM*NTOG+IOPT	MEM00790
	LP2=LP1+IM*JM*NTOG*IOPT+(1-IOPT)	MEM00800
	LP3=LP2+IM*JM*NTOG*IOPT+(1-IOPT)	MEM00810
	LPSD=LP3+IM*JM*NTOG*IOPT+(1-IOPT)	MEM00820
	LW=LPSD+(1-IOPT)*IM*JM*KM+IOPT	MEM00830
	LPD=LW+IM*JM*KM	MEM00840
	LW1=LPD+IM*JM*IOPT+(1-IOPT)	MEM00850
	LTOT=LW1+IM*JM*IOPT+(1-IOPT)	ME4 86
	IF(IASIZE-LTOT)210,230,230	MEM00870
210	IOPT=IOPT+1	MEM00880
	IF(IOPT.GT.1)GO TO 220	MEM00890
	GO TO 200	MEM00900
220	IMEM=5	MEM00910
	WRITE(6,1000)IASIZE,LTOT	MEM00920
	GO TO 300	MEM00930
230	WRITE(6,1010)IASIZE,LTOT	MEM00940
300	RETURN	MEM00950
	END	MEM00960

```

SUBROUTINE CALLER                                CAL00010
IMPLICIT REAL*8 (A-H,O-Z)                       CAL00020
INTEGER*2 MMAP,NPRMP                            CAL00030
COMMON/POINT/LV,LXI,LXIM,LXNU,LSIGF,LSIGR,LSIGT,LSIGS,LALAM,LBETA,CAL00040
1LXIP,LX,LY,LZ,LHX,LHY,LHZ,LIBP,LJBP,LKBP,LDD1,LDD2,LDD3,LDD4,LDD5,CAL00050
2LDD6,LDD7,LVO,LMMAP,LNPRMP,LPSI,LP1,LP2,LP3,LFRD,LFRN,LFO,LFN,LSRCCAL00060
3,LWA,LGA,LSOLN,LOMEG,LXFISS,LXINSC,LXREM,LXLEK,LTOT,LPSO,LW,LPO,LWCAL00070
41                                                CAL00071
COMMON/INTG/IASIZE,NNG,NDG,NTOG,NMAT,IM,JM,KM,IRM,JRM,KRM,NLBC,   CAL00080
INFBC,NBBC,VDNSCT,NPRG,IOPT,NTG,NXTP,NYTP,NZTP,IXTP(5),IYTP(5),   CAL00090
2IZTP(5),NSTEAD,IFLIN,IGEOM,ITITLE(20),NDIT,NIIT,NPIT,IJPSI,IODUMP,CAL00100
3IOFN,IOFO,IOPN,IOPD,ITEMP,ITEMP1,ITEMP2,ITEMP3,ITEMP4,ITEMP5,   CAL00110
4NTIT,IETIME,IFLOUT,IMX,JMX,KMX,IOSC1,IOSC2,NGX                  CAL00120
COMMON/FLOTE/EFFK,DRFP,EPS1,EPS2,TEMP,TEMP1,TEMP2,TEMP3,TEMP4,   CAL00130
1TEMP5,TEMPS,XFISS,XFISSO,ALAMN,ALAMO,TIME,FLXCON,BETAT         CAL00140
COMMON/ARRAY/A(1)                                                CAL00150
C CALL INPUT FOR REMAINDER OF INPUT DATA                        CAL00160
  CALL INPUT(A(LV),A(LXI),A(LXNU),A(LSIGF),A(LSIGR),A(LSIGT),      CAL00170
  1A(LSIGS),A(LALAM),A(LBETA),A(LXIP),A(LX),A(LY),A(LZ),A(LHX),   CAL00180
  2A(LHY),A(LHZ),A(LIBP),A(LJBP),A(LKBP),A(LMMAP),A(LOMEG),NNG,NDG, CAL00190
  3NDNSCT,NMAT,IM,JM,KM,IRM,JRM,KRM)                             CAL00200
C CALL EDIT TO PRINT OUT EDITED VERSION OF PROBLEM DESCRIPTION CAL00210
  CALL IDEDIT(A(LV),A(LXI),A(LXNU),A(LSIGF),A(LSIGR),A(LSIGT),   CAL00220
  1A(LSIGS),A(LALAM),A(LBETA),A(LXIP),A(LX),A(LY),A(LZ),A(LHX),   CAL00230
  2A(LHY),A(LHZ),A(LIBP),A(LJBP),A(LKBP),A(LMMAP),A(LOMEG),NNG,NDG, CAL00240
  3NDNSCT,NMAT,IM,JM,KM,IRM,JRM,KRM)                             CAL00250
C CALL FLUXIN TO INPUT INITIAL FLUX GUESS                       CAL00260
  CALL FLUXIN(A(LPSI),A(LP1),NNG,IM,JM,KM)                       CAL00270
C CALL SSTATE TO COMPUTE COEFFICIENTS, SET UP PROBLEM REGIONS, AND CAL00280
C COMPUTE STEADY STATE FLUXES(IF REQUESTED)                    CAL00290
  CALL SSTATE(A(LV),A(LXI),A(LXIM),A(LXNU),A(LSIGF),A(LSIGR),     CAL00300
  1A(LSIGT),A(LSIGS),A(LALAM),A(LBETA),A(LXIP),A(LX),A(LY),A(LZ),   CAL00310
  2A(LHX),A(LHY),A(LHZ),A(LIBP),A(LJBP),A(LKBP),A(LDD1),A(LDD2),   CAL00320
  3A(LDD3),A(LDD4),A(LDD5),A(LDD6),A(LDD7),A(LVO),A(LMMAP),A(LNPRMP),CAL00330
  4A(LPSI),A(LP1),A(LP2),A(LP3),A(LFRD),A(LFRN),A(LFO),A(LFN),A(LSRC)CAL00340
  5,A(LWA),A(LGA),A(LSOLN),A(LOMEG),A(LXFISS),A(LXINSC),A(LXREM),A(LXCAL00350

```

6LEK),NNG,NDG,NDNSCT,NMAT,IM,JM,KM,IRM,JRM,KRM,NPRG,NGX)	CAL00360
IF(ITEMP.NE.4)GO TO 200	CAL00370
IF(NSTEAD.EQ.2)GO TO 200	CAL00380
WRITE(6,1000)	CAL00390
1000 FORMAT(1H1,///,10X,'PROCEEDING INTO TIME-DEPENDENT CALCULATION')	CAL00400
C CALL FLUXTR TO WRITE FLUXES OUT ON IOSCI FOR PASSAGE TO TIMDEP	CAL00410
CALL FLUXTR(A(LPSI),A(LP2),NNG,IM,JM,KM)	CAL00420
C CALL MEMORY TO REBUILD STORAGE FOR TIME-DEPENDENT CALCULATION	CAL00430
IMEM=2	CAL00440
CALL MEMORY(IMEM)	CAL00450
IF(IMEM.EQ.5)GO TO 200	CAL00460
C CALL TIMDEP TO PERFORM TIME-DEPENDENT CALCULATION	CAL00470
CALL TIMDEP(A(LV),A(LXI),A(LXIM),A(LXNU),A(LSIGF),A(LSIGR),	CAL00480
1A(LSIGT),A(LSTGS),A(LALAM),A(LBETA),A(LXIP),A(LX),A(LY),A(LZ),A(LHC	CAL00490
2X),A(LHY),A(LHZ),A(LIBP),A(LJBP),A(LKBP),A(LDD1),A(LDD2),A(LDD3),	CAL00500
3A(LDD4),A(LDD5),A(LDD6),A(LDD7),A(LVO),A(LMMAP),A(LNPRMP),A(LPSI)	CAL00510
4,A(LP1),A(LP2),A(LP3),A(LPSO),A(LW),A(LPD),A(LW1),NNG,NDG,NTOG,	CAL00520
5NDNSCT,NMAT,IM,JM,KM,IRM,JRM,KRM,NPRG,NGX)	CAL00530
C NOW RETURN TO MAIN	CAL00540
200 RETURN	CAL00550
END	CAL00560

```
SUBROUTINE ETIME
IMPLICIT REAL*8 (A-H,O-Z)
INTEGER TNOW,TSTART,TREL,TI
CALL TIMING(TSTART,TIO)
RETURN
ENTRY ETIMEF(TI)
CALL TIMING(TNOW,TIO)
TREL=TNOW-TSTART
IF(TREL.LT.0)TREL=TREL+8640000
TI=TREL/6000.
RETURN
END
```

```
ETI00010
ETI00020
ETI00030
ETI00040
ETI00050
ETI00060
ETI00070
ETI00080
ETI00090
ETI00100
ETI00110
ETI00120
```



```

SUBROUTINE INPUT(V,XI,XNU,SIGF,SIGR,STGT,SIGS,ALAM,BETA,XIP,X,Y,Z,INP00010
1HX,HY,HZ,IBP,JBP,KBP,MMAP,OMEG,NGV,NDGV,NDNSCV,NMATV,IMV,JMV,KMV,INP00020
2IRMV,JRMV,KRMV) INP00030
  IMPLICIT REAL*8 (A-H,O-Z) INP00040
  INTEGER*2 MMAP,NPRMP INP00050
  COMMON/INTG/IASIZE,NNG,NDG,VTOG,NMAT,IM,JM,KM,IRM,JRM,KRM,NLBC, INP00100
  INFBC,NBFC,NDNSCT,NPRG,IQPT,NTG,NXTP,NYTP,NZTP,IXTP(5),IYTP(5), INP00110
  IZTP(5),NSTEAD,IFLIN,IGEDM,ITITLE(20),NOIT,NIIT,NPIT,IOPSI,IODUMP,INP00120
  3IOFN,IOFO,IOPN,IOPJ,ITEMP,ITEMP1,ITEMP2,ITEMP3,ITEMP4,ITEMP5, INP00130
  4NTIT,IETIME,IFLOUT,IMX,JMX,KMX,IOSC1,IOSC2,NGX INP00140
  COMMON/FLOTE/EFFK,DRFP,EPS1,EPS2,TEMP,TEMP1,TEMP2,TEMP3,TEMP4, INP00150
  1TEMP5,TEMPS,XFISST,XFISSO,ALAMN,ALAMD,TIME,FLXCON,BETAT INP00160
  DIMENSION V(NNGV),XI(NNGV),XNU(NMATV,NNGV),SIGF(NMATV,NNGV), INP00170
  1SIGR(NMATV,NNGV),SIGT(NMATV,NNGV),SIGS(NMATV,NNGV,NDNSCV),ALAM(NDGINP00180
  2V),BETA(NDGV),XIP(NNGV,NDGV),X(IMV),Y(JMV),Z(KMV),HX(IRMV), INP00190
  3HY(JRMV),HZ(KRMV),IBP(IRMV),JBP(JRMV),KBP(KRMV),MMAP(IRMV,JRMV, INP00200
  4KRMV),OMEG(NNGV) INP00210
  DO 100 I=1,5 INP00220
    IXTP(I)=0 INP00230
    IYTP(I)=0 INP00240
    IZTP(I)=0 INP00250
100 CONTINUE INP00260
C READ IN REMAINDER OF TIME-INDEPENDENT INFORMATION INP00270
C ONLY EFFK IS USED IF NSTEAD=0 INP00280
C READ CARD 3 INP00290
  READ(5,1000)EFFK,DRFP,EPS1,EPS2,NOIT,NIIT,NPIT INP00300
1000 FORMAT(D16.10,4X,3D10.4,3I4) INP00310
  WRITE(6,1010)EFFK,DRFP,EPS1,EPS2,NOIT,NIIT,NPIT INP00320
1010 FORMAT(11X,D16.10,4X,3D10.4,3I4) INP00330
  READ(5,1001)(OMEG(NG),NG=1,NNG) INP00340
1001 FORMAT(8E10.4) INP00350
  WRITE(6,1002)(OMEG(NG),NG=1,NNG) INP00360
1002 FORMAT(11X,8E10.4,/(10X,8E10.4)) INP00370
C READ CARDS 4 INP00380
  105 READ(5,1020)NLBC,(IBP(IR),HX(IR),IR=1,IRM) INP00390
  1020 FORMAT(I5,5(I5,E10.4)/5(I5,E10.4)) INP00400

```

WRITE(6,1030)NLBC,(IBP(IR),HX(IR),IR=1,IRM)	INP00410
1030 FORMAT(11X, I5, 5(I5, E10.4)/(10X, 5(I5, E10.4)))	INP00420
READ(5,1020)NFBC,(JBP(JR),HY(JR),JR=1,JRM)	INP00430
WRITE(6,1030)NFBC,(JBP(JR),HY(JR),JR=1,JRM)	INP00440
READ(5,1020)NBBC,(KBP(KR),HZ(KR),KR=1,KRM)	INP00450
WRITE(6,1030)NBBC,(KBP(KR),HZ(KR),KR=1,KRM)	INP00460
C GENERATE MESH SPACINGS AND MESH PLANE DISTANCES FROM ORIGIN	INP00470
IS=1	INP00480
ISS=2	INP00490
DO 120 IR=1,IRM	INP00500
HX(IR)=HX(IR)/(IBP(IR)-IS)	INP00510
IS=IBP(IR)	INP00520
DO 110 I=ISS,IS	INP00530
110 X(I)=X(I-1)+HX(IR)	INP00540
120 ISS=IBP(IR)+1	INP00550
IS=1	INP00560
ISS=2	INP00570
DO 140 JR=1,JRM	INP00580
HY(JR)=HY(JR)/(JBP(JR)-IS)	INP00590
IS=JBP(JR)	INP00600
DO 130 J=ISS,IS	INP00610
130 Y(J)=Y(J-1)+HY(JR)	INP00620
140 ISS=JBP(JR)+1	INP00630
IS=1	INP00640
ISS=2	INP00650
DO 160 KR=1,KRM	INP00660
HZ(KR)=HZ(KR)/(KBP(KR)-IS)	INP00670
IS=KBP(KR)	INP00680
DO 150 K=ISS,IS	INP00690
150 Z(K)=Z(K-1)+HZ(KR)	INP00700
160 ISS=KBP(KR)+1	INP00710
C READ TEST POINTS FOR KINETICS CALCULATIONS CARD 5	INP00720
READ(5,1040)(IXTP(I),I=1,NXTP),(IYTP(I),I=1,NYTP),(IZTP(I),I=1,NZT	INP00730
1P)	INP00740
WRITE(6,1050)(IXTP(I),I=1,NXTP),(IYTP(I),I=1,NYTP),(IZTP(I),I=1,NZ	INP00750
1TP)	INP00760

C	READ IN MATERIAL REGION MAP CARDS 6	INP00770
	DD 170 KR=1, KRM	INP00780
	READ(5,1040)((MMAP(IR,JR,KR),IR=1,IRM),JR=1,JRM)	INP00790
	WRITE(6,1050)((MMAP(IR,JR,KR),IR=1,IRM),JR=1,JRM)	INP00800
	170 CONTINUE	INP00810
	1040 FORMAT(20I4)	INP00820
	1050 FORMAT(11X,20I4)	INP00830
C	READ VELOCITIES CARD 7	INP00840
	READ(5,1060)(V(NG),NG=1,NNG)	INP00850
	WRITE(6,1070)(V(NG),NG=1,NNG)	INP00860
	1060 FORMAT(6E12.6)	INP00870
	1070 FORMAT(11X,6E12.6/(10X,6E12.6))	INP00880
C	READ FISSION SPECTRUM CARD 8	INP00890
	READ(5,1060)(XI(NG),NG=1,NNG)	INP00900
	WRITE(6,1070)(XI(NG),NG=1,NNG)	INP00910
C	READ MATERIAL PROPERTIES	INP00920
	DD 190 NM=1, NMAT	INP00930
C	READ CARD 9	INP00940
	DD 180 NG=1, NNG	INP00950
	READ(5,1060)XNU(NM,NG),SIGF(NM,NG),SIGR(NM,NG),SIGT(NM,NG)	INP00960
	180 WRITE(6,1070)XNU(NM,NG),SIGF(NM,NG),SIGR(NM,NG),SIGT(NM,NG)	INP00970
C	READ CARD 10	INP00980
	READ(5,1060)((SIGS(NM,NG,NDNSC),NDNSC=1,NDNSCT),NG=1,NNG)	INP00990
	WRITE(6,1070)((SIGS(NM,NG,NDNSC),NDNSC=1,NDNSCT),NG=1,NNG)	INP01000
	190 CONTINUE	INP01010
C	READ PRECURSOR DATA CARD 11	INP01020
	DD 200 ND=1, NDG	INP01030
	READ(5,1060)ALAM(ND),BETA(ND),(XIP(NG,ND),NG=1,NNG)	INP01040
	WRITE(6,1070)ALAM(ND),BETA(ND),(XIP(NG,ND),NG=1,NNG)	INP01050
	200 CONTINUE	INP01060
	RETURN	INP01070
	END	INP01080

```

SUBROUTINE IOEDIT(V,XI,XNU,SIGF,SIGR,SIGT,SIGS,ALAM,BETA,XIP,X,Y,ZINP00010
1,HX,HY,HZ,IBP,JBP,KBP,MMAP,OMEG,NNGV,NDGV,NDNSCV,NMATV,IMV,JMV,KMVINP00020
2,IRMV,JRMV,KRMV) INP00030
IMPLICIT REAL*8 (A-H,O-Z) INP00040
INTEGER*2 MMAP,NPRMP INP00050
COMMON/INTG/IASIZE,NNG,NDG,NTOG,NMAT,IM,JM,KM,IRM,JRM,KRM,NLBC, INP00100
1NFBC,NB3C,NDNSCT,NPRG,IQPT,NTG,NXTP,NYTP,NZTP,IXTP(5),IYTP(5), INP00110
2IZTP(5),NSTEAD,IFLIN,IGEOM,ITITLE(20),NDIT,NIIT,NPIT,IJPSI,IODUMP, INP00120
3IDFN,IDFO,IOPN,IOPD,ITEMP,ITEMP1,ITEMP2,ITEMP3,ITEMP4,ITEMP5, INP00130
4NTIT,JETIME,IFLOUT,IMX,JMX,KMX,IOSC1,IOSC2,NGX INP00140
COMMON/FLQTE/EFFK,DRFP,EPS1,EPS2,TEMP,TEMP1,TEMP2,TEMP3,TEMP4, INP00150
1TEMP5,TEMP6,XFISST,XFISSO,ALAMN,ALAMO,TIME,FLXCON,BETAT INP00160
DIMENSION V(NNGV),XI(NNGV),XNU(NMATV,NNGV),SIGF(NMATV,NNGV), INP00170
1SIGR(NMATV,NNGV),SIGT(NMATV,NNGV),SIGS(NMATV,NNGV,NDNSCV),ALAM(NDGINP00180
2V),BETA(NDGV),XIP(NNGV,NDGV),X(IMV),Y(JMV),Z(KMV),HX(IRMV), INP00190
3HY(JRMV),HZ(KRMV),IBP(IRMV),JBP(JRMV),KBP(KRMV),MMAP(IRMV,JRMV, INP00200
4KRMV),OMEG(NNGV) INP00210
WRITE(6,1000)(ITITLE(I),I=1,20) INP00220
1000 FORMAT(1H1,10X,'3DKIN RUN FOR',2X,20A4) INP00230
C WILL ADD REST OF EDITING ROUTINE LATER INP00240
RETURN INP00250
END INP00260

```

SUBROUTINE FLUXIN(PSI,PI,NGV,IMV,JMV,KMV)	FLU00010
IMPLICIT REAL*8 (A-H,O-Z)	FLU00020
INTEGER*2 MMAP,NPRMP	FLU00030
COMMON/INTG/IASIZE,NNG,NDG,NTOG,NMAT,IM,JM,KM,IRM,JRM,KRM,NLBC,	FLU00080
INFBC,NBBC,NDNSCT,NPRG,IOPT,NTG,NXTP,NYTP,NZTP,IXTP(5),IYTP(5),	FLU00090
2IZTP(5),NSTEAD,IFLIN,IGEOM,ITITLE(20),NDIT,NIIT,NPIT,IOPSI,IODUMP,	FLU00100
3IOFN,IOFD,IOPN,IOPD,ITEMP,ITEMP1,ITEMP2,ITEMP3,ITEMP4,ITEMP5,	FLU00110
4NTIT,IETIME,IFLOUT,IMX,JMX,KMX,IOSC1,IOSC2,NGX	FLU00120
COMMON/FLOTE/EFFK,ORFP,EPS1,EPS2,TEMP,TEMP1,TEMP2,TEMP3,TEMP4,	FLU00130
ITEMP5,TEMP5,XFISST,XFISSD,ALAMN,ALAMD,TIME,FLXCON,BETAT	FLU00140
DIMENSION PSI(NNGV,IMV,JMV,KMV),PI(IMV,JMV)	FLU00150
ITEMP=IFLIN+1	FLU00160
ITEMP1=IOPT+1	FLU00170
PI=3.1415926535897900	FLU00180
TWO=2.000	FLU00190
GO TO(100,300,400),ITEMP	FLU00200
0 BRANCH HERE FOR SINE FLUX GUESS	FLU00210
100 DO 200 NG=1,NNG	FLU00220
DO 200 K=1,KM	FLU00230
IF(NBBC.EQ.1)GO TO 110	FLU00240
TEMP1=DSIN((K-1)*PI/(KM-1))	FLU00250
GO TO 120	FLU00260
110 TEMP1=DCOS((K-1)*PI/(TWO*(KM-1)))	FLU00270
120 IF(K.EQ.KM)TEMP1=0.000	FLU00280
DO 190 J=1,JM	FLU00290
IF(NFBC.EQ.1)GO TO 130	FLU00300
TEMP2=DSIN((J-1)*PI/(JM-1))	FLU00310
GO TO 140	FLU00320
130 TEMP2=DCOS((J-1)*PI/(TWO*(JM-1)))	FLU00330
140 IF(J.EQ.JM)TEMP2=0.000	FLU00340
DO 180 I=1,IM	FLU00350
IF(NLBC.EQ.1)GO TO 150	FLU00360
TEMP3=DSIN((I-1)*PI/(IM-1))	FLU00370
GO TO 160	FLU00380
150 TEMP3=DCOS((I-1)*PI/(TWO*(IM-1)))	FLU00390
160 IF(I.EQ.IM)TEMP3=0.000	FLU00400

```

        IF(ITEMP1.EQ.2)GO TO 170
        PSI(NG,I,J,K)=TEMP1*TEMP2*TEMP3
        GO TO 180
170    P1(I,J)=TEMP1*TEMP2*TEMP3
180    CONTINUE
190    CONTINUE
        IF(ITEMP1.EQ.1)GO TO 200
        WRITE(IOPN) P1
200    CONTINUE
        GO TO 999
C     BRANCH HERE FOR FLUXES INPUT ON CARDS
300    DO 340 NG=1,NNG
        DO 340 K=1,KM
            GO TO(310,320),ITEMP1
310    READ(5,1000)((PSI(NG,I,J,K),I=1,IM),J=1,JM)
            IF(K.LT.KM)GO TO 330
            DO 315 J=1,JM
                DO 315 I=1,IM
315    PSI(NG,I,J,KM)=0.000
            GO TO 330
320    READ(5,1000)((P1(I,J),I=1,IM),J=1,JM)
            IF(K.LT.KM)GO TO 325
            DO 324 J=1,JM
                DO 324 I=1,IM
324    P1(I,J)=0.000
325    WRITE(IOPN)P1
330    CONTINUE
340    CONTINUE
1000  FORMAT(5D16.10)
        GO TO 999
C     BRANCH HERE FOR FLUXES INPUT ON TAPE
400    DO 440 NG=1,NNG
        DO 440 K=1,KM
            GO TO(410,420),ITEMP1
410    READ(IOPSI)((PSI(NG,I,J,K),I=1,IM),J=1,JM)
            IF(K.LT.KM)GO TO 430

```

```

FLU00410
FLU00420
FLU00430
FLU00440
FLU00450
FLU00460
FLU00470
FLU00480
FLU00490
FLU00500
FLU00510
FLU00520
FLU00530
FLU00540
FLU00550
FLU00560
FLU00570
FLU00580
FLU00590
FLU00600
FLU00610
FLU00620
FLU00630
FLU00640
FLU00650
FLU00660
FLU00670
FLU00680
FLU00690
FLU00700
FLU00710
FLU00720
FLU00730
FLU00740
FLU00750
FLU00760

```

```
DO 415 J=1, JM
DO 415 I=1, IM
415 PSI(NG, I, J, KM)=0.000
GO TO 430
420 READ(IOPSI)P1
IF(K.LT.KM)GO TO 425
DO 424 J=1, JM
DO 424 I=1, IM
424 P1(I, J)=0.000
425 WRITE(IOPN)P1
430 CONTINUE
440 CONTINUE
999 IF(ITEMP1.EQ.2)REWIND IOPN
RETURN
END
```

```
FLU00770
FLU00780
FLU00790
FLU00800
FLU00810
FLU00820
FLU00830
FLU00840
FLU00850
FLU00860
FLU00870
FLU00880
FLU00890
FLU00900
FLU00910
```

```

SUBROUTINE SSTATE(V,XI,XIM,XNU,SIGF,SIGR,SIGT,SIGS,ALAM,BETA,XIP,XSST00010
1,Y,Z,HX,HY,HZ,IBP,JBP,KBP,DD1,DD2,DD3,DD4,DD5,DD6,DD7,VO,MMAP,NPRMSST00020
2P,PSI,P1,P2,P3,FRO,FRN,FO,FN,SRC,WA,GA,SOLN,OMEG,XFISS,XINSC,XREM,SST00030
3XLEK,NNGV,NDGV,NDNSCV,NMATV,IMV,JMV,KMV,IRMV,JRMV,KRMV,NPRGV,NGXV)SST00040
  IMPLICIT REAL*8 (A-H,O-Z) SST00050
  INTEGER*2 MMAP,NPRMP SST00060
  COMMON/INTG/IASIZE,NNG,NDG,NTOG,NMAT,IM,JM,KM,IRM,JRM,KRM,NLBC, SST00110
  INFBC,NBBC,NDNSCT,NPRG,IOPD,NTG,NXTP,NYTP,NZTP,IXTP(5),IYTP(5), SST00120
  2IZTP(5),NSTEAD,IFLIN,IGEOM,ITITLE(20),NOIT,NIIT,NPIT,IOPSI,IODUMP,SST00130
  3IOPN,IOPD,IOPN,IOPD,ITEMP,ITEMP1,ITEMP2,ITEMP3,ITEMP4,ITEMP5, SST00140
  4NTIT,IETIME,IFLOUT,IMX,JMX,KMX,IOSC1,IOSC2,NGX SST00150
  COMMON/FLOTE/EFFK,DRFP,EPS1,EPS2,TEMP,TEMP1,TEMP2,TEMP3,TEMP4, SST00160
  1TEMP5,TEMP5,XFISST,XFISSO,ALAMN,ALAMO,TIME,FLXCON,BETAT SST00170
  DIMENSION V(NNGV),XI(NNGV),XIM(NNGV),XNU(NMATV,NNGV), SST00180
  1SIGF(NMATV,NNGV),SIGR(NMATV,NNGV),SIGT(NMATV,NNGV),SIGS(NMATV,NNGV)SST00190
  2,NDNSCV),ALAM(NDGV),BETA(NDGV),XIP(NNGV,NDGV),X(IMV),Y(JMV),Z(KMV)SST00200
  3,HX(IRMV),HY(JRMV),HZ(KRMV),IBP(IRMV),JBP(JRMV),KBP(KRMV),DD1(NPRGSST00210
  4V,NNGV),DD2(NPRGV,NNGV),DD3(NPRGV,NNGV),DD4(NPRGV,NNGV),DD5(NPRGV,SST00220
  5NNGV),DD6(NPRGV,NNGV),DD7(NPRGV,NGXV,NDNSCV),MMAP(IRMV,JRMV,KRMV),SST00230
  6NPRMP(IMV,JMV,KMV),PSI(NNGV,IMV,JMV,KMV),P1(IMV,JMV),P2(IMV,JMV), SST00240
  7P3(IMV,JMV),FRO(IMV,JMV,KMV),FRN(IMV,JMV,KMV),FO(IMV,JMV),FN(IMV,JSST00250
  8MV),SRC(IMV,JMV,KMV),WA(IMV),GA(IMV),SOLN(IMV),OMEG(NNGV),XFISS(NNSST00260
  9GV),XINSC(NNGV),XREM(NNGV),XLEK(NNGV),VO(NPRGV) SST00270
  WRITE(6,1000)(ITITLE(I),I=1,20) SST00280
1000 FORMAT(1H1,10X,'SSTATE ENTERED FOR',2X,20A4) SST00290
C CALL SETUP1 TO COMPUTE PROBLEM REGION NUMBERS, GENERATE NPRMP(I,J,K)SST00300
C AND COMPUTE COEFFICIENTS SST00310
  CALL SETUP1(V,XI,XNU,SIGF,SIGR,SIGT,SIGS,X,Y,Z,HX,HY,HZ,IBP,JBP, SST00320
  1KBP,DD1,DD2,DD3,DD4,DD5,DD6,DD7,VO,MMAP,NPRMP,NNG,NDG,NDNSCT,NMAT,SST00330
  2IM,JM,KM,IRM,JRM,KRM,NPRG,NGX) SST00340
C SWITCH FLUX TAPE DESIGNATIONS SST00350
  ITEMP=IOPD SST00360
  IOPD=IOPN SST00370
  IOPN=ITEMP SST00380
  ITEMP=4 SST00390
  ONE=1.000 SST00392

```


HALF=0.500	SST00393
BETAT=0.000	SST00394
DO 80 ND=1,NDG	SST00395
80 BETAT=BETAT+BETA(ND)	SST00396
DO 85 NG=1,NNG	SST00400
85 XIM(NG)=XI(NG)*(1.000-BETAT)/EFFK	SST00410
IF(NSTEAD.EQ.0) GO TO 540	SST00420
DO 90 NG=1,NNG	SST00430
IF(OMEG(NG).LT..95.OR.OMEG(NG).GT.1.05)GO TO 90	SST00440
GO TO 95	SST00450
90 CONTINUE	SST00460
GO TO 99	SST00470
95 CALL ORPEST(X,Y,Z,FX,HY,HZ,DD1,DD2,DD3,DD4,DD5,MMAP,NPRMP,PS I,	SST00480
IP1,P2,P3,FRD,FRN,FD,FN,SRG,WA,GA,SOLN,OMEG,XFISS,XINSC,XREM,	SST00490
ZXLEK,NNG,NMAT,IM,JM,KM,IRM,JRM,KRM,NPRG)	SST00500
C COMPUTE POINT FISSION SOURCE	SST00510
99 DO 140 NG=1,NNG	SST00520
XFISS(NG)=0.000	SST00530
VOLB=ONE	SST00531
VOLF=ONE	SST00532
VOLL=ONE	SST00533
IF(NB3C.EQ.1)VOLB=HALF	SST00534
DO 140 K=1,KM	SST00540
IF(K.GT.1)VOLB=ONE	SST00541
IF(NF3C.EQ.1)VOLF=HALF	SST00542
IF(IOPT.EQ.0) GO TO 100	SST00550
READ (IDPO)P2	SST00560
IF(K.EQ.KM) GO TO 140	SST00570
100 DO 130 J=1,JMX	SST00580
IF(J.GT.1)VOLF=ONE	SST00581
VOLC=VOLF*VOLB	SST00582
IF(NL3C.EQ.1)VOLL=HALF	SST00583
DO 130 I=1,IMX	SST00590
IF(I.GT.1)VOLL=ONE	SST00591
VOLD=VOLL*VOLC	SST00592
NPR=NPRMP(I,J,K)	SST00600

IF(IOPT.EQ.1) GO TO 110	SST00610
FRO(I,J,K)=FRO(I,J,K)+DD6(NPR,NG)*PSI(NG,I,J,K)	SST00620
XFISS(NG)=XFISS(NG)+DD6(NPR,NG)*PSI(NG,I,J,K)*VOLD	SST00630
GO TO 120	SST00640
C IF FISSION SOURCE ON I/O, STORE TEMPORARILY IN SRC(I,J,K)	SST00650
110 SRC(I,J,K)=SRC(I,J,K)+DD6(NPR,NG)*P2(I,J)	SST00660
XFISS(NG)=XFISS(NG)+DD6(NPR,NG)*P2(I,J)*VOLD	SST00670
120 CONTINUE	SST00680
130 CONTINUE	SST00690
140 CONTINUE	SST00700
XFISST=0.000	SST00710
TEMP=0.000	SST00720
IF(EFFK.LT.0.1.OR.EFFK.GT.10.0)EFFK=1.000	SST00730
ALAMN=ONE	SST00740
DO 150 NG=1,NNG	SST00750
150 TEMP=TEMP+XFISS(NG)	SST00760
DO 160 NG=1,NNG	SST00770
TEMP2=0.000	SST00772
DO 155 ND=1,NDG	SST00773
155 TEMP2=TEMP2+XIP(NG,ND)*BETA(ND)/EFFK	SST00775
XIM(NG)=XI(NG)*(1.000-BETAT)/EFFK	SST00780
XFISS(NG)=(XIM(NG)+TEMP2)*TEMP	SST00790
160 XFISST=XFISST+XFISS(NG)	SST00800
IF(IOPT.EQ.0) GO TO 180	SST00810
DO 170 K=1,KM	SST00820
170 WRITE (IDFJ)((SRC(I,J,K),I=1,IM),J=1,JM)	SST00830
REWIND IDFJ	SST00840
REWIND IDPJ	SST00850
C OUTER ITERATION LOOP STARTS HERE	SST00860
180 NJITT=0	SST00870
190 CONTINUE	SST00880
NTIT=0	SST00890
NG=1	SST00900
FLXCON=0.000	SST00910
200 CONTINUE	SST00920
C ZERO SOURCE AND ADD IN FISSION SOURCE	SST00930

```

TEMP=0.000
D3 205 ND=1,NDG
205 TEMP=TEMP+XIP(NG,ND)*BETA(ND)/EFFK
D3 240 K=1,KM
IF(IOPT.EQ.0) GO TO 210
READ(IOFO) FO
IF(K.EQ.KM) GO TO 240
210 D3 230 J=1,JMX
D3 230 I=1,IMX
SRC(I,J,K)=0.000
IF(IOPT.EQ.0) GO TO 220
SRC(I,J,K)=SRC(I,J,K)+(XIM(NG)+TEMP)*FO(I,J)
GO TO 230
220 SRC(I,J,K)=SRC(I,J,K)+(XIM(NG)+TEMP)*FRD(I,J,K)
IF(NG.EQ.1)FRN(I,J,K)=0.000
230 CONTINUE
240 CONTINUE
IF(IOPT.EQ.1) REWIND IOFO
C ADD IN SCATTERING SOURCES
ITEMP1=NG-NDNSCT
IF(ITEMP1.GE.1) GO TO 250
ITEMP1=1
250 ITEM2=NG-1
IF(ITEM2.LE.NDNSCT)GO TO 260
ITEM2=NDNSCT
260 IF(ITEM1.GE.NG) GO TO 310
C SCATTERING SOURCE TO GROUP NG FROM GROUP ITEM1
270 D3 300 K=1,KM
IF(IOPT.EQ.1) READ(IOPN)P2
IF(K.EQ.KM)GO TO 300
D3 290 J=1,JMX
D3 290 I=1,IMX
NPR=NPRMP(I,J,K)
IF(IOPT.EQ.1) GO TO 280
SRC(I,J,K)=SRC(I,J,K)+DD7(NPR,ITEMP1,ITEMP2)*PSI(ITEMP1,I,J,K)
GO TO 290

```

```

SST00931
SST00932
SST00933
SST00940
SST00950
SST00960
SST00970
SST00980
SST00990
SST01000
SST01010
SST01020
SST01030
SST01040
SST01050
SST01060
SST01070
SST01080
SST01090
SST01100
SST01110
SST01120
SST01130
SST01140
SST01150
SST01160
SST01170
SST01180
SST01190
SST01200
SST01210
SST01220
SST01230
SST01240
SST01250
SST01260

```

280	SRC(I,J,K)=SRC(I,J,K)+DD7(NPR,ITEMP1,ITEMP2)*P2(I,J)	SST01270
290	CONTINUE	SST01280
300	CONTINUE	SST01290
310	ITEMP1=ITEMP1+1	SST01300
	ITEMP2=ITEMP2-1	SST01310
	IF(ITEMP1.LT.NG)GO TO 270	SST01320
C	SOURCE NOW CALCULATED I/O DEVICE IOPD READY TO READ IN FIRST PLANE	SST01330
C	FOR GROUP NG IF IOPT=1	SST01340
	TEMP=0.000	SST01350
	VOLB=ONE	SST01351
	VOLF=ONE	SST01352
	VOLL=ONE	SST01353
	IF(NB8C.EQ.1)VOLB=HALF	SST01354
	DO 320 K=1,KMX	SST01360
	IF(K.GT.1)VOLB=ONE	SST01361
	IF(NF8C.EQ.1)VOLF=HALF	SST01362
	DO 320 J=1,JMX	SST01370
	IF(J.GT.1)VOLF=ONE	SST01371
	VOLC=VOLB*VOLF	SST01372
	IF(NL8C.EQ.1)VOLL=HALF	SST01373
	DO 320 I=1,IMX	SST01380
	IF(I.GT.1)VOLL=ONE	SST01381
	TEMP=TEMP+SRC(I,J,K)*VOLC*VOLL	SST01390
320	CONTINUE	SST01400
	XINSC(NG)=TEMP-XFISS(NG)	SST01410
C	NOW PERFORM INNER ITERATIONS FOR GROUP NG	SST01420
	ITEMP5=1	SST01430
	IF(NOITT.GT.0.AND.FLCOND.LT.1.0D-5)ITEMP5=5	SST01435
	IF(IOPT.EQ.1)GO TO 330	SST01440
	CALL INVER0(X,Y,Z,HX,HY,HZ,DD1,DD2,DD3,DD4,DD5,MMAP,NPRMP,PSI,P1,	SST01450
	1P2,P3,FJ,SRC,WA,GA,SOLN,OMEG,XFISS,XINSC,XREM,XLEK,NNG,NMAT,IM,	SST01460
	2JM,KM,IRM,JRM,KRM,NPRG,NG)	SST01470
	IF(TEMP3.GT.FLXCON)FLXCON=TEMP3	SST01480
	GO TO 400	SST01490
330	CALL INVER1(X,Y,Z,HX,HY,HZ,DD1,DD2,DD3,DD4,DD5,MMAP,NPRMP,PSI,P1,	SST01500
	1P2,P3,FJ,SRC,WA,GA,SOLN,OMEG,XFISS,XINSC,XREM,XLEK,NNG,NMAT,IM,	SST01510

2 JM, KM, IRM, JRM, KRM, NPRG, NG)	SST01520
IF(TEMP3.GT.FLXCON)FLXCON=TEMP3	SST01530
REWIND IOSCI	SST01540
DD 340 ITEMP4=1,NDNSCT	SST01550
DD 340 K=1, KM	SST01560
BACKSPACE IOPN	SST01570
340 CONTINUE	SST01580
C IOPN HAS NOW BEEN POSITIONED TO COMPUTE SCATTERING SOURCE FOR NEXT	SST01590
C GROUP. IOSCI CAN BE USED TO OBTAIN FLUXES FOR COMPUTING FN	SST01600
DD 380 K=1, KM	SST01610
READ(IOSCI)P2	SST01620
IF(K.EQ.KM)GO TO 380	SST01630
IF(NG.GT.1)GO TO 360	SST01640
DD 350 J=1, JMX	SST01650
DD 350 I=1, IMX	SST01660
NPR=NPRMP(I, J, K)	SST01670
350 SRC(I, J, K)=DD6(NPR, NG)*P2(I, J)	SST01680
GO TO 380	SST01690
360 READ(IOFN)FN	SST01700
DD 370 J=1, JMX	SST01710
DD 370 I=1, IMX	SST01720
NPR=NPRMP(I, J, K)	SST01730
370 SRC(I, J, K)=FN(I, J)+DD6(NPR, NG)*P2(I, J)	SST01740
380 CONTINUE	SST01750
IF(NG.GT.1)REWIND IOFN	SST01760
DD 390 K=1, KM	SST01770
WRITE(IOFN)((SRC(I, J, K), I=1, IM), J=1, JM)	SST01780
390 CONTINUE	SST01790
REWIND IOSCI	SST01800
REWIND IOFN	SST01810
GO TO 420	SST01820
400 DD 410 K=1, KM	SST01830
DD 410 J=1, JMX	SST01840
DD 410 I=1, IMX	SST01850
NPR=NPRMP(I, J, K)	SST01860
410 FRN(I, J, K)=FRN(I, J, K)+DD6(NPR, NG)*PSI(NG, I, J, K)	SST01870

```

420 NG=NG+1
    IF(NG.LE.NNG) GO TO 200
C   NOW ONE OUTER ITERATION HAS BEEN COMPLETED
C   NEW FISSION SOURCE IS STORED IN SRC IF IOPT=1
    FLCOND=FLXCON
    XFISSD=XFISST
    TEMP5=0.000
    TEMP6=0.000
    VOLB=ONE
    VOLF=ONE
    VOLL=ONE
    IF(NB3C.EQ.1)VOLB=HALF
    IF(IOPT.FQ.1) GO TO 450
    DO 430 K=1,KMX
    IF(K.GT.1)VOLB=ONE
    IF(NFBC.EQ.1)VOLF=HALF
    DO 430 J=1,JMX
    IF(J.GT.1)VOLF=ONE
    VOLC=VOLB*VOLF
    IF(NL3C.EQ.1)VOLL=HALF
    DO 430 I=1,IMX
    IF(I.GT.1)VOLL=ONE
    VOLD=VOLC*VOLL
    TEMP5=TEMP5+FRN(I,J,K)*VOLD
    FRN(I,J,K)=FRO(I,J,K)+ORFP*(FRN(I,J,K)-FRO(I,J,K))
430 TEMP6=TEMP6+FRN(I,J,K)*VOLD
    TEMP=TEMP5/TEMP6
    DO 440 K=1,KMX
    DO 440 J=1,JMX
    DO 440 I=1,IMX
440 FRO(I,J,K)=TEMP*FRN(I,J,K)
    GO TO 490
450 DO 460 K=1,KMX
    IF(K.GT.1)VOLB=ONE
    IF(NFBC.EQ.1)VOLF=HALF
    READ(IOFD) FO

```

```

SST01880
SST01890
SST01900
SST01910
SST01920
SST01930
SST01940
SST01950
SST01951
SST01952
SST01953
SST01954
SST01960
SST01970
SST01971
SST01972
SST01980
SST01981
SST01982
SST01983
SST01990
SST01991
SST01992
SST02000
SST02010
SST02020
SST02030
SST02040
SST02050
SST02060
SST02070
SST02080
SST02090
SST02091
SST02092
SST02100

```

```

DO 460 J=1, JMX
IF(J.GT.1)VOLF=ONE
VOLC=VOLB*VOLF
IF(NL3C.EQ.1)VOLL=HALF
DO 460 I=1, IMX
IF(I.GT.1)VOLL=ONE
VOLD=VOLC*VOLL
TEMP5=TEMP5+SRC(I, J, K)*VOLD
SRC(I, J, K)=FO(I, J)+DRFP*(SRC(I, J, K)-FO(I, J))
460 TEMP6=TEMP6+SRC(I, J, K)*VOLD
TEMP=TEMP5/TEMP6
DO 480 K=1, KMX
DO 470 J=1, JMX
DO 470 I=1, IMX
470 FN(I, J)=SRC(I, J, K)*TEMP
WRITE(IDFN)FN
480 CONTINUE
REWIND IOFJ
REWIND IOFN
REWIND IOPJ
REWIND IOPV
490 XFISST=0.000
DO 500 NG=1, NNG
TEMP1=0.000
DO 495 ND=1, NDG
495 TEMP1=TEMP1+BETA(ND)*XIP(NG, ND)/EFFK
XFISS(NG)=(XIM(NG)+TEMP1)*TEMP5
500 XFISST=XFISST+XFISS(NG)
ALAMQ=ALAMN
ALAMN=XFISST/XFISSQ
DO 510 NG=1, NNG
XFISS(NG)=XFISS(NG)/ALAMN
510 XIM(NG)=XIM(NG)/ALAMN
XFISST=XFISST/ALAMN
C CONVERGENCE TESTS
NGOTO=1

```

```

SST02110
SST02111
SST02112
SST02113
SST02120
SST02121
SST02122
SST02130
SST02140
SST02150
SST02160
SST02170
SST02180
SST02190
SST02200
SST02210
SST02220
SST02230
SST02240
SST02250
SST02260
SST02270
SST02280
SST02281
SST02282
SST02283
SST02290
SST02300
SST02310
SST02320
SST02330
SST02340
SST02350
SST02360
SST02370
SST02380

```

NDITT=NDITT+1	SST02390
IF(IETIME.EQ.0)GO TO 520	SST02400
CALL ETIMEF(TEMP)	SST02410
IF(TEMP.GT.TIME)NGOTO=2	SST02420
520 IF(NDITT.GE.NDIT)NGOTO=3	SST02430
IF(DABS(1.0DO-ALAMN).LE.EPS1.AND.FLXCJN.LE.EPS2)NGOTO=4	SST02440
C COMPUTE NEW K-EFFECTIVE	SST02450
EFFK=0.000	SST02460
TEMP=0.000	SST02470
DO 530 NG=1,NNG	SST02480
EFFK=EFFK+XIM(NG)	SST02490
530 TEMP=TEMP+XI(NG)	SST02500
EFFK=(TEMP/EFFK)*(1.000-BETAT)	SST02510
C SWITCH I/O DEVICES	SST02520
ITEMP1=IOPN	SST02530
IOPN=IOPO	SST02540
IOPO=ITEMP1	SST02550
ITEMP1=IOFN	SST02560
IOFN=IOFO	SST02570
IOFO=ITEMP1	SST02580
C IF IOPT=1, LATEST FLUXES ON IOPO AND LATEST FISSION SOURCE ON IOFO	SST02590
C CALL STEADY STATE ITERATION PRINT MONITOR	SST02600
CALL SSTOUT(PSI,P2,NNG,IM,JM,KM,NGOTO,NDITT)	SST02610
C IF NGOTO=1, LOOP TO 190 TO BEGIN ANOTHER OUTER ITERATION	SST02620
C IF NGOTO=2, HAVE EXCEEDED RUNNING TIME	SST02630
C IF NGOTO=3, HAVE REACHED MAX. NO. OF OUTER ITERATIONS	SST02640
C IF NGOTO=4, HAVE ACHIEVED CONVERGENCE, CAN GO ON TO TIME-DEP CALC.	SST02650
ITEMP=NGOTO	SST02660
GO TO (190,540,540,540),NGOTO	SST02670
540 CONTINUE	SST02680
RETURN	SST02690
END	SST02700


```

SUBROUTINE DRPEST(X,Y,Z,HX,HY,HZ,DD1,DD2,DD3,DD4,DD5,MMAP,NPRMP, ORP00010
1PSI,P1,P2,P3,FRD,FRN,FO,FN,SRG,WA,GA,SOLN,DMEG,XFISS,XINSC,XREM, ORP00020
2XLEK,NNGV,NMATV,IMV,JMV,KMV,IRMV,JRMV,KRMV,NPRGV) ORP00030
IMPLICIT REAL*8 (A-H,O-Z) ORP00040
INTEGER*2 MMAP,NPRMP ORP00050
COMMON/INTS/IASIZE,NNG,NDG,NTDG,NMAT,IM,JM,KM,IRM,JRM,KRM,NLBC, ORP00100
1NFRG,NBBC,NDNSCT,VPRG,IOPT,VTG,NXTP,NYTP,NZTP,IXTP(5),IYTP(5), ORP00110
2IZTP(5),NSTFAD,IFLIN,IGEOM,ITITLE(20),NIIT,NIIT,NPIT,IOPSI,IODUMP, ORP00120
3IOFN,IOFO,IOPN,IOPJ,ITEMP,ITEMP1,ITEMP2,ITEMP3,ITEMP4,ITEMP5, ORP00130
4NTIT,IETIME,IFLOUT,IMX,JMX,KMX,IOSC1,IOSC2,NGX ORP00140
COMMON/FLOTE/EFFK,DRFP,EPS1,EPS2,TEMP,TEMP1,TEMP2,TEMP3,TEMP4, ORP00150
1TEMP5,TEMP6,XFISST,XFISSD,ALAMN,ALAMO,TIME,FLXCJN,BETAT ORP00160
DIMENSION X(IMV),Y(JMV),Z(KMV),HX(IRMV),HY(JRMV),HZ(KRMV), ORP00170
1DD1(NPRGV,NNGV),DD2(NPRGV,NNGV),DD3(NPRGV,NNGV),DD4(NPRGV,NNGV), ORP00180
2DD5(NPRGV,NNGV),MMAP(IRMV,JRMV,KRMV),VPRMP(IMV,JMV,KMV), ORP00190
3PSI(NNGV,IMV,JMV,KMV),P1(IMV,JMV),P2(IMV,JMV),P3(IMV,JMV), ORP00200
4FRD(IMV,JMV,KMV),FRN(IMV,JMV,KMV),FO(IMV,JMV),FN(IMV,JMV), ORP00210
5SRG(IMV,JMV,KMV),WA(IMV),GA(IMV),SOLN(IMV),DMEG(NNGV),XFISS(NNGV), ORP00220
6XINSC(NNGV),XREM(NNGV),XLEK(NNGV) ORP00230
C SAVE NIIT AND NPIT ORP00240
ITEMP1=NIIT ORP00250
ITEMP2=NPIT ORP00260
ITEMP5=5 ORP00270
C INITIALIZE SRC ORP00280
DO 100 K=1,KM ORP00290
DO 100 J=1,JM ORP00300
DO 100 I=1,IM ORP00310
100 SRC(I,J,K)=0.000 ORP00320
DO 260 NG=1,NNG ORP00330
C STORE INITIAL FLUXES FOR GROUP NG IN FRD IF IOPT=0 ORP00340
IF(IOPT.EQ.1)GO TO 120 ORP00350
DO 110 K=1,KM ORP00360
DO 110 J=1,JM ORP00370
DO 110 I=1,IM ORP00380
110 FRD(I,J,K)=PSI(NG,I,J,K) ORP00390
GO TO 140 ORP00400

```

120	REWIND IOSCI	ORP00410
	DD 130 K=1, KM	ORP00420
	READ(IOP0)P2	ORP00430
	WRITE(IOSCI)P2	ORP00440
130	CONTINUE	ORP00450
C	NOW INITIALIZE SOME PARAMETERS	ORP00460
140	NPIT=1	ORP00470
	NIIT=5	ORP00480
	OMEGBJ=0.000	ORP00490
	OMEGBL=0.000	ORP00500
	ICT=0	ORP00510
	ALAMES=0.000	ORP00520
150	CONTINUE	ORP00530
	IF(IOPT.EQ.1)GO TO 170	ORP00540
	DD 160 K=1, KM	ORP00550
	DD 160 J=1, JM	ORP00560
	DD 160 I=1, IM	ORP00570
160	FRN(I, J, K)=PSI(NG, I, J, K)	ORP00580
	CALL INNER0(X, Y, Z, HX, HY, HZ, DD1, DD2, DD3, DD4, DD5, MMAP, NPRMP, PSI,	ORP00590
	1P1, P2, P3, F3, SRC, WA, GA, SOLN, OMEG, XFISS, XINSC, XREM, XLEK, NNG, NMAT,	ORP00600
	2IM, JM, KM, IRM, JRM, KRM, NPRG, NG)	ORP00610
	GO TO 180	ORP00620
170	CALL INNER1(X, Y, Z, HX, HY, HZ, DD1, DD2, DD3, DD4, DD5, MMAP, NPRMP, PSI,	ORP00630
	1P1, P2, P3, F3, SRC, WA, GA, SOLN, OMEG, XFISS, XINSC, XREM, XLEK, NNG, NMAT,	ORP00640
	2IM, JM, KM, IRM, JRM, KRM, NPRG, NG)	ORP00650
180	NIIT=!	ORP00660
	ICT=ICT+1	ORP00670
	IF(ICT.LE.1)GO TO 150	ORP00680
C	COMPUTE LAMBDA(M)	ORP00690
	TEMP5=0.000	ORP00700
	TEMP6=0.000	ORP00710
	IF(IOPT.EQ.1)GO TO 200	ORP00720
	DD 190 K=1, KM	ORP00730
	DD 190 J=1, JM	ORP00740
	DD 190 I=1, IM	ORP00750
	TEMP5=TEMP5+PSI(NG, I, J, K)*PSI(NG, I, J, K)	ORP00760

```

TEMP6=TEMP5+PSI(NG,I,J,K)*FRN(I,J,K)
190 CONTINUE
GO TO 230
200 REWIND IDSC2
REWIND IDSC1
DO 220 K=1,KMX
READ(IDSC1)P2
READ(IDSC2)P1
DO 210 J=1,JM
DO 210 I=1,IM
TEMP5=TEMP5+P2(I,J)*P2(I,J)
210 TEMP6=TEMP6+P1(I,J)*P2(I,J)
220 CONTINUE
230 ALAMES=TEMP5/TEMP5
TEMP4=DABS(1.000-1.000/TEMP4)
TEMP1=DABS(1.000-1.000/TEMP1)
ALAMES=DABS(1.000-ALAMES)
OMEGBU=2.000/(1.000+DSQRT(TEMP4))
OMEGBL=2.000/(1.000+DSQRT(TEMP1))
OMEGM=2.000/(1.000+DSQRT(ALAMES))
IF(DABS(OMEGBU-OMEGBL).LE.((2.000-OMEGM)/1.001))GO TO 240
IF(1CT.LT.15)GO TO 150
C NOW STORE OMEGM AS OMEG(NG)
240 OMEG(NG)=OMEGM
C STORE INITIAL FLUXES BACK INTO PSI IF IOPT=0
IF(IOPT.EQ.1)GO TO 260
DO 250 K=1,KM
DO 250 J=1,JM
DO 250 I=1,IM
PSI(NG,I,J,K)=FRD(I,J,K)
250 FRD(I,J,K)=0.000
260 CONTINUE
IF(IOPT.EQ.1)REWIND IOPO
WRITE(6,1000)(OMEG(NG),NG=1,NNG)
1000 FORMAT(1H0,10X,'OPTIMUM OMEGAS NOW COMPUTED'//(10X,6E15.8))
NIIT=ITEMP1

```

```

DRP00770
DRP00780
DRP00790
DRP00800
DRP00810
DRP00820
DRP00830
DRP00840
DRP00850
DRP00860
DRP00870
DRP00880
DRP00890
DRP00900
DRP00910
DRP00920
DRP00930
DRP00940
DRP00950
DRP00960
DRP00970
DRP00980
DRP00990
DRP01000
DRP01010
DRP01020
DRP01030
DRP01040
DRP01050
DRP01060
DRP01070
DRP01080
DRP01090
DRP01100
DRP01110
DRP01120

```

NPIT=ITEMP2
RETURN
END

DRP01130
DRP01140
DRP01150

```

SUBROUTINE SSTOUT(PSI,P2,NNGV,IMV,JMV,KMV,NGOTO,NOITT)          SST00010
  IMPLICIT REAL*8 (A-H,O-Z)                                    SST00020
  INTEGER*2 MMAP,NPRMP                                         SST00030
  COMMON/INTG/IASIZE,NNG,NDG,NTOG,NMAT,IM,JM,KM,IRM,JRM,KRM,NLBC, SST00080
  1NFBC,NBBC,NDNSCT,NPRG,IOPN,NTG,NXTP,NYTP,NZTP,IXTP(5),IYTP(5), SST00090
  2IZTP(5),NSTEAD,IFLIN,IGEDM,ITITLE(20),NOIT,NIIT,NPIT,IJPSI,IODUMP,SST00100
  3IOFN,IOPD,IOPN,IOPD,ITEMP,ITEMP1,ITEMP2,ITEMP3,ITEMP4,ITEMP5, SST00110
  4NTIT,IETIME,IFLOUT,IMX,JMX,KMX,IOSC1,IOSC2,NGX              SST00120
  COMMON/FLDTE/EFFK,DRFP,EPS1,EPS2,TEMP,TEMP1,TEMP2,TEMP3,TEMP4, SST00130
  1TEMP5,TEMP6,XFISST,XFISSQ,ALAMN,ALAMD,TIME,FLXCON,BFTAT     SST00140
  DIMENSION PSI(NNGV,IMV,JMV,KMV),P2(IMV,JMV)                SST00150
  TEMP1=DABS(1.000-ALAMD/ALAMN)                                 SST00160
  CALL ETIME=(TEMP)                                           SST00170
  IF(NOITT.GT.1)GO TO 100                                       SST00180
  WRITE(6,1010)                                                SST00190
1010 FORMAT(1H0,/,53X,'OUTER ITERATION SUMMARY',/)           SST00200
  WRITE(6,1020)                                                SST00210
1020 FORMAT(1H ,11X,'OUTER IT.',5X,'NO. OF INNER',6X,'TOTAL COMP.',7X, SST00220
  1'REL. FLUX',9X,'LAMBDA',27X,'ESTIMATED')                   SST00230
  WRITE(6,1030)                                                SST00240
1030 FORMAT(1H ,12X,'NUMBER',9X,'ITERATIONS',7X,'TIME(MIN.)',6X,' CONVESST00250
  1RGENCE',6X,'CONVERGENCE',8X,'LAMBDA',9X,'K-EFFECTIVE',/)   SST00260
  100 WRITE(6,1040)NOITT,NTIT,TEMP,FLXCON,TEMP1,ALAMN,EFFK    SST00270
1040 FORMAT(1H ,13X,I4,13X,I4,11X,F8.3,6X,3D17.9,1X,F16.12)  SST00280
  IF(NGOTO.EQ.1)GO TO 220                                       SST00290
  WRITE(6,1050)                                                SST00300
1050 FORMAT(1H0,10X,'STEADY STATE ITERATIONS TERMINATED')    SST00310
  IF(NGOTO.EQ.2)WRITE(6,1060)                                  SST00320
1060 FORMAT(1H ,15X,'INSUFFICIENT TIME REMAINING FOR ANOTHER ITERATION'SST00330
  1)                                                            SST00340
  IF(NGOTO.EQ.3)WRITE(6,1070)                                  SST00350
1070 FORMAT(1H ,15X,'MAXIMUM NUMBER OF OUTER ITERATIONS EXCEEDED') SST00360
  IF(NGOTO.EQ.4)WRITE(6,1080)                                  SST00370
1080 FORMAT(1H ,15X,'CONVERGENCE HAS BEEN ACHIEVED')         SST00380
  IF IFLOUT = 0, RETURN                                         SST00390
  IF(IFLOUT.EQ.0)GO TO 220                                     SST00400

```

```

C   IF IFLOUT = 1, 2, OR 3, PRINT FLUXES
    IF(IFLOUT.EQ.4)GO TO 180
    WRITE(6,1090)(ITITLE(I),I=1,20)
1090 FORMAT(1H1,///,10X,'FINAL FLUXES FOR THE RUN ',20A4)
    JME=JM
    IF(JM.GT.50)JME=50
    ITEMP2=50/JME
    JMS=1
    DO 170 NG=1,NNG
    DO 160 K=1,KM
    IF(K.GT.1.OR.NG.GT.1)WRITE(6,1100)
1100 FORMAT(1H1,/)
    WRITE(6,1110)NG,K
1110 FORMAT(1H0,10X,'FLUXES FOR GROUP ',I2,' , PLANE 'I2)
    IF(IOPT.EQ.1)READ(IOPO)P2
    JMS=1
    JME=JM
    IF(JM.GT.50)JME=50
    ITEMP2=50/JME
    ITEMP5=ITEMP2
    DO 140 I=1,IM,10
    IS=I
    IE=I+9
    IF(IE.GT.IM)IE=IM
    IF((I-1)/10.LT.ITEMP5)GO TO 110
    WRITE(6,1100)
    ITEMP5=ITEMP5+50/ITEMP2
110 WRITE(6,1120)(ITEMP3,ITEMP3=IS,IE)
1120 FORMAT(1H0,3X,'J / I',2X,I7,9I12)
    DO 130 ITEMP3=JMS,JME
    J=JME+1-ITEMP3
    IF(IOPT.EQ.1)GO TO 120
    WRITE(6,1130)J,(PSI(NG,II,J,K),II=IS,IE)
1130 FORMAT(1H ,2X,I2,6X,1P10D12.5)
    GO TO 130
120 WRITE(6,1130)J,(P2(II,J),II=IS,IE)

```

```

SST00410
SST00420
SST00430
SST00440
SST00450
SST00460
SST00470
SST00480
SST00490
SST00500
SST00510
SST00520
SST00530
SST00540
SST00550
SST00560
SST00570
SST00580
SST00590
SST00591
SST00600
SST00610
SST00620
SST00630
SST00640
SST00650
SST00660
SST00670
SST00680
SST00690
SST00700
SST00710
SST00720
SST00730
SST00740
SST00750

```

130	CONTINUE	SST00760
	IF(JME.GE.JM)GO TO 140	SST00770
	JMS=JME+1	SST00780
	JME=JMS+49	SST00790
	IF(JME.GT.JM)JME=JM	SST00800
	WRITE(6,1100)	SST00810
	GO TO 110	SST00820
140	CONTINUE	SST00830
	IF(IFLOUT.NE.2)GO TO 160	SST00840
	IF(IOPT.EQ.1)GO TO 150	SST00850
	WRITE(7,1140)((PSI(NG,I,J,K),I=1,IM),J=1,JM)	SST00860
1140	FORMAT(5D16.10)	SST00870
	GO TO 160	SST00880
150	WRITE(7,1140)((P2(I,J),I=1,IM),J=1,JM)	SST00890
160	CONTINUE	SST00900
170	CONTINUE	SST00910
	IF(IOPT.EQ.1)REWIND IOPD	SST00920
	IF(IFLOUT.LT.3)GO TO 220	SST00930
180	REWIND IOPSI	SST00940
	D3 210 NG=1,NNG	SST00950
	D3 200 K=1,KM	SST00960
	IF(IOPT.EQ.1)GO TO 190	SST00970
	WRITE(IOPSI)((PSI(NG,I,J,K),I=1,IM),J=1,JM)	SST00980
	GO TO 200	SST00990
190	READ(IOPD)P2	SST01000
	WRITE(IOPSI)P2	SST01010
200	CONTINUE	SST01020
210	CONTINUE	SST01030
	IF(IOPT.EQ.1)REWIND IOPD	SST01040
	REWIND IOPSI	SST01050
220	RETURN	SST01060
	END	SST01070

```

SUBROUTINE SETUP1(V,XI,XNU,SIGF,SIGR,SIGT,SIGS,X,Y,Z,HX,HY,HZ,IBP,SET00010
1 JBP,KBP,DDL,DD2,DD3,DD4,DD5,DD6,DD7,VJ,MMAP,NPRMP,NNGV,NDGV,NDNSCV,SET00020
2,NMATV,IMV,JMV,KMV,IRMV,JRMV,KRMV,NPRGV,NGXV) SET00030
IMPLICIT REAL*8 (A-H,O-Z) SET00040
INTEGER*2 MMAP,NPRMP SET00050
COMMON/INTS/IASIZE,NNG,NDG,NTOG,NMAT,IM,JM,KM,IRM,JRM,KRM,NLBC, SET00100
1NFBC,NBBC,NDNSCT,NPRG,IOP,NTG,NXTP,NYTP,NZTP,IXTP(5),IYTP(5), SET00110
2IZTP(5),NSTEAD,IFLIN,IGEOM,ITITLE(20),NOIT,NIIT,NPIT,IOPSI,IODUMP,SET00120
3IOFN,IOPD,IOPN,IOPJ,ITEMP,ITEMP1,ITEMP2,ITEMP3,ITEMP4,ITEMP5, SET00130
4NTIT,IETIME,IFLQUT,IMX,JMX,KMX,IOSC1,IOSC2,NGX SET00140
COMMON/FLOTE/EFFK,JRFP,EPS1,EPS2,TEMP,TEMP1,TEMP2,TEMP3,TEMP4, SET00150
1TEMP5,TEMP5,XFISST,XFISSO,ALAMN,ALAMD,TIME,FLXCJN,BETAT SET00160
DIMENSION V(NNGV),XI(NNGV),XNU(NMATV,NNGV), SET00170
1SIGF(NMATV,NNGV),SIGR(NMATV,NNGV),SIGT(NMATV,NNGV),SIGS(NMATV,NNGV,SET00180
2,NDNSCV),X(IMV),Y(JMV),Z(KMV),VO(NPRGV), SET00190
3HX(IRMV),HY(JRMV),HZ(KRMV),IBP(IRMV),JBP(JRMV),KBP(KRMV),DD1(NPRGV,SET00200
4,NNGV),DD2(NPRGV,NNGV),DD3(NPRGV,NNGV),DD4(NPRGV,NNGV),DD5(NPRGV,NSET00210
5NGV),DD6(NPRGV,NNGV),DD7(NPRGV,NGXV,NDNSCV),MMAP(IRMV,JRMV,KRMV), SET00220
6NPRMP(IMV,JMV,KMV) SET00230
DIMENSION HD(6),MN(8) SET00240
DO 102 NM=1,NMAT SET00250
DO 101 NG=1,NNG SET00260
DO 101 VDN=1,NDNSCT SET00270
SIGR(NM,NG)=SIGR(NM,NG)+SIGS(NM,NG,NDN) SET00280
101 CONTINUE SET00290
102 CONTINUE SET00300
C START WITH NESTED DO LOOPS OVER MATERIAL REGIONS SET00310
ITEMP1=1 SET00320
DO 560 KR=1,KRM SET00330
ITEMP2=1 SET00340
DO 550 JR=1,JRM SET00350
ITEMP3=1 SET00360
DO 540 IR=1,IRM SET00370
C HOMOGENEOUS REGION SET00380
NPR=4*IRM*JRM*(2*KR-1)+2*IRM*(2*JR-1)+2*IR SET00390
KF=KBP(KR)-1 SET00400

```



```

KS=KBP(KR-1)+1
IF(KR.EQ.1)KS=2
JE=JBP(JR)-1
JS=JBP(JR-1)+1
IF(JR.EQ.1)JS=2
IE=IBP(IR)-1
IS=IBP(IR-1)+1
IF(IR.EQ.1)IS=2
ITEMP5=1
NPRP=NPR
GO TO 500
110 HD(1)=HZ(KR)
HD(2)=HD(1)
HD(3)=HY(JR)
HD(4)=HD(3)
HD(5)=HX(IR)
HD(6)=HD(5)
DO 120 ITEMP4=1,8
MN(ITEMP4)=MMAP(IR,JR,KR)
120 CONTINUE
GO TO 530
C LOWER LEFT EDGE
130 NPRP=NPR-4*IRM*JRM-1
IS=IS-1
IE=IS
KS=KS-1
KE=KS
ITEMP5=2
GO TO 500
140 HD(1)=HZ(KR)
HD(2)=HZ(KR-1)
IF(KR.EQ.1)HD(2)=HD(1)
HD(5)=HX(IR)
HD(6)=HX(IR-1)
IF(IR.EQ.1)HD(6)=HD(5)
MN(1)=MMAP(IR,JR,KR-1)

```

```

SET00410
SET00420
SET00430
SET00440
SET00450
SET00460
SET00470
SET00480
SET00490
SET00500
SET00510
SET00520
SET00530
SET00540
SET00550
SET00560
SET00570
SET00580
SET00590
SET00600
SET00610
SET00620
SET00630
SET00640
SET00650
SET00660
SET00665
SET00670
SET00680
SET00690
SET00700
SET00710
SET00720
SET00730
SET00740
SET00750

```

```

IF(KR.EQ.1)MN(1)=MN(5)
MN(4)=MN(1)
MN(6)=MMAP(IR-1,JR,KR)
IF(IR.EQ.1)MN(6)=MN(5)
MN(7)=MN(6)
MN(2)=MMAP(IR-1,JR,KR-1)
IF(KR.EQ.1)MN(2)=MN(6)
IF(IR.EQ.1)MN(2)=MN(1)
MN(3)=MN(2)
GO TO 530
C LEFT SIDE
150 NPRP=NPR-1
KE=KRP(KR)-1
KS=KS+1
ITEMP5=3
GO TO 500
160 HD(2)=HD(1)
MN(4)=MN(8)
MN(1)=MN(5)
MN(2)=MN(6)
MN(3)=MN(7)
GO TO 530
C LEFT FRONT EDGE
170 NPRP=NPR-2*IRM-1
JS=JS-1
JE=JS
ITEMP5=4
GO TO 500
180 MN(8)=MMAP(IR,JR-1,KR)
IF(JR.EQ.1)MN(8)=MN(5)
MN(4)=MN(8)
MN(7)=MMAP(IR-1,JR-1,KR)
IF(IR.EQ.1)MN(7)=MN(8)
IF(JR.EQ.1)MN(7)=MN(6)
MN(3)=MN(7)
HD(4)=HY(JR-1)

```

```

SET00760
SET00770
SET00780
SET00790
SET00800
SET00810
SET00820
SET00830
SET00840
SET00850
SET00860
SET00870
SET00880
SET00890
SET00900
SET00910
SET00920
SET00930
SET00940
SET00950
SET00960
SET00970
SET00980
SET00990
SET01000
SET01010
SET01020
SET01030
SET01040
SET01050
SET01060
SET01070
SET01080
SET01090
SET01100
SET01110

```

```

        IF(JR.EQ.1)HD(4)=HD(3)
        GO TO 530
C    LOWER FRONT EDGE
190  KS=KS-1
        KE=KS
        IS=IS+1
        IE=IBP(IR)-1
        NPRP=VPR-4*IRM*JRM-2*IRM
        ITEMP5=5
        GO TO 500
200  HD(2)=HZ(KR-1)
        IF(KR.EQ.1)HD(2)=HD(1)
        HD(6)=HD(5)
        MN(6)=MV(5)
        MN(1)=MMAP(IR,JR,KR-1)
        IF(KR.EQ.1)MN(1)=MN(5)
        MN(2)=MV(1)
        MN(7)=MN(8)
        MN(4)=MMAP(IR,JR-1,KR-1)
        IF(KR.EQ.1)MN(4)=MV(8)
        IF(JR.EQ.1)MN(4)=MN(1)
        MN(3)=MV(4)
        GO TO 530
C    LOWER FRONT LEFT CORNER
210  NPRP=VPR-4*IRM*JRM-2*IRM-1
        IS=IS-1
        IE=IS
        ITEMP5=6
        GO TO 500
220  HD(6)=HX(IR-1)
        IF(IR.EQ.1)HD(6)=HD(5)
        MN(6)=MMAP(IR-1,JR,KR)
        IF(IR.EQ.1)MN(6)=MV(5)
        MN(2)=MMAP(IR-1,JR,KR-1)
        IF(IR.EQ.1)MN(2)=MN(1)
        IF(KR.EQ.1)MN(2)=MV(6)

```

```

SET01120
SET01130
SET01140
SET01150
SET01160
SET01170
SET01180
SET01190
SET01200
SET01210
SET01220
SET01230
SET01240
SET01260
SET01270
SET01280
SET01290
SET01300
SET01310
SET01320
SET01330
SET01340
SET01350
SET01360
SET01370
SET01380
SET01390
SET01400
SET01410
SET01420
SET01430
SET01440
SET01450
SET01460
SET01470
SET01480

```

```

MN(7)=MMAP(IR-1,JR-1,KR)
IF(IR.EQ.1)MN(7)=MN(8)
IF(JR.EQ.1)MN(7)=MN(6)
MN(3)=MMAP(IR-1,JR-1,KR-1)
IF(IR.EQ.1)MN(3)=MN(4)
IF(JR.EQ.1)MN(3)=MN(2)
IF(KR.EQ.1)MN(3)=MN(7)
GO TO 530
C   FRONT SIDE
230 NPRP=NPR-2*IRM
    IS=IS+1
    IE=IBP(IR)-1
    KS=KS+1
    KE=KBP(KR)-1
    ITEMP5=7
    GO TO 500
240 HD(2)=HD(1)
    HD(6)=HD(5)
    MN(4)=MN(8)
    MN(7)=MN(8)
    MN(3)=MN(8)
    MN(6)=MN(5)
    MN(1)=MN(5)
    MN(2)=MN(5)
    GO TO 530
C   BOTTOM SIDE
250 NPRP=NPR-4*IRM*JRM
    KS=KS-1
    KE=KS
    JS=JS+1
    JE=JBP(JR)-1
    ITEMP5=8
    GO TO 500
260 HD(2)=HZ(KR-1)
    IF(KR.EQ.1)HD(2)=HD(1)
    HD(4)=HD(3)

```

```

SET01490
SET01500
SET01510
SET01520
SET01530
SET01540
SET01550
SET01560
SET01570
SET01580
SET01590
SET01600
SET01610
SET01620
SET01630
SET01640
SET01650
SET01660
SET01670
SET01680
SET01690
SET01700
SET01710
SET01720
SET01730
SET01740
SET01750
SET01760
SET01770
SET01780
SET01790
SET01800
SET01805
SET01810
SET01820
SET01830

```

MN(8)=MN(5)	SET01840
MN(7)=MN(6)	SET01850
MN(1)=MMAP(IR, JR, KR-1)	SET01860
IF(KR.EQ.1)MN(1)=MN(5)	SET01870
MN(2)=MN(1)	SET01880
MN(3)=MN(1)	SET01890
MN(4)=MN(1)	SET01900
GO TO 530	SET01910
500 DO 520 K=KS, KE	SET01920
DO 520 J=JS, JE	SET01930
DO 510 I=IS, IE	SET01940
NPRMP(I, J, K)=NPRP	SET01950
510 CONTINUE	SET01960
520 CONTINUE	SET01970
GO TO (110, 140, 160, 180, 200, 220, 240, 260), ITEMP5	SET01980
530 CALL COEF1(XNU, SIGF, SIGR, SIGT, SIGS, DD1, DD2, DD3, DD4, DD5, DD6, DD7, VO, INNG, NDNSCT, NMAT, NPRG, HD, MN, NPRP, NGX)	SET01990
GO TO (130, 150, 170, 190, 210, 230, 250, 540), ITEMP5	SET02000
540 CONTINUE	SET02010
550 CONTINUE	SET02020
560 CONTINUE	SET02030
RETURN	SET02040
END	SET02050
	SET02060

```

SUBROUTINE COEF1(XNU,SIGF,SIGR,SIGT,SIGS,DD1,DD2,DD3,DD4,DD5,      COE00010
1DD6,DD7,VO,NNGV,NDNSCV,NMATV,NPRGV,HD,MN,NPRP,NGXV)          COE00020
  IMPLICIT REAL*8 (A-H,O-Z)                                    COE00030
  INTEGER*2 MMAP,NPRMP                                         COE00040
  COMMON/INT3/IASIZE,NNG,NDG,NTOG,NMAT,IM,JM,KM,IRM,JRM,KRM,NLBC, COE00090
1NFBC,NBBC,NDNSCT,NPRG,IOP,VTG,NXTP,NYTP,NZTP,IXTP(5),IYTP(5), COE00100
2IZTP(5),NSTEAD,IFLIN,IGEOM,ITITLE(20),N3IT,NIIT,NPIT,IOPSI,IODUMP, COE00110
3IOFN,IQFO,IOPN,IOPD,ITEMP,ITEMP1,ITEMP2,ITEMP3,ITEMP4,ITEMP5, COE00120
4NTIT,IETIME,IFLOUT,IMX,JMX,KMX,IOSC1,IOSC2,NGX              COE00130
  COMMON/FLOTE/EFFK,DRFP,EPS1,EPS2,TEMP,TEMP1,TEMP2,TEMP3,TEMP4, COE00140
1TEMP5,TEMP5,XFISST,XFISSO,ALAMN,ALAMO,TIME,FLXCON,BETAT     COE00150
  DIMENSION XNU(NMATV,NNGV),SIGF(NMATV,NNGV),SIGR(NMATV,NNGV),SIGT(NCOE00160
1MATV,NNGV),SIGS(NMATV,NNGV,NDNSCV),DD1(NPRGV,NNGV),          COE00170
2DD2(NPRGV,NNGV),DD3(NPRGV,NNGV),DD4(NPRGV,NNGV),DD5(NPRGV,NNGV), COE00180
3DD6(NPRGV,NNGV),DD7(NPRGV,NGXV,NDNSCV),VO(NPRGV)           COE00190
  DIMENSION HD(6),MN(8)                                       COE00200
C LOOP OVER ALL GROUPS                                         COE00210
  TEMP=1.20D1                                                  COE00220
  TEMP1=8.0D0                                                  COE00230
  NPR=NPRP                                                      COE00240
  VO(NPR)=((HD(1)+HD(2))*(HD(3)+HD(4))*(HD(5)+HD(5)))/TEMP1  COE00241
  DO 110 NG=1,NNG                                              COE00250
  DD1(NPR,NG)=((HD(3)*HD(2)/SIGT(MN(1),NG))+(HD(3)*HD(1)/SIGT(MN(5),COE00260
1NG))+(HD(4)*HD(2)/SIGT(MN(4),NG))+(HD(4)*HD(1)/SIGT(MN(8),NG)))/(HCOE00270
2D(5)*TEMP)                                                    COE00280
  DD2(NPR,NG)=((HD(5)*HD(2)/SIGT(MN(1),NG))+(HD(6)*HD(2)/SIGT(MN(2),COE00290
1NG))+(HD(6)*HD(1)/SIGT(MN(6),NG))+(HD(5)*HD(1)/SIGT(MN(5),NG)))/(HCOE00300
2D(3)*TEMP)                                                    COE00310
  DD3(NPR,NG)=((HD(4)*HD(5)/SIGT(MN(7),NG))+(HD(4)*HD(5)/SIGT(MN(8),COE00320
1NG))+(HD(3)*HD(5)/SIGT(MN(5),NG))+(HD(3)*HD(6)/SIGT(MN(6),NG)))/(HCOE00330
2D(1)*TEMP)                                                    COE00340
  DD4(NPR,NG)=DD1(NPR,NG)+DD2(NPR,NG)+DD3(NPR,NG)+((HD(3)*HD(2)/SIGTCOE00350
1(MN(2),NG))+(HD(4)*HD(2)/SIGT(MN(3),NG))+(HD(4)*HD(1)/SIGT(MN(7),NCOE00360
2G))+(HD(3)*HD(1)/SIGT(MN(6),NG)))/(HD(6)*TEMP)+(HD(6)*HD(2)/SIGT(COE00370
3MN(3),NG))+(HD(5)*HD(2)/SIGT(MN(4),NG))+(HD(5)*HD(1)/SIGT(MN(8),NGCOE00380
4))+(HD(5)*HD(1)/SIGT(MN(7),NG)))/(HD(4)*TEMP)+(HD(5)*HD(3)/SIGT(MCOE00390

```

```

5N(1),NG))+(HD(3)*HD(6)/SIGT(MN(2),NG))+(HD(4)*HD(6)/SIGT(MN(3),NG)COE00400
6)+(HD(4)*HD(5)/SIGT(MN(4),NG)))/(HD(2)*TEMP) COE00410
DD5(NPR,NG)=DD4(NPR,NG)+(HD(5)*HD(3)*HD(2)*SIGR(MN(1),NG)+HD(6)*HDCOE00420
1(3)*HD(2)*SIGR(MN(2),NG)+HD(6)*HD(4)*HD(2)*SIGR(MN(3),NG)+HD(5)*HDCOE00430
2(4)*HD(2)*SIGR(MN(4),NG)+HD(5)*HD(3)*HD(1)*SIGR(MN(5),NG)+HD(6)*HDCOE00440
3(3)*HD(1)*SIGR(MN(6),NG)+HD(6)*HD(4)*HD(1)*SIGR(MN(7),NG)+HD(5)*HDCOE00450
4(4)*HD(1)*SIGR(MN(8),NG))/TEMP1 COE00460
DD6(NPR,NG)=(HD(5)*HD(3)*HD(2)*SIGF(MN(1),NG)*XNU(MN(1),NG)+HD(6)*COE00470
1HD(3)*HD(2)*SIGF(MN(2),NG)*XNU(MN(2),NG)+HD(6)*HD(4)*HD(2)*SIGF(MNCOE00480
2(3),NG)*XNU(MN(3),NG)+HD(5)*HD(4)*HD(2)*SIGF(MN(4),NG)*XNU(MN(4),NCCOE00490
3G)+HD(5)*HD(3)*HD(1)*SIGF(MN(5),NG)*XNU(MN(5),NG)+HD(6)*HD(3)*HD(1COE00500
4)*SIGF(MN(5),NG)*XNU(MN(6),NG)+HD(6)*HD(4)*HD(1)*SIGF(MN(7),NG)*XNCOE00510
5U(MN(7),NG)+HD(5)*HD(4)*HD(1)*SIGF(MN(8),NG)*XNU(MN(8),NG))/TEMP1 COE00520
IF(NG.EQ.NNG)GO TO 110 COE00521
DO 100 NDN=1,NDNSCT COE00530
DD7(NPR,NG,NDN)=(HD(5)*HD(3)*HD(2)*SIGS(MN(1),NG,NDN)+HD(6)*HD(3)*COE00540
1HD(2)*SIGS(MN(2),NG,NDN)+HD(6)*HD(4)*HD(2)*SIGS(MN(3),NG,NDN)+HD(5COE00550
2)*HD(4)*HD(2)*SIGS(MN(4),NG,NDN)+HD(5)*HD(3)*HD(1)*SIGS(MN(5),NG,NCCOE00560
3DN)+HD(5)*HD(3)*HD(1)*SIGS(MN(6),NG,NDN)+HD(6)*HD(4)*HD(1)*SIGS(MNCOE00570
4(7),NG,NDN)+HD(5)*HD(4)*HD(1)*SIGS(MN(8),NG,NDN))/TEMP1 COE00580
100 CONTINUE COE00590
110 CONTINUE COE00600
RETURN COE00610
END COE00620

```

SUBROUTINE INNERO(X,Y,Z,HX,HY,HZ,DD1,DD2,DD3,DD4,DD5,MMAP,NPRMP,	INN00010
1 PSI,P1,P2,P3,FO,SRC,WA,GA,SOLN,OMEG,XFISS,XINSC,XREM,XLEK,	INN00020
2 NNGV,VMATV,IMV,JMV,KMV,IRMV,JRMV,KRMV,NPRGV,NG)	INN00030
IMPLICIT REAL*8 (A-H,O-Z)	INN00040
INTEGER*2 MMAP,NPRMP	INN00050
COMMON/INTG/IASIZE,VNG,NDG,VTOG,NMAT,IM,JM,KM,IRM,JRM,KRM,NLBC,	INN00100
1 NFBC,NB3C,NDNSCT,NPRG,IOP1,VTG,NXTP,NYTP,NZTP,IXTP(5),IYTP(5),	INN00110
2 IZTP(5),NSTEAD,IFLIN,IGEOM,ITITLE(20),NOIT,NIIT,NPIT,IJPSI,IODUMP,	INN00120
3 IOFN,IOFO,IOPN,IOPJ,ITEMP,ITEMP1,ITEMP2,ITEMP3,ITEMP4,ITEMP5,	INN00130
4 NIT, IETIME, IFLOUT, IMX, JMX, KMV, IOSC1, IOSC2, NGX	INN00140
COMMON/FLOTE/EFFK,DRFP,EPS1, EPS2, TEMP, TEMP1, TEMP2, TEMP3, TEMP4,	INN00150
1 TEMP5, TEMP6, XFISS, XFISSD, ALAMN, ALAMD, TIME, FLXCJN, BETAT	INN00160
DIMENSION X(IMV),Y(JMV),Z(KMV),HX(IRMV),HY(JRMV),HZ(KRMV),	INN00170
1 DD1(NPRGV,VNGV),DD2(NPRGV,VNGV),DD3(NPRGV,NNGV),DD4(NPRGV,NNGV),	INN00180
2 DD5(NPRGV,NNGV),MMAP(IRMV,JRMV,KRMV),NPRMP(IMV,JMV,KMV),	INN00190
3 PSI(NNGV,IMV,JMV,KMV),P1(IMV,JMV),P2(IMV,JMV),P3(IMV,JMV),	INN00200
4 SRC(IMV,JMV,KMV),WA(IMV),GA(IMV),SOLN(IMV),OMEG(NNGV),XFISS(NNGV),	INN00210
5 XINSC(NNGV),XREM(NNGV),XLEK(NNGV)	INN00220
IF(ITEMP5.EQ.5)GO TO 90	INN00230
CALL GRBAL(DD1,DD2,DD3,DD4,DD5,NPRMP,PSI,P1,P2,P3,XFISS,XINSC,	INN00240
1 XREM,XLEK,NNG,IM,JM,KM,NPRG,NG)	INN00250
90 NIT=0	INN00260
C START WITH BOTTOM PLANE	INN00270
100 CONTINUE	INN00280
XNLBC=NLBC	INN00290
TEMP1=0.000	INN00300
TEMP4=1.00+50	INN00310
K=1	INN00320
IF(NB3C.EQ.0)GO TO 200	INN00330
J=1	INN00340
IF(NFBC.EQ.0)GO TO 140	INN00350
NPR=NPRMP(1,1,1)	INN00360
WA(1)=-2.000*DD1(NPR,NG)*XNLBC/DD5(NPR,NG)	INN00370
GA(1)=((SRC(1,J,K)+2.000*(DD2(NPR,NG)*PSI(NG,1,2,1)+DD3(NPR,NG)*PSI	INN00380
1(NG,1,1,2)))*XNLBC)/DD5(NPR,NG)	INN00390
DO 110 I=2,IMX	INN00400

NPR=NPRMP(I,1,1)	INN00410
NPRX=NPRMP(I-1,1,1)	INN00420
TEMP=1.000/(DD5(NPR,NG)+DD1(NPRX,NG)*WA(I-1))	INN00430
WA(I)=-DD1(NPR,NG)*TEMP	INN00440
110 GA(I)=(SRC(I,J,K)+2.000*(DD2(NPR,NG)*PSI(NG,I,2,1)+DD3(NPR,NG)*PSI	INN00450
1(NG,I,1,2))+DD1(NPRX,NG)*GA(I-1))*TEMP	INN00460
SOLN(IM)=0.000	INN00470
DO 120 II=1,IMX	INN00480
I=IM-II	INN00490
120 SOLN(I)=GA(I)-WA(I)*SOLN(I+1)	INN00500
DO 130 I=1,IM	INN00510
TEMP2=PSI(NG,I,1,1)	INN00520
PSI(NG,I,1,1)=TEMP2+OMEG(NG)*(SOLN(I)-TEMP2)	INN00530
IF(PSI(NG,I,1,1).GT.0.000)GO TO 125	INN00540
PSI(NG,I,1,1)=0.000	INN00550
GO TO 130	INN00560
125 TEMP3=TEMP2/PSI(NG,I,1,1)	INN00570
IF(TEMP1.LT.TEMP3)TEMP1=TEMP3	INN00580
IF(TEMP4.GT.TEMP3)TEMP4=TEMP3	INN00590
130 CONTINUE	INN00600
140 DO 180 J=2,JMX	INN00610
NPR=NPRMP(I,J,1)	INN00620
NPRY=NPRMP(I,J-1,1)	INN00630
WA(1)=-2.000*DD1(NPR,NG)*XNLBC/DD5(NPR,NG)	INN00640
GA(1)=((SRC(I,J,K)+DD2(NPRY,NG)*PSI(NG,I,J-1,1)+DD2(NPR,NG)*PSI(NG,I	INN00650
1,1,J+1,1)+2.000*DD3(NPR,NG)*PSI(NG,I,J,2))*XNLBC)/DD5(NPR,NG)	INN00660
DO 150 I=2,IMX	INN00670
NPR=NPRMP(I,J,1)	INN00680
NPRX=NPRMP(I-1,J,1)	INN00690
NPRY=NPRMP(I,J-1,1)	INN00700
TEMP=1.000/(DD5(NPR,NG)+DD1(NPRX,NG)*WA(I-1))	INN00710
WA(I)=-DD1(NPR,NG)*TEMP	INN00720
150 GA(I)=(SRC(I,J,1)+DD2(NPRY,NG)*PSI(NG,I,J-1,1)+DD2(NPR,NG)*PSI(NG,I	INN00730
1I,J+1,1)+2.000*DD3(NPR,NG)*PSI(NG,I,J,2)+DD1(NPRX,NG)*GA(I-1))*TEM	INN00740
2P	INN00750
SOLN(IM)=0.000	INN00760

DO 160 II=1,IMX	INN00770
I=IM-II	INN00780
160 SOLN(I)=GA(I)-WA(I)*SOLN(I+1)	INN00790
DO 170 I=1,IM	INN00800
TEMP2=PSI(NG,I,J,1)	INN00810
PSI(NG,I,J,1)=TEMP2+OMEG(NG)*(SOLN(I)-TEMP2)	INN00820
IF(PSI(NG,I,J,1).GT.0.000)GO TO 165	INN00830
PSI(NG,I,J,1)=0.000	INN00840
GO TO 170	INN00850
165 TEMP3=TEMP2/PSI(NG,I,J,1)	INN00860
IF(TEMP1.LT.TEMP3)TEMP1=TEMP3	INN00870
IF(TEMP4.GT.TEMP3)TEMP4=TEMP3	INN00880
170 CONTINUE	INN00890
180 CONTINUE	INN00900
DO 190 I=1,IM	INN00910
190 PSI(NG,I,JM,1)=0.000	INN00920
C NOW COMPUTE FOR THE REST OF THE PLANES	INN00930
200 DO 300 K=2,KMX	INN00940
IF(NFBC.EQ.0) GO TO 240	INN00950
J=1	INN00960
NPR=NPRMP(1,1,K)	INN00970
NPRZ=NPRMP(1,1,K-1)	INN00980
WA(1)=-2.000*DD1(NPR,NG)*XNLBC/DD5(NPR,NG)	INN00990
GA(1)=((SRC(1,1,K)+2.000*DD2(NPR,NG)*PSI(NG,1,2,K)+DD3(NPR,NG)*PSI	INN01000
I(NG,1,1,K+1)+DD3(NPRZ,NG)*PSI(NG,1,1,K-1))*XNLBC)/DD5(NPR,NG)	INN01010
DO 210 I=2,IMX	INN01020
NPR=NPRMP(I,1,K)	INN01030
NPRX=NPRMP(I-1,1,K)	INN01040
NPRZ=NPRMP(I,1,K-1)	INN01050
TEMP=1.000/(DD5(NPR,NG)+DD1(NPRX,NG)*WA(I-1))	INN01060
WA(I)=-DD1(NPR,NG)*TEMP	INN01070
210 GA(I)=(SRC(I,1,K)+2.000*DD2(NPR,NG)*PSI(NG,I,2,K)+DD3(NPR,NG)*PSI	INN01080
ING,I,1,K+1)+DD3(NPRZ,NG)*PSI(NG,I,1,K-1)+DD1(NPRX,NG)*GA(I-1))*TEM	INN01090
2P	INN01100
SOLN(IM)=0.000	INN01110
DO 220 II=1,IMX	INN01120

	I=IM-1	INN01130
220	SOLN(I)=GA(I)-WA(I)*SOLN(I+1)	INN01140
	DO 230 I=1, IM	INN01150
	TEMP2=PSI(NG,I,1,K)	INN01160
	PSI(NG,I,1,K)=TEMP2+OMEG(NG)*(SOLN(I)-TEMP2)	INN01170
	IF(PSI(NG,I,1,K).GT.0.000)GO TO 225	INN01180
	PSI(NG,I,1,K)=0.000	INN01190
	GO TO 230	INN01200
225	TEMP3=TEMP2/PSI(NG,I,1,K)	INN01210
	IF(TEMP1.LT.TEMP3)TEMP1=TEMP3	INN01220
	IF(TEMP4.GT.TEMP3)TEMP4=TEMP3	INN01230
230	CONTINUE	INN01240
240	DO 280 J=2, JMX	INN01250
	NPR=NPRMP(1, J, K)	INN01260
	NPRY=NPRMP(1, J-1, K)	INN01270
	NPRZ=NPRMP(1, J, K-1)	INN01280
	WA(1)=-2.000*DD1(NPR, NG)*XNLBC/DD5(NPR, NG)	INN01290
	GA(1)=((SRC(1, J, K)+DD2(NPR, NG)*PSI(NG, 1, J+1, K)+DD2(NPRY, NG)*PSI(NG, 1, J-1, K)+DD3(NPR, NG)*PSI(NG, 1, J, K+1)+DD3(NPRZ, NG)*PSI(NG, 1, J, K-1)+2)*XNLBC)/DD5(NPR, NG)	INN01300
	DO 250 I=2, IMX	INN01310
	NPR=NPRMP(I, J, K)	INN01320
	NPRX=NPRMP(I-1, J, K)	INN01330
	NPRY=NPRMP(I, J-1, K)	INN01340
	NPRZ=NPRMP(I, J, K-1)	INN01350
	TEMP=1.000/(DD5(NPR, NG)+DD1(NPRX, NG)*WA(I-1))	INN01360
	WA(I)=-DD1(NPR, NG)*TEMP	INN01370
250	GA(I)=(SRC(I, J, K)+DD2(NPR, NG)*PSI(NG, I, J+1, K)+DD2(NPRY, NG)*PSI(NG, I, J-1, K)+DD3(NPR, NG)*PSI(NG, I, J, K+1)+DD3(NPRZ, NG)*PSI(NG, I, J, K-1)+2DD1(NPRX, NG)*GA(I-1))*TEMP	INN01380
	SOLN(IM)=0.000	INN01390
	DO 260 I=1, IMX	INN01400
	I=IM-1	INN01410
260	SOLN(I)=GA(I)-WA(I)*SOLN(I+1)	INN01420
	DO 270 I=1, IM	INN01430
	TEMP2=PSI(NG, I, J, K)	INN01440
		INN01450
		INN01460
		INN01470
		INN01480

PSI(NG,I,J,K)=TEMP2+OMEG(NG)*(SOLN(I)-TEMP2)	INN01490
IF(PSI(NG,I,J,K).GT.0.000)GO TO 265	INN01500
PSI(NG,I,J,K)=0.000	INN01510
GO TO 270	INN01520
265 TEMP3=TEMP2/PSI(NG,I,J,K)	INN01530
IF(TEMP1.LT.TEMP3)TEMP1=TEMP3	INN01540
IF(TEMP4.GT.TEMP3)TEMP4=TEMP3	INN01550
270 CONTINUE	INN01560
280 CONTINUE	INN01570
DO 290 I=1,IM	INN01580
290 PSI(NG,I,JM,K)=0.000	INN01590
300 CONTINUE	INN01600
C COMPLETE MESH NOW SWEEP	INN01610
C NOW COMPUTE LARGEST RESIDUAL	INN01620
TEMP2=DABS(1.000-TEMP1)	INN01630
TEMP3=DABS(1.000-TEMP4)	INN01640
IF(TEMP2-TEMP3)320,320,310	INN01650
310 TEMP3=TEMP2	INN01660
320 NTIT=NTIT+1	INN01670
NIT=NIT+1	INN01680
IF(NIT.GE.NIIT)GO TO 330	INN01690
IF(TEMP3.GT.EPS2)GO TO 100	INN01700
330 CONTINUE	INN01710
RETURN	INN01720
END	INN01730

SUBROUTINE GRBAL0(DD1,DD2,DD3,DD4,DD5,NPRMP,PSI,P1,P2,P3,XFISS,	GRB00010
1XINSC,XREM,XLEK,NNGV,IMV,JMV,KMV,NPRGV,NG)	GRB00020
IMPLICIT REAL*8 (A-H,O-Z)	GRB00030
INTEGER*2 MMAP,NPRMP	GRB00040
COMMON/INTS/IASIZE,NNG,NDG,NTOG,NMAT,IM,JM,KM,IRM,JRM,KRM,NLBC,	GRB00090
1NFBC,NBBC,NDNSCT,NPRG,IOPT,NTG,NXTP,NYTP,NZTP,IXTP(5),IYTP(5),	GRB00100
2IZTP(5),NSTEAD,IFLIN,IGEOM,ITITLE(20),NOIT,NIIT,NPIT,IJPSI,IODUMP,	GRB00110
3IOFN,IOFO,IOPN,IOPD,ITEMP,ITEMP1,ITEMP2,ITEMP3,ITEMP4,ITEMP5,	GRB00120
4NTIT,IETIME,IFLOUT,IMX,JMX,KMX,IOSC1,IOSC2,NGX	GRB00130
COMMON/FLOTE/EFFK,DRFP,EPS1,EPS2,TEMP,TEMP1,TEMP2,TEMP3,TEMP4,	GRB00140
ITEMP5,TEMP5,XFISST,XFISSO,ALAMN,ALAMD,TIME,FLXCJN,BETAT	GRB00150
DIMENSION DD1(NPRGV,NNGV),DD2(NPRGV,NNGV),DD3(NPRGV,NNGV),DD4(NPRGV,	GRB00160
1V,NNGV),DD5(NPRGV,NNGV),NPRMP(IMV,JMV,KMV),PSI(NNGV,IMV,JMV,KMV),	GRB00170
2P1(IMV,JMV),P2(IMV,JMV),P3(IMV,JMV),XFISS(NNGV),XINSC(NNGV),	GRB00180
3XREM(NNGV),XLEK(NNGV)	GRB00190
XREM(NG)=0.000	GRB00200
XLEK(NG)=0.000	GRB00210
ONE=1.000	GRB00211
HALF=0.500	GRB00212
VOLB=ONE	GRB00213
VOLF=ONE	GRB00214
VOLL=ONE	GRB00215
IF(NBBC.EQ.1)VOLB=HALF	GRB00216
DO 230 K=1,KMX	GRB00220
IF(K.GT.1)VOLB=ONE	GRB00221
IF(K.EQ.1.AND.NBBC.EQ.0) GO TO 230	GRB00230
IF(K.NE.2)GO TO 120	GRB00240
100 IF(NBBC.EQ.1)GO TO 120	GRB00250
C COMPUTE LEAKAGE FOR BOTTOM PLANE	GRB00260
IF(NFBC.EQ.1)VOLF=HALF	GRB00261
DO 110 J=1,JMX	GRB00270
IF(J.GT.1)VOLF=ONE	GRB00271
IF(NLBC.EQ.1)VOLL=HALF	GRB00272
DO 110 I=1,IMX	GRB00280
IF(I.GT.1)VOLL=ONE	GRB00281
NPR=NPRMP(I,J,1)	GRB00290

```

XLEK(NG)=XLEK(NG)+DD3(NPR,NG)*PSI(NG,I,J,2)*VOLF*VOLL
110 CONTINUE
C COMPUTE FRONT LEAKAGE
120 IF(NFBC.EQ.1) GO TO 140
    IF(NLBC.EQ.1)VOLL=HALF
    DO 130 I=1,IMX
        IF(I.GT.1)VOLL=ONE
        NPR=NPRMP(I,1,K)
130 XLEK(NG)=XLEK(NG)+DD2(NPR,NG)*PSI(NG,I,2,K)*VOLL*VOLB
C COMPUTE LEFT LEAKAGE
140 IF(NLBC.EQ.1) GO TO 160
    IF(NFBC.EQ.1)VOLF=HALF
    DO 150 J=1,JMX
        IF(J.GT.1)VOLF=ONE
        NPR=NPRMP(1,J,K)
150 XLEK(NG)=XLEK(NG)+DD1(NPR,NG)*PSI(NG,2,J,K)*VOLF*VOLB
C COMPUTE RIGHT LEAKAGE
160 IF(NFBC.EQ.1)VOLF=HALF
    DO 170 J=1,JMX
        IF(J.GT.1)VOLF=ONE
        NPR=NPRMP(IMX,J,K)
170 XLEK(NG)=XLEK(NG)+DD1(NPR,NG)*PSI(NG,IMX,J,K)*VOLF*VOLB
C COMPUTE BACK LEAKAGE
    IF(NLBC.EQ.1)VOLL=HALF
    DO 180 I=1,IMX
        IF(I.GT.1)VOLL=ONE
        NPR=NPRMP(I,JMX,K)
180 XLEK(NG)=XLEK(NG)+DD2(NPR,NG)*PSI(NG,I,JMX,K)*VOLL*VOLB
    IF(NFBC.EQ.1)VOLF=HALF
    DO 200 J=1,JMX
        IF(J.GT.1)VOLF=ONE
        VOLC=VOLB*VOLF
        IF(NLBC.EQ.1)VOLL=HALF
    DO 190 I=1,IMX
        IF(I.GT.1)VOLL=ONE
        VOLD=VOLL*VOLC

```

```

GRB00300
GRB00310
GRB00320
GRB00330
GRB00331
GRB00340
GRB00341
GRB00350
GRB00360
GRB00370
GRB00380
GRB00381
GRB00390
GRB00391
GRB00400
GRB00410
GRB00420
GRB00421
GRB00430
GRB00431
GRB00440
GRB00440
GRB00450
GRB00460
GRB00461
GRB00470
GRB00471
GRB00480
GRB00490
GRB00491
GRB00500
GRB00501
GRB00502
GRB00503
GRB00510
GRB00511
GRB00512

```

NPR=NPRMP(I,J,K)	GRB00520
190 XREM(NG)=XREM(NG)+(DD5(NPR,NG)-DD4(NPR,NG))*PSI(NG,I,J,K)*VOLD	GRB00530
200 CONTINUE	GRB00540
IF(K.LT.KMX) GO TO 230	GRB00550
C COMPUTE TOP LEAKAGE	GRB00560
IF(NFBC.EQ.1)VOLF=HALF	GRB00561
DD 220 J=1,JMX	GRB00570
IF(J.GT.1)VOLF=ONE	GRB00571
IF(NLBC.EQ.1)VOLL=HALF	GRB00572
DD 210 I=1,IMX	GRB00580
IF(I.GT.1)VOLL=ONE	GRB00581
NPR=NPRMP(I,J,KMX)	GRB00590
210 XLEK(NG)=XLEK(NG)+DD3(NPR,NG)*PSI(NG,I,J,KMX)*VOLL*VOLF	GRB00600
220 CONTINUE	GRB00610
230 CONTINUE	GRB00620
TEMP=(XFISS(NG)+XINSC(NG))/(XLEK(NG)+XREM(NG))	GRB00630
DD 250 K=1,KMX	GRB00640
DD 250 J=1,JM	GRB00650
DD 240 I=1,IM	GRB00660
240 PSI(NG,I,J,K)=TEMP*PSI(NG,I,J,K)	GRB00670
250 CONTINUE	GRB00680
XREM(NG)=TEMP*XREM(NG)	GRB00690
XLEK(NG)=TEMP*XLEK(NG)	GRB00700
RETURN	GRB00710
END	GRB00720

SUBROUTINE INNER1(X,Y,Z,HX,HY,HZ,DD1,DD2,DD3,DD4,DD5,MMAP,NPRMP,	INN00010
1PSI,P1,P2,P3,FO,SRC,WA,GA,SOLN,OMEG,XFISS,XINSC,XREM,XLEK,	INN00020
2NNGV,NMATV,IMV,JMV,KMV,IRMV,JRMV,KRMV,NPRGV,NG)	INN00030
IMPLICIT REAL*8 (A-H,O-Z)	INN00040
INTEGER*2 MMAP,NPRMP	INN00050
COMMON/INTS/IASIZE,NNG,NDG,NTOG,NMAT,IM,JM,KM,IRM,JRM,KRM,NLBC,	INN00100
1NFBC,NB3C,NDNSCT,NPRG,IOP,T,NTG,NXTP,NYTP,NZTP,IXTP(5),IYTP(5),	INN00110
2IZTP(5),NSTEAD,IFLIN,IGEQM,ITITLE(20),NOIT,NIIT,NPIT,IOPSI,IODUMP,	INN00120
3IOFN,IOFO,IOPN,IOPD,ITEMP,ITEMP1,ITEMP2,ITEMP3,ITEMP4,ITEMP5,	INN00130
4NTIT,IETIME,IFLOUT,IMX,JMX,KMX,IOSC1,IOSC2,NGX	INN00140
COMMON/FLOTE/EFFK,DRFP,EPS1,EPS2,TEMP,TEMP1,TEMP2,TEMP3,TEMP4,	INN00150
1TEMP5,TEMP5,XFISST,XFISSO,ALAMN,ALAMD,TIME,FLXCON,BETAT	INN00160
DIMENSION X(IMV),Y(JMV),Z(KMV),HX(IRMV),HY(JRMV),HZ(KRMV),	INN00170
1DD1(NPRGV,NNGV),DD2(NPRGV,NNGV),DD3(NPRGV,NNGV),DD4(NPRGV,NNGV),	INN00180
2DD5(NPRGV,NNGV),MMAP(IRMV,JRMV,KRMV),NPRMP(IMV,JMV,KMV),	INN00190
3PSI(NNGV,IMV,JMV,KMV),P1(IMV,JMV),P2(IMV,JMV),P3(IMV,JMV),	INN00200
4SRC(IMV,JMV,KMV),WA(IMV),GA(IMV),SOLN(IMV),OMEG(NNGV),XFISS(NNGV),	INN00210
5XINSC(NNGV),XREM(NNGV),XLEK(NNGV)	INN00220
IF(ITEMP5.EQ.5)GO TO 90	INN00230
CALL GRBAL1(DD1,DD2,DD3,DD4,DD5,NPRMP,PSI,P1,P2,P3,XFISS,XINSC,	INN00240
1XREM,XLEK,NNG,IM,JM,KM,NPRG,NG)	INN00250
90 NIT=0	INN00260
XNLBC=NLBC	INN00270
START WITH BOTTOM PLANE	INN00280
100 CONTINUE	INN00290
REWIND IOSC1	INN00300
REWIND IOSC2	INN00310
TEMP1=0.000	INN00320
TEMP4=1.00+50	INN00330
K=1	INN00340
READ(IOSC1)P1	INN00350
READ(IOSC1)P2	INN00360
IF(NBBC.EQ.0)GO TO 200	INN00370
DO 185 NP=1,NPIT	INN00380
IF(NP.LT.NPIT)GO TO 105	INN00390
TEMP1=0.000	INN00400

	TEMP4=1.0D+50	INN00410
105	J=1	INN00420
	IF(NFBC.EQ.0)GO TO 140	INN00430
	NPR=NPRMP(1,1,1)	INN00440
	WA(1)=-2.0D0*DD1(NPR,NG)*XNLBC/DD5(NPR,NG)	INN00450
	GA(1)=((SRC(1,J,K)+2.0D0*(DD2(NPR,NG)*P1(1,2)+DD3(NPR,NG)*P2(1,1))	INN00460
	1)*XNLBC)/DD5(NPR,NG)	INN00470
	DO 110 I=2,IMX	INN00480
	NPR=NPRMP(I,1,1)	INN00490
	NPRX=NPRMP(I-1,1,1)	INN00500
	TEMP=1.0D0/(DD5(NPR,NG)+DD1(NPRX,NG)*WA(I-1))	INN00510
	WA(I)=-DD1(NPR,NG)*TEMP	INN00520
110	GA(I)=(SRC(I,1,1)+2.0D0*(DD2(NPR,NG)*P1(I,2)+DD3(NPR,NG)*P2(I,1))	INN00530
	1+DD1(NPRX,NG)*GA(I-1))*TEMP	INN00540
	SOLN(IM)=0.0D0	INN00550
	DO 120 II=1,IMX	INN00560
	I=IM-II	INN00570
120	SOLN(I)=GA(I)-WA(I)*SOLN(I+1)	INN00580
	DO 130 I=1,IM	INN00590
	TEMP2=P1(I,1)	INN00600
	P1(I,1)=TEMP2+OMEG(NG)*(SOLN(I)-TEMP2)	INN00610
	IF(P1(I,1).GT.0.0D0)GO TO 125	INN00620
	P1(I,1)=0.0D0	INN00630
	GO TO 130	INN00640
125	TEMP3=TEMP2/P1(I,1)	INN00650
	IF(TEMP1.LT.TEMP3)TEMP1=TEMP3	INN00660
	IF(TEMP4.GT.TEMP3)TEMP4=TEMP3	INN00670
130	CONTINUE	INN00680
140	DO 180 J=2,JMX	INN00690
	NPR=NPRMP(1,J,1)	INN00700
	NPRY=NPRMP(1,J-1,1)	INN00710
	WA(1)=-2.0D0*DD1(NPR,NG)*XNLBC/DD5(NPR,NG)	INN00720
	GA(1)=((SRC(1,J,1)+DD2(NPRY,NG)*P1(1,J-1)+DD2(NPR,NG)*P1(1,J+1)+	INN00730
	12.0D0*DD3(NPR,NG)*P2(1,J))*XNLBC)/DD5(NPR,NG)	INN00740
	DO 150 I=2,IMX	INN00750
	NPR=NPRMP(I,J,1)	INN00760

NPRX=NPRMP(I-1,J,1)	INN00770
NPRY=NPRMP(I,J-1,1)	INN00780
TEMP=1.000/(DD5(NPR,NG)+DD1(NPRX,NG)*WA(I-1))	INN00790
WA(I)=-DD1(NPR,NG)*TEMP	INN00800
150 GA(I)=(SRC(I,J,1)+DD2(NPRY,NG)*P1(I,J-1)+DD2(NPR,NG)*P1(I,J+1)+	INN00810
12.000*DD3(NPR,NG)*P2(I,J)+DD1(NPRX,NG)*GA(I-1))*TEMP	INN00820
SOLN(IM)=0.000	INN00830
DO 160 II=1,IMX	INN00840
I=IM-II	INN00850
160 SOLN(I)=GA(I)-WA(I)*SOLN(I+1)	INN00860
DO 170 I=1,IM	INN00870
TEMP2=P1(I,J)	INN00880
P1(I,J)=TEMP2+OMEG(NG)*(SOLN(I)-TEMP2)	INN00890
IF(P1(I,J).GT.0.000)GO TO 165	INN00900
P1(I,J)=0.000	INN00910
GO TO 170	INN00920
165 TEMP3=TEMP2/P1(I,J)	INN00930
IF(TEMP1.LT.TEMP3)TEMP1=TEMP3	INN00940
IF(TEMP4.GT.TEMP3)TEMP4=TEMP3	INN00950
170 CONTINUE	INN00960
180 CONTINUE	INN00970
185 CONTINUE	INN00980
TEMP5=TEMP1	INN00990
TEMP6=TEMP4	INN01000
190 P1(I,IM)=0.000	INN01010
200 DO 310 K=2,KMX	INN01020
READ(IDSC1)P3	INN01030
DO 295 NP=1,NPIT	INN01040
IF(NP.LT.NPIT)GO TO 205	INN01050
TEMP1=0.000	INN01060
TEMP4=1.00+50	INN01070
205 J=1	INN01080
IF(NFBC.EQ.0)GO TO 240	INN01090
NPR=NPRMP(1,1,K)	INN01100
NPR7=NPRMP(1,1,K-1)	INN01110
	INN01120

WA(1)=-2.000*DD1(NPR,NG)*XNLBC/DD5(NPR,NG)	INN01130
GA(1)=((SRC(1,1,K)+2.000*DD2(NPR,NG)*P2(1,2)+DD3(NPR,NG)*P3(1,1)+	INN01140
1DD3(NPRZ,NG)*P1(1,1))*XNLBC)/DD5(NPR,NG)	INN01150
DO 210 I=2,IMX	INN01160
NPR=NPRMP(I,1,K)	INN01170
NPRX=NPRMP(I-1,1,K)	INN01180
NPRZ=VPRMP(I,1,K-1)	INN01190
TEMP=1.000/(DD5(NPR,NG)+DD1(NPRX,NG)*WA(I-1))	INN01200
WA(I)=-DD1(NPR,NG)*TEMP	INN01210
210 GA(I)=(SRC(I,1,K)+2.000*DD2(NPR,NG)*P2(I,2)+DD3(NPR,NG)*P3(I,1)+	INN01220
1DD3(NPRZ,NG)*P1(I,1)+DD1(NPRX,NG)*GA(I-1))*TEMP	INN01230
SOLN(IM)=0.000	INN01240
DO 220 II=1,IMX	INN01250
I=IM-II	INN01260
220 SOLN(I)=GA(I)-WA(I)*SOLN(I+1)	INN01270
DO 230 I=1,IM	INN01280
TEMP2=P2(I,1)	INN01290
P2(I,1)=TEMP2+OMEG(NG)*(SOLN(I)-TEMP2)	INN01300
IF(P2(I,1).GT.0.000)GO TO 225	INN01310
P2(I,1)=0.000	INN01320
GO TO 230	INN01330
225 TEMP3=TEMP2/P2(I,1)	INN01340
IF(TEMP1.LT.TEMP3)TEMP1=TEMP3	INN01350
IF(TEMP4.GT.TEMP3)TEMP4=TEMP3	INN01360
230 CONTINUE	INN01370
240 DO 280 J=2,JMX	INN01380
NPR=NPRMP(1,J,K)	INN01390
NPRY=VPRMP(1,J-1,K)	INN01400
NPRZ=VPRMP(1,J,K-1)	INN01410
WA(1)=-2.000*DD1(NPR,NG)*XNLBC/DD5(NPR,NG)	INN01420
GA(1)=((SRC(1,J,K)+DD2(NPR,NG)*P2(1,J+1)+DD2(NPRY,NG)*P2(1,J-1)+	INN01430
1DD3(NPR,NG)*P3(1,J)+DD3(NPRZ,NG)*P1(1,J))*XNLBC)/DD5(NPR,NG)	INN01440
DO 250 I=2,IMX	INN01450
NPR=NPRMP(I,J,K)	INN01460
NPRX=VPRMP(I-1,J,K)	INN01470
NPRY=VPRMP(I,J-1,K)	INN01480

NPRZ=NPRMP(I,J,K-1)	INN01490
TEMP=1.000/(DD5(NPR,NG)+DD1(NPRX,NG)*WA(I-1))	INN01500
WA(I)=-DD1(NPR,NG)*TEMP	INN01510
250 GA(I)=(SRC(I,J,K)+DD2(NPR,NG)*P2(I,J+1)+DD2(NPRY,NG)*P2(I,J-1)+	INN01520
1DD3(NPR,NG)*P3(I,J)+DD3(NPRZ,NG)*P1(I,J)+DD1(NPRX,NG)*GA(I-1))*TEM	INN01530
2P	INN01540
SOLN(IM)=0.000	INN01550
DO 260 II=1,IMX	INN01560
I=IM-II	INN01570
260 SOLN(II)=GA(II)-WA(II)*SOLN(II+1)	INN01580
DO 270 I=1,IM	INN01590
TEMP2=P2(I,J)	INN01600
P2(I,J)=TEMP2+OMEG(NG)*(SOLN(I)-TEMP2)	INN01610
IF(P2(I,J).GT.0.000)GO TO 255	INN01620
P2(I,J)=0.000	INN01630
GO TO 270	INN01640
265 TEMP3=TEMP2/P2(I,J)	INN01650
IF(TEMP1.LT.TEMP3)TEMP1=TEMP3	INN01660
IF(TEMP4.GT.TEMP3)TEMP4=TEMP3	INN01670
270 CONTINUE	INN01680
280 CONTINUE	INN01690
DO 290 I=1,IM	INN01700
290 P2(I,IM)=0.000	INN01710
295 CONTINUE	INN01720
C TEST MIN AND MAX FLUX RATIO FOR THIS PLANE	INN01730
IF(TEMP1.GT.TEMP5)TEMP5=TEMP1	INN01740
IF(TEMP4.LT.TEMP6)TEMP6=TEMP4	INN01750
WRITE(IJSC2)P1	INN01760
DO 305 J=1,JM	INN01770
DO 305 I=1,IM	INN01780
P1(I,J)=P2(I,J)	INN01790
305 P2(I,J)=P3(I,J)	INN01800
310 CONTINUE	INN01810
C COMPLETE MESH NOW SWEEP	INN01820
WRITE(IJSC2)P1	INN01830
WRITE(IJSC2)P2	INN01840

```

C SWITCH DATASET DESIGNATIONS
  ITEMP4=IOSC2
  IOSC2=IOSC1
  IOSC1=ITEMP4
C NOW COMPUTE LARGEST RESIDUAL
  TEMP1=TEMP5
  TEMP4=TEMP6
  TEMP2=DABS(1.000-TEMP1)
  TEMP3=DABS(1.000-TEMP4)
  IF(TEMP2-TEMP3)330,330,320
320 TEMP3=TEMP2
330 NTIT=NTIT+1
  NIT=NIT+1
  IF(NIT.GE.NIIT)GO TO 340
  IF(TEMP3.GT.EPS2)GO TO 100
C INNER ITERATION CONVERGES, WRITE FLUXES ON IOPN
340 CONTINUE
  REWIND IOSC1
  IF(ITEMP5.EQ.5)GO TO 360
  DJ 350 K=1,KM
  READ(IOSC1)P2
  WRITE(IOPN)P2
350 CONTINUE
360 RETURN
  END

```

```

INN01850
INN01860
INN01870
INN01880
INN01890
INN01900
INN01910
INN01920
INN01930
INN01940
INN01950
INN01960
INN01970
INN01980
INN01990
INN02000
INN02010
INN02020
INN02030
INN02040
INN02050
INN02060
INN02070
INN02080
INN02090

```

SUBROUTINE GRBAL1(DD1,DD2,DD3,DD4,DD5,NPRMP,PSI,P1,P2,P3,XFISS,	GRB00010
1XINSC,XREM,XLEK,NNGV,IMV,JMV,KMV,NPRGV,NG)	GRB00020
IMPLICIT REAL*8 (A-H,O-Z)	GRB00030
INTEGER*2 MMAP,NPRMP	GRB00040
COMMON/INTG/IASIZE,NNG,NDG,NTDG,NMAT,IM,JM,KM,IRM,JRM,KRM,NLBC,	GRB00090
1NFBC,NBBC,NDNSCT,NPRG,IOPD,NTG,NXTP,NYTP,NZTP,IXTP(5),IYTP(5),	GRB00100
2IZTP(5),NSTEAD,IFLIN,IGEDM,ITITLE(20),NDIT,NIIT,NPIT,IOPSI,IODUMP,	GRB00110
3IOPN,IOPD,IOPN,IOPD,ITEMP,ITEMP1,ITEMP2,ITEMP3,ITEMP4,ITEMP5,	GRB00120
4NTIT,IETIME,IFLOUT,IMX,JMX,KMX,IOSC1,IOSC2,NGX	GRB00130
COMMON/FLOTE/EFFK,ORFP,EPS1,EPS2,TEMP,TEMP1,TEMP2,TEMP3,TEMP4,	GRB00140
1TEMP5,TEMP6,XFISST,XFISSO,ALAMN,ALAMO,TIME,FLXCON,BETAT	GRB00150
DIMENSION DD1(NPRGV,NNGV),DD2(NPRGV,NNGV),DD3(NPRGV,NNGV),DD4(NPRGV,	GRB00160
1V,NNGV),DD5(NPRGV,NNGV),NPRMP(IMV,JMV,KMV),PSI(NNGV,IMV,JMV,KMV),	GRB00170
2P1(IMV,JMV),P2(IMV,JMV),P3(IMV,JMV),XFISS(NNGV),XINSC(NNGV),	GRB00180
3XREM(NNGV),XLEK(NNGV)	GRB00190
XREM(NG)=0.000	GRB00200
XLEK(NG)=0.000	GRB00210
REWIND IOSC1	GRB00220
REWIND IOSC2	GRB00230
ONE=1.000	GRB00231
HALF=0.500	GRB00232
VOLB=ONE	GRB00233
VOLF=ONE	GRB00234
VOLL=ONE	GRB00235
IF(NBBC.EQ.1)VOLB=HALF	GRB00236
DO 230 K=1,KMX	GRB00240
READ(IOPD)P2	GRB00250
WRITE(IOSC2)P2	GRB00260
IF(K.GT.1)VOLB=ONE	GRB00261
IF(K.EQ.1.AND.NBBC.EQ.0) GO TO 230	GRB00270
IF(K.NE.2)GO TO 120	GRB00280
100 IF(NBBC.EQ.1)GO TO 120	GRB00290
C COMPUTE LEAKAGE FOR BOTTOM PLANE	GRB00300
IF(NFBC.EQ.1)VOLF=HALF	GRB00301
DO 110 J=1,JMX	GRB00310
IF(J.GT.1)VOLF=ONE	GRB00311

```

        IF(NLBC.EQ.1)VOLL=HALF
        DO 110 I=1,IMX
        IF(I.GT.1)VOLL=ONE
        NPR=NPRMP(I,J,1)
        XLEK(NG)=XLEK(NG)+DD3(NPR,NG)*P2(I,J)*VOLF*VOLL
110 CONTINUE
C COMPUTE FRONT LEAKAGE
120 IF(NFBC.EQ.1) GO TO 140
        IF(NLBC.EQ.1)VOLL=HALF
        DO 130 I=1,IMX
        IF(I.GT.1)VOLL=ONE
        NPR=NPRMP(I,1,K)
130 XLEK(NG)=XLEK(NG)+DD2(NPR,NG)*P2(I,2)*VOLL*VOLB
C COMPUTE LEFT LEAKAGE
140 IF(NLBC.EQ.1) GO TO 160
        IF(NFBC.EQ.1)VOLF=HALF
        DO 150 J=1,JMX
        IF(J.GT.1)VOLF=ONE
        NPR=NPRMP(I,J,K)
150 XLEK(NG)=XLEK(NG)+DD1(NPR,NG)*P2(2,J)*VOLF*VOLB
C COMPUTE RIGHT LEAKAGE
160 IF(NFBC.EQ.1)VOLF=HALF
        DO 170 J=1,JMX
        IF(J.GT.1)VOLF=ONE
        NPR=NPRMP(IMX,J,K)
170 XLEK(NG)=XLEK(NG)+DD1(NPR,NG)*P2(IMX,J)*VOLF*VOLB
C COMPUTE BACK LEAKAGE
        IF(NLBC.EQ.1)VOLL=HALF
        DO 180 I=1,IMX
        IF(I.GT.1)VOLL=ONE
        NPR=NPRMP(I,JMX,K)
180 XLEK(NG)=XLEK(NG)+DD2(NPR,NG)*P2(I,JMX)*VOLL*VOLB
        IF(NFBC.EQ.1)VOLF=HALF
        DO 200 J=1,JMX
        IF(J.GT.1)VOLF=ONE
        VOLC=VOLB*VOLF

```

```

GRB00312
GRB00320
GRB00321
GRB00330
GRB00340
GRB00350
GRB00360
GRB00370
GRB00371
GRB00380
GRB00381
GRB00390
GRB00400
GRB00410
GRB00420
GRB00421
GRB00430
GRB00431
GRB00440
GRB00450
GRB00460
GRB00461
GRB00470
GRB00471
GRB00480
GRB00490
GRB00500
GRB00501
GRB00510
GRB00511
GRB00520
GRB00530
GRB00531
GRB00540
GRB00541
GRB00542

```

IF(NLBC.EQ.1)VOLL=HALF	GRB00543
DO 190 I=1,IMX	GRB00550
IF(I.GT.1)VOLL=ONE	GRB00551
VOLD=VOLL*VOLC	GRB00552
NPR=NPR4P(I,J,K)	GRB00560
190 XREM(NG)=XREM(NG)+(DD5(NPR,NG)-DD4(NPR,NG))*P2(I,J)*VOLD	GRB00570
200 CONTINUE	GRB00580
IF(K.LT.KMX) GO TO 230	GRB00590
C COMPUTE TOP LEAKAGE	GRB00600
IF(NF3C.EQ.1)VOLF=HALF	GRB00601
DO 220 J=1,JMX	GRB00610
IF(J.GT.1)VOLF=ONE	GRB00610
IF(NLBC.EQ.1)VOLL=HALF	GRB00612
DO 210 I=1,IMX	GRB00620
IF(I.GT.1)VOLL=ONE	GRB00621
NPR=NPR4P(I,J,KMX)	GRB00630
210 XLEK(NG)=XLEK(NG)+DD3(NPR,NG)*P2(I,J)*VOLL*VOLF	GRB00640
220 CONTINUE	GRB00650
230 CONTINUE	GRB00660
READ(IDPO)P2	GRB00670
WRITE(IJSC2)P2	GRB00680
REWIND IDSC2	GRB00690
TEMP=(XFISS(NG)+XINSC(NG))/(XLEK(NG)+XREM(NG))	GRB00700
DO 260 K=1,KM	GRB00710
READ(IDSC2)P2	GRB00720
DO 250 J=1,JM	GRB00730
DO 250 I=1,IM	GRB00740
250 P2(I,J)=TEMP*P2(I,J)	GRB00750
WRITE(IJSC1)P2	GRB00760
260 CONTINUE	GRB00770
XREM(NG)=TEMP*XREM(NG)	GRB00780
XLEK(NG)=TEMP*XLEK(NG)	GRB00790
RETURN	GRB00800
END	GRB00810

SUBROUTINE FLUXTR(PSI,P2,NNGV,IMV,JMV,KMV)	FLU00010
IMPLICIT REAL*8 (A-H,O-Z)	FLU00020
INTEGER*2 MMAP,NPRMP	FLU00030
COMMON/INTG/IASIZE,NNG,NDG,NTOG,NMAT,IM,JM,KM,IRM,JRM,KRM,NLBC,	FLU00040
1NFBC,VBBC,VDNSCT,NPRG,IOPT,NTG,NXTP,NYTP,NZTP,IXTP(5),IYTP(5),	FLU00050
2IZTP(5),NSTEAD,IFLIN,IGEOM,ITITLE(20),NOIT,NIIT,NPIT,IJPSI,IODUMP,	FLU00060
3IJFN,IJFO,IOPN,IOPD,ITEMP,ITEMP1,ITEMP2,ITEMP3,ITEMP4,ITEMP5,	FLU00070
4NTIT,IETIME,IFLOUT,IMX,JMX,KMX,IOSC1,IOSC2,NGX	FLU00080
COMMON/FLDTE/EFFK,DRFP,EPS1,EPS2,TEMP,TEMP1,TEMP2,TEMP3,TEMP4,	FLU00130
1TEMP5,TEMP6,XFISST,XFISSD,ALAMN,ALAMD,TIME,FLXCON,BETAT	FLU00140
DIMENSION PSI(NNGV,IMV,JMV,KMV),P2(IMV,JMV)	FLU00150
0 WILL USE IOSC1 TO BUILD FLUXES FOR TRANSMITTAL TO TIMDEP	FLU00160
REWIND IOSC1	FLU00170
IF(IOPT.EQ.1)GO TO 200	FLU00180
DO 100 K=1,KM	FLU00190
DO 100 NG=1,NNG	FLU00200
WRITE(IJSC1)((PSI(NG,I,J,K),I=1,IM),J=1,JM)	FLU00210
100 CONTINUE	FLU00220
REWIND IOSC1	FLU00230
GO TO 300	FLU00240
200 CONTINUE	FLU00250
K=0	FLU00260
210 K=K+1	FLU00270
ITEMP2=K-1	FLU00280
IF(ITEMP2.EQ.0)GO TO 230	FLU00290
DO 220 ITEMP=1,ITEMP2	FLU00300
READ(IOPO)	FLU00310
220 CONTINUE	FLU00320
230 DO 250 ITEMP=1,NNG	FLU00330
READ(IOPO)P2	FLU00340
WRITE(IJSC1)P2	FLU00350
IF(ITEMP.EQ.NNG)GO TO 250	FLU00360
DO 240 ITEMP3=1,KMX	FLU00370
READ(IOPO)	FLU00380
240 CONTINUE	FLU00390
250 CONTINUE	FLU00400

REWIND IOPD
IF(K.LT.KM)GO TO 210
REWIND IOSCI
300 RETURN
END

FLU00410
FLU00420
FLU00430
FLU00440
FLU00450

```

SUBROUTINE TIMDEP(V,XI,XIM,XNU,SIGF,SIGR,SIGT,SIGS,ALAM,BETA,XIP, TIM00010
1X,Y,Z,HX,HY,HZ,IBP,JBP,KBP,DD1,DD2,DD3,DD4,DD5,DD6,DD7,VO,MMAP,NPRTIM00020
2MP,PSI,P1,P2,P3,PSO,W,PO,WI,NNGV,NDGV,NTDGV,NDNSCV,NMATV,IMV,JMV,KTIM00030
3MV,IRMV,JRMV,KRMV,NPRGV,NGXV) TIM00040
  IMPLICIT REAL*8 (A-H,O-Z) TIM00050
  INTEGER*2 MMAP,NPRMP TIM00060
  COMMON/INTG/IASIZE,NNG,NDG,NTDGV,NMAT,IM,JM,KM,IRM,JRM,KRM,NLBC, TIM00070
1NFBC,NB3C,NDNSCT,NPRG,IOPT,NTG,NXTP,NYTP,NZTP,IXTP(5),IYTP(5), TIM00080
2IZTP(5),NSTEAD,IFLIN,IGEOM,ITITLE(20),NOIT,NIIT,NPIT,IOPSI,IODUMP,TIM00090
3IOFN,IOFO,IOPN,IOPD,ITEMP,ITEMP1,ITEMP2,ITEMP3,ITEMP4,ITEMP5, TIM00100
4NTIT,IETIME,IFLOUT,IMX,JMX,KMX,IOSC1,IOSC2,NGX TIM00110
  COMMON/FLOTE/EFFK,DRFP,EPS1,EPS2,TEMP,TEMP1,TEMP2,TEMP3,TEMP4, TIM00160
1TEMP5,TEMP6,XFISST,XFISSO,ALAMN,ALAMO,TIME,FLXCON,BETAT TIM00170
  COMMON/TIMINT/LASZON,ISTPCH,ILINCH,I PRSTP,MNSCH(5),MNLCH(5), TIM00180
1ISTEP,ICHHT TIM00190
  COMMON/TIMFLO/T,HT,HMIN,HMAX,TSTART,TEND,DELSFS(5,4),DELSRS(5,4), TIM00200
1DELSTS(5,4),DELS1S(5,4),DELS2S(5,4),DELSFL(5,4),DELSRL(5,4), TIM00210
2DELSTL(5,4),DELS1L(5,4),DELS2L(5,4) TIM00220
  DIMENSION V(NNGV),XI(NNGV),XIM(NNGV),XNU(NMATV,NNGV), TIM00230
1SIGF(NMATV,NNGV),SIGR(NMATV,NNGV),SIGT(NMATV,NNGV),SIGS(NMATV,NNGV)TIM00240
2,NDNSCV),ALAM(NDGV),BETA(NDGV),XIP(NNGV,NDGV),X(IMV),Y(JMV),Z(KMV)TIM00250
3,HX(IRMV),HY(JRMV),HZ(KRMV),IBP(IRMV),JBP(JRMV),KBP(KRMV),DD1(NPRG)TIM00260
4V,NNGV),DD2(NPRGV,NNGV),DD3(NPRGV,NNGV),DD4(NPRGV,NNGV),DD5(NPRGV,TIM00270
5NNGV),DD6(NPRGV,NNGV),DD7(NPRGV,NGXV,NDNSCV),MMAP(IRMV,JRMV,KRMV),TIM00280
6NPRMP(IMV,JMV,KMV),PSI(NTDGV,IMV,JMV,KMV),P1(NTDGV,IMV,JMV), TIM00290
7P2(NTDGV,IMV,JMV),P3(NTDGV,IMV,JMV),PSO(IMV,JMV,KMV),W(IMV,JMV,KMV)TIM00300
8),PO(IMV,JMV),WI(IMV,JMV),VO(NPRGV) TIM00310
  IF(IOPT.EQ.0) GO TO 100 TIM00320
  REWIND IOPD TIM00330
  REWIND IOPN TIM00340
  REWIND IOFO TIM00350
  REWIND IOFN TIM00360
100 DO 105 NPR=1,NPRG TIM00365
  DO 105 NG=1,NNG TIM00370
  DD4(NPR,NG)=0.5DO*DD4(NPR,NG) TIM00375
  DD5(NPR,NG)=DD5(NPR,NG)-DD4(NPR,NG)-XIM(NG)*DD6(NPR,NG) TIM00380

```

```

105 CONTINUE
C CALL DELAYS TO COMPUTE INITIAL DELAYED NEUTRON PRECURSOR DENSITIES
C AND READ FLUXES FROM IOSCI
CALL DELAYS(ALAM,BETA,XIP,DD6,VD,NPRMP,PSI,P2,PSD,PD,NVG,NDG,NTOG,
INMAT,IM,JM,KM,NPRG)
DO 120 ND=1,NDG
DO 110 NG=1,NNG
110 XIP(NG,VD)=XIP(NG,ND)*ALAM(ND)
120 ALAM(ND)=ALAM(ND)/2.000
C ZERO FREQUENCY VECTOR
DO 130 K=1,KM
DO 130 J=1,JM
DO 130 I=1,IM
130 W(I,J,K)=0.000
TSTART=0.000
ISTEP=0
C START LOOP HERE OVER TIME ZONES BY CALLING TIMINP
200 CALL TIMINP
NFLAG1=1
IF(ISTPCH.GT.0)CALL CHANGE(XIM,XNU,SIGF,SIGR,SIGT,SIGS,HX,HY,HZ,
1IBP,JBP,KBP,DD1,DD2,DD3,DD4,DD5,DD6,DD7,MMAP,NNG,NDNSCT,NMAT,IM,JM
2,KM,IRM,JRM,KRM,NPRG,NFLAG1,NGX)
T=TSTART
HT=HMIN
NFLAG2=1
IF(ISTEP.EQ.0)CALL TIMOUT(PSI,P2,W,W1,NTOG,IM,JM,KM,NFLAG2)
210 IF(IOPT.EQ.1)GO TO 230
CALL STEPA0(V,XIM,ALAM,BETA,XIP,X,Y,Z,HX,HY,HZ,DD1,DD2,DD3,DD4,DD5
1,DD6,DD7,VD,NPRMP,PSI,W,NVG,NDG,NTOG,NDNSCT,IM,JM,KM,IRM,JRM,KRM,
2NPRG,NGX)
CALL STEPB0(V,XIM,ALAM,BETA,XIP,X,Y,Z,HX,HY,HZ,DD1,DD2,DD3,DD4,DD5
1,DD6,DD7,VD,NPRMP,PSI,W,NVG,NDG,NTOG,NDNSCT,IM,JM,KM,IRM,JRM,KRM,
2NPRG,NGX)
CALL FREQ0(PSI,PSD,W,NTOG,IM,JM,KM)
DO 220 K=1,KM
DO 220 J=1,JM

```

```

TIM00390
TIM00400
TIM00410
TIM00420
TIM00430
TIM00431
TIM00432
TIM00433
TIM00434
TIM00440
TIM00450
TIM00460
TIM00470
TIM00480
TIM00490
TIM00500
TIM00510
TIM00520
TIM00530
TIM00540
TIM00550
TIM00560
TIM00570
TIM00580
TIM00590
TIM00600
TIM00610
TIM00620
TIM00630
TIM00640
TIM00650
TIM00660
TIM00670
TIM00680
TIM00690
TIM00700

```

DO 220 I=1, IM	TIM00710
220 PSO(I, J, K)=PSI(NTG, I, J, K)	TIM00720
GO TO 250	TIM00730
230 CONTINUE	**TEMP**
C 230 CALL STEPAL(V, XIM, ALAM, BETA, XIP, X, Y, Z, HX, HY, HZ, DD1, DD2, DD3, DD4,	TIM00740
C 1DD5, DD6, DD7, NPRMP, P1, P2, P3, W, PO, W1, NNG, NDG, NTOG, NDNSCT, IM, JM, KM,	TIM00750
C 2IRM, JRM, KRM, NPRG)	TIM00760
C CALL STEPBI(V, XIM, ALAM, BETA, XIP, X, Y, Z, HX, HY, HZ, DD1, DD2, DD3, DD4,	TIM00770
C 1DD5, DD6, DD7, NPRMP, P1, P2, P3, W, PO, W1, NNG, NDG, NTOG, NDNSCT, IM, JM, KM,	TIM00780
C 2IRM, JRM, KRM, NPRG)	TIM00790
C CALL FREQ1(P2, PO, W, W1, NTOG, IM, JM, KM)	TIM00800
250 T=T+2.000*HT	TIM00810
ISTEP=ISTEP+1	TIM00820
NFLAG1=2	TIM00830
NFLAG2=0	TIM00840
IF(ILINCH.GT.0)CALL CHANGE(XIM, XNU, SIGF, SIGR, SIGT, SIGS, HX, HY, HZ,	TIM00850
1IBP, JBP, KBP, DD1, DD2, DD3, DD4, DD5, DD6, DD7, MMAP, NNG, NDNSCT, NMAT, IM, JM,	TIM00860
2, KM, IRM, JRM, KRM, NPRG, NFLAG1, NGX)	TIM00870
IF(DABS(T-TEND).LT.1.00-10)NFLAG2=1	TIM00880
IF(NFLAG2.EQ.1.OR.MOD(ISTEP, IPRSTP).EQ.0)CALL TIMEOUT(PSI, P2, W, W1,	TIM00890
INTOG, IM, JM, KM, NFLAG2)	TIM00900
IF(ICHHT.EQ.1)CALL TALTER	TIM00910
CALL ETIMEF(TEMP)	TIM00920
IF(TEMP.LT.TIME)GO TO 270	TIM00930
NFLAG2=2	TIM00940
LASZON=1	TIM00950
CALL TIMEOUT(PSI, P2, W, W1, NTOG, IM, JM, KM, NFLAG2)	TIM00960
GO TO 280	TIM00970
270 IF(NFLAG2.EQ.0)GO TO 210	TIM00980
TSTART=T	TIM00990
IF(LASZON.GT.0)GO TO 200	TIM01000
280 IF(IOPT.EQ.0)GO TO 300	TIM01010
REWIND IOFJ	TIM01020
REWIND IOFN	TIM01030
REWIND IOPJ	TIM01040
REWIND IOPN	TIM01050

REWIND IO SC1
REWIND IO SC2
300 RETURN
END

TIM01060
TIM01070
TIM01080
TIM01090

```

SUBROUTINE TIMINP
IMPLICIT REAL*8 (A-H,O-Z)
INTEGER*2 MMAP,NPRMP
COMMON/INTG/IASIZE,NNG,NDG,VTDG,NMAT,IM,JM,KM,IRM,JRM,KRM,NLBC,
1NFBC,NBRC,NDNSCT,NPRG,IOPT,VTG,NXTP,NYTP,NZTP,IXTP(5),IYTP(5),
2IZTP(5),NSTEAD,IFLIN,IGEOM,ITITLE(20),NDIT,NIIT,NPIT,IOPSI,IODUMP,
3IOFN,IOFO,IOPN,IOPJ,ITEMP,ITEMP1,ITEMP2,ITEMP3,ITEMP4,ITEMP5,
4NTIT,IETIME,IFLOUT,IMX,JMX,KMX,IOSC1,IOSC2,NGX
COMMON/FLOTE/EFFK,DRFP,EPS1,EPS2,TEMP,TEMP1,TEMP2,TEMP3,TEMP4,
ITEMP5,TEMP5,XFISST,XFISSD,ALAMN,ALAMO,TIME,FLXCON,BETAT
COMMON/TIMINT/LASZON,ISTPCH,ILINCH,IPRSTP,MNSCH(5),MNLCH(5),
LISTEP,ICHHT
COMMON/TIMFLO/T,HT,HMIN,HMAX,TSTART,TEND,DELSFS(5,4),DELSRS(5,4),
1DELSTS(5,4),DELSIS(5,4),DELS2S(5,4),DELSFL(5,4),DELSRL(5,4),
2DELSTL(5,4),DELS1L(5,4),DELS2L(5,4)
C READ IN FIRST TIME ZONE DESCRIPTION CARD (CARD TYPE 13)
100 READ(5,1000)LASZON,ISTPCH,ILINCH,IPRSTP,ICHHT,IFLOUT,HMIN,HMAX,TENTIM00210
1D TIM00211
1000 FORMAT(6I5,3D12.5) TIM00220
IF(ISTEP.GT.0)WRITE(6,1010) TIM00230
1010 FORMAT(1H1,/) TIM00240
IF(LASZON.GT.0)GO TO 110 TIM00250
LTMZON=LTMZON+1 TIM00260
GO TO 120 TIM00270
110 LTMZON=LASZON TIM00280
120 WRITE(6,1020)LTMZON TIM00290
1020 FORMAT(1H0,/,15X,'EDITED INPUT FOR TIME ZONE',I3,/) TIM00300
WRITE(6,1030)LASZON,ISTPCH,ILINCH,IPRSTP,ICHHT,IFLOUT,HMIN,HMAX,TETIM00310
1ND TIM00311
C IF ISTPCH GT 0, READ IN STEP CHANGE INFORMATION TIM00320
IF(ISTPCH.EQ.0)GO TO 140 TIM00330
DO 130 MN=1,ISTPCH TIM00340
DO 130 NG=1,NNG TIM00350
READ(5,1040)MNSCH(MN),DELSFS(MN,NG),DELSRS(MN,NG),DELSTS(MN,NG),
1DELS1S(MN,NG),DELS2S(MN,NG) TIM00360
WRITE(6,1050)MNSCH(MN),DELSFS(MN,NG),DELSRS(MN,NG),DELSTS(MN,NG), TIM00380

```

1DFLS1S(MN,NG),DELS2S(MN,NG)	TIM00390
130 CONTINUE	TIM00400
1030 FORMAT(11X,6I5,3D12.5)	TIM00410
1040 FORMAT(I5,5X,5D12.5)	TIM00420
1050 FORMAT(11X,I5,5X,5D12.5)	TIM00430
140 IF(ILINCH.EQ.0)GO TO 160	TIM00440
DO 150 MN=1,ILINCH	TIM00450
DO 150 NG=1,NNG	TIM00460
READ(5,1040)MNLCH(MN),DELSFL(MN,NG),DELSRL(MN,NG),DELSTL(MN,NG),	TIM00470
1DELS1L(MN,NG),DELS2L(MN,NG)	TIM00480
WRITE(6,1050)MNLCH(MN),DELSFL(MN,NG),DELSRL(MN,NG),DELSTL(MN,NG),	TIM00490
1DELS1L(MN,NG),DELS2L(MN,NG)	TIM00500
150 CONTINUE	TIM00510
C NOW PRINT OUT EDITED INFORMATION	TIM00520
160 WRITE(6,1060)HMIN,4MAX,TEND	TIM00530
1060 FORMAT(1H0,10X,'MIN. TIME STEP(SEC)= ',D12.6,' MAX. TIME STEP(SECT	TIM00540
1)= ',D12.6,' ZONE END TIME(SEC)= ',D12.6)	TIM00550
IF(ISTPCH.EQ.0)GO TO 180	TIM00560
WRITE(6,1070)ISTPCH	TIM00570
1070 FORMAT(1H0,10X,'STEP CHANGES IN ',I2,' MATERIALS IN THIS TIME ZONE	TIM00580
1')	TIM00590
WRITE(6,1080)	TIM00600
1080 FORMAT(1H0,55X,'TOTAL CHANGE (IN CM-1) IN CROSS-SECTIONS',/11X,	TIM00610
1'MATERIAL',4X,'GROUP',70X,'SCATTERING',/,35X,'FISSION',10X,	TIM00620
2'ABSORPTION',8X,'TRANSPORT',10X,'G TO G+1',10X,'G TO G+2',/)	TIM00630
DO 170 MN=1,ISTPCH	TIM00640
DO 170 NG=1,NNG	TIM00650
WRITE(6,1090)MNSCH(MN),NG,DELSFS(MN,NG),DELSRS(MN,NG),DELSTS(MN,NG	TIM00660
1),DELS1S(MN,NG),DELS2S(MN,NG)	TIM00670
170 CONTINUE	TIM00680
1090 FORMAT(1H ,14X,I2,7X,I2,2X,5(4X,D14.7))	TIM00690
180 IF(ILINCH.EQ.0)GO TO 200	TIM00700
WRITE(6,1100)ILINCH	TIM00710
1100 FORMAT(1H0,10X,'RAMP CHANGES IN ',I2,' MATERIALS IN THIS TIME ZONE	TIM00720
1')	TIM00730
WRITE(6,1080)	TIM00740

DO 190 MN=1,ILINCH	TIM00750
DO 193 NG=1,NNG	TIM00760
WRITE(6,1090)MNLCH(MN),NG,DELSFL(MN,NG),DELSRL(MN,NG),DELSTL(MN,NG)	TIM00770
1),DELSIL(MN,NG),DELSZL(MN,NG)	TIM00780
190 CONTINUE	TIM00790
200 WRITE(6,1110)	TIM00800
1110 FORMAT(1H0,/,10X,'BEGIN TIME-DEPENDENT CALCULATION FOR THIS ZONE'	TIM00810
1)	TIM00820
RETURN	TIM00830
END	TIM00840

```

SUBROUTINE TALTER
IMPLICIT REAL*8 (A-H,O-Z)
INTEGER*2 MMAP,NPRMP
COMMON/INTS/IASIZE,NNG,NDG,NTOG,NMAT,IM,JM,KM,IRM,JRM,KRM,NLBC,
1NFBC,NBBC,NDNSCT,NPRG,IOPD,NTG,NXTP,NYTP,NZTP,IXTP(5),IYTP(5),
2IZTP(5),NSTEAD,IFLIN,IGEOM,ITITLE(20),NDIT,NIIT,NPIT,IOPSI,IODUMP,
3IOFN,IOFO,IOPN,IOPD,ITEMP,ITEMP1,ITEMP2,ITEMP3,ITEMP4,ITEMP5,
4NTIT,IETIME,IFLOUT,IMX,JMX,KMX,IOSC1,IOSC2,NGX
COMMON/FLOTE/EFFK,DRFP,EPS1,EPS2,TEMP,TEMP1,TEMP2,TEMP3,TEMP4,
ITEMP5,TEMP6,XFISST,XFISSD,ALAMN,ALAMO,TIME,FLXCJN,BETAT
COMMON/TIMINT/LASZON,ISTPCH,ILINCH,IPRSTP,MNSCH(5),MNLCH(5),
1ISTEP,ICHHT
COMMON/TIMFLO/T,HT,HMIN,HMAX,TSTART,TEND,DELSFS(5,4),DELSRS(5,4),
1DELSTS(5,4),DELSIS(5,4),DELS2S(5,4),DELSFL(5,4),DELSRL(5,4),
2DELSTL(5,4),DELSIL(5,4),DELS2L(5,4)
C THE FOLLOWING LOGIC ASSURES THAT HT IS AN INTEGER MULTIPLE OF TIME
C ZONE LENGTH
TEMP5=(TEND-TSTART)/(2.000*HT)
ITEMP5=TEMP5
TEMP6=ITEMP5
IF((TEMP5-TEMP6).LT.1.00-11)GO TO 110
1000 FORMAT(1H0,15X,'*****INPUT HMIN (=HT) IS NOT AN INTEGER MULTIPLE OF
IF TIME ZONE LENGTH*****')
HT=(TEND-TSTART-2.000*HT)/(TEMP6-1.000)
WRITE(6,1000)
WRITE(6,1010)HT
1010 FORMAT(1H ,15X,'HT HAS BEEN CHANGED TO ',D20.13,' SECONDS AND WILL
) BE HELD FIXED AT THAT VALUE')
110 ICHHT=0
RETURN
END
TAL00010
TAL00020
TAL00030
TAL00040
TAL00050
TAL00060
TAL00070
TAL00080
TAL00130
TAL00140
TAL00150
TAL00160
TAL00170
TAL00180
TAL00190
TAL00200
TAL00210
TAL00220
TAL00230
TAL00240
TAL00250
TAL00260
TAL00270
TAL00280
TAL00290
TAL00300
TAL00310
TAL00320
TAL00330
TAL00340
TAL00350

```

```

SUBROUTINE DSIMQ(A,B,N,KS)
C THIS SUBROUTINE HAS BEEN TAKEN FROM THE IBM SCIENTIFIC
C SUBROUTINE PACKAGE AND CONVERTED TO DOUBLE PRECISION
  IMPLICIT REAL*8 (A-H,O-Z)
  DIMENSION A(1),B(1)

C
C   FORWARD SOLUTION
C
  TOL=0.0
  KS=0
  JJ=-N
  DO 65 J=1,N
  JY=J+1
  JJ=JJ+N+1
  BIGA=0
  IT=JJ-J
  DO 30 I=J,N

C
C   SEARCH FOR MAXIMUM COEFFICIENT IN COLUMN
C
  IJ=IT+I
  IF(DABS(BIGA)-DABS(A(IJ))) 20,30,30
20  BIGA=A(IJ)
  IMAX=I
30  CONTINUE

C
C   TEST FOR PIVOT LESS THAN TOLERANCE (SINGULAR MATRIX)
C
  IF(DABS(BIGA)-TOL) 35,35,40
35  KS=1
  RETURN

C
C   INTERCHANGE ROWS IF NECESSARY
C
40  I1=J+N*(J-2)
  IT=IMAX-J

```

```

SI00010
SI00020
SI00030
SI00040
SI00050
SI00060
SI00070
SI00080
SI00090
SI00100
SI00110
SI00120
SI00130
SI00140
SI00150
SI00160
SI00170
SI00180
SI00190
SI00200
SI00210
SI00220
SI00230
SI00240
SI00250
SI00260
SI00270
SI00280
SI00290
SI00300
SI00310
SI00320
SI00330
SI00340
SI00350
SI00360

```

```

DO 50 K=J,N
I1=I1+N
I2=I1+IT
SAVE=A(I1)
A(I1)=A(I2)
A(I2)=SAVE
C
C      DIVIDE EQUATION BY LEADING COEFFICIENT
C
50 A(I1)=A(I1)/BIGA
SAVE=B(IMAX)
B(IMAX)=B(J)
B(J)=SAVE/BIGA
C
C      ELIMINATE NEXT VARIABLE
C
IF(J-N) 55,70,55
55 IQS=N*(J-1)
DO 65 IX=JY,N
IXJ=IQS+IX
IT=J-IX
DO 60 JX=JY,N
IXJX=N*(JX-1)+IX
JJX=IXJX+IT
60 A(IXJX)=A(IXJX)-(A(IXJ)*A(JJX))
65 B(IX)=B(IX)-(B(J)*A(IXJ))
C
C      BACK SOLUTION
C
70 NY=N-1
IT=N*N
DO 80 J=1,NY
IA=IT-J
IB=N-J
IC=N
DO 80 K=1,J

```

```

SI00370
SI00380
SI00390
SI00400
SI00410
SI00420
SI00430
SI00440
SI00450
SI00460
SI00470
SI00480
SI00490
SI00500
SI00510
SI00520
SI00530
SI00540
SI00550
SI00560
SI00570
SI00580
SI00590
SI00600
SI00610
SI00620
SI00630
SI00640
SI00650
SI00660
SI00670
SI00680
SI00690
SI00700
SI00710
SI00720

```

```
B( IB)=B( IB)-A( IA)*B( IC)  
IA=IA-N  
80 IC=IC-1  
RETURN  
END
```

```
SI00730  
SI00740  
SI00750  
SI00760  
SI00770
```

```

SUBROUTINE TIMOUT(PSI,P2,W,N1,NTOGV,IMV,JMV,KMV,NFLAG2)      TIM00010
IMPLICIT REAL*8 (A-H,O-Z)      TIM00020
INTEGER*2 MMAP,NPRMP      TIM00030
COMMON/INTG/IASIZE,NNG,NDG,NTDG,NMAT,IM,JM,KM,IRM,JRM,KRM,NLBC,      TIM00040
INFBC,NBBC,NDNSCT,NPRG,IOPT,NTG,NXTP,NYTP,NZTP,IXTP(5),IYTP(5),      TIM00050
ZIZTP(5),NSTEAD,IFLIN,IGEOM,ITITLE(20),NOIT,NIIT,NPIT,IDPSI,IODUMP,      TIM00060
3IOFN,IJFO,IOPN,IOPD,ITEMP,ITEMP1,ITEMP2,ITEMP3,ITEMP4,ITEMP5,      TIM00070
4NTIT,IETIME,IFLOUT,IMX,JMX,KMX,IOSC1,IOSC2,NGX      TIM00080
COMMON/FLOTE/EFFK,DRFP,EPS1,EPS2,TEMP,TEMP1,TEMP2,TEMP3,TEMP4,      TIM00130
ITEMP5,TEMP6,XFISST,XFISSO,ALAMN,ALAMO,TIME,FLXCON,BETAT      TIM00140
COMMON/TIMINT/LASZON,ISTPCH,ILINCH,IPRSTP,MNSCH(5),MNLCH(5),      TIM00150
IISTEP,ICHHT      TIM00160
COMMON/TIMFLO/T,HT,HMIN,HMAX,TSTART,TEND,DELSFS(5,4),DELSRS(5,4),      TIM00170
1DELS1S(5,4),DELS1S(5,4),DELS2S(5,4),DELSFL(5,4),DELSRL(5,4),      TIM00180
2DELS1L(5,4),DELS1L(5,4),DELS2L(5,4)      TIM00190
DIMENSION PSI(NTOGV,IMV,JMV,KMV),P2(NTOGV,IMV,JMV),W(IMV,JMV,KMV),      TIM00200
IW1(IMV,JMV)      TIM00210
CALL ETIMEF(TEMP)      TIM00220
WRITE(6,1000)      TIM00230
1000 FORMAT(1H1,/)      TIM00240
IF(ISTEP.GT.0)GO TO 100      TIM00250
WRITE(6,1010)(ITITLE(I),I=1,20)      TIM00260
1010 FORMAT(1H,10X,'INITIAL FLUXES FOR THE PROBLEM ',20A4)      TIM00270
ISSAVE=ISTEP      TIM00280
100 WRITE(6,1020)ISTEP,T,HT,TEMP      TIM00290
1020 FORMAT(1H0,5X,'STEP NUMBER',I4,2X,'TRANSIENT TIME(SEC)=',1PD14.7      TIM00300
1,2X,'1/2 TIME STEP(SEC)=',1PD14.7,2X,'ELAPSED CPU TIME(MIN)=',      TIM00310
20PF10.4)      TIM00320
IF(ISTEP.EQ.0)GO TO 230      TIM00330
C WRITE OUT FREQUENCIES AT TEST POINTS      TIM00340
WRITE(6,1030)      TIM00350
1030 FORMAT(1H0,/,15X,'FREQUENCIES AT TEST POINTS',/)      TIM00360
DO 130 K=1,NZTP      TIM00370
IF(K.GT.1)GO TO 110      TIM00380
WRITE(6,1040)(IXTP(I),I=1,NXTP)      TIM00390
1040 FORMAT(1H,24X,'J / I',7X,5(I3,15X))      TIM00400

```

110	WRITE(6,1050)IZTP(K)	TIM00410
1050	FORMAT(1H0,12X,'PLANE ',I2)	TIM00420
	DO 120 JJ=1,NYTP	TIM00430
	J=NYTP+1-JJ	TIM00440
	WRITE(6,1060)IYTP(J),(W(IXTP(I)),IYTP(J),IZTP(K)),I=1,NXTP)	TIM00450
120	CONTINUE	TIM00460
1060	FORMAT(1H ,22X,I3,2X,5(4X,1PD14.7))	TIM00470
130	CONTINUE	TIM00480
	IF(IFLOUT.GT.0.AND.NFLAG2.GT.0)GO TO 220	TIM00490
C	GO HERE FOR WRITING OUT FLUXES AT TEST POINTS ONLY	TIM00500
	IF((NZTP*(NYTP+2)).GT.26)WRITE(6,1000)	TIM00510
	WRITE(6,1070)	TIM00520
1070	FORMAT(1H0,/,15X,'FLUXES AT TEST POINTS',/)	TIM00530
	LINCT=(NZTP*(NYTP+2))+14	TIM00540
	IF((NZTP*(NYTP+2)).GT.26)LINCT=10	TIM00550
C	IF IOPT=1, ASSUME NEW FLUXES ON IOPO AND THAT IOPO IS REWOUND	TIM00560
	KS=1	TIM00570
	DO 210 K=1,NZTP	TIM00580
	IF(K.GT.1)GO TO 140	TIM00590
	WRITE(6,1040)(IXTP(I),I=1,NXTP)	TIM00600
140	IF(IOPT.EQ.0)GO TO 170	TIM00610
	KD=IZTP(K)-KS	TIM00620
	IF(KD.EQ.0)GO TO 160	TIM00630
	DO 150 ITEMP3=1,KD	TIM00640
	READ(IOPO)	TIM00650
150	CONTINUE	TIM00660
160	READ(IOPO)P2	TIM00670
170	DO 200 NG=1,NNG	TIM00680
	ND=NG-NNG	TIM00690
	IF(NG.LE.NNG)WRITE(6,1080)IZTP(K),NG	TIM00700
	IF(NG.GT.NNG)WRITE(6,1090)IZTP(K),ND	TIM00710
1080	FORMAT(1H0,12X,'PLANE ',I2,' , NEUTRON GROUP ',I2)	TIM00720
1090	FORMAT(1H0,12X,'PLANE ',I2,' , PRECURSOR GROUP ',I2)	TIM00730
	DO 190 JJ=1,NYTP	TIM00740
	J=NYTP+1-JJ	TIM00750
	IF(IOPT.EQ.0)GO TO 180	TIM00760

WRITE(6,1060)IYTP(J), (P2(NG,IXTP(I),IYTP(J)),I=1,NXTP)	TIM00770
GO TO 190	TIM00780
180 WRITE(6,1050)IYTP(J), (PSI(NG,IXTP(I),IYTP(J),IZTP(K)),I=1,NXTP)	TIM00790
190 CONTINUE	TIM00800
LINECT=LINECT+NYTP+2	TIM00810
IF((LINECT+NYTP+2).LE.60)GO TO 200	TIM00820
WRITE(6,1000)	TIM00830
WRITE(6,1070)	TIM00840
WRITE(6,1040)(IXTP(I),I=1,NXTP)	TIM00850
LINECT=7	TIM00860
200 CONTINUE	TIM00870
KS=IZTP(K)	TIM00880
210 CONTINUE	TIM00890
GO TO 290	TIM00900
2 BRANCH HERE FOR COMPLETE FLUX DUMP	TIM00910
220 WRITE(6,1000)	TIM00920
WRITE(6,1100)(ITITLE(I),I=1,20)	TIM00930
1100 FORMAT(1H0,10X,'FLUXES FOR THE PROBLEM',20A4)	TIM00940
230 DO 280 K=1,KM	TIM00950
IF(IOPT.EQ.1)READ(IOPO)P2	TIM00960
DO 280 NG=1,NTOG	TIM00970
ND=NG-NNG	TIM00980
IF(K.GT.1.OR.NG.GT.1)WRITE(5,1110)	TIM00990
1110 FORMAT(1H1, /)	TIM01000
IF(NG.LE.NNG)WRITE(6,1120)K,NG	TIM01010
IF(NG.GT.NNG)WRITE(6,1130)K,ND	TIM01020
1120 FORMAT(1H0,10X,'NEUTRON FLUXES FOR PLANE ',I2,' , GROUP ',I2)	TIM01030
1130 FORMAT(1H0,10X,'PRECURSOR CONC. FOR PLANE ',I2,' , GROUP ',I2)	TIM01040
JMS=1	TIM01050
JME=JM	TIM01060
IF(JM.GT.50)JME=50	TIM01070
ITEMP2=50/JME	TIM01080
ITEMP4=ITEMP2	TIM01090
DO 270 I=1,IM,10	TIM01100
IS=I	TIM01110
IE=I+9	TIM01120

IF(IE.GT.IM)IE=IM	TIM01130
IF((I-1)/10.LT.ITEMP4)GO TO 240	TIM01140
WRITE(6,1110)	TIM01150
ITEMP4=ITEMP4+ITEMP2	TIM01160
240 WRITE(6,1140)(ITEMP3,ITEMP3=IS,IE)	TIM01170
1140 FJRMAT(1H0,3X,'J / I',2X,I7,9I12)	TIM01180
WRITE(6,1150)	TIM01190
1150 FJRMAT(1H ,3X)	TIM01200
DD 260 ITEMP3=JMS,JME	TIM01210
J=JME+1-ITEMP3	TIM01220
IF(IOPT.EQ.1)GO TO 250	TIM01230
WRITE(6,1150)J,(PSI(NG,II,J,K),II=IS,IE)	TIM01240
1160 FJRMAT(1H ,2X,I2,6X,1P10D12.5)	TIM01250
GO TO 260	TIM01260
250 WRITE(6,1150)J,(P2(NG,II,J),II=IS,IE)	TIM01270
260 CONTINUE	TIM01280
IF(JME.GE.JM)GO TO 270	TIM01290
JMS=JME+1	TIM01300
JME=JMS+49	TIM01310
IF(JME.GT.JM)JME=JM	TIM01320
WRITE(6,1110)	TIM01330
GO TO 240	TIM01340
270 CONTINUE	TIM01350
280 CONTINUE	TIM01360
CALL ETIMEF(TEMP)	TIM01370
WRITE(6,1180)TEMP	TIM01380
1180 FJRMAT(1H0,10X,'FLUX PRINTOUT COMPLETED, ELAPSED TIME(MIN) = ',F10	TIM01390
1.4)	TIM01400
IF(NFLAG2.EQ.2)WRITE(6,1170)	TIM01410
1170 FJRMAT(1H1,10X,'HAVE USED ALLOTTED CPU TIME')	TIM01420
290 CONTINUE	TIM01430
IF(IOPT.EQ.1)REWIND IOPO	TIM01440
RETURN	TIM01450
END	TIM01460

```

SUBROUTINE CHANGE(XIM,XNU,SIGF,SIGR,SIGT,SIGS,HX,HY,HZ,IBP,JBP,KBP,SET00010
1,DD1,DD2,DD3,DD4,DD5,DD6,DD7,MMAP,NGV,NDNSCV,NMATV,IMV,JMV,KMV, SET00020
2IRMV,JRMV,KRMV,NPRGV,NFLAG1,NGXV) SET00030
IMPLICIT REAL*8 (A-H,O-Z) SET00040
INTEGER*2 MMAP,NPRMP SET00050
COMMON/INTG/IASIZE,NNG,NDG,NTOG,NMAT,IM,JM,KM,IRM,JRM,KRM,NLBC, SET00060
INFBC,NBBC,NDNSCT,NPRG,IOP,NTG,NXTP,NYTP,NZTP,IXTP(5),IYTP(5), SET00070
2IZTP(5),NSTEAD,IFLIN,IGEOM,ITITLE(20),NDIT,NIIT,NPIT,IOPSI,IODUMP,SET00080
3IDFN,IOFO,IOPN,IOPD,ITEMP,ITEMP1,ITEMP2,ITEMP3,ITEMP4,ITEMP5, SET00090
4NTIT,IETIME,IFLOUT,IMX,JMX,KMX,IOSC1,IOSC2,NGX SET00100
COMMON/FLOTE/EFFK,ORFP,EPS1,EPS2,TEMP,TEMP1,TEMP2,TEMP3,TEMP4, SET00150
ITEMP5,TEMP6,XFISST,XFISSD,ALAMN,ALAMO,TIME,FLXCON,BETAT SET00160
COMMON/TIMINT/LASZON,ISTPCH,ILINCH,I PRSTP,MNSCH(5),MNLCH(5), SET00170
1ISTEP,ICHHT SET00180
COMMON/TIMFLO/T,HT,HMIN,HMAX,TSTART,TEND,DELSFS(5,4),DELSRS(5,4), SET00190
1DELSTS(5,4),DELS1S(5,4),DELS2S(5,4),DELSFL(5,4),DELSRL(5,4), SET00200
2DELSTL(5,4),DELS1L(5,4),DELS2L(5,4) SET00210
DIMENSION XIM(NGV),XNU(NMATV,NGV),SIGF(NMATV,NGV),SIGR(NMATV, SET00220
1NNGV),SIGT(NMATV,NGV),SIGS(NMATV,NGV,NDNSCV),HX(IRMV),HY(JRMV), SET00230
2HZ(KRMV),IBP(IRMV),JBP(JRMV),KBP(KRMV),DD1(NPRGV,NGV),DD2(NPRGV, SET00240
3NNGV),DD3(NPRGV,NGV),DD4(NPRGV,NGV),DD5(NPRGV,NGV),DD6(NPRGV, SET00250
4NNGV),DD7(NPRGV,NGXV,NDNSCV),MMAP(IRMV,JRMV,KRMV) SET00260
DIMENSION HD(6),MN(8) SET00270
TEMP=1.2D1 SET00280
TEMP1=8.0D0 SET00290
C FIRST ALTER CROSS SECTIONS SET00300
IF(NFLAG1.EQ.2)GO TO 110 SET00310
ITEMP1=ISTPCH SET00320
TEMP2=1.0D0 SET00330
GO TO 120 SET00340
110 ITEMPI=ILINCH SET00350
TEMP2=2.0D0*HT/(TEND-TSTART) SET00360
120 DJ 600 ITEMPI=1,ITEMPI SET00370
IF(NFLAG1.EQ.2)GO TO 150 SET00380
130 NM=MNSCH(ITEMPI) SET00390
MM=ITEMPI SET00395

```

	DO 140 NG=1,NNG	SET00400
	SIGF(NM,NG)=SIGF(NM,NG)+DELSFS(MM,NG)	SET00410
	SIGR(NM,NG)=SIGR(NM,NG)+DELSRS(MM,NG)+DELS1S(MM,NG)+DELS2S(MM,NG)	SET00420
	SIGT(NM,NG)=SIGT(NM,NG)+DELSTS(MM,NG)	SET00430
	SIGS(NM,NG,1)=SIGS(NM,NG,1)+DELS1S(MM,NG)	SET00440
	IF(NDNSCT.LT.2)GO TO 140	SET00450
	SIGS(NM,NG,2)=SIGS(NM,NG,2)+DELS2S(MM,NG)	SET00460
140	CONTINUE	SET00470
	GO TO 170	SET00480
150	NM=MNLCH(ITEMP2)	SET00490
	MM=ITEMP2	SET00495
	DO 160 NG=1,NNG	SET00500
	SIGF(NM,NG)=SIGF(NM,NG)+TEMP2*DELSFL(MM,NG)	SET00510
	SIGR(NM,NG)=SIGR(NM,NG)+TEMP2*(DELSRL(MM,NG)+DELS1L(MM,NG))	SET00520
	SIGT(NM,NG)=SIGT(NM,NG)+TEMP2*DELSTL(MM,NG)	SET00530
	SIGS(NM,NG,1)=SIGS(NM,NG,1)+TEMP2*DELS1L(MM,NG)	SET00540
	IF(NDNSCT.LT.2)GO TO 160	SET00550
	SIGR(NM,NG)=SIGR(NM,NG)+TEMP2*DELS2L(MM,NG)	SET00560
	SIGS(NM,NG,2)=SIGS(NM,NG,2)+TEMP2*DELS2L(MM,NG)	SET00570
160	CONTINUE	SET00580
C	LOOP OVER MATERIAL REGIONS, CHANGING COEFFICIENTS WHENEVER MMAP(IR,J	SET00590
C	R,KR)=NM	SET00600
170	DO 550 KR=1,KRM	SET00610
	DO 540 JR=1,JRM	SET00620
	DO 530 IR=1,IRM	SET00630
	IF(MMAP(IR,JR,KR).NE.NM)GO TO 530	SET00640
C	HOMOGENEOUS REGION	SET00650
	NPR=4*IRM*JRM*(2*KR-1)+2*IRM*(2*JR-1)+2*IR	SET00660
	ITEMP5=1	SET00670
	NPRP=NPR	SET00680
	HD(1)=HZ(KR)	SET00690
	HD(2)=HD(1)	SET00700
	HD(3)=HY(JR)	SET00710
	HD(4)=HD(3)	SET00720
	HD(5)=HX(IR)	SET00730
	HD(6)=HD(5)	SET00740

```

        DD 180 ITEMP4=1,8
        MN(ITEMP4)=MMAP(IR,JR,KR)
180 CONTINUE
        GO TO 500
C   LOWER LEFT EDGE
200 NPRP=NPR-4*IRM*JRM-1
        ITEMP5=2
        HD(1)=HZ(KR)
        HD(2)=HZ(KR-1)
        IF(KR.EQ.1)HD(2)=HD(1)
        HD(5)=HX(IR)
        HD(6)=HX(IR-1)
        IF(IR.EQ.1)HD(6)=HD(5)
        MN(1)=MMAP(IR,JR,KR-1)
        IF(KR.EQ.1)MN(1)=MN(5)
        MN(4)=MN(1)
        MN(6)=MMAP(IR-1,JR,KR)
        IF(IR.EQ.1)MN(6)=MN(5)
        MN(7)=MN(6)
        MN(2)=MMAP(IR-1,JR,KR-1)
        IF(KR.EQ.1)MN(2)=MN(6)
        IF(IR.EQ.1)MN(2)=MN(1)
        MN(3)=MN(2)
        GO TO 500
C   LEFT SIDE
210 NPRP=NPR-1
        ITEMP5=3
        HD(2)=HD(1)
        MN(4)=MN(8)
        MN(1)=MN(5)
        MN(2)=MN(6)
        MN(3)=MN(7)
        GO TO 500
C   LEFT FRONT EDGE
220 NPRP=NPR-2*IRM-1
        ITEMP5=4

```

```

SET00750
SET00760
SET00770
SET00780
SET00790
SET00800
SET00810
SET00820
SET00830
SET00840
SET00850
SET00860
SET00870
SET00880
SET00890
SET00900
SET00910
SET00920
SET00930
SET00940
SET00950
SET00960
SET00970
SET00980
SET00990
SET01000
SET01010
SET01020
SET01030
SET01040
SET01050
SET01060
SET01070
SET01080
SET01090
SET01100

```

MN(8)=MMAP(IR,JR-1,KR)
IF(JR.EQ.1)MN(8)=MN(5)
MN(4)=MN(8)
MN(7)=MMAP(IR-1,JR-1,KR)
IF(IR.EQ.1)MN(7)=MN(8)
IF(JR.EQ.1)MN(7)=MN(6)
MN(3)=MN(7)
HD(4)=HY(JR-1)
IF(JR.EQ.1)HD(4)=HD(3)
GO TO 500

C LOWER FRONT EDGE

230 NPRP=VPR-4*IRM*JRM-2*IRM
ITEMP5=5
HD(2)=HZ(KR-1)
IF(KR.EQ.1)HD(2)=HD(1)
HD(6)=HD(5)
MN(6)=MN(5)
MN(1)=MMAP(IR,JR,KR-1)
IF(KR.EQ.1)MN(1)=MN(5)
MN(2)=MN(1)
MN(7)=MN(8)
MN(4)=MMAP(IR,JR-1,KR-1)
IF(KR.EQ.1)MN(4)=MN(8)
IF(JR.EQ.1)MN(4)=MN(1)
MN(3)=MN(4)
GO TO 500

C LOWER FRONT LEFT CORNER

240 NPRP=NPR-4*IRM*JRM-2*IRM-1
ITEMP5=5
HD(6)=HX(IR-1)
IF(IR.EQ.1)HD(6)=HD(5)
MN(6)=MMAP(IR-1,JR,KR)
IF(IR.EQ.1)MN(6)=MN(5)
MN(2)=MMAP(IR-1,JR,KR-1)
IF(IR.EQ.1)MN(2)=MN(1)
IF(KR.EQ.1)MN(2)=MN(6)

SET01110
SET01120
SET01130
SET01140
SET01150
SET01160
SET01170
SET01180
SET01190
SET01200
SET01210
SET01220
SET01230
SET01240
SET01250
SET01260
SET01270
SET01280
SET01290
SET01300
SET01310
SET01320
SET01330
SET01340
SET01350
SET01360
SET01370
SET01380
SET01390
SET01400
SET01410
SET01420
SET01430
SET01440
SET01450
SET01460

```

MN(7)=MMAP(IR-1,JR-1,KR)
IF(IR.EQ.1)MN(7)=MN(8)
IF(JR.EQ.1)MN(7)=MN(6)
MN(3)=MMAP(IR-1,JR-1,KR-1)
IF(IR.EQ.1)MN(3)=MN(4)
IF(JR.EQ.1)MN(3)=MN(2)
IF(KR.EQ.1)MN(3)=MN(7)
GO TO 500
C FRONT SIDE
250 NPRP=NPR-2*IRM
ITEMP5=7
HD(2)=HD(1)
HD(6)=HD(5)
MN(4)=MN(8)
MN(7)=MN(8)
MN(3)=MN(8)
MN(6)=MN(5)
MN(1)=MN(5)
MN(2)=MN(5)
GO TO 500
C BOTTOM SIDE
260 NPRP=NPR-4*IRM*JRM
ITEMP5=8
HD(2)=HZ(KR-1)
IF(KR.EQ.1)HD(2)=HD(1)
HD(4)=HD(3)
MN(8)=MN(5)
MN(7)=MN(6)
MN(1)=MMAP(IR,JR,KR-1)
IF(KR.EQ.1)MN(1)=MN(5)
MN(2)=MN(1)
MN(3)=MN(1)
MN(4)=MN(1)
GO TO 500
C BOTTOM RIGHT EDGE (9)
270 IF(IR.EQ.IRM)GO TO 360

```

```

SET01470
SET01480
SET01490
SET01500
SET01510
SET01520
SET01530
SET01540
SET01550
SET01560
SET01570
SET01580
SET01590
SET01600
SET01610
SET01620
SET01630
SET01640
SET01650
SET01660
SET01670
SET01680
SET01690
SET01700
SET01710
SET01720
SET01730
SET01740
SET01750
SET01760
SET01770
SET01780
SET01790
SET01800
SET01810
SET01820

```

```

NPRP=NPR-4*IRM*JRM+1
ITEMP5=9
HD(5)=HX(IR+1)
MN(5)=MMAP(IR+1,JR,KR)
MN(8)=MN(5)
MN(1)=MMAP(IR+1,JR,KR-1)
IF(KR.EQ.1)MN(1)=MN(5)
MN(4)=MV(1)
GO TO 500
C FRONT BOTTOM RIGHT CORNER (10)
280 NPRP=NPR-4*IRM*JRM-2*IRM+1
ITEMP5=10
IF(JR.EQ.1)GO TO 285
HD(4)=HY(JR-1)
MN(7)=MMAP(IR,JR-1,KR)
MN(3)=MMAP(IR,JR-1,KR-1)
MN(8)=MMAP(IR+1,JR-1,KR)
MN(4)=MMAP(IR+1,JR-1,KR-1)
IF(KR.NE.1)GO TO 285
MN(3)=MN(7)
MV(4)=MV(8)
285 GO TO 500
C FRONT RIGHT EDGE
290 NPRP=NPR-2*IRM+1
HD(2)=HD(1)
ITEMP5=11
IF(KR.EQ.1)GO TO 295
MN(4)=MN(8)
MN(3)=MV(7)
MN(1)=MN(5)
MN(2)=MN(6)
295 GO TO 500
C FRONT TOP RIGHT CORNER (12)
300 IF(KR.EQ.KRM)GO TO 320
NPRP=NPR+4*IRM*JRM-2*IRM+1
ITEMP5=12

```

```

SET01830
SET01840
SET01850
SET01860
SET01870
SET01880
SET01890
SET01900
SET01910
SET01920
SET01930
SET01940
SET01950
SET01960
SET01970
SET01980
SET01990
SET02000
SET02010
SET02020
SET02030
SET02040
SET02050
SET02060
SET02070
SET02080
SET02090
SET02100
SET02110
SET02120
SET02130
SET02140
SET02150
SET02160
SET02170
SET02180

```

```

      HD(1)=HZ(KR+1)
      MN(6)=MMAP(IR,JR,KR+1)
      MN(5)=MMAP(IR+1,JR,KR+1)
      MN(8)=MMAP(IR+1,JR-1,KR+1)
      MN(7)=MMAP(IR,JR-1,KR+1)
      IF(JR.NE.1)GO TO 305
      MN(8)=MN(5)
      MN(7)=MN(6)
305 GO TO 500
C   TOP RIGHT EDGE (13)
310 NPRP=NPR+4*IRM*JRM+1
      ITEMP5=13
      IF(JR.EQ.1)GO TO 315
      HD(4)=HD(3)
      MN(7)=MN(6)
      MN(8)=MN(5)
      MN(4)=MN(1)
      MN(3)=MN(2)
315 GO TO 500
C   RIGHT SIDE (14)
320 NPRP=NPR+1
      ITEMP5=14
      IF(KR.NE.KRM)GO TO 325
      IF(JR.EQ.1)GO TO 325
      HD(4)=HD(3)
      MN(4)=MN(1)
      MN(3)=MN(2)
325 MN(8)=MN(4)
      MN(5)=MN(1)
      MN(7)=MN(3)
      MN(6)=MN(2)
      HD(1)=HD(2)
      GO TO 500
C   BACK BOTTOM RIGHT CORNER (15)
330 IF(JR.EQ.JRM)GO TO 420
      NPRP=NPR-4*IRM*JRM+2*IRM+1

```

```

SET02190
SET02200
SET02210
SET02220
SET02230
SET02240
SET02250
SET02260
SET02270
SET02280
SET02290
SET02300
SET02310
SET02320
SET02330
SET02340
SET02350
SET02360
SET02370
SET02380
SET02390
SET02400
SET02410
SET02420
SET02430
SET02440
SET02450
SET02460
SET02470
SET02475
SET02480
SET02490
SET02500
SET02510
SET02520
SET02530

```



```

ITEMP5=15
HD(3)=HY(JR+1)
MN(5)=MMAP(IR+1, JR+1, KR)
MN(6)=MMAP(IR, JR+1, KR)
MN(2)=MV(6)
MN(1)=MN(5)
IF(KR.EQ.1)GO TO 335
HD(2)=HZ(KR-1)
MN(2)=MMAP(IR, JR+1, KR-1)
MN(1)=MMAP(IR+1, JR+1, KR-1)
MN(3)=MMAP(IR, JR, KR-1)
MN(4)=MMAP(IR+1, JR, KR-1)
335 GO TO 500
C BACK RIGHT EDGE (16)
340 NPRP=NPR+2*IRM+1
ITEMP5=16
IF(KR.EQ.1)GO TO 345
HD(2)=HZ(KR)
MN(1)=MN(5)
MN(2)=MN(6)
MN(3)=MV(7)
MN(4)=MN(8)
345 GO TO 500
C BACK TOP RIGHT CORNER (17)
350 IF(KR.EQ.KRM)GO TO 370
NPRP=VPR+4*IRM*JRM+2*IRM+1
ITEMP5=17
HD(1)=HZ(KR+1)
MN(5)=MMAP(IR+1, JR+1, KR+1)
MN(6)=MMAP(IR, JR+1, KR+1)
MN(7)=MMAP(IR, JR, KR+1)
MN(8)=MMAP(IR+1, JR, KR+1)
GO TO 500
C BACK TOP EDGE (18)
360 IF(JR.EQ.JRM)GO TO 420
IF(KR.EQ.KRM)GO TO 370

```

```

SET02540
SET02550
SET02560
SET02570
SET02580
SET02590
SET02600
SET02610
SET02620
SET02630
SET02640
SET02650
SET02660
SET02670
SET02680
SET02690
SET02700
SET02710
SET02720
SET02730
SET02740
SET02750
SET02760
SET02770
SET02775
SET02780
SET02785
SET02790
SET02800
SET02810
SET02820
SET02830
SET02840
SET02850
SET02860
SET02865
SET02870

```

```

NPRP=NPR+4*IRM*JRM+2*IRM
ITEMP5=18
IF(IR.NE.IRM)GO TO 365
HD(1)=HZ(KR+1)
HD(2)=HZ(KR)
HD(3)=HY(JR+1)
MN(2)=MMAP(IR,JR+1,KR)
MN(3)=MMAP(IR,JR,KR)
MN(6)=MMAP(IR,JR+1,KR+1)
MN(7)=MMAP(IR,JR,KR+1)
365 MN(1)=MN(2)
MN(4)=MN(3)
MN(5)=MN(6)
MN(8)=MN(7)
HD(5)=HD(6)
GO TO 500
C BACK SIDE (19)
370 NPRP=NPR+2*IRM
ITEMP5=19
IF(IR.NE.IRM.AND.KR.NE.KRM)GO TO 375
MN(2)=MMAP(IR,JR+1,KR)
MN(3)=MMAP(IR,JR,KR)
HD(2)=HD(1)
HD(3)=HY(JR+1)
HD(5)=HD(6)
MN(4)=MN(3)
MN(1)=MN(2)
375 HD(1)=HZ(KR)
MN(5)=MN(1)
MN(6)=MN(2)
MN(7)=MN(3)
MN(8)=MN(4)
GO TO 500
C BACK BOTTOM EDGE (20)
380 NPRP=NPR-4*IRM*JRM+2*IRM
ITEMP5=20

```

```

SET02875
SET02880
SET02890
SET02900
SET02910
SET02920
SET02930
SET02940
SET02950
SET02960
SET02970
SET02980
SET02990
SET03000
SET03010
SET03020
SET03030
SET03040
SET03050
SET03060
SET03062
SET03064
SET03066
SET03068
SET03070
SET03080
SET03090
SET03100
SET03110
SET03120
SET03130
SET03140
SET03150
SET03160
SET03170
SET03180

```

```

IF(KR.EQ.1)GO TO 385
HD(2)=HZ(KR-1)
MN(1)=MMAP(IR,JR+1,KR-1)
MN(2)=MN(1)
MN(3)=MMAP(IR,JR,KR-1)
MN(4)=MN(3)
385 GO TO 500
C BACK BOTTOM LEFT CORNER (21)
390 NPRP=NPR-4*IRM*JRM+2*IRM-1
ITEMP5=21
IF(IR.EQ.1)GO TO 395
HD(6)=HX(IR-1)
MN(6)=MMAP(IR-1,JR+1,KR)
MN(7)=MMAP(IR-1,JR,KR)
MN(3)=MN(7)
MN(2)=MN(6)
IF(KR.EQ.1)GO TO 395
MN(3)=MMAP(IR-1,JR,KR-1)
MN(2)=MMAP(IR-1,JR+1,KR-1)
395 GO TO 500
C BACK LEFT EDGE (22)
400 NPRP=NPR+2*IRM-1
ITEMP5=22
IF(KR.EQ.1)GO TO 405
MN(1)=MN(5)
MN(2)=MN(6)
MN(3)=MN(7)
MN(4)=MN(8)
HD(2)=HD(1)
405 GO TO 500
C BACK TOP LEFT CORNER (23)
410 IF(KR.EQ.KRM)GO TO 530
NPRP=NPR+4*IRM*JRM+2*IRM-1
ITEMP5=23
HD(1)=HZ(KR+1)
MN(5)=MMAP(IR,JR+1,KR+1)

```

```

SET03190
SET03200
SET03210
SET03220
SET03230
SET03240
SET03250
SET03260
SET03270
SET03280
SET03290
SET03300
SET03310
SET03320
SET03330
SET03340
SET03350
SET03360
SET03370
SET03380
SET03390
SET03400
SET03410
SET03420
SET03430
SET03440
SET03450
SET03460
SET03470
SET03480
SET03490
SET03500
SET03510
SET03520
SET03530
SET03540

```

```

MN(8)=MMAP(IR,JR,KR+1)
MN(6)=MN(5)
MN(7)=MN(8)
IF(IR.EQ.1)GO TO 415
MN(6)=MMAP(IR-1,JR+1,KR+1)
MN(7)=MMAP(IR-1,JR,KR+1)
415 GO TO 500
C TOP LEFT EDGE (24)
420 IF(KR.EQ.KRM)GO TO 530
NPRP=NPR+4*IRM*JRM-1
ITEMP5=24
IF(IR.NE.IRM.AND.JR.NE.JRM)GO TO 425
HD(1)=HZ(KR+1)
HD(2)=HZ(KR)
HD(5)=HX(IR)
MN(8)=MMAP(IR,JR,KR+1)
MN(4)=MMAP(IR,JR,KR)
MN(7)=MN(8)
MN(3)=MN(4)
IF(IR.EQ.1)GO TO 425
HD(6)=HX(IR-1)
MN(7)=MMAP(IR-1,JR,KR+1)
MN(3)=MMAP(IR-1,JR,KR)
425 HD(3)=HD(4)
MN(1)=MN(4)
MN(2)=MN(3)
MN(5)=MN(8)
MN(6)=MN(7)
GO TO 500
C FRONT TOP LEFT CORNER
430 NPRP=NPR+4*IRM*JRM-2*IRM-1
ITEMP5=25
IF(JR.EQ.1)GO TO 435
HD(4)=HY(JR-1)
MN(4)=MMAP(IR,JR-1,KR)
MN(8)=MMAP(IR,JR-1,KR+1)

```

```

SET03550
SET03560
SET03570
SET03580
SET03590
SET03600
SET03610
SET03620
SET03630
SET03635
SET03640
SET03650
SET03660
SET03665
SET03670
SET03680
SET03690
SET03700
SET03705
SET03710
SET03720
SET03730
SET03740
SET03750
SET03760
SET03770
SET03780
SET03790
SET03800
SET03810
SET03820
SET03830
SET03840
SET03850
SET03860
SET03870

```

MN(3)=MN(4)	SET03880
MN(7)=MN(8)	SET03890
IF(IR.EQ.1)GO TO 435	SET03900
MN(3)=MMAP(IR-1,JR-1,KR)	SET03910
MN(7)=MMAP(IR-1,JR-1,KR+1)	SET03920
435 GO TO 500	SET03930
C TOP FRONT EDGE	SET03940
440 NPRP=VPR+4*IRM*JRM-2*IRM	SET03950
ITEMP5=26	SET03960
IF(IR.EQ.1)GO TO 445	SET03970
HD(6)=HD(5)	SET03980
MN(2)=MN(1)	SET03990
MN(3)=MN(4)	SET04000
MN(6)=MN(5)	SET04010
MN(7)=MN(8)	SET04020
445 GO TO 500	SET04030
C TOP SIDE (27)	SET04040
450 NPRP=NPR+4*IRM*JRM	SET04050
ITEMP5=27	SET04060
IF(JR.EQ.1)GO TO 455	SET04070
HD(4)=HD(3)	SET04080
MN(4)=MN(1)	SET04090
MN(3)=MN(2)	SET04100
MN(7)=MN(6)	SET04110
MN(8)=MN(5)	SET04120
455 GO TO 500	SET04130
C BRANCH HERE TO COMPUTE COEFFICIENTS	SET04140
500 NRP=NPRP	SET04150
TEMP3=1.000	SET04160
DO 520 NG=1,NNG	SET04170
DD1(NRP,NG)=((HD(3)*HD(2)/SIGT(MN(1),NG))+(HD(3)*HD(1)/SIGT(MN(5),	SET04180
1NG))+(HD(4)*HD(2)/SIGT(MN(4),NG))+(HD(4)*HD(1)/SIGT(MN(8),NG)))*	SET04190
2(TEMP3/(HD(5)*TEMP))	SET04200
DD2(NRP,NG)=((HD(5)*HD(2)/SIGT(MN(1),NG))+(HD(6)*HD(2)/SIGT(MN(2),	SET04210
1NG))+(HD(6)*HD(1)/SIGT(MN(6),NG))+(HD(5)*HD(1)/SIGT(MN(5),NG)))*	SET04220
2(TEMP3/(HD(3)*TEMP))	SET04230

```

DD3(NRP,NG)=((HD(4)*HD(5)/SIGT(MN(7),NG))+(HD(4)*HD(5)/SIGT(MN(8),SET04240
1NG))+(HD(3)*HD(5)/SIGT(MN(5),NG))+(HD(3)*HD(6)/SIGT(MN(6),NG))) * SET04250
2(TEMP3/(HD(1)*TEMP)) SET04260
DD4(NRP,NG)=DD1(NRP,NG)+DD2(NRP,NG)+DD3(NRP,NG)+(((HD(3)*HD(2)/SIGSET04270
1T(MN(2),NG))+(HD(4)*HD(2)/SIGT(MN(3),NG))+(HD(4)*HD(1)/SIGT(MN(7),SET04280
2NG))+(HD(3)*HD(1)/SIGT(MN(6),NG)))/(HD(6)*TEMP)+(HD(6)*HD(2)/SIGTSET04290
3(MN(3),NG))+(HD(5)*HD(2)/SIGT(MN(4),NG))+(HD(5)*HD(1)/SIGT(MN(8),NSET04300
4G))+(HD(6)*HD(1)/SIGT(MN(7),NG)))/(HD(4)*TEMP)+(HD(5)*HD(3)/SIGT(SET04310
5MN(1),NG))+(HD(3)*HD(6)/SIGT(MN(2),NG))+(HD(4)*HD(6)/SIGT(MN(3),NGSET04320
6))+(HD(4)*HD(5)/SIGT(MN(4),NG)))/(HD(2)*TEMP))*TEMP3 SET04330
DD4(NRP,NG)=0.5D0*DD4(NRP,NG) SET04340
DD5(NRP,NG)=DD4(NRP,NG)+(HD(5)*HD(3)*HD(2)*S IGR(MN(1),NG)+HD(6)*HDSET04350
1(3)*HD(2)*S IGR(MN(2),NG)+HD(6)*HD(4)*HD(2)*S IGR(MN(3),NG)+HD(5)*HDSET04360
2(4)*HD(2)*S IGR(MN(4),NG)+HD(5)*HD(3)*HD(1)*S IGR(MN(5),NG)+HD(6)*HDSET04370
3(3)*HD(1)*S IGR(MN(5),NG)+HD(6)*HD(4)*HD(1)*S IGR(MN(7),NG)+HD(5)*HDSET04380
4(4)*HD(1)*S IGR(MN(8),NG))*(TEMP3/TEMP1) SET04390
DD6(NRP,NG)=(HD(5)*HD(3)*HD(2)*S IGF(MN(1),NG)*XNU(MN(1),NG)+HD(6)*HD(6)*SET04400
1HD(3)*HD(2)*S IGF(MN(2),NG)*XNU(MN(2),NG)+HD(6)*HD(4)*HD(2)*S IGF(MNSET04410
2(3),NG)*XNU(MN(3),NG)+HD(5)*HD(4)*HD(2)*S IGF(MN(4),NG)*XNU(MN(4),NSET04420
3G)+HD(5)*HD(3)*HD(1)*S IGF(MN(5),NG)*XNU(MN(5),NG)+HD(6)*HD(3)*HD(1SET04430
4)*S IGF(MN(6),NG)*XNU(MN(6),NG)+HD(6)*HD(4)*HD(1)*S IGF(MN(7),NG)*XNSET04440
5U(MN(7),NG)+HD(5)*HD(4)*HD(1)*S IGF(MN(8),NG)*XNU(MN(8),NG))*(TEMP3SET04450
6/TEMP1) SET04460
DD5(NRP,NG)=DD5(NRP,NG)-XIM(NG)*DD6(NRP,NG) SET04470
IF(NG.EQ.NNG)GO TO 520 SET04471
DJ 510 NDN=1,NDNSCT SET04480
DD7(NRP,NG,NDN)=(HD(5)*HD(3)*HD(2)*S IGS(MN(1),NG,NDN)+HD(6)*HD(3)*SET04490
1HD(2)*S IGS(MN(2),NG,NDN)+HD(6)*HD(4)*HD(2)*S IGS(MN(3),NG,NDN)+HD(5SET04500
2)*HD(4)*HD(2)*S IGS(MN(4),NG,NDN)+HD(5)*HD(3)*HD(1)*S IGS(MN(5),NG,NSET04510
3DN)+HD(5)*HD(3)*HD(1)*S IGS(MN(6),NG,NDN)+HD(6)*HD(4)*HD(1)*S IGS(MNSET04520
4(7),NG,NDN)+HD(5)*HD(4)*HD(1)*S IGS(MN(8),NG,NDN))*(TEMP3/TEMP1) SET04530
510 CONTINUE SET04540
520 CONTINUE SET04550
GO TO (200,210,220,230,240,250,260,270,280,290,300,310,320,330,340SET04560
1,350,360,370,380,390,400,410,420,430,440,450,530),ITEMP5 SET04570
530 CONTINUE SET04580

```

540 CONTINUE
550 CONTINUE
600 CONTINUE
RETURN
END

SET04590
SET04600
SET04610
SET04620
SET04630

```

SUBROUTINE DELAYS(ALAM,BETA,XIP,DD6,VO,NPRMP,PSI,P2,PSJ,PO,NNGV,NNDEL00010
1GV,NTOGV,NMATV,IMV,JMV,KMV,NPRGV) DEL00020
IMPLICIT REAL*8 (A-H,O-Z) DEL00030
INTEGER*2 NMAP,NPRMP DEL00040
COMMON/INTG/IASIZE,NNG,NDG,NTOG,NMAT,IM,JM,KM,IRM,JRM,KRM,NLBC, DEL00050
1NFBC,NB3C,VDNSCT,NPRG,IOPT,NTG,NXTP,NYTP,NZTP,IXTP(5),IYTP(5), DEL00060
2IZTP(5),NSTEAD,IFLIN,IGEOM,ITITLE(20),NDIT,NIIT,NPIT,IJPSI,IODUMP, DEL00070
3IOFN,IJFO,IOPN,IOPD,ITEMP,ITEMP1,ITEMP2,ITEMP3,ITEMP4,ITEMP5, DEL00080
4NTIT,IETIME,IFLOUT,IMX,JMX,KMX,IOSC1,IOSC2,NGX DEL00090
COMMON/FLOTE/EFFK,DRFP,EPS1,EPS2,TEMP,TEMP1,TEMP2,TEMP3,TEMP4, DEL00140
1TEMP5,TEMP6,XFISST,XFISSO,ALAMN,ALAMO,TIME,FLXCON,BETAT DEL00150
COMMON/TIMINT/LASZON,ISTPCH,ILINCH,IIRSTP,MVSCH(5),MNLCH(5), DEL00160
1ISTEP,ICHHT DEL00170
COMMON/TIMFLO/T,HT,HMIN,HMAX,TSTART,TEND,DELSFS(5,4),DELSRS(5,4), DEL00180
1DELSTS(5,4),DELS1S(5,4),DELS2S(5,4),DELSFL(5,4),DELSRL(5,4), DEL00190
2DELSTL(5,4),DELS1L(5,4),DELS2L(5,4) DEL00200
DIMENSION ALAM(NDGV),BETA(NDGV),XIP(NNGV,NDGV),DD6(NPRGV,NNGV), DEL00210
1NPRMP(IMV,JMV,KMV),PSI(NTOGV,IMV,JMV,KMV),P2(NTOGV,IMV,JMV), DEL00220
2PSD(IMV,JMV,KMV),PO(IMV,JMV),VO(NPRGV) DEL00230
IF(IOPT.EQ.1)GO TO 200 DEL00240
DO 180 K=1,KM DEL00250
DO 110 NG=1,NNG DEL00260
READ(IDSC1)((PSI(NG,I,J,K),I=1,IM),J=1,JM) DEL00270
IF(NG.NE.NTG)GO TO 110 DEL00280
DO 100 J=1,JM DEL00290
DO 100 I=1,IM DEL00300
100 PSD(I,J,K)=PSI(NTG,I,J,K) DEL00310
110 CONTINUE DEL00320
NDL=NNG+1 DEL00330
DO 170 J=1,JM DEL00340
DO 170 I=1,IM DEL00350
IF(K.EQ.KM)GO TO 150 DEL00360
NPR=NPRMP(I,J,K) DEL00370
TEMP=0.000 DEL00380
DO 120 NG=1,NNG DEL00390
120 TEMP=TEMP+DD6(NPR,NG)*PSI(NG,I,J,K) DEL00400

```



```

TEMP=TEMP/(EFFK*VO(NPR))
DO 140 NG=NDL,NTOG
ND=NG-NNG
IF(J.EQ.JM.OR.I.EQ.IM)GO TO 130
PSI(NG,I,J,K)=BETA(ND)*TEMP/ALAM(ND)
GO TO 140
130 PSI(NG,I,J,K)=0.000
140 CONTINUE
GO TO 170
150 DO 160 NG=NDL,NTOG
160 PSI(NG,I,J,KM)=0.000
170 CONTINUE
180 CONTINUE
GO TO 300
C BRANCH HERE IF IOPT=1
200 DO 280 K=1,KM
DO 210 NG=1,NNG
READ(10SC1)((P2(NG,I,J),I=1,IM),J=1,JM)
210 CONTINUE
WRITE(10FD)((P2(NTG,I,J),I=1,IM),J=1,JM)
NDL=NNG+1
DO 270 J=1,JM
DO 270 I=1,IM
IF(K.EQ.KM)GO TO 250
NPR=NPRMP(I,J,K)
TEMP=0.000
DO 220 NG=1,NNG
220 TEMP=TEMP+DD6(NPR,NG)*P2(NG,I,J)/(EFFK*VO(NPR))
DO 240 NG=NDL,NTOG
ND=NG-NNG
IF(I.EQ.IM.OR.J.EQ.JM)GO TO 230
P2(NG,I,J)=BETA(ND)*TEMP/ALAM(ND)
GO TO 240
230 P2(NG,I,J)=0.000
240 CONTINUE
GO TO 270

```

```

DEL00405
DEL00410
DEL00420
DEL00430
DEL00440
DEL00450
DEL00460
DEL00470
DEL00480
DEL00490
DEL00500
DEL00510
DEL00520
DEL00530
DEL00540
DEL00550
DEL00560
DEL00570
DEL00580
DEL00590
DEL00600
DEL00610
DEL00620
DEL00630
DEL00640
DEL00650
DEL00660
DEL00670
DEL00680
DEL00690
DEL00700
DEL00710
DEL00720
DEL00730
DEL00740
DEL00750

```

250 DO 260 NG=NDL,NTOG
260 P2(NG,I,J)=0.000
270 CONTINUE
 WRITE(IOPO)P2
280 CONTINUE
 REWIND IOPJ
 REWIND IOFO
300 REWIND IOSC1
 RETURN
 END

DEL00760
DEL00770
DEL00780
DEL00790
DEL00800
DEL00810
DEL00820
DEL00830
DEL00840
DEL00850

```

SUBROUTINE STEPA0(V,XIM,ALAM,BETA,XIP,X,Y,Z,HX,HY,HZ,DD1,DD2,DD3, STE00010
1 DD4,DD5,DD6,DD7,VO,NPRMP,PSI,W,NGV,NDGV,NTDGV,NDNSCV,IMV,JMV,KMV, STE00020
2 IRMV,JRMV,KRMV,NPRGV,NGXV) STE00030
  IMPLICIT REAL*8 (A-H,O-Z) STE00040
  INTEGER*2 MMAP,NPRMP STE00050
  COMMON/INTG/IASIZE,NNG,NDG,NTDGV,NMAT,IM,JM,KM,IRM,JRM,KRM,NLBC, STE00060
1 NFBC,NBBC,NDNSCT,NPRG,IOP,NTG,NXTP,NYTP,NZTP,IXTP(5),IYTP(5), STE00070
2 IZTP(5),NSTEAD,IFLIN,IGEOM,ITITLE(20),NDIT,NIIT,NPIT,IOPSI,IODUMP, STE00080
3 IOFN,IOFO,IOPN,IOPJ,ITEMP,ITEMP1,ITEMP2,ITEMP3,ITEMP4,ITEMP5, STE00090
4 NTIT,IETIME,IFLOUT,IMX,JMX,KMX,IOSC1,IOSC2,NGX STE00100
  COMMON/FLOTE/EFFK,DRFP,EPS1,EPS2,TEMP,TEMP1,TEMP2,TEMP3,TEMP4, STE00150
1 TEMP5,TEMP6,XFISST,XFISSO,ALAMN,ALAMO,TIME,FLXCON,BETAT STE00160
  COMMON/TIMINT/LASZON,ISTPCH,ILINCH,IPRSTP,MNSCH(5),MNLCH(5), STE00170
1 ISTEP,ICHHT STE00180
  COMMON/TIMFLO/T,HT,HMIN,HMAX,TSTART,TEND,DELSFS(5,4),DELSRS(5,4), STE00190
1 DELSTS(5,4),DELS1S(5,4),DELS2S(5,4),DELSFL(5,4),DELSRL(5,4), STE00200
2 DELSTL(5,4),DELS1L(5,4),DELS2L(5,4) STE00210
  DIMENSION V(NGV),XIM(NGV),ALAM(NDGV),BETA(NDGV),XIP(NGV,NDGV), STE00220
1 X(IMV),Y(JMV),Z(KMV),HX(IRMV),HY(JRMV),HZ(KRMV),DD1(NPRGV,NGV), STE00230
2 DD2(NPRGV,NGV),DD3(NPRGV,NGV),DD4(NPRGV,NGV),DD5(NPRGV,NGV), STE00240
3 DD6(NPRGV,NGV),DD7(NPRGV,NGXV,NDNSCV),NPRMP(IMV,JMV,KMV), STE00250
4 PSI(NTDGV,IMV,JMV,KMV),W(IMV,JMV,KMV),VO(NPRGV) STE00260
  DIMENSION CC(4,4),DD(4) STE00270
C FIRST TRANSFORM ALL POINTS STE00280
  DO 110 K=2,KMX STE00290
  DO 110 J=1,JMX STE00300
  DO 110 I=1,IMX STE00310
  TEMP1=DEXP(W(I,J,K)*HT) STE00320
  DO 100 NG=1,NNG STE00330
100 PSI(NG,I,J,K)=TEMP1*PSI(NG,I,J,K) STE00340
110 CONTINUE STE00350
C NOW SET STARTING I,J,AND K INDICES ASSUMING NO SYMMETRY BOUNDARIES STE00360
  IS=2 STE00370
  JS=2 STE00380
  KS=2 STE00390
  HINV=1.000/HT STE00400

```

500	DO 850 K=KS,KMX	STE02370
	IF(NFBC.EQ.0)GO TO 660	STE02380
	DO 620 NG=1,NNG	STE02390
	TEMP=1.000/(V(NG)*HT)	STE02400
	DO 550 J=1,2	STE02410
	DO 550 I=1,2	STE02420
	NPR=NPRMP(I,J,K)	STE02430
	II=2*(J-1)+I	STE02440
	DD(II)=0.000	STE02450
	DO 520 NGP=1,NTOG	STE02460
	IF(NGP.GT.NNG)GO TO 510	STE02470
	IF(NGP.EQ.NG)GO TO 520	STE02480
	DD(II)=DD(II)+XIM(NG)*DD6(NPR,NGP)*PSI(NGP,I,J,K)	STE02490
	GO TO 520	STE02500
510	ND=NGP-NNG	STE02510
	DD(II)=DD(II)+XIP(NG,ND)*PSI(NGP,I,J,K)*VO(NPR)	STE02520
520	CONTINUE	STE02530
	DO 530 NDN=1,NDNSCT	STE02540
	ITEMP1=NG-NDN	STE02550
	IF(ITEMP1.LE.0)GO TO 530	STE02560
	DD(II)=DD(II)+DD7(NPR,ITEMP1,NDN)*PSI(ITEMP1,I,J,K)	STE02570
530	CONTINUE	STE02580
	PTEM=TEMP*VO(NPR)	STE02581
	DD(II)=DD(II)+(PTEM-DD4(NPR,NG))*PSI(NG,I,J,K)+DD1(NPR,NG)*PSI(NG,	STE02590
	I+1,J,K)+DD2(NPR,NG)*PSI(NG,I,J+1,K)+DD3(NPR,NG)*PSI(NG,I,J,K+1)+	STE02600
	2DD3(NPRMP(I,J,K-1),NG)*PSI(NG,I,J,K-1)	STE02610
	DO 540 ITEMP2=1,4	STE02620
540	CC(II,ITEMP2)=0.000	STE02630
	CC(II,II)=(TEMP+W(I,J,K)/V(NG))*VO(NPR)+DD5(NPR,NG)	STE02640
550	CONTINUE	STE02650
	NPR=NPRMP(1,1,K)	STE02660
	CC(1,2)=-DD1(NPR,NG)	STE02670
	CC(1,3)=-DD2(NPR,NG)	STE02680
	CC(2,4)=-DD2(NPRMP(2,1,K),NG)	STE02690
	CC(3,4)=-DD1(NPRMP(1,2,K),NG)	STE02700
	CC(2,1)=CC(1,2)	STE02710

CC(3,1)=CC(1,3)	STE02720
CC(4,2)=CC(2,4)	STE02730
CC(4,3)=CC(3,4)	STE02740
C CALL DSIMQ TO SOLVE SYSTEM	STE02750
NEQ=4	STE02760
CALL DSIMQ(CC,DD,NEQ,ISING)	STE02770
DO 560 J=1,2	STE02780
DO 560 I=1,2	STE02790
II=2*(J-1)+I	STE02800
560 PSI(NG,I,J,K)=DD(II)	STE02810
DO 620 I=3,IMX	STE02820
DO 570 II=1,4	STE02830
570 DD(II)=0.000	STE02840
NPRY=NPRMP(I,1,K)	STE02850
DO 610 J=1,2	STE02860
NPR=NPRMP(I,J,K)	STE02870
DO 590 VGP=1,NTDG	STE02880
IF(NGP.GT.NNG)GO TO 580	STE02890
IF(NGP.EQ.NG)GO TO 590	STE02900
DD(J)=DD(J)+XIM(NG)*DD6(NPR,NG)*PSI(NGP,I,J,K)	STE02910
GO TO 590	STE02920
580 ND=NGP-NNG	STE02930
DD(J)=DD(J)+XIP(NG,ND)*PSI(VGP,I,J,K)*VO(NPR)	STE02940
590 CONTINUE	STE02950
DO 600 VDN=1,NDNSCT	STE02960
ITEMP1=VG-NDN	STE02970
IF(ITEMP1.LE.0)GO TO 600	STE02980
DD(J)=DD(J)+DD7(NPR,ITEMP1,VDN)*PSI(ITEMP1,I,J,K)	STE02990
600 CONTINUE	STE03000
PTEM=TEMP*VO(NPR)	STE03001
DD(J)=DD(J)+{PTEM-DD4(NPR,VG)}*PSI(NG,I,J,K)+DD1(NPR,NG)*PSI(NG,I,	STE03010
1 I,J,K)+DD2(NPR,NG)*PSI(NG,I,J+1,K)+DD1(NPRMP(I-1,J,K),VG)*PSI(NG,I	STE03020
2-1,J,K)+DD3(NPR,NG)*PSI(NG,I,J,K+1)+DD3(NPRMP(I,J,K-1),NG)*PSI(NG,	STE03030
3 I,J,K-1)	STE03040
610 DD(J+2)=(TEMP+W(I,J,K)/V(NG))*VO(NPR)+DD5(NPR,NG)	STE03051
TEMP5=DD(3)*DD(4)-(DD2(NPRY,NG)**2.000)	STE03060

	PSI(NG,I,1,K)=(DD(1)*DD(4)+DD(2)*DD2(NPRY,NG))/TEMP5	STE03070
	PSI(NG,I,2,K)=(DD(2)*DD(3)+DD(1)*DD2(NPRY,NG))/TEMP5	STE03080
620	CONTINUE	STE03090
	DD 650 J=1,2	STE03100
	DD 650 I=1,IMX	STE03110
	NPR=NPRMP(I,J,K)	STE03120
	DD 640 ND=1,NDG	STE03130
	NG=ND+NNG	STE03140
	TEMP1=0.000	STE03150
	DD 630 NGP=1,NNG	STE03160
630	TEMP1=TEMP1+BETA(ND)*DD6(NPR,NGP)*PSI(NGP,I,J,K)	STE03170
	TEMP1=TEMP1/(EFFK*VO(NPR))	STE03180
640	PSI(NG,I,J,K)=((HINV-ALAM(ND))*PSI(NG,I,J,K)+TEMP1)/(HINV+ALAM(ND))	STE03190
	1)	STE03200
650	CONTINUE	STE03210
	JS=3	STE03220
660	DD 840 J=JS,JMX	STE03230
	IF(NLBC.EQ.0)GO TO 760	STE03240
	DD 720 NG=1,NNG	STE03250
	TEMP=1.000/(V(NG)*HT)	STE03260
	DD 670 II=1,4	STE03270
670	DD(II)=0.000	STE03280
	NPRX=NPRMP(1,J,K)	STE03290
	DD 710 I=1,2	STE03300
	NPR=NPRMP(I,J,K)	STE03310
	DD 690 VGP=1,NTDG	STE03320
	IF(NGP.GT.NNG)GO TO 680	STE03330
	IF(NGP.EQ.NG)GO TO 690	STE03340
	DD(I)=DD(I)+XIM(NG)*DD6(NPR,NGP)*PSI(NGP,I,J,K)	STE03350
	GO TO 690	STE03360
680	ND=NGP-NNG	STE03370
	DD(I)=DD(I)+XIP(NG,ND)*PSI(VGP,I,J,K)*VO(NPR)	STE03380
690	CONTINUE	STE03390
	DD 700 NDN=1,NDNSCT	STE03400
	ITEMP1=NG-NDN	STE03410
	IF(ITEMP1.LE.0)GO TO 700	STE03420

DD(I)=DD(I)+DD7(NPR,ITEMP1,NDN)*PSI(ITEMP1,I,J,K)	STE03430
700 CONTINUE	STE03440
PTEM=TEMP*VD(NPR)	STE03441
DD(I)=DD(I)+(PTEM-DD4(NPR,NG))*PSI(NG,I,J,K)+DD1(NPR,NG)*PSI(NG,I+STE03450	
11,J,K)+DD2(NPR,NG)*PSI(NG,I,J+1,K)+DD2(NPRMP(I,J-1,K),NG)*PSI(NG,ISTE03460	
2,J-1,K)+DD3(NPR,NG)*PSI(NG,I,J,K+1)+DD3(NPRMP(I,J,K-1),NG)*PSI(NG STE03470	
3,I,J,K-1)	STE03480
710 DD(I+2)=(TEMP+W(I,J,K)/V(NG))*VD(NPR)+DD5(NPR,NG)	STE03490
TEMP5=DD(3)*DD(4)-(DD1(NPRX,NG)**2.000)	STE03500
PSI(NG,1,J,K)=(DD(1)*DD(4)+DD(2)*DD1(NPRX,NG))/TEMP5	STE03510
PSI(NG,2,J,K)=(DD(2)*DD(3)+DD(1)*DD1(NPRX,NG))/TEMP5	STE03520
720 CONTINUE	STE03530
DD 750 I=1,2	STE03540
NPR=NPRMP(I,J,K)	STE03550
DD 740 ND=1,NDG	STE03560
NG=ND+NNG	STE03570
TEMP1=0.000	STE03580
DD 730 NGP=1,NNG	STE03590
730 TEMP1=TEMP1+BETA(ND)*DD6(NPR,NGP)*PSI(NGP,I,J,K)	STE03600
TEMP1=TEMP1/(EFFK*VD(NPR))	STE03610
740 PSI(NG,I,J,K)=((HINV-ALAM(ND))*PSI(NG,I,J,K)+TEMP1)/(HINV+ALAM(ND)STE03620	
1)	STE03630
750 CONTINUE	STE03640
IS=3	STE03650
760 DD 830 I=IS,IMX	STE03660
NPR=NPRMP(I,J,K)	STE03670
NPRX=NPRMP(I-1,J,K)	STE03680
NPRY=NPRMP(I,J-1,K)	STE03690
NPRZ=NPRMP(I,J,K-1)	STE03700
DD 800 NG=1,NNG	STE03710
TEMP=1.000/(V(NG)*HT)	STE03720
TEMP1=0.000	STE03730
DD 780 NGP=1,NTOG	STE03740
IF(NGP.GT.NNG)GO TO 770	STE03750
IF(NGP.EQ.NG)GO TO 780	STE03760
TEMP1=TEMP1+XIM(NG)*DD6(NPR,NGP)*PSI(NGP,I,J,K)	STE03770

GO TO 780	STE03780
770 ND=NGP-NNG	STE03790
TEMP1=TEMP1+XIP(NG,ND)*PSI(NGP,I,J,K)*VO(NPR)	STE03800
780 CONTINUE	STE03810
DO 790 VDN=1,NDNSCT	STE03820
ITEMP1=NG-NDN	STE03830
IF(ITEMP1.LE.0)GO TO 790	STE03840
TEMP1=TEMP1+DD7(NPR,ITEMP1,VDN)*PSI(ITEMP1,I,J,K)	STE03850
790 CONTINUE	STE03860
PTEM=TEMP*VO(NPR)	STE03861
PSI(NG,I,J,K)=((PTEM-DD4(NPR,NG))*PSI(NG,I,J,K)+DD1(NPR,NG)*PSI(NG,STE03870	
1,I+1,J,K)+DD1(NPRX,NG)*PSI(NG,I-1,J,K)+DD2(NPR,NG)*PSI(NG,I,J+1,K)STE03880	
2+DD2(NPRY,NG)*PSI(NG,I,J-1,K)+DD3(NPR,NG)*PSI(NG,I,J,K+1)+DD3(NPRZSTE03890	
3,NG)*PSI(NG,I,J,K-1)+TEMP1)/((TEMP+W(I,J,K)/V(NG))*VO(NPR)+DD5(NPRSTE03900	
4,NG))	STE03901
800 CONTINUE	STE03910
DO 820 ND=1,NDG	STE03920
NG=ND+NNG	STE03930
TEMP1=0.000	STE03940
DO 810 NGP=1,NNG	STE03950
810 TEMP1=TEMP1+BETA(ND)*DD6(NPR,NGP)*PSI(NGP,I,J,K)	STE03960
TEMP1=TEMP1/(EFFK*VO(NPR))	STE03970
820 PSI(NG,I,J,K)=((HINV-ALAM(ND))*PSI(NG,I,J,K)+TEMP1)/(HINV+ALAM(ND)STE03980	
1)	STE03990
830 CONTINUE	STE04000
840 CONTINUE	STE04010
850 CONTINUE	STE04020
RETURN	STE04030
END	STE04040


```

SUBROUTINE STEPBO(V, XIM, ALAM, BETA, XIP, X, Y, Z, HX, HY, HZ, DD1, DD2, DD3, STE00010
1DD4, DD5, DD6, DD7, VO, NPRMP, PSI, W, NNGV, NDGV, NTOGV, NDNSCV, IMV, JMV, KMV, STE00020
2IRMV, JRMV, KRMV, NPRGV, NGXV) STE00030
  IMPLICIT REAL*8 (A-H, O-Z) STE00040
  INTEGER*2 MMAP, NPRMP STE00050
  COMMON/INTG/ IASIZE, NNG, NDG, NTOG, NMAT, IM, JM, KM, IRM, JRM, KRM, NLBC, STE00060
  1NFBC, NBBC, NDNSCT, NPRG, IOPT, NTG, NXTP, NYTP, NZTP, IXTP(5), IYTP(5), STE00070
  2IZTP(5), NSTEAD, IFLIN, IGEOM, ITITLE(20), NOIT, NIIT, NPIT, IJPSI, IODUMP, STE00080
  3IOFN, IOFO, IOFN, IOPO, ITEMP, ITEMP1, ITEMP2, ITEMP3, ITEMP4, ITEMP5, STE00090
  4NTIT, IETIME, IFLOUT, IMX, JMX, KMX, IOSC1, IOSC2, NGX STE00100
  COMMON/FLOTE/EFFK, DRFP, EPS1, EPS2, TEMP, TEMP1, TEMP2, TEMP3, TEMP4, STE00150
  1TEMP5, TEMP6, XFISST, XFISSO, ALAMN, ALAMO, TIME, FLXCON, BETAT STE00160
  COMMON/TIMINT/LASZDN, ISTPCH, ILINCH, IPRSTP, MNSCH(5), MNLCH(5), STE00170
  1ISTEP, ICHHT STE00180
  COMMON/TIMELO/T, HT, HMIN, HMAX, TSTART, TEND, DELSFS(5,4), DELSRS(5,4), STE00190
  1DELSTS(5,4), DELS1S(5,4), DELS2S(5,4), DELSFL(5,4), DELSRL(5,4), STE00200
  2DELSTL(5,4), DELS1L(5,4), DELS2L(5,4) STE00210
  DIMENSION V(NNGV), XIM(NNGV), ALAM(NDGV), BETA(NDGV), XIP(NNGV, NDGV), STE00220
  1X(IMV), Y(JMV), Z(KMV), HX(IRMV), HY(JRMV), HZ(KRMV), DD1(NPRGV, NNGV), STE00230
  2DD2(NPRGV, NNGV), DD3(NPRGV, NNGV), DD4(NPRGV, NNGV), DD5(NPRGV, NNGV), STE00240
  3DD6(NPRGV, NNGV), DD7(NPRGV, NGXV, NDNSCV), NPRMP(IMV, JMV, KMV), STE00250
  4PSI(NTOGV, IMV, JMV, KMV), W(IMV, JMV, KMV), VO(NPRGV) STE00260
  KE=KMX-1 STE00270
  JE=JMX-1 STE00290
  IF(NFBC.EQ.1)JE=JMX-2 STE00300
  HINV=1.000/HT STE00310
  IE=IMX-1 STE00320
  DO 340 KK=1, KE STE00330
  K=KM-KK STE00340
  DO 220 JJ=1, JE STE00350
  J=JM-JJ STE00360
  DO 210 II=1, IE STE00370
  I=IM-II STE00380
  NPR=NPRMP(I, J, K) STE00390
  NPRX=NPRMP(I-1, J, K) STE00400
  NPRY=NPRMP(I, J-1, K) STE00410

```

NPRZ=NPRMP(I,J,K-1)	STE00420
DO 160 NG=1,NNG	STE00430
TEMP=1.0DD0/(V(NG)*HT)	STE00440
110 TEMP1=0.0DD0	STE00450
DO 130 NGP=1,NTOG	STE00460
IF(NGP.GT.NNG)GO TO 120	STE00470
IF(NGP.EQ.NG)GO TO 130	STE00480
TEMP1=TEMP1+XIM(NG)*DD6(NPR,NGP)*PSI(NGP,I,J,K)	STE00490
GO TO 130	STE00500
120 ND=NGP-NNG	STE00510
TEMP1=TEMP1+XIP(NG,ND)*PSI(NGP,I,J,K)*VO(NPR)	STE00520
130 CONTINUE	STE00530
DO 140 NDN=1,NDNSCT	STE00540
ITEMP1=NG-NDN	STE00550
IF(ITEMP1.LE.0)GO TO 140	STE00560
TEMP1=TEMP1+DD7(NPR,ITEMP1,NDN)*PSI(ITEMP1,I,J,K)	STE00570
140 CONTINUE	STE00580
PTEM=TEMP*VO(NPR)	STE00581
IF(I.EQ.1)GO TO 150	STE00590
TEMP2=PSI(NG,I,J,K)	STE00600
PSI(NG,I,J,K)={(PTEM-DD4(NPR,NG))*TEMP2+DD1(NPR,NG)*PSI(NG,I+1,J,K)	STE00610
1)+DD1(NPRX,NG)*PSI(NG,I-1,J,K)+DD2(NPR,NG)*PSI(NG,I,J+1,K)+DD2(NPR	STE00620
2Y,NG)*PSI(NG,I,J-1,K)+DD3(NPR,NG)*PSI(NG,I,J,K+1)+DD3(NPRZ,NG)*PSI	STE00630
3(NG,I,J,K-1)+TEMP1)/((TEMP+W(I,J,K)/V(NG))*VO(NPR)+DD5(NPR,NG))	STE00640
IF(I.GT.2)GO TO 160	STE00650
IF(NL3C.EQ.0)GO TO 160	STE00660
I=1	STE00670
NPR=NPRMP(1,J,K)	STE00680
GO TO 110	STE00690
150 PSI(NG,1,J,K)={(PTEM-DD4(NPR,NG))*PSI(NG,1,J,K)+DD1(NPR,NG)*{PSI(NG	STE00700
1G,2,J,K)+TEMP2)+DD2(NPR,NG)*PSI(NG,1,J+1,K)+DD2(NPRMP(1,J-1,K),NG)	STE00710
2*PSI(NG,1,J+1,K)+DD3(NPR,NG)*PSI(NG,1,J,K+1)+DD3(NPRMP(1,J,K-1),NG)	STE00720
3)*PSI(NG,1,J,K-1)+TEMP1)/((TEMP+W(I,J,K)/V(NG))*VO(NPR)+DD5(NPR,NG)	STE00730
4))	STE00731
NPR=NPRMP(2,J,K)	STE00740
I=2	STE00750

160	CONTINUE	STE00760
	DO 200 ND=1,NDG	STE00770
	NG=ND+NNG	STE00780
170	TEMP1=0.0DD	STE00790
	DO 180 NGP=1,NNG	STE00800
180	TEMP1=TEMP1+BETA(ND)*DD6(NPR,NGP)*PSI(NGP,I,J,K)	STE00810
	TEMP1=TEMP1/(EFFK*VO(NPR))	STE00820
	PSI(NG,I,J,K)=((HINV-ALAM(ND))*PSI(NG,I,J,K)+TEMP1)/(HINV+ALAM(ND))	STE00830
	1)	STE00840
	IF(I.EQ.1)GO TO 190	STE00850
	IF(I.GT.2)GO TO 200	STE00860
	IF(NLBC.EQ.0)GO TO 200	STE00870
	I=1	STE00880
	NPR=NPR4P(1,J,K)	STE00890
	GO TO 170	STE00900
190	I=2	STE00910
	NPR=NPR4P(2,J,K)	STE00920
200	CONTINUE	STE00930
210	CONTINUE	STE00940
220	CONTINUE	STE00950
	IF(NFBC.EQ.0)GO TO 340	STE00960
	DO 300 NG=1,NNG	STE00970
	TEMP=1.0DD/(V(NG)*HT)	STE00980
	DO 290 II=1,IE	STE00990
230	TEMP2=PSI(NG,I,1,K)	STE01000
	DO 270 JJ=1,2	STE01010
	J=3-JJ	STE01020
	NPR=NPRMP(I,J,K)	STE01030
	NPRX=NPRMP(I-1,J,K)	STE01040
	NPRY=NPRMP(I,1,K)	STE01050
	NPRZ=NPRMP(I,J,K-1)	STE01060
	TEMP1=0.0DD	STE01070
	DO 250 NGP=1,NTOG	STE01080
	IF(NGP.GT.NNG)GO TO 240	STE01090
	IF(NGP.LE.NG)TEMP1=TEMP1+DD6(NPR,NGP)*PSI(NGP,I,J,K)	STE01100
	IF(NGP.EQ.NNG)TEMP1=TEMP1*XIM(NG)	STE01110

GO TO 250	STE01120
240 ND=NGP-NNG	STE01130
TEMP1=TEMP1+XIP(NG,ND)*PSI(NGP,I,J,K)*VO(NPR)	STE01140
250 CONTINUE	STE01150
TEMP3=PSI(NG,I,2,K)	STE01160
PTEM=TEMP*VO(NPR)	STE01161
IF(I.EQ.1)GO TO 260	STE01170
PSI(NG,I,J,K)=((PTEM-DD4(NPR,NG))*PSI(NG,I,J,K)+DD1(NPR,NG)*PSI(NG,I,I+1,J,K)+DD1(NPRX,NG)*PSI(NG,I-1,J,K)+DD2(NPR,NG)*PSI(NG,I,J+1,K)+DD2(NPRY,NG)*TEMP2+DD3(NPR,NG)*PSI(NG,I,J,K+1)+DD3(NPRZ,NG)*PSI(NG,I,J,K-1)+TEMP1)/((TEMP+W(I,J,K)/V(NG))*VO(NPR)+DD5(NPR,NG))	STE01180
TEMP2=TEMP3	STE01190
GO TO 270	STE01200
260 PSI(NG,I,J,K)=((PTEM-DD4(NPR,NG))*PSI(NG,I,J,K)+DD1(NPR,NG)*(TEMP4+PSI(NG,2,J,K))+DD2(NPR,NG)*PSI(NG,1,J+1,K)+DD2(NPRY,NG)*TEMP2+DD3(NPR,NG)*PSI(NG,1,J,K+1)+DD3(NPRZ,NG)*PSI(NG,1,J,K-1)+TEMP1)/3((TEMP+W(1,J,K)/V(NG))*VO(NPR)+DD5(NPR,NG))	STE01210
TEMP4=TEMP5	STE01220
TEMP2=TEMP3	STE01230
270 CONTINUE	STE01240
IF(I.EQ.2)GO TO 280	STE01250
IF(I.NE.3)GO TO 290	STE01260
TEMP4=PSI(NG,2,2,K)	STE01270
TEMP5=PSI(NG,2,1,K)	STE01280
GO TO 290	STE01290
280 I=1	STE01300
GO TO 230	STE01310
290 CONTINUE	STE01320
300 CONTINUE	STE01330
DO 330 II=1,IMX	STE01340
I=IM-II	STE01350
DO 330 JJ=1,2	STE01360
J=3-JJ	STE01370
NPR=NPRMP(I,J,K)	STE01380
DO 320 ND=1,NDG	STE01390
NG=ND+NNG	STE01400
	STE01410
	STE01420
	STE01430
	STE01440
	STE01450
	STE01460

TEMP1=0.0D0	STE01470
DO 310 NGP=1,NNG	STE01480
310 TEMP1=TEMP1+BETA(ND)*DD6(NPR,NGP)*PSI(NGP,I,J,K)	STE01490
TEMP1=TEMP1/(EFFK*VO(NPR))	STE01500
320 PSI(NG,I,J,K)=((HINV-ALAM(ND))*PSI(NG,I,J,K)+TEMP1)/(HINV+ALAM(ND)	STE01510
1)	STE01520
330 CONTINUE	STE01530
340 CONTINUE	STE01540
C NOW CARRY OUT EXP(W*H) TRANSFORMATION	STE01550
350 DO 370 K=2,KMX	STE01560
DO 370 J=1,JMX	STE01570
DO 370 I=1,IMX	STE01580
TEMP1=DEXP(W(I,J,K)*HT)	STE01590
DO 360 VG=1,NNG	STE01600
360 PSI(NG,I,J,K)=TEMP1*PSI(NG,I,J,K)	STE01610
370 CONTINUE	STE01620
RETURN	STE01630
END	STE01640

SUBROUTINE FREQ0(PSI,PS0,W,NT0GV,IMV,JMV,KMV)	FRE00010
IMPLICIT REAL*8 (A-H,O-Z)	FRE00020
INTEGER*2 MMAP,NPRMP	FRE00030
COMMON/INT3/IASIZE,NNG,NDG,NT0G,NMAT,IM,JM,KM,IRM,JRM,KRM,NLBC,	FRE00040
1NFBC,NB8C,NDNSCT,NPRG,I0PT,NTG,NXTP,NYTP,NZTP,IXTP(5),IYTP(5),	FRE00050
2IZTP(5),NSTEAD,IFLIN,IGEQM,ITITLE(20),NOIT,NIIT,NPIT,IOPSI,I0DUMP,	FRE00060
3I0FN,I0FO,I0PN,I0PD,ITEMP,ITEMP1,ITEMP2,ITEMP3,ITEMP4,ITEMP5,	FRE00070
4NTIT,IETIME,IFL0UT,IMX,JMX,KMX,I0SC1,I0SC2,NGX	FRE00080
COMMON/FLOTE/EFFK,DRFP,EPS1,EPS2,TEMP,TEMP1,TEMP2,TEMP3,TEMP4,	FRE00130
1TEMP5,TEMP6,XFISST,XFIS80,ALAMN,ALAMD,TIME,FLXCJN,BETAT	FRE00140
COMMON/TIMINT/LASZ0N,ISTPC4,ILINCH,I0RSTP,MNSCH(5),MNLCH(5),	FRE00150
1ISTEP,ICHHT	FRE00160
COMMON/TIMFLO/T,HT,HMIN,HMAX,TSTART,TEND,DELSFS(5,4),DELSRS(5,4),	FRE00170
1DELS(5,4),DELS1S(5,4),DELS2S(5,4),DELSFL(5,4),DELSRL(5,4),	FRE00180
2DELSL(5,4),DELS1L(5,4),DELS2L(5,4)	FRE00190
DIMENSION PSI(NT0GV,IMV,JMV,KMV),PS0(IMV,JMV,KMV),W(IMV,JMV,KMV)	FRE00200
TEMP5=1.000/(2.000*HT)	FRE00210
C COMPUTE FREQUENCIES	FRE00220
DD 120 K=2,KMX	FRE00230
DD 120 J=1,JMX	FRE00240
DD 120 I=1,IMX	FRE00250
IF(PSJ(I,J,K).LT.1.00-30)GO TO 110	FRE00260
TEMP4=PSI(NTG,I,J,K)/PS0(I,J,K)	FRE00270
IF(DABS(1.000-TEMP4).LT.1.00-08)GO TO 110	FRE00280
W(I,J,K)=TEMP5*DLOG(TEMP4)	FRE00290
GO TO 120	FRE00300
110 W(I,J,K)=0.000	FRE00310
120 CONTINUE	FRE00320
RETURN	FRE00330
END	FRE00340